

**AN INVESTIGATION INTO THE USE OF AERIAL DIGITAL PHOTOGRAPHY FOR
MONITORING COASTAL SAND DUNES**

ESTHER EDWARDS

A thesis submitted in partial fulfilment of the requirements of the University of the West of
England, Bristol for the degree of Doctor of Philosophy at Bath Spa University College

Faculty of Applied Sciences, Bath Spa University College

March 2001

ABSTRACT

The coastal zone is a highly dynamic entity both spatially and temporally and when shoreline changes (and in particular retreat) occur on a human time-scale, measurement of the rate of change becomes a pressing issue. This dynamism presents an excellent scenario for monitoring change using remote sensing techniques, and in the case of coastal sand dunes, where the requirement is to measure small scale changes such as erosion or accretion in the region of 10 or 20 m, aerial photography is the preferred source of remotely sensed data.

The rapid developments in digital camera technology and real time satellite differential Global Positioning Systems have yielded new opportunities for mapping and monitoring environmental change when used with image processing and mapping software and state-of-the-art digital photogrammetric workstations. Despite the progress in digital technologies, however, there is still considerable lack of awareness on the part of potential users, and it is in response to this that the processing chain for data collection through to orthophoto production described here has been developed. This study explores the major issues that affect quality, mission logistics and cost and will demonstrate the methodology and application of digital techniques for producing georectified imagery and contoured orthophoto maps of coastal environments. This will be achieved through a series of case studies of dynamic dune environments in south-west England and France.

Digital imagery was captured using a colour infrared Aerial Digital Photographic System and ground control was collected using differential Global Positioning Systems. This study seeks to assess the application of this imagery to coastal dune monitoring, putting these new techniques within the grasp of coastal dune managers, enabling them to make use of digital imagery captured to different specifications depending on the accuracy requirement of the end product.

The results indicate that this type of imagery and the techniques used can provide the dune manager with information which would otherwise be too costly or time consuming to acquire. 2D rectification of the imagery provided maps of dune retreat and accretion with errors in the region of $\pm 1.5\text{m}$, and rectification to a higher order using 3D photogrammetric correction provided 1:5000 contoured orthophotographs with mean xy errors in the region of 2.5m and mean elevation errors in the region of 1.5m.

CONTENTS

Abstract	i
Acknowledgements	iii
Index	iv
List of Figures	xiii
List of Tables	xvi
List of Plates	xviii
Chapter 1 The Coastal Zone ~ a suitable case for monitoring change	1
Chapter 2 Coastal Dunes ~ physical background	14
Chapter 3 Coastal Dunes ~ pressures and perspectives	26
Chapter 4 Coastal Dunes Management ~ issues and techniques	33
Chapter 5 Aerial Photography and Videography	51
Chapter 6 The Aerial Digital Photographic System [ADPS]	81
Chapter 7 Aerial photographs and photogrammetry	114
Chapter 8 Methodology	125
Chapter 9 Case Study 1 ~ surface change at Ile d'Oleron	144
Chapter 10 Case study 2 ~ at Dossen	163
Chapter 11 Case Study 3 ~ surface change at Ile de Noirmoutier	180
Chapter 12 Case Study 4 ~ orthophoto at Holywell Bay	206
Chapter 13 Summary	236
References	244
Appendix 1	273
Appendix 2	280
Appendix 3	311
Appendix 4	312

ACKNOWLEDGEMENTS

The author is grateful to Bath Spa University College for the opportunity to carry out this research and for financial support during the first three years of the programme.

The author wishes to acknowledge the help and support of many individuals and in particular special thanks are due to:

Dr. Richard Curr for all his help and encouragement and for his valuable comments and constructive advice on the text of this thesis.

Alexander Koh without whose help none of the primary data capture would have been possible, and for his help and advice on the more technical aspects of the image processing and the text of the thesis.

Andy Skellem and Fiona Strawbridge for help and advice.

Adrian Barralet and his trusty Partanavia for flying the survey team backwards and forwards across the English Channel and up and down the dune coasts of France and England.

Finally, my thanks to all my family for all their patience and encouragement throughout the long duration of this work.

INDEX

	Page
Chapter 1 The Coastal Zone ~ a suitable case for monitoring change	1
1.1 Introduction	1
1.2 Aims and objectives	2
1.3 Change in space and time	3
1.3.1 The question of time	3
1.3.2 The question of scale	4
1.4 Delineation of the coastal zone	6
1.5 The coastal resource	8
1.6 Natural and anthropogenic impacts on the coastal zone	9
1.6.1 Population Pressure At The Coastal Zone	9
1.6.2 Sea Level Rise	10
1.7 Coastal management	12
Chapter 2 Coastal Dunes ~ physical background	14
2.1 Sand Dune Development	14
2.1.1 Global distribution	14
2.1.2 Sediment sources	14
2.1.3 Sediment dynamics	16
2.1.3.1 <i>Sediment transport models</i>	17
2.2 Dune Morphology	18
2.2.1 Morphology and wind regime	19
2.2.2 Evolution of the system	19
2.2.3 Blowouts	21
2.3 Dune Classification	23
2.3.1 Geomorphologic classification	23

2.3.1.1	<i>Foredunes</i>	24
2.3.1.2	<i>Mobile dunes</i>	24
2.3.1.3	<i>Transition dunes</i>	24
2.3.1.4	<i>Fixed dunes</i>	24
2.4	Summary	25
Chapter 3	Coastal Dunes ~ pressures and perspectives	26
3.1	Perceptions and Mis-Conceptions	26
3.1.1	Dune Vulnerability	26
3.1.2	Societal Perceptions	27
3.2	Historic And Modern Perspectives	29
3.2.1	Historic Perspectives	29
3.2.2	Modern Perspectives	30
3.3	Summary	32
Chapter 4	Coastal Dunes Management ~ issues and techniques	33
4.1	Introduction to current management issues	33
4.2	Human impacts on sand dunes	33
4.2.1	Industrialisation	34
4.2.2	Sand extraction	35
4.2.3	Farming	36
4.2.3.1	<i>Stock grazing</i>	36
4.2.3.2	<i>Rabbit grazing</i>	36
4.2.3.3	<i>Cultivation</i>	37
4.2.4	Tourism and Recreation	38
4.2.4.1	<i>A contextual overview</i>	38
4.2.4.2	<i>Trampling</i>	41
4.2.4.3	<i>Off-Road Vehicles and Cycles</i>	43

4.2.4.4	<i>Horse Riding</i>	43
4.2.4.5	<i>Golf courses</i>	44
4.2.5	Urbanisation	45
4.2.5.1	<i>Housing</i>	45
4.2.5.2	<i>Drinking water catchments</i>	46
4.2.6	Exotic Introductions	47
4.2.7	Military Use	48
4.2.8	Coastal Protection Works	49
4.2.9	Assessment of change	49
4.3	Management Techniques	50
4.3.1	Management ethos	50
4.3.2	Managing the physical environment	51
4.3.2.1	<i>Planting, fencing and thatching</i>	51
4.3.2.2	<i>Beach nourishment and dredging</i>	55
4.3.3	Managing the human element	57
4.4	Monitoring and Measurement	59
Chapter 5	Aerial Photography And Videography	61
5.1	A brief history of small format aerial photography	61
5.1.1	The early years	61
5.1.2	Evolution of small format camera technology	61
5.2	The advent of solid state	62
5.2.1	The evolution of video cameras	62
5.2.1.1	<i>Airborne video</i>	62
5.2.1.2	<i>Analogue video</i>	63
5.2.1.3	<i>Digital video</i>	65
5.2.2	The evolution of digital cameras	65
5.2.2.1	<i>Early developments</i>	65

5.3	The choice of sensors ~ film or digital	67
5.3.1	Making the choice	67
5.3.2	General film and digital issues	68
5.3.3	Digital image capture	69
5.3.4	Image scale and resolution	71
5.3.5	Aliasing	72
5.3.6	Data security and quality control	73
5.3.7	Cost considerations	74
5.3.7.1	<i>Capital cost</i>	74
5.3.7.2	<i>Developing, printing scanning</i>	74
5.3.7.3	<i>Block survey and orthophoto production</i>	75
5.4	True colour and colour infrared digital imaging	77
5.4.1	Digital image display	77
5.4.2	Producing multiband images	78
5.5	Continuing developments	79
Chapter 6	The Aerial Digital Photographic System [ADPS]	81
6.1	Development of the system	81
6.1.1	The choice of sensor	81
6.1.2	Evolution of the ADPS	83
6.2	General system specifications	84
6.3	The ADPS cameras	85
6.3.1	The Kodak Digital Science 420 and 460 series	85
6.3.2	Digital file formats and data storage in the Kodak DS series	87
6.3.3	Spectral Sensitivity	89
6.3.3.1	<i>Spectral range and quantum efficiency</i>	89
6.3.3.2	<i>Survey altitude and poor light levels</i>	90
6.3.4	The Kodak Colour Filter Array	91

6.3.5	CIR and True Colour Filters	94
6.3.6	Spatial resolution of the image	96
6.4	The intervalometer	99
6.4.1	Power supply to the camera	99
6.4.2	Firing the camera	101
6.5	The camera mount	102
6.6	The mission planner	104
6.6.1	Flight track planning	104
6.6.2	Issues related to the array size of the sensor	106
6.6.3	Issues related to the download time	107
6.6.4	Issues related to the maximum storage capacity of the storage medium	107
6.6.5	Other Issues	108
6.6.5.1	<i>Exposure compensation</i>	108
6.6.5.2	<i>Pixel translation</i>	110
6.6.6	Navigation	110
6.7	The future	113
Chapter 7	Aerial Photographs and Photogrammetry	114
7.1	Geometry of an aerial photograph	114
7.1.1	Types of aerial photographs	114
7.1.2	Scale	115
7.1.3	Image displacement and distortion	116
7.1.3.1	<i>Topographic displacement</i>	116
7.1.3.2	<i>Tilt displacement</i>	118
7.2	Orthophotographs	119
7.2.1	Introduction	119
7.2.2	Measurement of height from stereo photography	120

7.2.3	Stereo cover in a block survey	122
7.2.4	Digital photogrammetry	123
Chapter 8	Methodology	125
8.1	Introduction	125
8.2	Data description	125
8.2.1	General description	125
8.3	Data collection and analysis	128
8.3.1	Organisation of the study	128
8.3.2	Logistics and mission planning	129
8.3.2.1	<i>Assessing the type of imagery required</i>	130
8.3.2.2	<i>Air and ground survey logistics and cost</i>	131
8.3.2.3	<i>Camera metrics</i>	131
8.3.2.4	<i>Mission and flight track planning</i>	133
8.3.2.5	<i>Ground control point planning</i>	133
8.3.2.6	<i>Meteorological constraints</i>	133
8.3.3	Primary data acquisition	134
8.3.3.1	<i>Digital image data</i>	134
8.3.3.2	<i>Data archiving and photoindex generation</i>	135
8.3.3.3	<i>Reflight identification</i>	135
8.3.3.4	<i>Ground control data</i>	136
8.3.4	Methodology for data analysis	137
8.3.4.1	<i>Data processing and data analysis</i>	137
8.3.5	Geometric correction	137
8.3.6	Photogrammetric processing	139
8.3.6.1	<i>Defining the input and output parameters</i>	139
8.3.6.2	<i>Interior and exterior orientation</i>	140
8.3.6.3	<i>Relative and absolute orientation</i>	140

8.3.6.4	<i>Generation of the DEM and orthoimage</i>	142
8.3.6.5	<i>Mosaicing</i>	142
8.4	Summary	143
Chapter 9	Case Study 1 ~ measurement of recession at Ile d'Olcron	144
9.1	Introduction	144
9.2	Site description	144
9.3	Image registration	149
9.3.1	Mosaicing and registration	149
9.3.2	Error analysis	151
9.3.2.1	<i>Determination of registration error</i>	151
9.3.2.2	<i>Determination of the sample size</i>	153
9.4	Measurement of the dune cliff retreat	154
9.5	Overwash deposits	158
Chapter10	Case Study 2 ~ redistribution of sediment at Dossen	163
10.1	Introduction	163
10.2	Site description	165
10.3	Image registration and error assessment	168
10.3.1	Image registration	168
10.3.2	Error analysis	168
10.4	Change detection	169
10.5	Sediment redistribution	174
10.5.1	Sand deposited on the beach	174
10.5.2	Aeolian deposits on the dune	177

Chapter 11	Case Study 3 ~ measurement of surface change at Ile de Noirmoutier	180
11.1	Introduction	180
11.2	Ile de Noirmoutier - the physical context	181
11.3	Surface changes between Village de la Tresson and le Midi ~ erosion	183
11.3.1	Site description	183
11.3.2	Image analysis of blowouts between Village de la Tresson and Le Midi	190
11.3.2.1	Image registration	190
11.3.2.2	Change detection	192
11.4	Surface changes between La Frandiere and Pointe de la Fosse ~ Accretion	200
11.4.1	Site description	200
11.4.2	Image analysis of accretion between La Frandiere and La Fosse	202
Chapter 12	CASE STUDY 4 ~ measurement of volume at Holywell Bay	206
12.1	Introduction	206
12.2	Site Description	207
12.3	Ground control	210
12.4	Photogrammetric processing	212
12.4.1	Data input	212
12.4.2	Block and model setup	213
12.4.3	Interior. relative and absolute orientations	213
12.4.4	DEM / DTM extraction	213
12.4.5	Contoured orthophoto	215
12.4.6	Perspective views	217
12.4.7	Orthophotomosaic	220

12.4.8	Quality assurance report	220
12.5	Determination of blowout volume	222
12.5.1	Introduction	226
12.5.2	Photogrammetric processing at a higher resolution	226
12.5.3	Calculating the volume of the blowouts	227
12.5.3.1	<i>Editing the DEM</i>	229
12.5.4	Results of the calculation of the volume of the blowouts	231
12.5.5	Estimation of the error	233
12.6	Summary	234
Chapter 13	SUMMARY	236
13.1	Introduction	236
13.2	The main conclusions	237
13.2.1	Measurement of dune recession at Ile d'Oleron	237
13.2.2	Redistribution of sediment at Dossen	238
13.2.3	Measurement of surface changes at Ile de Noirmoutier	238
13.2.4	Measurement of volume at Holywell Bay	239
13.3	Evaluation of the methodology and the data	240
13.4	Recommendations for future research	242
	REFERENCES	244
	APPENDIX 1	273
	APPENDIX 2	280
	APPENDIX 3	311
	APPENDIX 4	312

LIST OF FIGURES

Chapter 1

Figure 1.1	Some stress related pressures at the coastal zone	10
------------	---	----

Chapter 2

Figure 2.1	Sediment exchange at the nearshore / beach/ dune interface	15
Figure 2.2	The dynamic dune environment	23

Chapter 5

Figure 5.1	Imaging route from sensor to storage device in a digital camera	67
Figure 5.2	Charge coupling, charges are 'clocked' to the shift register across a potential difference	70
Figure 5.3	Cross section of a CCD	70
Figure 5.4	Digital / analogue costings for orthophoto production at 0.5m pixel resolution for 3 survey block sizes	76
Figure 5.5	Digital / analogue costings for orthophoto production at 1m pixel resolution for 4 survey block sizes	76
Figure 5.6	True colour and colour infrared image display	77

Chapter 6

Figure 6.1	Image capture components of the video system and ADPS	83
Figure 6.2	Comparative sensor sizes of a 35mm film camera, the 420 and 460 cameras	86
Figure 6.3	Screen grab of import window showing TIF-EP and image attribute data	87
Figure 6.4	Spectral sensitivity of the sensor (Eastman Kodak Company)	90
Figure 6.5	Colour Filter Array (CFA)	92
Figure 6.6	True colour image production using CFA and infrared cut filter	93
Figure 6.7	False colour infrared image production using CFA and minus blue filter	93
Figure 6.8	Spectral response of the 650BP300 filter	95
Figure 6.9	Spectral response of the vis filter	95
Figure 6.10	Flight line planning using the mission planner and GPS	112

Chapter 7

Figure 7.1	Classification of aerial photographs	114
Figure 7.2	The relationship between focal length, field of view and scale of an object	116
Figure 7.3	The effect of topography on scale	117
Figure 7.4	Relief displacement of an object in a vertical photograph	117
Figure 7.5	The three rotations of a camera: ω (roll); ϕ (pitch); κ (yaw)	118
Figure 7.6	The effects of rotations in ω (roll); ϕ (pitch); κ (yaw) on scale and orientation of a vertical aerial photograph over flat terrain	119
Figure 7.7	Height measurement from a stereo pair of photographs using differential parallax	122
Figure 7.8a	Forward overlap in a single flightline	123
Figure 7.8b	Side overlap in two flight lines	123

Chapter 8

Figure 8.1	Map showing location of the 4 case study sites	127
Figure 8.2	The 4 major elements of the processing chain	128
Figure 8.3	Logistics and mission planning	130
Figure 8.4	Convergent network of 8 images of the test pattern projected onto a near planar wall	132
Figure 8.5	A processing chain for primary data acquisition	134
Figure 8.6	Image index in MapInfo for easy retrieval of image locations	136
Figure 8.7	The image analysis routes for stereo and non-stereo digital photography	137
Figure 8.8	The block setup window showing input and output parameters	139
Figure 8.9	The relative orientation window in Virtuoso	141

Chapter 9

Figure 9.1	Outline map of Ile d'oleron with inset showing La Rochelle to the north and the River Gironde and Bordeaux to the south	145
Figure 9.2	Map of the southern end of Ile d'Oleron showing study area	146
Figure 9.3	Sample point locations along the baseline, Ile d'Oleron	155
Figure 9.4	Position of the dune cliff in 1996, 1997 and 1999, Ile d'Oleron	156
Figure 9.5	Retreat of the dune front 1996 –1997 ($\pm 1.12\text{m}$) and 1996 –1999 ($\pm 1.76\text{m}$)	161

Chapter 10	Map showing the location of the dune site at Dossen to the west of Roscoff on the north coast of Brittany	165
Figure 10.1	The dune site at Dossen showing region of interest	166
Figure 10.2	Part of the dune field with digitised dune fronts for three epochs showing areas of erosion and deposition	170
Figure 10.3	Erosion 1997-1999 & 1996-1997 at Dossen, Foret de Santec, Brittany	171
Figure 10.4 (a)	Accretion 1997-1999 & 1996-1997 at Dossen, Foret de Santec, Brittany	172
Figure 10.4 (b)	The progressive shift of sand lobes along the dune face and displacement of the estuarine channel of the River Horn, Dossen	176
Figure 10.5	Extent of the wind blown deposit on the dune at the southern end of Dossen site, May 1999	178
Figure 10.6		
Chapter 11		
Figure 11.1	Outline map of the Ile de Noirmoutier with inset showing its location south of the River Loire	181
Figure 11.2	Southern section of Ile de Noirmoutier. showing the major settlements and dune sites	182
Figure 11.3	Stages in producing a red-green difference image	193
Figure 11.4	Digitised blowouts as source data for Tables 11.3 and 11.4. and relate to change detection shown in Plates 11.11, 11.12 and 11.13	197
Figure 11.5	Chart showing increase in area of the three blowouts 1996 to 1999	198
Figure 11.6	Relationship between blowout area and perimeter, Village de la Tresson	200
Chapter 12		
Figure 12.1	Map of Holywell Bay, Cornwall	208
Figure 12.2	Cross section of a blowout in the dune with estimated pre-erosion surface	227
Figure 12.3	Workflow for calculation of blowout volumes using DEM of difference	228
Figure 12.4	Orthophoto drape showing selected blowouts	229

LIST OF TABLES

Chapter 5

Table 5.1	Digital / analogue costings for orthophoto production at 0.5m pixel resolution for 3 survey block sizes	75
Table 5.2	Digital / analogue costings for orthophoto production at 1m pixel resolution for 4 survey block sizes	76

Chapter 6

Table 6.1	Framing Rates and File Sizes of the Kodak Digital Science Camera Series	88
Table 6.2	Storage capacity of PCMCIA type III cards	89
Table 6.3	A comparison of the mean image spread function in a CIR and a True Colour digital image captured simultaneously	98
Table 6.4	The ground sampled distance and angular resolving power for each camera, computer and hardcopy image	99
Table 6.5	The flight track component of the ADPS mission and flight track planner	105
Table 6.6	Navigation section of the mission planner	112

Chapter 8

Table 8.1	Camera calibration parameters for the DS 460 CIR camera with a 28mm focal length lens at infinity	132
Table 8.2	Camera series and filter type used for each survey at each site	135

Chapter 9

Table 9.1	Summary statistics for misregistration between the 1996 mosaic and the 1997 and 1999 mosaics for Ile d'Oleron	152
Table 9.2	Minimum sample size required to assess the error in registration	153
Table 9.3	Erosion of the dune cliff at 90 sample points, Ile d'Oleron	157

Chapter 10

Table 10.1	Summary statistics for registration errors between the three epochs, Dossen	169
Table 10.2	Erosion and deposition resulting in changes in the surface area of the dune between 1996 and 1999, Dossen	173

Chapter 11

Table 11.1	Summary statistics for registration errors between the three epochs	192
Table 11.2	Mean digital value for dry bare sand, dune vegetation and windblown deposit on the dune	193
Table 11.3	Area of blowouts south of Village de la Tresson June 1996 to June 1999	198
Table 11.4	Increase in the area of the blowouts 1996–1997, 1997-1999 & 1996-1999 and percentage increase over the same periods	199
Table 11.5	Co-registration of the CIR images of the southern part of Noirmoutier	203

Chapter 12

Table 12.1	The mean standard deviation for differential correction of the GCPs	211
Table 12.2	Absolute orientation residual values for models 1.2 and 3	220
Table 12.3	Extract of DEM (0)	226
Table 12.4	Extract of DEM (0) reformatted in Excel and with UTM northings and eastings	227
Table 12.5	Calculation of the volume of Blowouts 1 and 2 from the DEM of difference	228
Table 12.6	The estimated mass and volume of material eroded from blowouts 1, 2 and 3	229
Table 12.7	The impact of the elevation accuracy on volume calculation	230

LIST OF PLATES

Chapter 1

- Plate 1.1 Landsat TM subscene of Newquay, Cornwall, England and aerial digital photograph at Holywell Bay, Cornwall 5

Chapter 2

- Plate 2.1 True colour digital aerial photograph of the dune system at Northam Burrows, Devon, England 17
- Plate 2.2 Barchan dune form and vegetated dunes 19
- Plate 2.3 Dune cliffing by the sea at Pea Island, Oregon 20
- Plate 2.4 'Stellate' erosional features at minor path nodes in the foredunes at Holywell Bay, Cornwall 22
- Plate 2.5 CIR digital photograph showing serious erosion of the dune front 22

Chapter 3

- Plate 3.1 Dwelling at Hourtin Plage, Aquitaine, France partially engulfed by sand, September, 1998 28

Chapter 4

- Plate 4.1 Industrial development on the dunes at Kenfig, South Wales, May 1997 35
- Plate 4.2 Arable fields on the dunes at Tronoen, Brittany, May 1997 38
- Plate 4.3 Development on the dunes along the Belgian coast, July 1997 39
- Plate 4.4 Property development at the dune – beach interface 40
- Plate 4.5 Washover deposits destroy the forest and result in loss of sand 40
- Plate 4.6 Penhale Sands, Cornwall. Paths from the beach leading into the dunes provide a wind corridor and an easy route for high tides to penetrate the dune. 41
- Plate 4.7 La Fosse, Cotes du Nord, France. CIR aerial photograph showing numerous paths through the dunes spreading out from access points on the road at the back of the dunes. 42
- Plate 4.8 Housing development built on the dune front 45
- Plate 4.9 Stands of Sea Buckthorn (*Hippophae rhamnoides*) at Merthyr Mawr, South Wales 48

Plate 4.10	Planting with marram grass on the foredunes at Holywell Bay, Cornwall	52
Plate 4.11	Dune enhancement using marram grass to stabilise the dunes, Texel, The Netherlands	52
Plate 4.12	Three different methods of fencing to trap sand reflecting differing conditions at the dune site	54
Plate 4.13	Ile d'Oleron, Poitou-Charentes, France. Thatching to prevent deflation on the dune	55
Plate 4.14	Pumping sediment onto the beach to raise beach levels and protect the dune front properties	56 58
Plate 4.15	Materials used for beach access path management in Europe	
 Chapter 6		
Plate 6.1	The ADPS comprising a Kodak DS 460 CIR camera, aircraft mounting plate, intervalometer and PCMCIA type III card	84
Plate 6.2	Digital Science colour infrared image of an open cast mine	91
Plate 6.3	A visual comparison of the detail discernible in a colour infrared (left) and true colour image (right). Red response ($\approx 550 - 700\text{nm}$) centre and green response ($\approx 450 - 600\text{nm}$) bottom	97
Plate 6.4	The ADPS universal mount: from the front (TL) from the back (TR) from above (BL) and from below (BR)	103
Plate 6.5	Series of photographs captured with the DS 420 CIR camera with exposure compensation set between 0 and -3.3	109
Plate 6.6	DS 460 CIR image captured with exposure compensation set at -2.3 and autolevelled to produce an image with a full dynamic range	110
 Chapter 9		
Plate 9.1	Aerial view of the harbour at La Perroche, Ile d'Oleron	147
Plate 9.2	Sand cliffs resulting from rapid erosion of the dune front. Ile d'Oleron, Sept. 1998	149
Plate 9.3	Relative orientation of the photographs of Ile d'Oleron from the 1996 epoch	150
Plate 9.4	Composite image showing misregistration between images	152
Plate 9.5	Lobe-shaped overwash deposit at Ile d'Oleron, Sept. 1998	158

Plate 9.6	Aerial view of overwash deposits at southern end of Ile d'Oleron, May 1999	159
Plate 9.7	Ile d'Oleron, 1997 mosaic in green channel, 1999 mosaic in red channel.	160
 Chapter 10		
Plate 10.1a	DS 460 CIR photograph, May 1997, Dossen	164
Plate 10.1b	DS 460 CIR photograph, May 1999, Dossen	164
Plate 10.2	Enrochement in front of the dune at Dossen	167
Plate 10.3	Clumps of dune building grasses forming embryo dunes at Dossen	168
Plate 10.4	Colour infrared digital photograph showing sand deposit in the estuary of the R. Horn and wind blown sand on the dune at Dossen, May 1999	175
 Chapter 11		
Plate 11.1	Educational notice boards at Les Sables d'Or and La Tresson, Ile de Noirmoutier	183
Plate 11.2	Broken fencing and cliffing at Village de la Tresson, Ile de Noirmoutier, Sept. 1998	184
Plate 11.3	New zig-zag fencing at Village de la Tresson, Ile de Noirmoutier, May 1999	184
Plate 11.4	New zig-zag fencing on dune at Village de la Tresson, looking north-east, Sept. 1999	185
Plate 11.5	Aerial view of part of the dune between Village de la Tresson and le Midi, May 1999	186
Plate 11.6	View of blowouts and blockhouses from the top of the first dune ridge, September 1999	186
Plate 11.7	Blowouts, housing and camp site at Plage du Midi, Ile de Noirmoutier, May 1999	188
Plate 11.8	Campsite, dune and beach at Plage du Midi, Ile de Noirmoutier	189
Plate 11.9	Re colonisation of foredune immediately to south of campsite at Le Midi	189
Plate 11.10	Georectified mosaic of the study area, showing blowouts in the north and accretion in the south	191

Plate 11.11	Bi-temporal image (1996 green, 1997 red) showing active	194
Plate 11.12	blowouts south of the Village de la Tresson , Ile de Noirmoutier, France.	195
Plate 11.13	Bi-temporal image (1997 green, 1999 red) showing active blowouts south of the Village de la Tresson , Ile de Noirmoutier, France	196
Plate 11.14	Bi-temporal image (1996 green, 1999 red) showing active blowouts south of the Village de la Tresson , Ile de Noirmoutier, France	201
Plate 11.15	Large deposits of sand offshore at the southern end of the dunes at La Fosse. Ile de Noirmoutier, May 1997	202
Plate 11.16	Prograding dune at La Fosse. Ile de Noirmoutier, September 1998 Inverted NIR responses of the 1997 image (green channel) and 1999 image (red channel) displayed as a composite image showing vegetation colonisation of the accreting dune coast near La Fosse, Ile de Noirmoutier, France.	204

Chapter 12

Plate 12.1	Uncontrolled mosaic of Holywell bay showing the dunes, golf course and town of Holywell. Cornwall	208
Plate 12.2	Setting up the GPS base station on a prominent outcrop with an open view of the sky	211
Plate 12.3	The location of the GCPs and the base station at Holywell Bay	212
Plate 12.4a	Contoured orthophoto created from Model 1	215
Plate 12.4b	Detail of the dune front (left). and the headland north of the dune system (right)	216
Plate 12.5	Contoured orthophoto created from Model 2	216
Plate 12.6	Contoured orthophoto created from model number 3	217
Plate 12.7a	Draped orthophoto and isometric view of the DEM grid looking east	218
Plate 12.7b	Perspective view of a subset of Model 2 looking north	218
Plate 12.7c	Perspective view of Model 2 looking north west	219
Plate 12.8	CIR contoured orthophoto mosaic with 2m contour interval of the dune front at Holywell Bay	221
Plate 12.9a	Perspective view of the mosaic looking east	222

Plate 12.9b	Perspective view of the mosaic looking north west	223
Plate 12.9c	Perspective view of the mosaic looking south east	224
Plate 12.10	Contoured orthophoto with 2m contour interval of a subset of model 2	227

THE COASTAL ZONE ~ a suitable case for monitoring change

1.1. INTRODUCTION

The final decade of the 20th century has been marked by the extraordinary pace of technological change, commonly referred to as the 'digital revolution'. In Earth Science, Geography and Remote Sensing this change includes the ready availability of desk top computers with hitherto unprecedented computational speed and power, as well as specially developed software such as GIS, softcopy photogrammetry and user friendly remote sensing packages. These developments have created real opportunities for, amongst others, geomorphologists, biologists, ecologists and planners to map distributions and monitor change in the environment. In addition, the digital revolution has placed a range of tools in the hands of these researchers which provide data for advanced techniques in analysis, and these include miniature data loggers, micro-processor circuits, Global Positioning Systems (GPS) receivers and digital cameras.

It is an evaluation of the opportunities presented by the advent of the large array digital camera which forms the subject of this thesis, founded on the need for new techniques of rapid acquisition of environmental data for planning, management and prediction. Recognition of the needs of the environmental community and the opportunities presented by the availability of these cameras resulted in the development of the Aerial Digital Photographic System (ADPS) by GeoTechnologies at Bath Spa University College, thereby providing the means by which aerial digital photographic data could be obtained.

1.2. AIMS AND OBJECTIVES

The aim of this study is the evaluation of small format aerial digital photography as a qualitative and quantitative tool for use in environmental monitoring. In achieving this aim, six objectives must be realised. These are:-

- An understanding of the values and limitations of digital cameras.
- Development of a methodology of data collection using the ADPS.
- A reasoned selection of a test environment in which evaluation of the ADPS can take place.
- Application of the ADPS in the selected environment with subsequent evaluation of its performance in monitoring environmental change.
- An appreciation of the methodologies of image processing using remote sensing software and soft-copy photogrammetry as applied to digital photography within the context of this study.
- Recommendations with regard to future deployment of digital photographic systems in environmental monitoring.

The performance of the small format digital camera and the Aerial Digital Photographic System (ADPS) will therefore be tested in a variety of contexts within coastal sand dune environments. Before any evaluation of its performance can be made, it will be necessary to have an understanding of the characteristics of the environment in which the digital camera will be tested. It is not only to ensure that the opportunities provided by this tool will be correctly identified and grasped. To this end, this chapter will give a brief account of some of the major issues, problems and monitoring needs in the coastal zone in general, and this will, in chapters 2 to 4, lead into a more in-depth account of their relevance to coastal sand dunes in particular.

The use of large array, small format digital cameras in environmental monitoring is a developing field, and, as indicated in the aims and objectives, the characteristics of the camera and system must also be fully explored before the evaluation can take place. Chapter 5 will give an overview of digital photography and digital cameras in general, followed by a more detailed account of the particular digital cameras used in this investigation and the techniques employed to elicit data from the imagery (chapters 6 to 8). The study will culminate in several applications of the ADPS in coastal sand dune environments (chapters 9 to 12), each case study designed to rigorously test the usefulness of the approach in general, and small format digital photography in particular.

1.3. CHANGE IN SPACE AND TIME

In the natural sciences, the element of time is an important consideration in choosing the subject matter for short-term research projects centred on change detection using contemporaneous data, *i.e.*, it would be useful for at least some measurable change to have occurred within the time frame of the research. For example, illegally deforested tropical rain forest, encroachment into National Parks, areas subject to flooding and areas subject to landslides are potential candidates, but the changes here are episodic and they may not actually occur within the time frame of the project. In contrast the coastal zone is a highly dynamic entity both spatially and temporally where the interactions of natural processes with socio-economic factors create stresses which gives rise to a continuously changing environment.

1.3.1. The question of time

When shoreline changes (and in particular retreat) occur on a human time-scale, measurement of the rate of change becomes a pressing issue for many reasons. These include scientific investigation into natural processes and sediment budgets *per se*. which may then be applied by engineers to study the effectiveness of shoreline protection structures or the construction of safe set-back lines. Planners and Insurers need to make decisions regarding existing property and land

use and future development and managers need to make management decisions which will not become obsolete in the very short term.

The rate of change at the coastal zone has accelerated markedly over the past 50 years (1.5) and mapping the differences has not always kept pace with the change. Indeed, many of the changes take place around the immediate boundary between the sea and the land, in the subtidal zone, the intertidal zone, the backshore and at the dune, cliff or marsh. These areas are usually not mapped in detail simply because they are changing incessantly. Scientists, engineers and coastal managers are looking for new, cost effective ways of monitoring and mapping the coastal zone that are not constrained by the inertia that often accompanies national mapping campaigns and for data that can fill in the 'missing details' associated with even relatively large scale maps (e.g. 1:2500) that are so often vital for investigations at the very margin between the land and the sea.

1.3.2. **The question of scale**

The dynamism of the coastal zone presents an excellent scenario for monitoring change using remote sensing techniques and Cracknell (1999 p. 485) has cited the coastal zone as:

"the last remaining frontier of opportunity for remote sensing techniques. The key to success, or otherwise, of remote sensing in coastal or estuarine studies lies in the question of scale".

This 'question of scale' is important in terms of the physical dimensions of the area of interest, the magnitude of the changes, the type of information that is required and the scale of the final output, all of which are related to the resolution of the sensor. Therefore, it is of the utmost importance to select data that is acquired at the appropriate scale so that the information desired is obtained with the least data (Atkinson & Curran, 1997). For example, both pictures shown in Plate 1.1 are false colour infrared images, but the type of information that can be derived from them is very different

for each. The image on the right is a small subset of a Landsat TM scene imaged at 30 m ground pixel resolution and the image on the left is part of the same area (indicated with an arrow) photographed with a digital camera with a ground pixel of 50 cm.

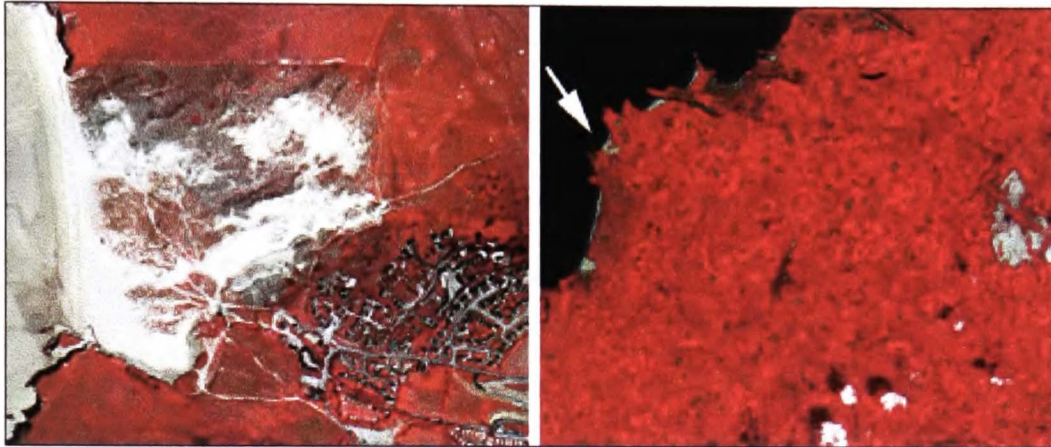


Plate 1.1 Landsat TM subszene of Newquay, Cornwall, England and aerial digital photograph at Holywell Bay, Cornwall

Whilst the Landsat image gives an excellent overview of a relatively large area and shows that it is a coastal area, it is difficult to define with certainty the type of beaches and their sediment characteristics. In contrast, the aerial digital image of a sand dune system shows individual dune ridges, paths through the dunes, a golf course and a small settlement, although it does not provide a contextual view of the area. Where typically small scale changes such as erosion or accretion of say 10 or 20 m of sand dune are to be measured, the use of Landsat imagery would be totally inappropriate and aerial photography would be the obvious choice. If, on the other hand, it were necessary to monitor remotely the land use in a region, then Landsat TM imagery would probably be the more appropriate data to use, as was the case in the 1990s when the National Remote Sensing Centre was charged with checking inventories submitted by farmers in the U.K. regarding the hectareage of crops and set-aside land on individual farms.

Whereas there have been innumerable studies using satellite imagery for small scale mapping and monitoring at the coast where extensive features and general trends are of interest (Brivio & Zilioli, 1996; Ramsey & Laine, 1997; Green *et al.*, 1998; Ciavola *et al.*,1999), there have been few, if any, studies using small format aerial digital photography for large scale mapping, where detailed information regarding changes in the position, size and morphology of coastal features is required.

Of all the coastal landforms, coastal dunes, composed of unconsolidated sediments - easily eroded by wind, waves and trampling, probably offer one of the best opportunities for testing aerial digital photography and its related technologies within a relatively short time scale. For, not only are dunes characterised by near continuous multidimensional changes (length, width, height and position), as opposed to say hard rock environments, they are also subject to significant surface character changes such as alterations in vegetation cover and erosion of new blowouts and paths. In addition, they are easily accessible for field work, and are not subject to tidal constraints as are some coastal environments such as salt marsh and mud flats. Coastal dunes account for only one part of the spectrum of coastal landforms and many of the problems encountered at the dune coast are common to and influenced by issues related to the coastal zone as a whole. It is important therefore to examine issues in the broader context of the coastal zone and in doing so the potential to use aerial digital photography beyond the singular application to sand dune coasts might be considered. One of the most basic questions for coastal scientists lies in the fundamental problem of defining what actually constitutes a coastal zone

1.4. DELINEATION OF THE COASTAL ZONE

Arriving at a definition of the coastal zone that satisfies everybody is problematic for a variety of reasons. In the first place, the boundary between the land and sea is difficult to define because the

coast is a dynamic entity both spatially and temporally. There are areas where strong interactions take place between the land and the sea including beaches, marshes, coral reefs and rivers but it may be difficult to decide where to draw the boundary. For example, in the case of rivers, the boundary might be drawn at the limit of the tidal influence or at a level that includes the entire watershed bearing in mind the delivery of water, pollutants and sediments into the coastal zone.

In addition to political and physical factors there is a cultural dimension that cannot be ignored. In western cultures the limits of the coastal zone are indeed often determined by the geographical extent of the natural processes and human activities that take place, or by administrative boundaries, and so can extend as far inland and seaward as is required by management objectives (McInnes *et al.*, 1998). However, this approach is felt to be inappropriate in other cultures where the delineation along artificial boundaries is intrinsically unacceptable and where the coast has traditionally been viewed as a transitional region between land and sea (Kay & Alder, 1999).

Based on the premise that the coast is an area that shows a connection between land and sea, Ketchum (1972) defined the coastal zone as:

The band of dry land and adjacent ocean space (water and submerged land) in which terrestrial processes and land uses direct oceanic processes and uses, and vice versa.

This definition is very imprecise, and for management purposes it is often necessary to take a more pragmatic approach in order to achieve management objectives within the available resource allocation (Soulsby, 1998). This belief is reiterated by Sorensen (1997), who has remarked that the boundaries of the coastal zone should extend as far inland and as far seaward as is necessary to enable the management issues to be resolved. The World Bank Environment Department (1993) states that:

“For practical purposes, the coastal zone is the special area endowed with special characteristics, of which the boundaries are often determined by the special problems to be tackled”.

In many instances the area of interest lies just either side of the interface between the water and the land and the typical swath width of the Aerial Digital Photographic System at 1 km lends itself to efficient and economical survey.

1.5. THE COASTAL RESOURCE

Coastal areas are increasingly valued by society for a diverse range of uses including living space, tourism, port and harbour development, and waste assimilation (CCIRG, 1996). Natural resources including fisheries, forestry, oil, gas and marine aggregates are all exploited at the coast and, in addition, coastal areas are now seen as areas of worthy of conservation for the protection of biodiversity (Kay & Alder, 1999). The actual value of the coastal resource is difficult to assess since some facets of coastal zone development and uses for industry, commerce and tourism can be characterised in economic terms, whereas the ecological-economic aspects pose a complex problem regarding evaluation in monetary terms. The UK annual turnover by the marine related sector of the economy has been estimated at £51.2 billion (1994-1995 prices) and the total marine related value added has been put at £27.8 billion (OST, 1997). In contrast, estimates of the value of natural resources such as storm buffering and coastal ecosystem biodiversity (such as the estimate of \$1.28 trillion on a global scale, by Costanza *et al.*, (1997)) are very difficult to quantify and are often thought to be fictitious (Turner *et al.*, 1998). Nevertheless, approximate as these values may be, the implied high monetary value of the coastal zone underlines the importance of developing tools for large scale data acquisition.

1.6. NATURAL AND ANTHROPOGENIC IMPACTS ON THE COASTAL ZONE

1.6.1. Population Pressure At The Coastal Zone

Walter Reid (1997), Vice President for Programs at the World Resources Institute has suggested that there will be more people living at the coastal zone in 2020 than were living in the world in 1997. Public pressure on coastal zones around the world has increased dramatically in the last 50 years and there have been numerous estimates of the percentage of the world's population now living at the coast, as well as innumerable forecasts of the potential increase over the next few decades. For example, in the Mediterranean region there are 132 million permanent residents, with a further 97 million national and international tourists each year (Paraskevas & Lekkas 1997). The USA has experienced an estimated 27% increase in the population living at the coast within the past decade, bringing the current total to around 54% and in Australia, some 83% of the population was living near the coast during the 1980's (Carter, 1988). In Latin America over 50% of the coast is believed to be under development pressure with the consequent rapid population growth and urbanisation (IDB, 1997). The Belgian coastal population grew by 225% in the 50 years between 1919 and 1968 (Charlier & Charlier, 1995). Cyprus has experienced a rapid increase in tourism in the past two decades, 90% of which has taken place at the coast (Loizidou & Iacouvo, 1997), and the Egyptian population along the Red Sea and Mediterranean coasts is predicted to rise by between 81% and 125% by 2025 (Khalil, 1997). It has been estimated that 50% of the population of the industrialised world lives within 1 km of the coast and that this population is set to grow by 1.5% p.a. over the next decade (Goldberg, 1994).

These few examples share a common trait indicating an inexorable rise in the actual and predicted population living at the coast. As a consequence of this increased population pressure, coastal zones are under severe stress, a condition which has led Eke (1997) to remark that economic dynamism is often accompanied by loss of natural resources, loss of fertile agricultural land and increase in environmental degradation. The problems are compounded by natural phenomena

such as erosion, loss of sediment, and by indirect anthropogenic pressures such as enhanced global warming and its associated sea level rise. This brief analysis clearly underlines the need for readily accessible monitoring and mapping at the coastal zone and new digital technologies seem to offer the opportunity to achieve this to a wide spectrum of users. Figure 1.1 outlines some of the pressures which cause stress at the coastal zone, ultimately giving rise to change.

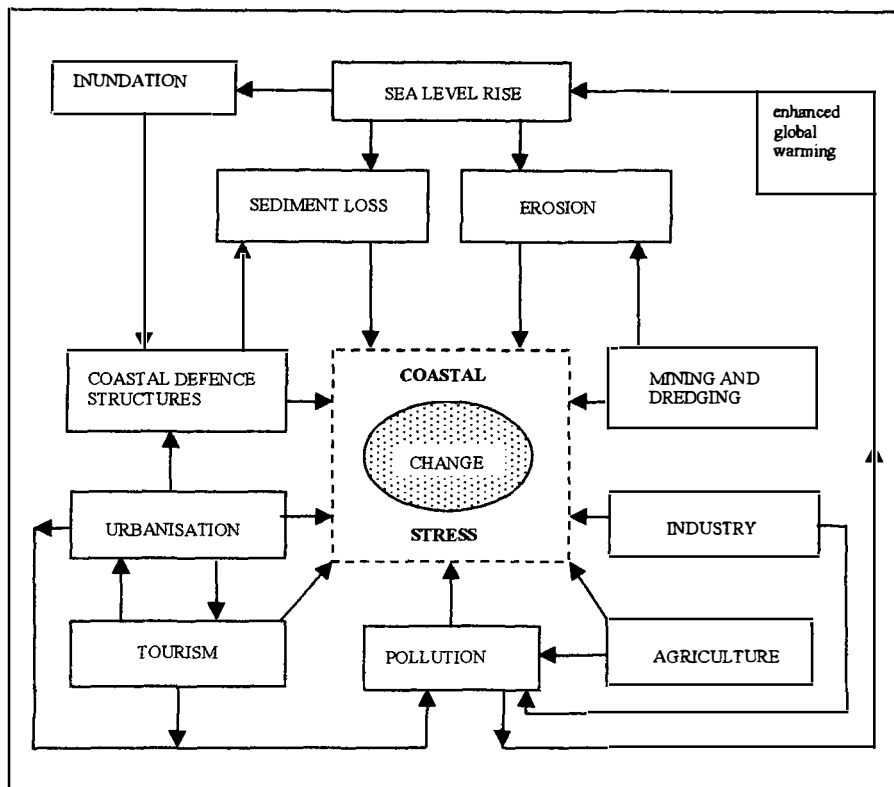


Figure 1.1 Some stress related pressures at the coastal zone

1.6.2. Sea Level Rise

Sea level rise is arguably one of the most important potential impacts of global climate change in terms of environmental and social consequences (IPCC, 1995). In worldwide studies of sea level trends there are difficulties in separating natural changes in sea level from those induced by an increase in ocean volume resulting from anthropogenic global warming (Pirazzoli, 1993) or

indeed from apparent changes due to changes in land level (Harvey *et al.*, 1999). Furthermore, there is no hard evidence of accelerated sea level rise this century (Gornitz & Seeber, 1990; Shennan & Woodworth, 1992; Gornitz, 1995). Although significant uncertainties still remain in estimating the amount of future warming and its impact on sea-level, the IPCC recognised in 1996 that evidence suggested that there was a discernible human influence on the climate (CCIRG, 1996) and a total rise in the order of 230 mm by 2050 and 480 mm by 2100 (4 mm per annum) has been forecast recently (Bray *et al.*, 1997), as compared with 'background' levels of a mean sea level rise of 1.8 ± 0.1 mm per annum over the period of 1880 – 1980 (IPCC, 1995).

A recently published article in 'The Observer' (McKie, 2000), revealed that between 1764 and 1793, Captain William Hutchinson, a dockmaster at Liverpool, measured the high-tide mark twice a day for 30 years, whereas generally in the U.K. measurements of sea levels were not started systematically until well after the industrial revolution had begun. Hutchinson's measurements give a record of sea levels which precedes the build up of anthropogenic greenhouse gases in the atmosphere and adds a valuable new dimension to the records showing that until the 1840's there was relatively little change in sea levels at Liverpool, providing another piece of evidence that there is indeed a human impact on the climate and hence sea-level rise.

Change in mean sea-level is of paramount importance to coastal managers as coastal defence strategies and estimates of risk of flooding are based on magnitude and frequency calculations for storm surges and extremely high tides; return periods are likely to decrease with increasing global warming. Rising sea levels and changing patterns of storm activity have the potential to increase nearshore wave energy with implications for future flooding, patterns of erosion, sediment transport and deposition (*ibid.*)

The impact of sea level rise will depend, in part, on the type of coastal environment. It is thought that coasts protected by artificial defences will not be able to adjust to rising sea levels (Pilkey &

Wright, 1988); gravel beaches will be highly vulnerable (Brunsdon 1992; Orford *et al.*, 1995) and wetlands, occupying a limited vertical range, will be the most vulnerable (Pethick, 1992, 1993). Sandy beaches, although susceptible to increased erosion as sea level rises, will be able to adjust effectively providing that there are backshore sediment stores e.g. dunes, and that the backshore is allowed to retreat (Brunn, 1988). In many countries, these backshore sediment stores are not mapped in sufficient detail, for reliable management decisions to be made. Traditional methods involving ground based profiling are very time consuming and expensive in man-power. The development of a cost effective, rapid method for calculating the extent and volumes of these sediment stores using aerial digital photography and digital photogrammetry would provide a useful tool for dune managers to monitor the progress of change.

1.7. COASTAL MANAGEMENT

Given the fact that the population at the coast is large and increasing, coastal managers must find new ways to manage the coast that allow harmonisation of human interests with the natural processes of dynamic evolution that has always characterised the coast (Tooley & Shennon, 1987). Integrated coastal management (ICM) is an holistic approach to coastal management which takes account of human, physical and biological processes at the coast and which promotes integrated planning to enhance management of this valuable resource (McInnes *et al.*, 1998). Although ICM has been practiced in some parts of the developed world, e.g. United States of America and Australia for around thirty years, it is only of late that the concept has gained sufficient momentum to be practiced, to a greater or lesser extent, on a global scale. There has been much discussion in recent decades regarding integrated coastal management (ICM) and one of the conclusions drawn from this is that globally, efforts to achieve ICM are piecemeal, lack co-ordination, sufficient funding and often outright sincerity (Charlier & Charlier, 1995). This belief has led prominent figures worldwide to call for renewed action, and, since the beginning of the

1990's, the adoption of nationally integrated management and planning has been promoted by several international organisations. These include; Intergovernmental Panel on Climate Change (IPCC), 1992; Council of the European Communities, 1992; United Nations Conference on Environment and Development, in Rio de Janeiro, 1992; and the Organisation for Economic Cooperation and Development (OECD) 1993. What is clear, is that data related to all facets of the coastal zone will be necessary to enable ICM, and the broad panoply of aerial survey techniques represent a major component in acquiring data to undertake that task.

Such sustainable management strategies must be based on detailed knowledge of all types of coastal systems. With particular reference to sand dune management, Davis (1992) has remarked that much still remains to be achieved before comprehensive and effective management can be implemented which will ensure their sustainability for future generations and although coastal dunes have been studied over a period of many years, numerous aspects of their formation and evolution remain poorly understood. This thesis will concentrate on assessing the value of the ADPS in recording distributions and detecting change in the dune and beach morphology and the vegetation cover. If assessment and measurement of these environmental changes proves to be successful, then its value in monitoring the less subtle changes in infrastructure and buildings in the coastal zone will almost certainly be possible.

COASTAL DUNES ~ physical background**2.1. SAND DUNE DEVELOPMENT**

This chapter is not intended to be an all-inclusive discussion on the physical nature of sand dune systems, rather, it is intended to review the physical dynamics that make dunes susceptible to pressure and adjustment. A knowledge of the physical character of dunes will allow an appreciation of the type of evidence that makes them a suitable testbed for this new technology.

2.1.1. Global distribution

On a global basis sand dunes are most common on dissipative coasts (characterised by flat shoaling slopes and wide surf zones) with strong onshore winds and a plentiful supply of sand sized sediment (Carter, 1988). However, in Europe, they occur in a variety of different coastal settings from exposed Atlantic coasts to more sheltered North Sea coasts and from the Baltic to the Mediterranean. The extent and morphology of dune systems also vary considerably: from the extensive hindshore systems of the Holland coast in The Netherlands and the chains of barrier dune islands of southern Iberia, to small exposed bay dunes often found in predominantly rocky coastlines such as south-west England and Brittany (Doody, 1991, Guilcher & Hallegouet, 1991; Radley, 1992; Arens & Wiersma, 1994).

2.1.2. Sediment sources

Coastal sand dunes are dynamic geomorphologic features that receive, store and release excess beach sand. These exchanges of sediment take place over all time scales from thousands of years to minutes and with spatial dimensions of millimetres to kilometres (Carter, 1991).

The seas surrounding Europe are relatively shallow and provide a vast reservoir of sand, gravels and muds derived for the most part from the last glaciation. Most of the European Holocene dunes have formed within the last 5 000 years, and many are less than 1 000 years old (Klinj, 1990a; Guilcher & Hallegouet, 1991; Haslett *et al.*, 2000). They are mainly composed of glaciogenic sands that were stranded during a minor sea level regression some 5 - 6 000 years B.P., and which have been reworked and incorporated into the coastal system.

Present day sources of sediment include the products of cliff erosion, especially in areas of soft rock geology and from glacial till deposits and fluvial sources, particularly in areas where coarse (sand grade) sediments dominate the bedload. These sediments may then be transported alongshore and then delivered immediately to the beach or they may be transported first to offshore bars where they are stored temporarily, and subsequently transported to the beach by wave action (King, 1973; May, 1985). This exchange of sediment is continuous but particular phases in the cycle are dominant, depending on the prevailing conditions (Figure 2.1).

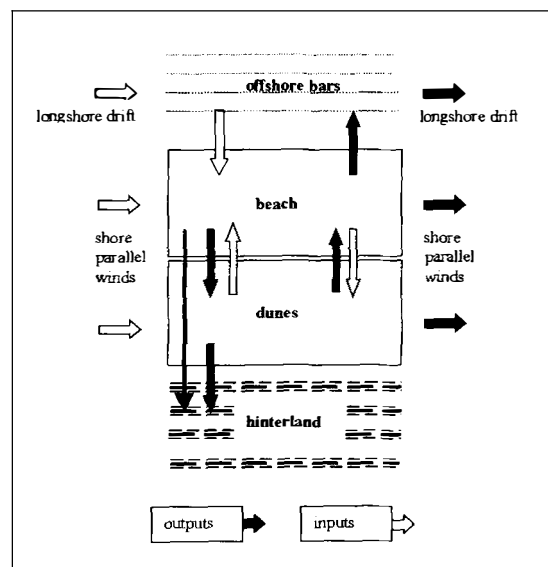


Figure 2.1 Sediment exchange at the nearshore / beach/ dune interface

For example, during summer, the cycle is dominated by a net movement of sediment from offshore bars onto the beach and into the dunes, whereas, during winter storms the cycle is

dominated by marine erosion of the dunes and beach resulting in a net sediment transport from the beach to offshore bars. In addition, there may be increased aeolian erosion where dune sand may be deposited on the beach or in the dune hinterland, depending on wind direction. Some of the sand removed from the dune system during storm surges is incorporated into the foredunes afterwards and this dynamic sediment exchange between dunes and beach ensures the morphological stability and ecological diversity of dune systems (Arens & Weirsmas, 1994).

There are numerous quantitative studies that demonstrate the dynamic nature of coastal dunes, for example, Bennet and Olyphant (1998) found that the backshore width varied from about 40 m in summer to 25 m in winter months. Relative rates of aeolian transport varied by more than two orders of magnitude depending on topography, vegetation cover, sand fetch and the direction of wind approach. De Ruig (1989) calculated an average transport rate of 3 - 3.5 $\text{m}^3\text{m}^{-1}\text{yr}^{-1}$, whereas Carter (1988), quoted 50 000 m^3km^{-1} supply of sand to a beach due to dune face failure and recession in a matter of hours. Arens & Weirsmas (1994) calculated maximum aeolian transport rates of 50 $\text{m}^3\text{m}^{-1}\text{yr}^{-1}$ for a severely eroding coast.

2.1.3. Sediment dynamics

Dunes depend on the transfer of sand, by wind, from drying intertidal areas. Sand is deposited first in the intertidal zone and then on to the nearshore when currents and wave action transport sediment from offshore and alongshore deposits. As the sand dries, particles (usually between 0.05 mm and 3 mm in diameter) are prepared for aeolian transport and once the wind reaches the critical entrainment velocity, particles are carried downwind in the air or by rolling and saltation until they are trapped by vegetation or other physical barriers.

When sand is lost from a beach the level drops and the intertidal zone becomes narrower. One of the symptoms of this condition is a failure of the sediment to dry sufficiently for aeolian transport between tides, characterised by a wet intertidal zone. Wet sand on the beach is a good indicator of an inadequate sand supply for dune building and is a feature which is easily recognised in aerial photographs as can be seen in Plate 2.1.



Plate 2.1 True colour digital aerial photograph of the dune system at Northam Burrows, Devon, England

The dune system at Northam Burrows is under considerable pressure as the dune is not only separated from the beach by a pebble ridge (Popple Ridge), but the beach level has dropped to such an extent that the sand apron remains wet, as evidenced by the darker tone compared with the dry sand exposed on the dune and in the bunkers on the golf course. This condition severely restricts the sand supply to the dune system.

2.1.3.1. Sediment transport models

A comprehensive understanding of beach-dune interactions is fundamental to any judicious management philosophy and the dynamics of aeolian transport are central to this ideal. The beach - dune aeolian system is extraordinarily complex and there have been numerous attempts during the past 60 years to establish a quantitative foundation for aeolian sediment transport rates, to enable both measurement and the development of predictive models, e.g., Bagnold (1936); Horikawa and Shen (1960); Illenberger and Rust (1986); Sherman (1990). The problem has proved arduous because most models are based on theory and laboratory

work and rely on a set of enabling assumptions: these include, steadiness of wind, a planar, horizontal and unobstructed surface, clean, dry and uniform sediments and an absence of vegetation ~ none of which may be reliably satisfied in a natural, dynamic, coastal environment. This has led Sherman *et al.*, (1994, p.477) to remark that 'All of these assumptions are violated, some seriously, in coastal aeolian systems'.

Never-the-less, models have been devised, and in most of these the transport rate depends on only three parameters which are critical to the estimation of threshold shear velocity, these are; shear velocity, sediment grain size and sediment density. For average size particles threshold velocity is reached at about 4 m s^{-1} , but substantial sand movement is only achieved at high wind velocities since the rate of sand flow varies as the cube of the wind velocity, once the threshold has been reached (Bagnold, 1936).

Deposition occurs when obstacles in the wind-run, such as vegetation and tidal debris, disturb the flow, saltation ceases, and small shadow dunes form in the lee of such obstacles (Hesp, 1984). The type of vegetation and the density and height of the stand all contribute to the final form of the incipient dune (Carter, 1988).

2.2. DUNE MORPHOLOGY

The morphology of dunes is constantly changing and reliable maps of dunefields are rare. This situation presents an opportunity to test aerial digital photography and digital photogrammetry as a cost effective means of producing and updating maps from contoured orthophotographs derived from true colour and colour infrared stereo photography. A basic knowledge of the morphology of sand dunes is necessary to enable an understanding of the implications of changes for the dune manager.

2.2.1. Morphology and wind regime

The relationship between dune morphology and wind flow is extremely complex where either one may influence the other. For example, as the dune increases in height, wind velocity over the crest increases, particularly if the crestline is sharp, when acceleration of the wind may be up to twice the freestream velocity. Changes in wind strength and direction cause rapid re-sedimentation often changing the dune surface by the hour, especially on sparsely vegetated sites. Established dune fields can alter the surface wind pattern and in front of high foredunes shore parallel winds are common, irrespective of the prevailing wind direction (Carter, 1988; Klinj, 1990b; Arens, 1992). The presence of vegetation fundamentally alters the shape of a dune, whereas a bare surface will result in a barchan form i.e. a shallow windward slope and a steep leeward slope at around 32° , (the angle of repose for loose clean sand, (Selby, 1993)) a vegetated slope becomes more steep on the windward side and more shallow on the landward side. A barchan dune form is shown on the left of Plate 2.2 and a typical vegetated dune system is shown on the right.



Plate 2.2 Barchan dune form and vegetated dunes

2.2.2. Evolution of the system

The initial growth habit of coastal dunes is in a linear or curvilinear direction, parallel with the strandline but subsequent development depends upon geographic location and on sediment supply giving rise to dune systems that vary in fundamental ways. They may stabilise at a low level, erode and recycle as in a small bay or continue to accumulate as in

open coast sites with a plentiful supply of sediments (Ranwell, 1975). If the coast is prograding, as is the case of many of the dune sites in Aquitaine, a series of ridges are formed with the youngest ridge to seaward, the older ridges becoming stable in a relatively short period. On eroding coasts where sediment supply is limited the seaward ridge undergoes a cycle of erosion and deposition and may move landward, either as a parabolic dune or as a complete ridge. This type of system is inherently unstable and can remain mobile for centuries (Boorman, 1977). Seaward growth of the dune is limited by storm tide height which can undercut the dune to form a near vertical seaward face, an example of dune cliffing can be seen in Plate 2.3. These photographs of Pea Island, near Oregon Inlet were taken during a small storm in March, 1988.



Plate 2.3 Dune cliffing by the sea at Pea Island, Oregon

Source: Pilkey & Thieler (1992).

Where this condition prevails, the windward face may continue to erode and the sand may be re-deposited on the leeward slope. In this way the dune continues to grow in height but undergoes a progressive landward shift. A flat-bottomed dune valley or slack may form between dune ridges when the eroding surface reaches the water table. This type of dune development is common on the western coast of the UK, where the prevailing Atlantic winds are onshore, and is independent of human interference (Boorman, 1977). Dune slacks can also be formed when prograding foredunes leave inter-dune hollows which may be subsequently colonised by a diverse community of physiologically and morphologically adapted species (Carter, 1988).

2.2.3. Blowouts

Blowouts are basin shaped wind hollows within the dunes. They may develop as a result of natural gaps in the dune line which are subsequently eroded by wind action, or they may form where there is a poorly vegetated area on the dune. Once a small hollow forms it may be rapidly extended by deflation and then avalanching along the flanks. Blowout cycles are natural phenomena which provide free sand within the system enabling a state of dynamic equilibrium to develop. In time many blowouts stabilise and revegetate.

Problems arise when anthropogenic pressure either prevents existing natural blowouts from healing or actually causes the formation of numerous blowouts in a system. An early warning sign of potential blowout development due to trampling pressure can be seen where paths through the dunes meet and coalesce forming 'stellate' features. Aerial photography gives an excellent overview of features such as blowouts as can be seen in Plates 2.4 and 2.5.

Plate 2.4 shows the development of numerous stellate features due to path coalescence in the foredunes at Holywell Bay, Cornwall, U.K. This situation should be monitored carefully because although the individual blowouts are relatively small, many in the region of 2 m in diameter, (pers. obs.) they are numerous and the dune vegetation is very fragmented. This degree of erosion could be controlled fairly easily with appropriate management strategies unlike the rather more serious problem identified in Plate 2.5.



Plate 2.4 'Stellate' erosional features at minor path nodes in the foredunes at Holywell Bay, Cornwall

Plate 2.5 is a colour infrared digital photograph showing part of a dune coast which is seriously eroded. A number of large blowouts have coalesced and the first dune ridge has largely disappeared leaving a huge area of bare sand. This state of affairs is potentially very costly as the road running parallel with the coast and developments along the road will need protection from the sea.



Plate 2.5 CIR digital photograph showing serious erosion of the dune front

In contrast, over-management which inhibits blowout formation is also detrimental to the system as this stabilises too much sand preventing the natural evolution of the system (Gares and Nordstrom, 1991).

2.3. DUNE CLASSIFICATION

2.3.1. Geomorphologic classification

The chaotic relief of many dune systems has confounded simple description and a rigorous process - response classification of dunes is impossible because of the complex relationship between topography and forcing processes, but geomorphologically relevant classifications have been made on the basis of age (Van Straaten, 1961; Hesp, 1984) structure (Goldsmith, 1978), morphology (King, 1972) and shoreline morphodynamics (Ranwell & Boar, 1986; Rust & Illenberger, 1996). The most universally applied typology is based on an amalgamation of several of these classifications including morphological, positional, age and stability factors (Carter *et al.*, 1990). Such a typology is described by Houston (1992a) who considers a dynamic environment where foredunes develop at the seaward edge of the dunefield leading to mobile dunes, transitional dunes and finally fixed dunes. Figure 2.2 describes the dynamic dune environment put forward by Houston.

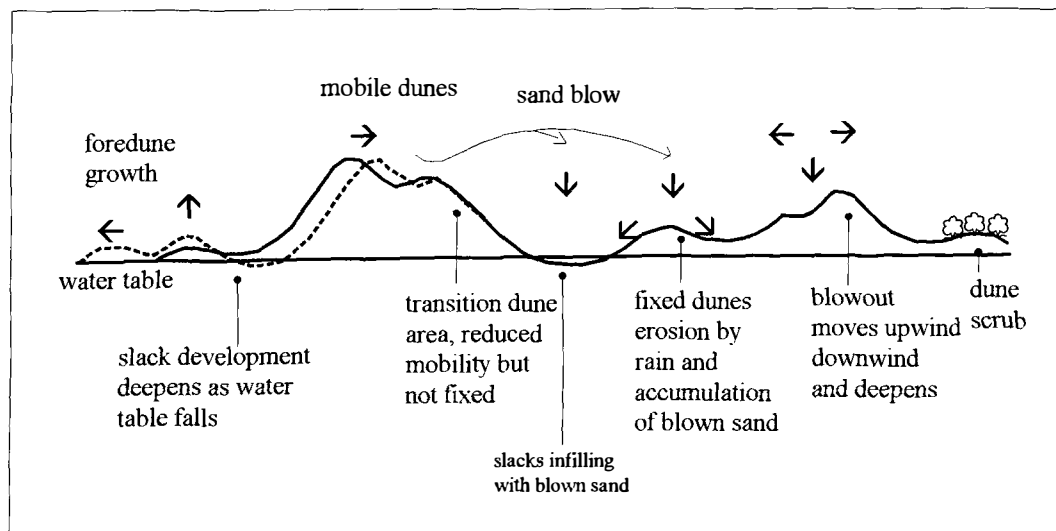


Figure 2.2 The dynamic dune environment

Source: Houston, 1992a

2.3.1.1. *Foredunes*

Foredune growth is a symptom of a positive sand budget and on natural coastlines is in a seaward direction. They develop where incipient (embryo) dunes in the litter zone become colonised by annuals which are rapidly succeeded by perennial dune building grass species, tolerant of high salinity and drought such as *Ammophila arenaria* (marram grass), *Elymus farctus* (sand couch grass) and *Leymus arenarius* (sea lyme grass). These dune building grasses respond positively to sand deposition and can extend the foredune depositional area seaward by 5 - 15 m in a few months (Carter, 1988).

2.3.1.2. *Mobile dunes*

Mobile dunes are generally ridges that have attained their maximum height and then move downwind. They are fed by sand released from foredunes and from blowouts within the dunes and by sand exposed on the beach by coastal erosion. Often mobile dunes have an eroded windward face and a marram covered leeward face. The mobility of the dune is controlled, to a large extent, by the degree of vegetation on the leeward face: movement is steady and predictable if the face is well vegetated and unpredictable if the face is bare.

2.3.1.3. *Transition dunes*

Transition dunes are generally stable with a dominance of marram as the substrate contains little soil. Through the process of succession, a wide variety of plant species become established so that the transition dune eventually becomes more fixed.

2.3.1.4. *Fixed dunes*

Fixed dunes are the final landform and are characterised by a low hummocky morphology with a permanent grassland vegetation cover. In this more inland part of the dune system typical species include *Agrostis stolonifera*, *Festuca rubra*, and *Carex arenaria* in the wetter areas with *Calluna* heath developing in dry areas.

2.4. SUMMARY

In their paper entitled “Engineering geomorphology on the coast: lessons from west Dorset, Brunsdon and Moore (1999, p. 392) remarked that:

“the first general consideration in the development of an applied geomorphological investigation (assuming that the problem has been identified, the objectives are known, and the brief has been written!) is to determine the nature of the resource which is to be managed and to understand public attitudes toward it.”

This chapter has looked briefly at some of the physical characteristics of sand dunes. It has clearly demonstrated the impermanent nature of dunes and their susceptibility to often rapid and frequent physical change, thus confirming the rationale for selecting coastal dunes as a test bed for the evaluation of the ADPS. Chapter 3 will consider the relationship between humankind and the dune landscape.

COASTAL DUNES ~ pressures and perspectives

3.1. PERCEPTIONS AND MIS-CONCEPTIONS

3.1.1. Dune Vulnerability

In 1864, George P. Marsh first wrote about the impact of humankind on sand dunes and contemplated "in what degree the naked condition of most dunes is to be ascribed to the improvidence and indiscretion of man" (Marsh, 1864, p. 410). Considerable debate as to the vulnerability and fragility of dune systems prevails to this day, and whilst some authorities e.g. Nordstrom and Lotstein (1989) believe that the dynamic nature of dune systems enables them to readjust to stress, most workers accept that there is a threshold beyond which degradation and destruction is inevitable (Alveirinho-Dias *et al.*, 1994).

In a study of dune systems in the Eastern Cape Province South Africa, Rust and Illenberger (1996, p. 166) have suggested that

"certain coastal dune systems are extremely fragile and sensitive to even low-level impacts, whereas other dune components are physically robust, resilient and capable of rapid restoration, even under conditions of comparatively heavy impact".

This perspective seems to encapsulate the views expressed by other workers in the field and brings together even those viewpoints that at first seem to be diametrically opposed to each other. In the light of this more comprehensive approach, judicious management strategies for coastal dune systems should encompass a broad spectrum of procedures to cater for the many differences in sensitivity. Efforts have been made to address this, for example Davies *et al.*, (1995) and Simeoni *et al.*, (1999) have devised multi-parameter checklists which seek to investigate the pressures on the dunes and the management strategies in place in order to evaluate the status of the system before implementing new management measures. One of the problems associated with this

approach is that such checklists are time consuming to use and depend on the survey of discrete areas of the dune system. In contrast aerial survey using digital cameras could give a synoptic view of an entire dune system or even entire coastline in a matter of hours.

3.1.2. Societal Perceptions

One fundamental problem that must be addressed with respect to the sustainable use of dune coasts is that of past societal perceptions and misconceptions, a phenomenon which exerts a powerful influence over the condition of this coastal landform. The fear of engulfment of hinterland developments by shifting sands and inundation by seawater in active coastal dunefields appears to have been universal, and such fears have prompted extensive programmes of dune stabilisation and reclamation all around the world; for example, Goudie, (2000) claims that the Japanese first began to stabilise coastal dunes using vegetation in the seventeenth century; McLachlan *et al.*, (1994) have reported such programmes in the Eastern Cape Province, South Africa; Houston, (1992b) has cited examples from Denmark; Mourik *et al.*, (1995) have described stabilisation with *Leymus arenarius* in The Netherlands whilst Favennec (1996) has described planting regimes in the Aquitaine using a number of *Pinus* species. In the USA Seabloom and Wiedemann (1994) have reported the use of *Ammophila arenaria* (a non-native American dune grass) for planting schemes throughout the west coast of North America since the early 1900's and Mauriello (1989) has described the continued use of planting and fencing techniques to stabilise dunes fronting coastal properties in the barrier islands of New Jersey in the 1980's.

Drawings and paintings and old photographs showing churches, houses and whole communities partially buried by sand are fairly common in the literature but the lessons of the past have not always been heeded and Plate 3.1 shows a modern day example of engulfment, on the Aquitaine coast of France at Hourtin Plage, where a relatively new development is under threat of burial by sand. The house is quite clearly occupied as evidenced by the open shutters and laundry on the washing line.



Plate 3.1 Dwelling at Hourtin Plage, Aquitaine, France partially engulfed by sand, September, 1998

Prevailing attitudes towards the management of coastal dunes are shaped by past experiences and these are different everywhere. For example, in the Netherlands, around 55% of the country is below sea level (Klein *et al.*, 1998) and because much of the Dutch coast is flanked by dunes (de Ruig, 1995) dune coasts are of major importance. They are a means of natural coastal defence, since they act as a buffer to extreme wind and waves, sheltering landward communities, but they also pose a direct threat to hinterland settlements from sand engulfment. They have been an important means of producing a biologically clean, potable water supply since Mediaeval times (Louisse & Van der Meulen, 1991), and in recent years this has become one of the major functions of the Dutch dune coasts, providing one third of Holland's drinking water (Houston, 1992b). For these reasons dune management has always been given high priority, although it is only in recent years that any serious consideration has been given to the ecological value of dune coasts (Janssen, 1995).

In contrast, the UK coastal dunes have hitherto been regarded as mere wastelands fit only for development into some more profitable use (Houston, 1992a) such as golf courses, military training grounds and grazing. It is only fairly recently that sand dunes have come to be seen as a cost effective, natural and sustainable means of coastal defence (English Nature, 1992) which merit conservation for their ecological and geomorphological value.

3.2. HISTORIC AND MODERN PERSPECTIVES

3.2.1. Historic Perspectives

Dune sites have been used by mankind for hundreds and even thousands of years (Higgins, 1939) and the extent of the human impact on coastal sand dunes has been so great throughout history that there are very few dunes that are “natural” in the strictest sense of the word. Farming, mineral extraction, recreation and military training have created such an impact on dune systems that in some instances they have undergone complete structural and ecological modification, moreover, many European coasts are lined with artificial dunes, some 300-400 years old (Carter, 1988).

Farmers have used dunes for centuries for low intensity agriculture that could be readily abandoned or adjusted to mirror the natural dynamic character of the dune system, and they could maintain a relatively high standard of living providing they did not attempt to exceed the carrying capacity of the land. This they achieved by careful cultivation and fertilization of the dune soils, thus avoiding nutrient stripping, ensuring that the land was not overgrazed and by cutting only as much fuel wood and fodder as the ecosystem could sustain. In this way a delicate balance was struck between the needs of the people and the inherent potential of the land (Houston, 1992a).

Many coastal communities lived in this way, but from the sixteenth to the early nineteenth centuries, huge areas of the European coast were devastated by blowing sand, due to the destruction of dune systems. The problem was caused by a shift in climatic conditions in Europe which was known to have given rise to temperatures one or two degrees lower than today's

temperatures and to exceptionally stormy conditions (Hauerbach, 1992). This decrease in temperature was sufficient to cause a general lowering of sea-level through an increase in the extent of polar sea ice with a consequent marked increase in the expanse of the foreshore around Europe's coasts and hence an increase in the volume of sand available for aeolian transport.

The environmental and social catastrophe that ensued gave rise to the first recorded attempts at dune management. Higgins (1939), discovered historical evidence indicating dune management practice at the mouth of the River Ogmere at Merthyr Mawr between 1514 and 1573 and Carter (1988), reported that remedial planting and regrading of slopes had been practised even in Mediaeval times. Mediaeval Dutch dune managers used a simple sand trapping barrier made from reeds, poplar or willow, known as a 'Dutch Fence', to create sand dykes at the top of the beach which enclosed the low lying polders behind; these were then kept drained using windmill powered pumps. In Jutland, western Denmark, the problem of drifting sand was particularly severe, so that even 9 km inland whole communities were enveloped by huge 'wandering dunes'. In 1539, Christian III of Denmark issued an ordinance aimed at protection of dune vegetation. Much later, in 1792 the Sand Drift Act was drawn up which ordered the conscription of labourers from communities within 24 km of the coast. over a 60 year period, to try to stem the tide of drifting sand. The problem was finally addressed by thatching the dune surface with cut heather to prevent aeolian sand loss and planting with marram grass (Jensen, 1994). Such management practice was totally pragmatic in nature, reflecting the urgent need to control sand drifting onto adjacent lands and to maintain a sea defence, unlike the most modern approach which also involves preserving the dune-scape *per se*.

3.2.2. Modern Perspectives

Much of the past legislation concerning dunes has been centred on the need to protect the land behind the dunes, but this has led to many systems becoming over stabilised with a loss of geomorphic and ecological diversity. Over the last few decades there has been a shift in policy to one which relies on the use of the naturally functioning beach and dune system as a means of

coastal protection (Nordstrom and Psuty, 1980), and even those nations who have suffered badly in the past are adopting an approach which places more emphasis on protection of the ecological environment. Examples of this new philosophy can be found around the world, for example, although the main priority of the Danish dune management legislation concerns the prevention of sand drift, the 1992 Nature Protection Act explicitly states that consideration should be taken of nature and landscape (Jensen, 1994). In the case of The Netherlands, Tekke, (1995) has pointed to recent concerns held throughout Dutch society for nature conservation.

In the late 1970's the US government designated 'barrier-island' systems as worthy of protection, and dune preservation districts were established where natural dunes, designed to provide protection for shorefront structures and to serve as wildlife habitat, were created (Nordstrom and Psuty, 1980). This action prompted much research in the barrier islands, and in the early 1990's, contrary to popular belief, Gares and Nordstrom (1991) demonstrated that the development of blowouts in the dune system of the Island Beach State Park, New Jersey was desirable because these facilitated sediment transport into the dune system, reinvigorating existing plant species and increasing species diversity.

On the island of Romo, Denmark, work is currently underway to remove sand traps and managed paths in favour of a non-intervention style of management to preserve the 'wilderness' element of the dune landscape (pers. com., Reimers, 1998).

In the Alexandria dunefield in Algoa Bay, South Africa, dunes have been artificially stabilised through planting schemes with the resultant net loss of breeding habitats for indigenous birds. Watson *et al.*, (1997) have proposed new management strategies that will return the dunes to their natural state to provide breeding sites; these strategies include a moratorium on planting, fencing breeding sites to protect them from off-road vehicles and public education.

The Netherlands has a long tradition of coastal management using stringent dune management and hard engineering structures but this has resulted in a coastline that has very little natural resilience and is unable to evolve naturally. The current philosophy which has grown out of studies such as the World Wide Fund for Nature's *Growing with the Sea* (Helmer *et al.*, 1996) envisions a dynamic coast with space for natural processes to occur. Through managed retreat the safety of coastal communities could be maintained at a lower financial cost and with additional benefits such as nature conservation. (Klein *et al.*, 1998). This philosophy has been embraced, at least in part, by the Ministry of Transport, Public Works and Water Management which is now investigating ways in which new developments can be designed which could enhance coastal resilience (Rijkswaterstaat, 1998).

3.3. SUMMARY

This chapter has indicated how deep seated, historical perceptions of sand dunes have prevailed to some extent until today and because of this dune managers are faced with a variety of different types of problems, some stemming from over-stabilisation of dunes and others from lack of regard for the natural value of dunes. Management policies are clearly evolving as perceptions change, and there are strong incentives to base the implementation and modification of those policies on a secure knowledge of the current form and use of the dunes. In addition, there is a need to monitor the response of dune systems to the newly evolving management ethos and policy in order to ensure that management decisions are appropriate in the context of the now established value of coastal sand dunes. The following chapter will therefore look at current management issues and at some of the management techniques commonly in use.

COASTAL DUNE MANAGEMENT ~ issues and techniques

4.1. INTRODUCTION TO CURRENT MANAGEMENT ISSUES

Huge areas of dunes have been lost all over Europe during this century due to industrialisation, urbanisation and tourism. All of these causes are destructive to some extent, and in each case the dune can no longer function as a natural dynamic landscape. The impact of human intervention is however, far more complex than simply giving dune systems over to development for some commercial activity and current management issues arise out of a complex set of interrelated conditions, both natural and anthropogenic in origin.

If the Mediaeval period saw massive sand drifting related to lower sea levels, then currently rising sea levels (1.5.2) due to both natural and anthropogenic factors, with its concomitant loss of sediment for dune replenishment, poses different problems for dune management today. The Brunn model (1988) implies that sandy beaches, although susceptible to increased erosion as sea level rises, will be able to adjust effectively, providing that there are backshore sediment stores e.g. dunes, and that the backshore is allowed to retreat. but Bray *et al.*, (1997) have warned that the adjustments may not be instantaneous and that considerable lags are likely with respect to redistribution of sediment so that erosion would be enhanced. It is important for coastal managers to be aware of the implications of sea level rise at the local level as this will be different everywhere (ibid).

4.2. HUMAN IMPACTS ON SAND DUNES

Although many of the management issues of the past have prevailed until the present day, others are distinctly contemporaneous reflecting the anthropogenic impacts of 20th century industrial

developments and modern lifestyles. The range of these anthropogenic forcings is wide and varied and includes: industrialisation, sand extraction, farming, recreation, tourism, urbanisation, military use and coastal protection works within the coastal cell (Carter, 1988; Jensen, 1994; Nordstrom, 1994; Simeoni *et al.*, 1999), and some dune systems such as the Wilderness dune cordons of the Western Cape South Africa, are used as rubbish dumps (Illenberger & Burkinshaw, 1996). The scale of human alterations to dunes

"runs the gamut from unconscious actions taken by individual shorefront residents or visitors to preplanned and massive construction projects that convert entire natural landscapes employing a considerable investment of capital and labour",
(Nordstrom, 1994, p448).

Some of the factors involved in the destruction of dune systems are given below and although they are dealt with under separate headings many are interrelated.

4.2.1. Industrialisation

Industrial development is often responsible for the total loss of dunes and examples can be seen all around the coasts of Europe (Ritchie, 1981; Ranwell & Boar, 1986; Killemaes & Herrier, 1998; Meur & Ruz, 1998). Industrial developments often require erosion control to protect the site from wind blown sand (Ranwell & Boar, 1986; Meur-Ferrec & Ruz, 1998) and this in turn can upset sediment delivery at adjacent coastal sites (McLachlan *et al.*, 1994). In addition, there may be localised risk of damage to dune ecosystems from water/air-borne pollutants (Ranwell & Boar, 1986). Williams and Randerson (1989) reported that as a result of urbanisation and industrialisation in South Wales, the once extensive coastal dunes have been mostly destroyed. Plate 4.1, a true colour digital aerial photograph of the north-east end of Kenfig National Nature Reserve near Port Talbot in South Wales shows a typical industrial development on a dune system. The development includes manufacturing and storage units as well as the associated

infrastructure such as the rail yard and road built to carry material to Port Talbot for the construction of a breakwater in the late 1960's.



Plate 4.1 Industrial development on the dunes at Kenfig, South Wales, May 1997

This represents just one part of the dune coast in Swansea Bay which has been subjected to intensive industrialisation because of its proximity to vast coal reserves and because of the easy establishment of land and sea transport links. Heavy industry such as metal smelting and the Port Talbot steel works soon followed and once the basic infrastructure was in place new industrial estates were spawned. The expansion of industry resulted in a massive population increase in the area and this in turn put further pressure on the remaining dune systems from recreational activities.

4.2.2. Sand extraction

Although less sand extraction from dunes and foreshores occurs nowadays than in the past it remains a significant problem in some areas. Sand is exploited by industry for construction, glass making, and winning heavy metals and by farmers for nourishing calcium poor soils (Mather &

Ritchie, 1977; Heathershaw *et al.*, 1978; Ranwell & Boar, 1986; Gillham, 1987; Guilcher & Hallegouet, 1991; Flinn, 1997; Simeoni *et al.*, 1999). Removal of sand from the shore can prevent dune growth creating a continuously eroding seaward face and removal of sand from the dune itself causes destabilisation and deflation.

4.2.3. Farming

4.2.3.1. Stock grazing

Some of the dune systems in the U.K. have a very long history of grazing management, for example, at Sandscale Haws, Cumbria, grazing has occurred for at least 800 years (Burton, 1998) and in The Netherlands grazing is the oldest continuous type of land use of the dunes (Coops 1953; Boerboom, 1957; van der Vegte *et al.*, 1985). In the 1960's and 1970's grazing dune systems by cattle and sheep came to be seen as detrimental to the dunes (Frame, 1971; Band, 1979; Band, 1981; Doody, 1985; Chapman, 1989; de Bonte *et al.*, 1999) because cattle and sheep create deflation hollows and erode tracks by trampling and crop the turf short, thus reducing the sand trapping capacity of the dune vegetation. Boorman (1977) reported a general movement away from extensive stock farming on dunes in the U.K. The notion has come full circle and currently grazing for conservation using domestic livestock is seen as an effective means of managing over-stabilisation resulting from excessive protection (Burton, 1998, Hoffman *et al.*, 1998) and of increasing species diversity (de Bonte, *et al.*, 1999).

4.2.3.2. Rabbit grazing

Rabbits were a deliberate introduction to dune systems in England and Wales during Norman times and were exploited commercially providing a cheap, available source of meat (Rhind *et al.*, 1998) and many of the dune systems in England and Wales are actually called 'warrens' or 'burrows' as in Newborough Warren, Anglesey and Braunton Burrows, Devon. Wild populations established easily and spread rapidly causing considerable damage to dune systems because burrows and scrapes are readily enlarged by wind erosion and these may coalesce to form craters up to 10m deep (Ranwell & Boar, 1986). Rabbits alter the plant community structure by

preferentially grazing some species, particularly the grasses and sedges that are then outcompeted by low growing herbs. This phenomenon was demonstrated at Newborough Warren, Anglesey, Wales, where in the first three years following the outbreak of myxomatosis, in the 1950's, there was a great increase in the growth of indigenous dune grasses and sedges, and within 10 years there was a significant reduction in the area of bare sand (Rhind *et al.*, 1998). This latter point is seen to be a disadvantage and the reduction in rabbit grazing due to myxomatosis is often quoted as one of the main causes of dune stabilisation in Britain and The Netherlands (Ranwell & Boar, 1986; de Bonte *et al.*, 1999) although in the case of Newborough warren, Rhind *et al.*, (1998) suggest that the reduction in strong winds and a continuous reduction in the quantity of offshore sand in the same time interval would also have resulted in a more stable system. In reality it is probably a combination of many factors working together which brings about significant changes on large dune systems.

4.2.3.3. *Cultivation*

Cultivation is practised in the hinterland of many large dune sites (Ranwell & Boar, 1986). In Belgium the dunes have been used intensively for growing crops such as potatoes, rye and vegetables (Hoffman *et al.*, 1998); in North Western France vegetables and flower bulbs are grown (Guilcher & Hallegouet, 1991), and in The Netherlands a whole range of arable crops and bulbs are grown on the dunes (van der Vegte *et al.*, 1985; van der Meulen & van der Maarel, 1989). Plate 4.2 shows arable fields on the dunes at Tronoen, Brittany.

Cultivation alters the texture and structure of dune soils through tillage and the addition of fertilisers and has a significant impact on dune ecology and landscape. In sensitive sites, such as machair lands in Scotland, cultivation can cause severe erosion (Ranwell & Boar, 1986); in less sensitive areas cultivation of the landward side of the dunes is not thought to cause problems for coastal protection.



Plate 4.2 Arable fields on the dunes at Tronoen, Brittany, May 1997

4.2.4. Tourism And Recreation

4.2.4.1. A contextual overview.

In the more recent past the major cause of impact has changed from low intensity farming to episodic, high intensity recreation and during the past century the impact of recreation has been steadily increasing (1.5.1). Traditional landuse has declined for a variety of reasons such as modern farming methods and the decline of small holdings, decline in the resin trade etc. and by and large this has been replaced by tourism which has paralleled increases in leisure time, expendable income and mobility.

In developed countries, the proximity of large cities to coastal dunes has led to high recreation pressure on the dunes, for example, 35% of Denmark's dunes has been lost due to afforestation and recreation (Doody, 1993), and some 75% is estimated to have been lost from the dunes of Mediterranean region (Gehu, 1985) due to tourism and urbanisation.

At Camber Sands in Sussex, England, Ranwell, (1975 p. 478) quoted "... as many as 17 000 people a day may descend on only 57 hectares of dune", this represents a huge influx of visitors

since Carter (1988) has suggested the overall carrying capacity for dunes to be around 100 people per hectare. However, visitor pressure *per se* is only one facet of the problem and at some dune coasts, hotels and holiday villages have been built on the dunes, in some cases completely obliterating the dunes. A typical scenario is shown in Plate 4.3, a CIR digital aerial photograph taken in July, 1997 along the Belgian coast. This photograph shows a small part of an enormously developed coastline where mere fragments of the dune remain. Sand traps have been placed on the beach to hold the sand in front of the hotels as the natural exchange of sand between the dune and the beach is no longer possible since the sediment store of the dunes has been removed. A considerable number of visitors can be seen on the beach.



Plate 4.3 Development on the dunes along the Belgian coast, July 1997

Plate 4.4 shows another example of property built in the dunes. This photograph shows a holiday home built directly in the dunes in northern Christchurch, Canterbury, New Zealand. To accommodate this building, part of the dune has been removed. This type of construction lowers the profile of the dune and may lead to extensive flooding inland during storms and huge deposits of sand washed over into the land behind the dunes. Where the dune is backed by land of relatively high value, such as the timber in Plate 4.5, the cost in terms of loss of the crop can be

very high and furthermore, large volumes of sand can be lost to the sediment budget in this way.

In addition, properties such as this have a very short life expectancy.

Plate 4.4 Property development at the dune – beach interface (source, Scholle, 1996)

Plates 4.4, 4.5, 4.8, 4.11 and 4.14 have been removed from the digitized thesis for copyright reasons.

Plate 4.5 Washover deposits destroy the forest and result in loss of sand (source: Scholle, 1996)

These types of development are not uncommon in developed countries but one recent, unusual example of destruction of a dune environment related to recreation is that of Maya Bay, Phi Phi

Leh, Thailand, where Twentieth Century Fox's production crew reconstructed the landscape to film 'The Beach', scheduled for release in February 2000. The crew created two large gaps in the cove's sand dune system which the monsoon tides subsequently ripped apart destroying the beach (R.E., 2000).

4.2.4.2. *Trampling*

The impact of visitors on many types of natural landscapes can often be characterised by erosional features (Bayfield, 1979; Liddle, M., 1997; Tallis, 1997, Wainwright, 1999) and sand dunes are no exception. Carter (1988) has remarked that dune degradation is usually paralleled by a developing network of paths and tracks and trampling pressure has been shown by many to compact dune soils, alter species composition and destroy vegetation (Willis, 1963; Burden & Randerson, 1972; Liddle & Greig-Smith, 1975a, 1975b; Hylgaard & Liddle, 1981; Bowles & Maun, 1982; Sothorn *et al.*, 1985; Williams & Randerson, 1989; Louisse & van der Meulen, 1991; Koehler *et al.*, 1996). Trampling diminishes the system's ability to recover from stress through a loss in species diversity and is thought to be the major anthropogenic factor in dune erosion in many sand dune systems (Ranwell & Boar, 1986). This type of damage exposes bare sand to erosional forces and can lead to the development of low elevation passes and fragmentation of the dune front forming wind corridors and allowing inundation by the sea. An example can be seen in Plate 4.6.



Plate 4.6 Penhale Sands, Cornwall, paths from the beach leading into the dunes provide a wind corridor and an easy route for high tides to penetrate the dune

Boorman (1976) found that 10 trampling passes per month reduced turf height by 60% at Winterton, Norfolk, and by more than 75% with 40 passes per month. Boorman & Fuller (1977) estimated that bare ground would result when trampling pressure reached 80 passes per month. Hylgaard & Liddle (1981) found that one person walking to and from the beach across the dune heath at Skallingen, Denmark, created a path 24 cm wide and 15mm deep within 200 passages over a period of 3 months. During this time the vegetation cover was reduced by 50% and there was a 75% reduction in species diversity. These results have clear implications for dune sites that are visited by large numbers of tourists in the holiday season.

Uncontrolled path networks are often fan shaped spreading out from an inland access point, such as a car park, and path density often increases near the sea. This can be seen in Plate 4.7, a colour infrared digital image, showing a badly eroded dune system with numerous paths spreading out from access points on the road at the back of the dunes.

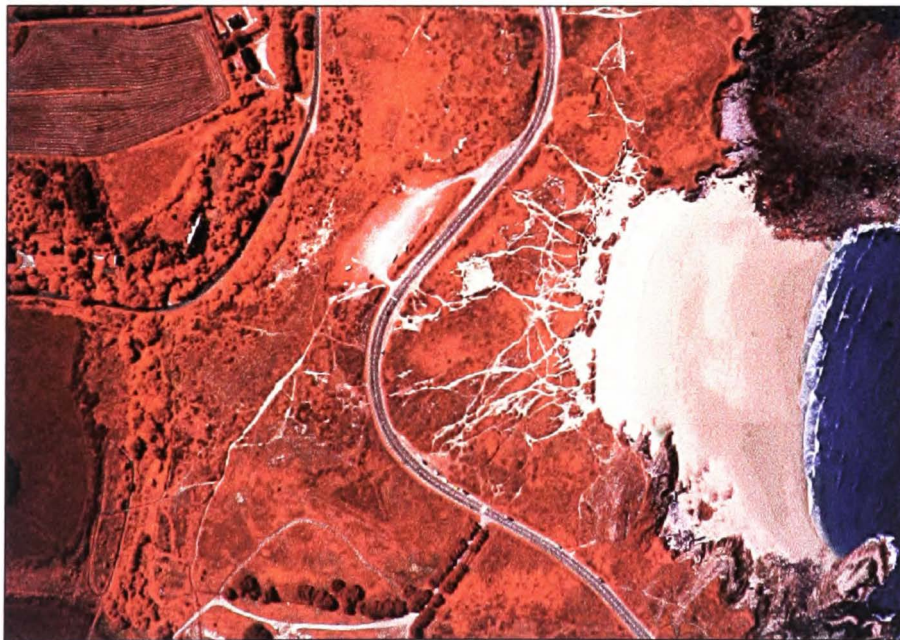


Plate 4.7 CIR aerial photograph showing numerous paths through the dunes spreading out from access points on the road at the back of the dunes

Once paths become devoid of vegetation the bare sand becomes difficult to walk on and new areas are often eroded alongside existing paths. These newly eroded areas may coalesce with the original path causing significant widening, or may remain intact increasing the path network density. In addition, where crossing paths meet, enlarged areas of bare sand occur and these are particularly susceptible to aeolian erosion and can eventually form large blowouts in the dune with a windward deflation area and a downwind deposition area, the latter derived from the former (Bate & Ferguson, 1996). This condition has already been shown in Plates 2.4 and 2.5

4.2.4.3. Off-Road Vehicles And Cycles

Off-road vehicles and cycles have a substantial effect on dune vegetation that can eventually lead to destruction of the dune system (Liddle & Grieg-Smith 1975b; Leatherman & Godfrey, 1979; Ranwell & Boar, 1986; Rust & Illenberger, 1996; Watson *et al.*, 1997) through deflation of exposed sand. Leatherman and Godfrey (1979) reported transportation of some 2000cm³ of sand by one vehicle on an 8° slope, and predicted that over time the dune profile could be lowered by as much as 0.6m annually in areas of uncontrolled vehicular access. The recovery process on the foredune area can take up to 4 years but in the backdune area recovery may take up to 8 years (*ibid*).

4.2.4.4. Horse Riding

In some countries, e.g. England, Wales and France, horse riding is a popular leisure pursuit whose environmental impact can be considerable (Boorman, 1977; Ranwell & Boar, 1986; Williams and Randerson, 1989). Evolution of the horse has ensured that each 'foot' is actually only a single digit and hoofs are modified toenails. This means that the entire weight of the horse (and rider) is concentrated on three, two, or one, very hard small points (depending on the gait) when the horse is moving. On a soft substrate like sand dune the hoofs pierce the sward causing considerable damage. Where there are riding establishments at the dune site, riders usually use the same paths through the dunes so that the paths never have time to recover.

4.2.4.5. *Golf courses*

In Europe there are over 5,200 existing golf courses, covering in excess of 250,000 hectares. Although concentrated in the British Isles there are smaller numbers in Scandinavia, The Netherlands, Belgium, France and Iberia. Golf courses are commonly sited at coastal locations and around one third of the sand dune systems in the UK are used this way (Ranwell, 1975; Stubbs, 1998). There has been a long and on-going debate as to the environmental impact of golf courses on dune environments and it has been claimed that they are both beneficial and detrimental.

Golf courses can contain important fragments of semi-natural vegetation, often with a high biological diversity. In particular, they support valuable patches of coastal vegetation, notably dune slacks and fixed dune communities (A typical 18 hole golf course may occupy 50-60 hectares of open space, much of which receives little direct management or disturbance). Indeed, on some coastal sites, golf courses have provided a last line of defence against encroaching urbanisation, tourist development or intensive agriculture (EGAEU, 1995; 1997). Furthermore, exclusion of the general public protects the natural dune vegetation within the perimeter from trampling damage.

Originally golf courses were virtually unmodified dune landscapes using the natural vegetation and topography but over time they have evolved and changed from their original 'natural' state. The maintenance of the close-mown greens and fairways has been shown to radically alter the species diversity of the site. For example a case study on Jersey, UK, showed that the number of floral species was typically reduced from 30 to 40 species per 25 m², to communities of 5 to 10 species per 25 m², mostly consisting of grasses and common herbs (Ranwell, 1975).

In southern Europe, the number of coastal golf courses has increased dramatically in recent decades with the advent of golf tourism. These new resorts attract the majority of their golfing clientele during the winter, enabling year-round tourism to flourish in these areas and this

prolonged 'tourist season' is having a major detrimental impact on the coastal environment (Stubbs, 1998).

4.2.5. Urbanisation

4.2.5.1. Housing

There are a number of different impacts on dunes that stem from urbanisation depending on the size and type of the development as well as the local conditions. Many areas of coastal dune were developed before the hazards to such developments were understood, and these now pose difficult management problems because of the cost of protection and because of the conflict that management techniques create between groups with different vested interests. Plate 4.8 shows a housing development on the remnant of what was once a continuous dune.



Plate 4.8 Housing development built on the dune front

Source: Scholle, 1996

In many countries legislation now exists which permits maintenance of existing properties but forbids new development (Cartright, 1987; Jensen, 1994; Alveirinho Dias, 1998 pers com.). The

problems for the protection of coastal dune developments could be said to fall into two major categories: First where sediment supply is abundant and large volumes of drifting sand can engulf buildings and infrastructure (Jensen, 1994) or can accumulate to form extensive foredunes which obliterate the ocean-view of ocean front properties (Cartright, 1987). An example of this was shown in Chapter 3 Plate 3.1. Second, where sediment supply is low and erosion of the dunes may become irreversible increasing the danger of inundation of settlements by the sea (Carter, 1980).

Aside from the problems of protection of the property itself, other problems result from the provision of services to the property, for example, sewage pipelines laid through the dunes have been exposed following erosion of the dune resulting in fracture of the pipes (Ranwell & Boar, 1986). Housing developments also bring the risk of the introduction of undesirable exotic species from gardens that may change the ecological integrity of the dune system (Ranwell & Boar, 1986; Garcia Mora *et al.*, 1998).

4.2.5.2. *Drinking water catchments*

The use of dune systems in Holland as water catchments for urban areas has had a significant impact on the dune environment by altering the natural hydrology and the ecological balance of the dune systems so that grass and scrub communities now dominate Dutch dune landscapes (Van der Hagen *et al.*, 1998). This problem can be attributed to excessive water extraction from sub-dune aquifers over the past 100 years that resulted in salinisation of the polderland behind the dunes in the early 1950's. In an attempt to remedy this situation, the aquifers have been artificially recharged by percolating water abstracted and diverted from the river Rhine to the dunes, to be filtered before extraction for public water supply. An unforeseen result of this action was the loss of most of the rare species previously found in the dune slacks because the river water was richer in both pollutants and nutrients (Louisse & van der Meulen, 1991). Currently the Amsterdam Water Supply Dunes at Zandvoort provide 70 million m³ of drinking water each year (Cousin, *et*

al., 1998) and the Amsterdam Municipal Water Supply now has a department dedicated to nature conservation and research (Van der Meulen, 1997).

4.2.6. Exotic Introductions

Exotic introductions can be found on dune sites all around the world. The major problems associated with planting schemes using exotic species arise from the fact that the plant in question is often chosen for its vigour and ability to establish readily, attributes which make it very difficult and costly to eradicate. The deep shade created by mature stands of forest and shrubs may eliminate the natural ground flora changing the balance of the ecosystem and in addition, depletion of the water table due to high transpiration rates of trees and shrubs compounds the damage to the ecosystem (Ovington, 1951; Tinley, 1985; Doody, 1989). Furthermore, the aesthetic value of the site may be impaired.

Sea buckthorn (*Hippophae rhamnoides*) is a native shrub that has been introduced extensively to dune systems in the U.K. in stabilisation programmes. It is very vigorous and as a result of reduced grazing by rabbits following the Myxomatosis epidemic, the shrub has spread out of control on many dune systems (Ranwell, 1975) forming impenetrable thickets as at Merthyr Mawr, SouthWales (see Plate 4.9). Mourik, *et al.*, (1995) have reported a 700% increase in the distribution of this shrub in a part of the dune system at Zandvoort, the Netherlands.



Plate 4.9 Stands of Sea Buckthorn (*Hippophae rhamnoides*) at Merthyr Mawr, South Wales.

In Denmark the pine (*Pinus mugo*) that was planted to stabilise the dunes has spread naturally to adjacent dune areas with the result that the intrinsic value of the dune area is diminished or lost (Jensen, 1994). Bitou bush (*Chrysanthemoides monilifera*) was accidentally introduced to the New South Wales dunes, Australia, from southern Africa. It was used for sand drift control in the late 1940s until its recommendation was withdrawn in 1972 following the discovery of its detrimental effects on indigenous species (Chapman *et al.*, 1987). Paradoxically, Australian Wattle (*Acacia cyclops*) was introduced in the 1970s to stabilise the dunes at Bushman's River, South Africa and was also found to be problematic (Booyesen, 1994).

4.2.7. Military Use

As with golf courses the impact of military activity on sand dunes has been both detrimental and beneficial (Ranwell & Boar, 1986; Guilcher & Hallegouet, 1991). Military activity has caused significant damage to dune systems through a variety of activities including sand mining for construction of concrete anti-tank structures, block houses and access roads; the destruction of the dunescape by military vehicles; and the creation of craters from ship to shore bombardment and

air to ground explosions during training exercises. On the other hand, the exclusion of the general public has protected the dunes from visitor pressure allowing wildlife to flourish in seclusion. In recent years the MOD has been working towards striking a balance between military use, public access and wildlife conservation (Baker, 1998).

4.2.8. Coastal Protection Works

Coastal protection works such as groynes, jetties, sea walls, harbour-building and dune stabilisation can cause serious erosion problems for down-transport areas when sediment supply is interrupted or stopped (Arens & Weirsmas, 1994; Nordstrom, 1994). For example, Mlenberger (1993) reported 140 m recession in 45 years (1940 - 1985) or 3.1 m yr^{-1} on the downdrift side of the harbour breakwater at Port Elizabeth, South Africa. Similar problems have been reported around the world (Kelletat, 1992; Moller, 1992; Correia *et al.*, 1996). The problem of inadequate sediment delivery to some dune coasts is further exacerbated by the construction of dams that act as sediment traps reducing fluvial sediment supply to the coast. On the Adriatic coast of southern Italy Simeoni *et al.* (1999) have estimated that damming the Rivers Fortore and Biferno has caused a retreat of the shoreline between 1957 - 1980 of up to 11 m yr^{-1} . The Aswan High Dam is reputed to have caused a 50% drop in sediment yield and enhanced erosion of the Nile delta at a rate of 30 m yr^{-1} since its construction in 1964 (Kassas, 1971; Sharaf El Din, 1974; Khedr, 1998).

4.2.9. Assessment of change

The morphological changes on the dunes that have been reported in 4.1 and 4.2 are precisely the types of scenarios that offer a subject for testing the aerial digital photographic system as many of the changes are relatively large and may occur in a short time span. For example, the development of new paths and increased erosion of old paths can occur within the space of one holiday season and conversely remedial action can restore damaged areas in the interval between successive holiday seasons (Sothorn *et al.*, 1985). The initial indications are that the ADPS is potentially a useful instrument for monitoring, measuring and mapping such phenomena.

4.3.MANAGEMENT TECHNIQUES

4.3.1. Management ethos

With new found understanding of coastal processes there has been a change in management ethos and practice over recent years from hard engineering using sea walls and groynes to a softer approach using beach nourishment and subsequent management (Turner *et al.*, 1998; O'Brien *et al.*, 1999). Furthermore, since much of the existing coastal protection around the world is in need of constant attention and costly repair, the dynamic coast which can maintain safety at a lower financial cost and with additional benefits such as nature conservation (Klein *et al.*, 1998) is increasingly viewed as a very attractive option.

Although the modern philosophy on dune management embraces this natural approach (3.2.2) there are problems associated with it, and the importance of sustainability is relegated to a lower order of concern as vested interests cause conflict over policy and planning, so that compromise becomes inevitable. For example, in the Zeeland estuaries, in The Netherlands, safety requirements (do and must) dictate most of the management activities because in most places only a single foredune ridge protects the hinterland from the sea (Arens & Weirsmas, 1994). In the case of the UK there is no mechanism to award compensation for erosional loss at the coast, a cause of both anxiety and conflict for property owners. To satisfy the needs of all stakeholders in developed coastal areas dune managers need to adopt a pragmatic approach that allows both natural and socio-economic systems to interact dynamically (Turner *et al.*, 1998). Decision making in management of the coastal zone requires rapid access to spatial and temporal information. Aerial digital photography using the ADPS can potentially provide this because it can be deployed rapidly, can often operate in conditions prohibitive to conventional aerial cameras and the data can be processed in a fraction of the time required for film processing (5.3.6).

4.3.2. Managing the physical environment

To protect high value property and amenities behind the dunes, managers use a range of techniques, some of which were first used in Mediaeval times (3.2.1). Often these techniques rely on methods that mimic natural processes of dune construction, particularly those which aim to build new dunes such as the use of fencing to trap sediment and direct seeding with natural vegetation. In other cases preventing loss and damage is the object and mitigating against the impacts of visitor pressure using techniques such as managed paths and strategically sited car parks.

4.3.2.1. *Planting, fencing and thatching*

Planting with natural vegetation has been used almost ubiquitously both for stabilisation of eroding dunes and to encourage new dune growth and development (Cartright, 1987; Avis, 1989; Van der Putten, 1990; Mendelsshon, *et al.*, 1991; McLachlan *et al.*, 1994; Seabloom & Wiedemann, 1994; Barron & Dalton, 1996). Planting schemes have been most successful on the upper beach where there is often an abundant sediment supply and a low risk of storm damage but limited success has also been achieved in blowouts and inter-dune areas. The planted area may be fertilised and temporarily stabilised using materials such as bitumen mulch, chopped straw, compost, and geotextiles (Van der Putten, 1990; Mendelssohn *et al.*, 1991; Barron & Dalton, 1996).

Plate 4.10 shows a small scale planting of marram grass on the upper beach at Holywell Bay Cornwall to rehabilitate a severely eroded corner of the southern section of the dune front. Plants were protected in small enclosures of nylon mesh and the whole area was fenced. A planting scheme on a much larger scale, again using marram grass, but this time on the Island of Texel, The Netherlands is shown in Plate 4.11.

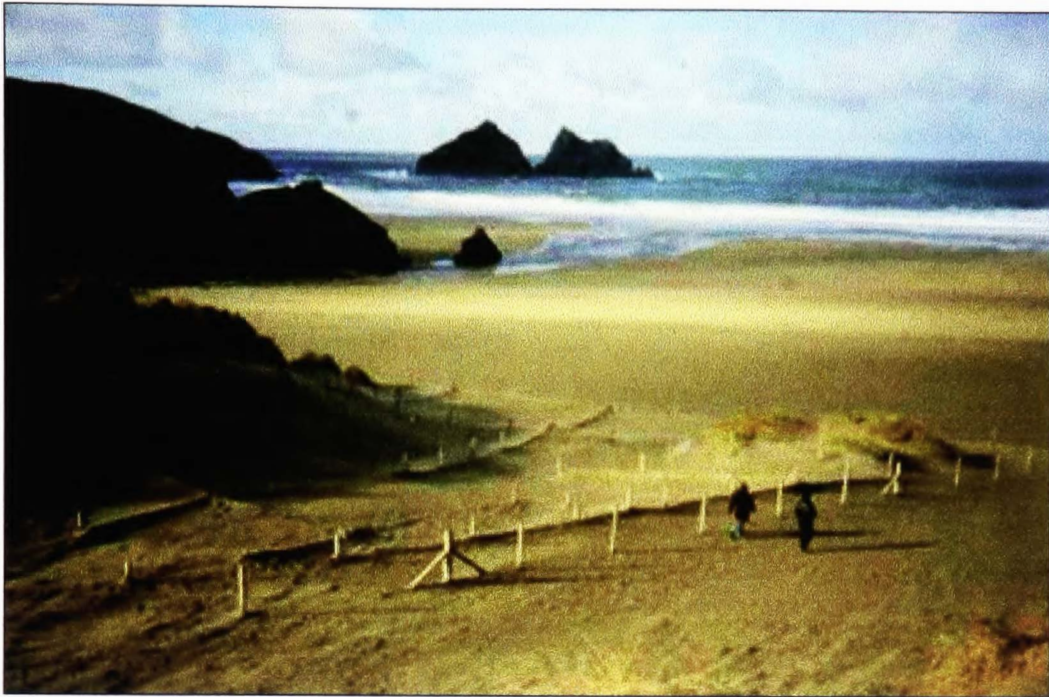


Plate 4.10 Planting with marram grass on the foredunes at Holywell Bay, Cornwall

Plate 4.11, Dune enhancement using marram grass to stabilise the dunes, Texel, The Netherlands

Source: Scholle, 1996

Planting schemes can improve habitat diversity by providing shelter for dune species, but, although there have been numerous successes, planting schemes are not without their fair share of disasters so careful consideration is required before management decisions are made. The choice of species and particular planting regime depends upon a number of factors including: climate, aspect, and the desired outcome, e.g., in areas where public pressure is likely to be high, such as designated dune amenity areas e.g. campsites, pathways, and picnic spots, hardy grass mixtures are planted which require minimal maintenance.

Fencing and thatching have long been used as relatively inexpensive and easily constructed means of trapping sand by disrupting the surface airflow (Van der Putten, 1990; Gares & Nordstrom, 1991, Mendelsshon *et al.*, 1991; Kelletat, 1992). These sand traps are commonly made from straw bales, palings, brushwood, *etc.*, the choice of material reflecting the cost and availability of material in the vicinity of the dune site.

A variety of different strategies are used for fencing depending on the prevailing conditions at the site. Sometimes new fences may be placed upwind or downwind of the original fence to encourage horizontal as well as vertical growth of the dune. Ultimately, the original fence may become buried and the siting of a new fence will depend on the current status of the dune. Plate 4.12 shows 3 different types of fencing, each at a different dune site managed by the Office de Forets Nationale in France. The choice of fence type reflects the particular conditions at the sites: in the top photograph the paling fences have been erected in succession, evidenced by the weathered appearance and degree of burial of some of the panels with new sections erected to increase the height of the dune. This is the primary function of this type of fence but it also controls trampling as it is difficult to cross. The zig-zag fencing constructed in the centre photograph is commonly used to trap sand where the wind direction is variable (Savage, 1962; Willets & Phillips, 1978) and at this site the dune front is severely eroded at the entrance to a popular resort beach. The fenced area is enclosed by a sturdy rustic post-and-wire fence to deter visitors from using the v-shaped enclosures of the windbreak fence as convenient picnic spots.

The third type of fencing shown in the bottom photograph has no visitor control function at all and is simply used to prevent deflation by lowering the wind speed across the beach.



Plate 4.12 Three different methods of fencing to trap sand reflecting differing conditions at the dune site

The short-term results of planting schemes alone do not often achieve the rates of dune growth and development promoted by fencing, but in the longer-term dune growth is usually sustained (Dahl *et al.*, 1975; Mendelsohn *et al.*, 1991). Results vary according to the wind regime, sediment supply, type of planting and type of fencing. Planting with fencing often gives the best results. For example, in a trial site on a sand deficient barrier island, accumulation of only $0.6 \text{ m}^3 \text{ m}^{-1} \text{ yr}^{-1}$ was achieved using planting alone, whereas $4.2 \text{ m}^3 \text{ m}^{-1} \text{ yr}^{-1}$ was achieved with planting and fencing (Mendelsohn *et al.*, 1991). In other combined planting and fencing strategies Dahl *et al.* (1975) reported an average accumulation of $10 \text{ m}^3 \text{ m}^{-1} \text{ shoreline yr}^{-1}$, Knutson (1980) recorded

14 m³m⁻¹yr⁻¹ at Cape Cod and Savage and Woodhouse (1978) measured 16 m³m⁻¹yr⁻¹ at Ocracoke Island, North Carolina.

Thatching the surface is often used where scrub clearance is taking place on a different part of the dune. Plate 4.13 shows the use of brushwood to trap sand on a dune where the vegetation has been destroyed. A close-up of the type of material used is also shown.



Plate 4.13, Thatching to prevent deflation on the dune, Ile d'Oleron, France

In the main photograph the thatching material has begun to decay, and not only is this unsightly but it can also be hazardous to barefoot visitors when it becomes obscured just beneath the surface of the sand.

4.3.2.2. Beach nourishment and dredging

Sand nourishment is an attractive management technique because it is flexible and allows cost-spreading, it does not disturb recreational beaches, it is less expensive than hard engineering structures and it matches the natural character of the coast (Valverde *et al.*, 1999; van Nootwijk &

Peerbolte, 2000). In similar vein, Kelletat (1992) remarked that hard structures such as tetrapods and groynes are expensive, obtrusive features in sandy environments and are sometimes dangerous to bathers. Beach nourishment schemes, however do cause some ecological damage both at the extraction site and at the nourishment site, impacting on benthic communities and this in turn can affect organisms higher up the food chain, so timing of the nourishment to minimise impact is very important (Loffler & Coosen, 1995).

Beach nourishment is common around the world (Newman, 1976; Dixon & Pilkey, 1991; Kelletat, 1992; Moller, 1992; O'Brien *et al.*, 1999). The sand is usually supplied either from dredging offshore and pumping onto the beach (Plate 4.14) or duneface (hydraulic dredging) or by dumping individual truckloads of sand on the upper beach (truck haul) (Creed *et al.*, 2000).

Plate 4.14 Pumping sediment onto the beach to raise beach levels and protect the dune front properties source: Scholle, 1996

In The Netherlands, beach nourishment is necessary to protect valuable dune areas and the high value hinterlands that are densely populated. Each year about 7 million m³ of sand are supplied to

maintain areas of the coastline subject to permanent erosion. Currently the cost of this operation is about 70 million Dutch guilders (van Noortwijk & Peerbolte, 2000). Similar nourishment regimes on the German North sea coast reportedly require 3 million m³ that are pumped from the offshore or the leeward side of the islands to the outer beaches (Kelleat, 1992). Nourishment episodes on the Great Lakes beaches have cost between \$ 6000 - \$ 2 451 000 U.S., depending on the source of the sediments and the volumes involved (O'Brien *et al.*, 1999).

Simeoni *et al.* (1999) have advocated nourishment and sub-aerial reprofiling to assuage erosion and increase sand supply to the dunes in cases of high instability in the foredunes, and only limited nourishment together with remodelling of the beach and dune, in cases of medium - high instability. In cases of low instability management activities which control or stimulate natural processes e.g. planting and fencing are recommended. To protect the village of Fabrica and the clam and oyster beds in the lagoon behind Cacela peninsula, Algarve, Portugal, the inner channel was dredged and some 325 000 m³ of sediment was used for dune replenishment (Matias *et al.*, in press). The new dune was fenced to trap sand and prevent trampling and 2 elevated foot-bridges were built to allow visitors to cross the replenished areas.

4.3.3. Managing the human element

Visitor pressure is responsible for considerable impact on dune systems, but careful planning and design of a system can significantly reduce the damage sustained (Kelleat, 1992). Providing well designed access roads and strategically placed car parks contains vehicle pressure, restricting it to small areas and preventing indiscriminate wear and tear throughout the dunes. In the same way, channelling visitors to the beach along sign-posted and fenced walkways encourages people to use the preferred routes and discourages trespass onto fragile surfaces, especially if the walkway is constructed of an easy to walk on material such as wooden slats or plastic / raffia mesh. Carter (1988) advocates planting the edge of the walkway with spiky vegetation to prevent widening of footpaths and careful contouring to minimise the 'wind tunnel' effect. Similarly, camp sites which

may accommodate hundreds of visitors throughout the holiday season, should be sited and organised so that erosion is contained.

Often people will respond positively to instruction and providing visitors with well-marked boundaries and information at the dune site can prove very satisfactory. In the U.K. there have been many initiatives in recent years aimed at educating the public through interpretation centres and publications, funded by bodies such as English Nature, The National Trust, the European Union, county councils and numerous private sector organisations. General environmental education in schools and through the media has gained ground in the recent past and this should raise awareness among future generations of beach users.



Plate 4.15 Materials used for beach access path management in Europe

Plate 4.15 shows a number of different materials used for path management at various dune sites in Europe, ranging from a channelled walkway without surface protection, a nylon mesh walkway,

a makeshift straw bale and fenced path and a wooden boardwalk to an expensive well constructed bridge and steps.

4.4. MONITORING AND MEASUREMENT

Despite the fact that numerous studies of dune sites have clearly documented the features, processes and stages of dune degradation (Louisse & van der Meulen, 1991; Arens, 1992; Nordstrom, 1994), site specific extents and rates of such environmental changes are often less well known (Curr *et al.*, 2000). In recent decades management of the environment has become a high profile issue and this has prompted governments, local authorities, land-owners and other interested parties to look more closely at the types of management in place. Management intervention to prevent or control dune degradation has often been haphazard, misguided, under funded and sometimes too late and in common with coastal management in general, has often been stimulated by 'crisis response' strategies (Healy, 1995).

The dune manager needs information regarding the condition of the dune system both before and after management intervention so that a baseline can be established against which all subsequent measurements can be evaluated (Van der Hagen *et al.*, 1998). Effective management decisions depend upon the timely availability of quality information which is objectively measured rather than anecdotal and this enables dune managers to identify spatial and temporal variations in the degradation of dune sites, significantly enhancing the strategic decision making process (Ricketts, 1992; Davies *et al.*, 1995). This information is required at scales ranging from the species to the landscape and in broad terms, the dune manager's interest is particularly focussed on the loss and development of vegetation as a means of assessing the current condition of a dune system. Monitoring such dynamic coastal environments in the field is very time consuming and tedious because of the large spatial scales involved so new methods that can provide cost effective data, rapidly and over large areas are required.

Remote sensing techniques are capable of providing such data but it is imperative that it is acquired at the appropriate scale (1.2.2). For instance, the spatial resolution of all but the most recent high resolution satellite data is too coarse for detailed investigation on coastal sand dunes and even Space Imaging's Ikonos data, (1m panchromatic and 4m colour at nadir) cannot equal the resolution of aerial photography 'at the high resolution end' (10cm - 1m), (Walker, 1999) and may not be of sufficiently high resolution for detailed mapping. Aerial photography using film is a well established form of remote sensing but airborne digital photography is a new remote sensing technique using state-of-the-art digital cameras. Although it has not been tested extensively, Fraser (1994), Bobbe & McKean (1995) and King (1995) have demonstrated its potential as an alternative means of imaging for landcover analysis. The trend in using digital is set to continue (Light, 1996; Walker, 1999) and now that the technology is in place, there is a need for further research to prove the concept of this exciting new data gathering facility in new application areas. Monitoring change on sand dune systems is an ideal application area because of the highly dynamic nature of this coastal feature.

AERIAL PHOTOGRAPHY AND VIDEOGRAPHY

5.1. A BRIEF HISTORY OF SMALL FORMAT AERIAL PHOTOGRAPHY

5.1.1. The early years

In 1858 the first aerial photographs of the earth's surface were taken from balloons. The advent of powered aircraft heralded the next stage in the evolutionary process and World War I saw an increase in research into aerial photography using handheld Kodak aerial cameras for reconnaissance (Campbell, 1987). As early as the 1920's oblique aerial photography was used in Canada and the United States for basic mapping purposes; applications included timber resource inventory, forest fire damage and wildlife habitat and infrastructure mapping (Zsilinszky, 1997). Large scale photography (LSP) was already a research concept in the late 1950's and by the mid 1960's vertical aerial LSP was standard for most resource management applications. It soon became apparent that there were severe limitations to its use because large format cameras were (and are) both bulky and expensive. In the early days only black and white film was an option, furthermore, because of the cost, a 10 year revisit time was standard practice (Meyer, 1997), and in this long time interval any maps produced were usually out of date well before the next aerial campaign.

5.1.2. Evolution of small format camera technology

The need to acquire aerial photographs more frequently and at an affordable price spawned the search for a new solution to the problems of air survey. At the same time, rapid developments in 35 mm film and camera technology raised people's awareness and expectations of the products of film (particularly colour film), and a logical progression for the aerial photography fraternity was to investigate the potential of small format cameras, either 70 mm or 35 mm format (Warner *et al.*, 1996). In the first place, 70 mm cameras such as the Hasselblad and Hulcher were more widely

used as there were few 35 mm cameras available with motor drive, but in the 1970's and 1980's the wider availability of 35 mm cameras with motor drives enabled their take-up as a cost effective alternative to large format photography for some applications. There are numerous examples of the use of small format cameras in the literature including crop mapping (Warner, 1994), natural resource management (Zsilinszky *et al.*, 1979; Knapp *et al.*, 1997; Rowe *et al.*, 1999), monitoring land degradation (Marzloff & Ries, 1997) and mapping coastal vegetation (Van der Hagen *et al.*, 1998; Everitt *et al.*, 1999a).

5.2. THE ADVENT OF SOLID STATE

5.2.1. The evolution of video cameras

5.2.1.1. Airborne video

The phenomenon of electronic imaging provided practitioners with another element of choice regarding the type of camera to use for aerial work and the development of solid state technology has enabled rapid progress in the electronic imaging world. Before its advent in the late 1970's, the use of airborne videography was possible but not practical because the equipment was both fragile and very bulky, but, since the development of the earliest solid state sensor in 1981 by Hodgeson *et al.*, (1981) the use of airborne videography and digital photography has increased dramatically. Indeed, low cost solid state video and digital camera technology has progressed at such a rate over the last 10 years that these sensors, available 'off the shelf', are now a realistic alternative to high cost, sophisticated sensors for some applications in commercial mapping and scientific research market places (King, 1995).

Airborne video has found a niche where relatively large scale imaging is required and it is a very cost effective tool for imaging long narrow corridors such as pipelines and coastlines for 'quick-look' monitoring (Meisner, 1986; Edirisinghe *et al.*, 1999; Um & Wright, 1999a). Video is attractive because of the near-real time availability of the imagery and it has been increasingly

used for natural resource assessment over the past 20 years or so (Meisner & Lindstrom, 1985; Nixon *et al.*, 1987, King & Vlcek, 1990; Everitt *et al.*, 1995; Everitt *et al.* 1999a, 1999b). There are however several processes involved in moving from the analogue to digital environment and the size of the unit pixel changes in the course of digitising which impacts on image quality. The resolution of the final image is only as good as the lowest resolution component in the system (Lee & Faig, 1999). For photogrammetric work, interior orientation is difficult because video camera geometry is frequently unstable and furthermore it also depends on the configuration of the frame grabber.

5.2.1.2. *Analogue video*

In a video, the sensor converts light energy into electrical signals and the voltage of the signal is proportional to the brightness of the image (Meisner, 1986). The image is composed of a series of horizontal scan lines, scanned from left to right and top to bottom. The image is transferred from the camera to the tape by an analogue TV signal. The resolution of the transfer is constrained by TV standards for encoding and decoding video signals, e.g., NTSC calls for a video frame to be scanned at one thirtieth of a second, but at this rate flicker is perceptible. To overcome this the frame is split into 2 fields each containing alternate scan lines which are then displayed every sixtieth of a second (60Hz), and the one row misalignment is imperceptible to the human eye. When a video frame is 'frozen' using a frame grabber the odd and even lines are viewed in sequence and misalignment is clear. In addition, the spatial resolution of the recording tape is lower than professional grade cameras (typically 540 lines) at 230 horizontal lines for VHS tape and 400 lines for SVHS tape.

Video imaging systems are not radiometrically calibrated (Everitt & Nixon, 1995) and spectral brightness variations including vignetting, change in viewing geometry, bidirectional reflectance variation and atmospheric scattering pose problems for quantitative work (Pickup *et al.*, 1995a) although there has been much research into radiometric calibration for custom built cameras with

a fair degree of success (King, 1991; Richardson *et al.*, 1993; Louise *et al.*, 1995; Pickup *et al.*, 1995; Edirisinghe *et al.*, 1999).

The sampling frequency and radiometric linearity determine the geometric and radiometric resolutions of the output image, respectively, of the frame grabber. A typical imaging board matrix is 768 (H) x 576 (V), which is well above the spatial resolution of SVHS tape but there are other factors that relate to the digitising process which must be considered. For example, the video signal carries timing information so that the horizontal lines are aligned correctly, and, during the digitisation process the frame grabber generates its own pixel clock which locks onto the video time signal. Pixel jitter occurs when the two timing signals are not synchronised and this causes objects in the image to be displaced (Raynor & Seitz, 1990), however, recent developments in synchronisation performance have begun to address this problem (Um & Wright, 1999b). Further loss of geometric integrity occurs due to image capture from a sensor on board a moving platform, for example, given an aircraft true ground speed of 50 ms^{-1} using a 50 Hz system and a ground sampled distance of 30cm, a displacement of approximately 3 pixels would occur. These deficiencies have been addressed to a certain extent by software designed to shift the odd and even line displacement (Neale *et al.*, 1994).

Until recently, one of the major drawbacks of using video imagery has been the time consuming and tedious procedure of converting the analogue signal to a digital format if digital analysis of the imagery is required, particularly if a large number of frames is involved. There have been several attempts to overcome this problem by designing systems with direct digitisation capabilities in flight (Pearson *et al.* 1994; Everitt *et al.*, 1996; Mao & Kettler, 1996) but these are expensive systems compared with off the shelf digital video cameras (Um & Wright, 1999b). Moreover these systems which use more than one video camera to collect multispectral data require time consuming image co-registration to produce a single composite multispectral image because the different image bands are significantly misaligned through rotation, shift and scale change (Mao & Howard, 1996). In addition, Heitschmidt *et al.*, (1996) found that mosaicing such images

presented problems because the transformations created in mosaicing the first band could not be used for the other two bands because the file sizes and mosaic geometry were different for each of the bands. The difficulties encountered with imaging using analogue video has delayed widespread acceptance of video technology and researchers have looked to other technologies to satisfy the needs of end users (Um & Wright, 1999b). Digital still camera technology is considered to be a great advancement by some resource specialists accustomed to using video (Bobbe, 1997), and the emergence of 'off-the-shelf' digital video cameras has been favoured by others (Um & wright,1999b).

5.2.1.3. Digital video

The advent of the low cost multimedia PC and the availability of CODEC (compressor / decompressor) cards enabling direct input video format to a computer (producing outputs such as MPEG, Indeo and Cinepak) could be exploited for aerial video, although even newer technology now exists which does not require CODEC cards to compress and decompress the data (Doyle, 1999). The latest technology, digital video, has a world-wide unified format decided in consideration of high definition TV (HDTV) signals which has more than 1000 lines. Digital video dispenses with all the losses of image quality due to analogue to digital conversion since the resulting captured video is the original itself (*ibid.*). Picture quality is likely to be more than 25% improved over SVHS because there is no radiometric or spatial resolution loss due to data conversion (Morgan, 1995).

5.2.2. The evolution of digital cameras

5.2.2.1. Early developments

The Sony Mavica, which was launched in 1980, was a precursor of the modern digital camera in as much as it was a CCD camera. It used a 50mm floppy disk to store the data instead of film, but the output was analogue and not digital. This camera was viewed more as a curiosity than a potential commercial camera, and Graham (1998) considers that one of the main reasons for its failure of uptake was that it was too advanced for the status quo of the supporting technologies,

i.e. personal computers and peripherals were of low specification, were expensive and were not universally available, as is the case today.

The first generation digital cameras on the market required permanent connection to a computer for power supply, image acquisition and storage (Peipe & Schneider, 1995). For example, Kodak's DCS 100 camera, although compact, needed to be connected to a large external digital storage unit and this detracted from its uptake (Graham, 1998). Technological evolution has allowed the development of completely independent cameras which carry an internal power supply and storage medium (Peipe & Schneider, 1995), making them far more versatile than was previously possible.

Although, broadly speaking this is true, and the internal power supply and storage are adequate for applications such as photo-journalism, these two elements of the Kodak digital cameras used for this research posed difficulties for air survey operation for all but the smallest survey blocks. This was because of the limited capacity of the battery (1100 mAh) and because of the number of frames that could be stored on one PCMCIA card. To overcome these problems an integral power supply unit and intervalometer was designed to power and control the camera (6.4) and meticulous mission planning via an interactive mission planner (6.6) was designed to manage the storage medium and cost the survey.

Regardless of the make of digital camera they all share the same basic architecture that allows energy to be captured and recorded as an electrical signal, corresponding to the brightness of the scene. This analogue signal is converted to a digital value corresponding to the voltage of the signal and is then stored to a magnetic medium in compressed format. Figure 5.1 is a schematic representation of a digital camera.

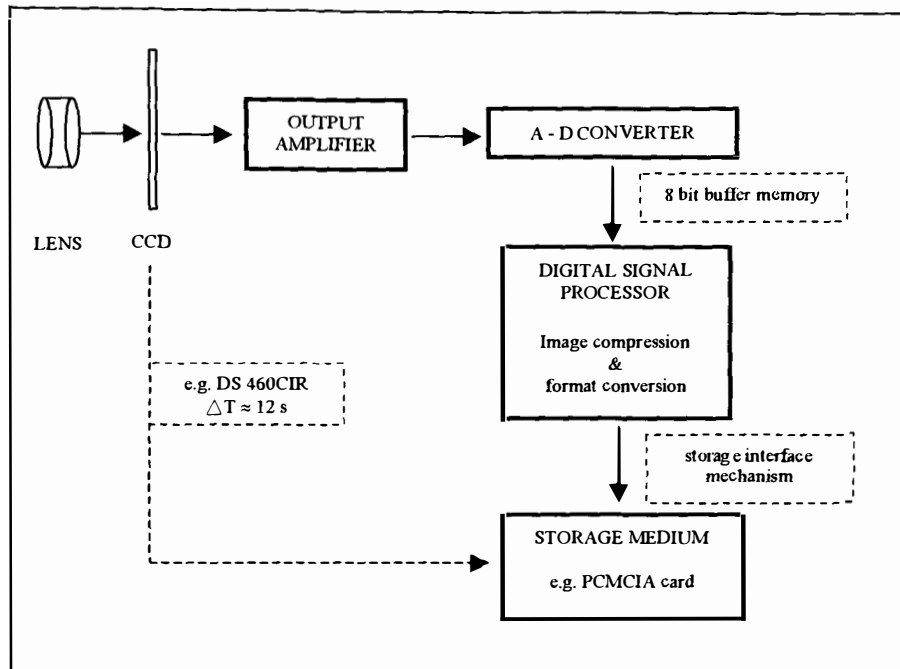


Figure 5.1 Imaging route from sensor to storage device in a digital camera

5.3. THE CHOICE OF SENSORS ~ film or digital

5.3.1. Making the choice

It is now possible to make choices about the type of sensor to use and there are a number of factors including cost and application to be considered before any such choice can be exercised. The new approach using low cost videography and digital photography has been born out of the realization in recent years that cost effectiveness has previously been given low priority and that applications have often been developed only after commitment to an expensive technology. The result is that many organisations are now awash with expensive data for which they have no immediate meaningful use (King, 1995).

The opportunity for decision making regarding the type of imagery to acquire presents itself with regularity since the shelf life of data can be very short, especially where natural or anthropogenic change is continual and/or rapid. However, making the change from tried and tested technology

to very new technology is likely to take some time as it not only requires forward thinking, but also sufficient funds for implementation of contingency plans should the new product not meet expectations. Commenting, almost twenty years ago, on the general reluctance of professionals to embrace new imaging technology Crawley (1981) remarked:

"That announcement of a prototype solid-state imaging camera by Sony should cause nervousness and apprehension is very difficult to understand, especially when one considers that electronic imagery will only broaden the whole scope of photography and its associated industry and trade".

In fact, traditional aerial photography using film is still widely used today in the coastal sciences e.g. coastal resource management and planning (La Cock *et al.*, 1992; Welch *et al.*, 1992; Ferguson *et al.*, 1993; Chauvaud *et al.*, 1998), the study of estuarine sedimentology (McManus & Soulsby, 1994), monitoring morphological change over time (Lyon & Green, 1990; Hellstrom & Lubke, 1993; Jiminez *et al.*, 1997; Gorman, *et al.*, 1998; Leys & Werritty, 1999; Oostwoud Wijdenes *et al.*, 2000), monitoring coastal wetlands (Ramsey & Laine, 1997), monitoring coastal sand dunes (Bate & Ferguson, 1996; Johnson, 1997; Sanderson, *et al.*, 1998; Brown & Arbogast, 1999), but it is a relatively expensive data format which does not lend itself to modern computerised approaches to data handling for resource management and planning. Even though film technology still prevails, other industries including mapping and charting and GIS have now embraced digital technology and so it is imperative for the imaging side to be able to interface with these industries allowing them to take full advantage of the digital revolution. This requirement in itself highlights the need for application led research into the capability of digital cameras.

5.3.2. General film and digital issues

There are fundamental differences in image capture, storage and transmission between photographic and electronic imaging devices. Whereas conventional aerial cameras use film for recording images which must be processed chemically to reveal the acquired image, digital

cameras use a camera body and lens but record the image with charge-coupled devices (CCDs) and the images are stored in digital format usually on computer disks. Film (particularly CIR) suffers from degradation induced by fluctuating temperature and humidity and there are problems of consistency associated with film emulsion batches. A further significant disadvantage is that film is prone to deform during both the survey and subsequent processing, reducing the geometric integrity of any derived maps. In contrast, airborne digital photography neither requires specialist laboratory processing nor suffers from deformation. The images integrate seamlessly with other digital technologies such as Global Positioning Systems (GPS), computer assisted cartography and Geographic Information Systems (GIS) (Greve, 1996). Images can be readily enhanced using image processing software to reveal subtle details which might not otherwise be visible in a print.

5.3.3. Digital image capture

Digital images are captured using charge-coupled devices or CCDs. A CCD is made up of a string of metal oxide semiconductor (MOS) capacitors that collect and transfer photon-generated charge. By connecting up the MOS capacitors in groups of 3 and applying 3 step voltages to them, clocked in sequence (t_1 , t_2 , t_3), each charge signal is moved from well 1 to well 2 to well 3 to the output register (Figure 5.2). In this way the charge is coupled through each line of MOS capacitors in the array.

In the case of area array CCDs these capacitors are closely spaced in a regular grid arrangement. A cross section of this arrangement is shown in Figure 5.3. When radiation strikes each sensor, electrons are released and then stored in the capacitors' potential wells (a potential well is a negatively charged depletion area, created at each Si-SiO₂ interface). The magnitude of the charge (number of electrons released) is proportional to the amount of incident radiation. After the charge is collected in each pixel site, the charge is clocked down each column (kept intact by electronic fields induced by applied clock voltages), and into the serial shift register in a method that is often referred to as a "bucket brigade". When the charge reaches the serial shift register, it is transferred perpendicularly along another shift register to one or multiple amplifiers before it

can be read out of the array. The charge is moved from well to well to an output diode via a semi-transparent polysilicon gate by applying a step voltage (ϕ_1, ϕ_2, ϕ_3) as the surface potential as illustrated in Figure 5.3.

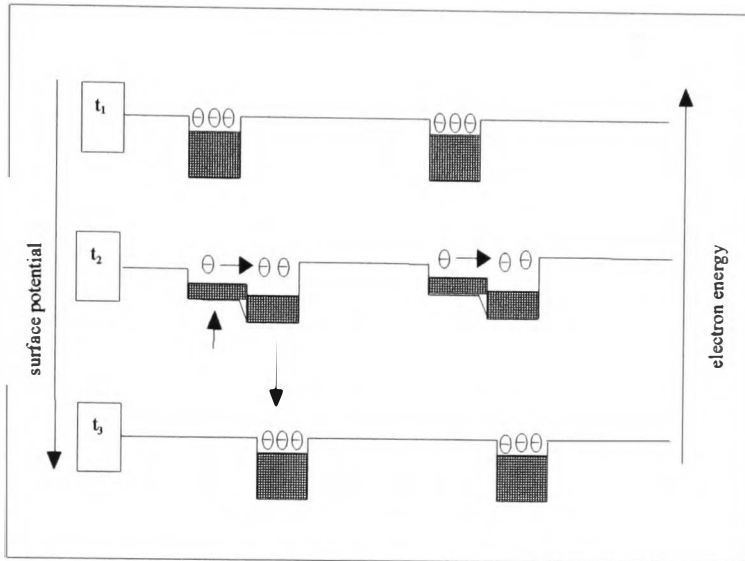


Figure 5.2 Charge coupling, charges are 'clocked' to the shift register across a potential difference (Graham, 1998)

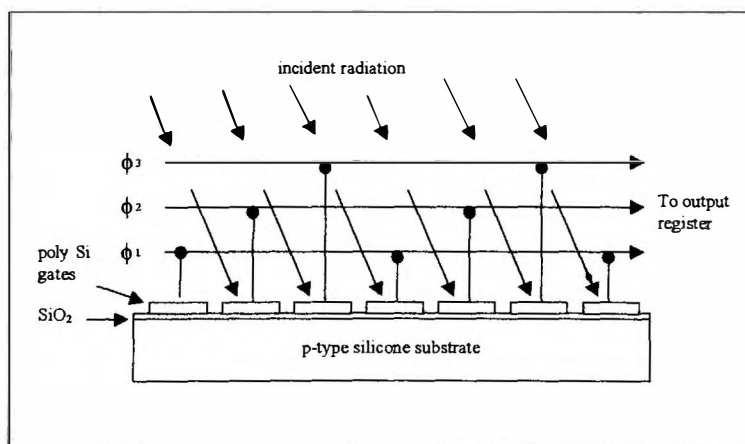


Figure 5.3 Cross section of a CCD (Graham, 1998)

One of the critical parameters of the frame transfer CCD is the speed at which the charge can be transferred to the storage medium and this has implications for aerial survey work because it is a

controlling factor in the collection of stereo photographs (6.6.3). Digital file formats and data storage in the Kodak DS series will be described in 6.3.2.

5.3.4. Image Scale and Resolution

Because hardcopy digital imagery bears a very close resemblance to film photography there is a tendency to use terminology based on traditional methods such as scale, line pairs per millimetre (lp mm^{-1}) and ground resolved distance when describing the resolution of digital imagery (Thompson, 1995; Comer *et al.*, 1998). Problems arise because of the very properties of a digital image. For instance, scale is a fundamental measure of the usefulness and quality of print, and aerial photographs are characterised accordingly. Users will specify a particular scale of photography for an application and be confident that their expectations of the photography will be met. However, a digital image does not have a scale in the same sense, as it can be printed and displayed at many different scales and this has led to confusion in both the film and digital communities.

The level of detail which may be discerned in a photograph depends not only on the scale of image capture, but also upon the film granularity and the degree of contrast within the scene (Graham & Read, 1986). High resolution film currently produces the best resolution attainable of all remote sensing sensors and film resolution is often described in line pairs per millimetre (lp mm^{-1}). This measurement represents the limiting spatial frequency for which a regular line pattern can still be distinguished, and the line pair is the centre of one bar to the centre of the next in the test target. Typical values for black and white aerial photographs are between 30 and 60 lp mm^{-1} , corresponding to distances of between 33 and 16 μm on the photo, (although experience has shown that atmosphere and other attenuating factors in flight always reduce resolution to $< 40 \text{ lp mm}^{-1}$ (Light, 1996). For typical image scale of 1:10 000 these values translates to a ground spatial resolution of between 33 cm and 16 cm.

Ground sampled distance (GSD) provides an indication of the smallest objects that can be detected on the ground and is a more appropriate metric for digital imagery. However, since the conventional expression of resolution of a photograph is its scale, it is inevitable that those familiar with this expression wish to equate it to ground sampled distance. If the spatial frequency of CCD pixels were described in terms of lp mm⁻¹ it might be assumed that 1 line pair could be resolved by 2 pixels but in practice it has been found that 2 pixels often fail to resolve 1 line pair. Several different proposals have been put forward including 2.8 pixels = 1 line pair (Konecny *et al.*, 1982) and 3.3 pixels = 1 line pair (Makarovic & Tempfil, 1979). Graham, (1998, p. 51) recommends a compromise somewhere between the two and that for practical purposes 3 pixels = 1 line pair. In terms of digital imagery captured at 50cm ground pixel resolution, this would equate to a resolution of 1.5m per line pair and this would be equivalent to film based photography at a scale of 1:40 000 (assuming 40 lpmm⁻¹).

Although GSD has come to be the expression of digital image resolution that is favoured by the Remote Sensing community (Thompson, 1994), this must be clearly defined to avoid ambiguity because digital imagery may be resampled to alter the GSD. In effect, the GSD at collection may be very different from that of the final product (Comer *et al.*, 1998). Thompson (1994, p.129) has suggested that the GSD can be determined at any stage in the photographic reproduction cycle by measurement of the image spread function and he has suggested that: “*For a photographic system, the ISF is characterised as the smallest observable pixels that remain visible as separate levels of grey (or Colour) in the image*”. In this paper he describes a method for the determination of GSD and the results of an investigation into the spatial resolution of the Kodak Digital Science 460 CIR camera are given in Chapter 6 section 6.3.6.

5.3.5. Aliasing

In digital imaging aliasing occurs when artefacts are created in an image. This is a fundamental limitation of all solid state image sensors because they have discrete sensor elements. Aliasing is manifested as jagged edges on straight lines or as a ‘rainbow effect’ or chromatic aliasing in

colour imaging and occurs when the intensity minima and maxima in the image do not fully coincide with the sensor elements. This phenomenon obeys the Nyquist sampling theorem which states that: “ *The sampling of any signal that has a spatial frequency close to the sampling frequency of the sensor (or multiples thereof) gives rise to intensity modulations in the displayed image in the form of beats between the two frequencies*”. As the spatial frequency of the sampling system improves to higher values the problem becomes less important. To remove colour aliasing artefacts, an anti-aliasing filter can be installed in the camera to lower the high frequency / high contrast in the image, but this also affects the low frequency data and has an overall smoothing effect on the image, thus decreasing sharpness in the image.

5.3.6. Data security and quality control

A significant advantage of the digital approach lies in security and control of data where CIR film processing is unavailable. In-flight quality control is possible since imagery can be seen in near-real time allowing immediate verification before leaving the project region, eliminating costly reflights and remobilisation (Burger, 1996). Where data obsolescence is problematic during time-critical investigations, e.g. pollution incidents and precision farming applications with typical data lives of 24 to 48 hours, a rapid turn-around time is imperative.

Goodpasture (1996) has reported the routine delivery of images, including hardcopy, highlighting crop anomalies to growers within 48 hrs, at annual cost of around \$10 per acre. Bobbe (1997), of the USDA forest, service was able to map an area of 25,000 acres of burnt forest in less than 1 week using a Kodak Digital Science 420 CIR camera, whereas it would have taken several weeks using conventional film cameras, and, at the same time realizing a saving of \$ 250 000 over traditional methods. In June 1999, the aerial digital photographic system (ADPS) was used to photograph the 250 km² district of San Cayetano, Columbia, to map the area for landslides in 4 days, when the client was unable to locate any other survey team prepared to deliver the product in such a short turn-around time (pers. obs.).

5.3.7. Cost considerations

5.3.7.1. Capital cost

The capital cost of most airborne cameras is in the order of \$500 000 plus, with relatively high operational costs owing to the need for larger, more expensive aircraft (Roberts and Anderson 1999). In addition, the logistical and navigation support for these large-format systems could add an additional \$150000 to the capital investment and facilities for scanning must be provided for. The complete system used for this research, based on the Kodak DS 460 CIR camera, costs less than £ 40 000 (\$ 60 000) with modest operational cost, typically £200 - £300 (~\$450) per hour for aircraft hire as it does not require survey-dedicated aircraft.

5.3.7.2. Developing, printing scanning

Comparing the costs of film and digital survey is a complex matter because the two are inherently different, for example, the cost of chemicals for developing and printing film, and their expensive disposal imposed by environmental regulation, is considerable. This is particularly pertinent to CIR (colour infrared) film since it requires specialist processing, available only at a few professional laboratories in the U.S. The Netherlands and Japan, whereas, there are no such costs incurred with a digital system because the images are stored directly to disk. The cost is also dependent on the required product, for example, if the end product is needed in digital format then film must be scanned.

Scanning is a time consuming (20 minutes per photograph at 7.5 μm (Hohle, 1996)) and costly operation, (\$100 per 23cm x 23cm print, (Light, 1996)), and furthermore, there is often a loss of radiometric detail and geometric integrity in the scanning process (Bakker & Kootwijk, 1993; Burger, 1996). Mills and Newton (1996) have remarked that the increased cost of a digital camera compared with its 35mm film counterpart is easily offset by the cost of a high-resolution flat bed scanner.

5.3.7.3. *Block survey and orthophoto production*

For block air survey operations the area of photocoverage for a given ground pixel resolution dictates the economic feasibility of using one format in preference to the other. The largest commercial off-the-shelf CCD is the Kodak M6 that has sensor dimensions of 27mm by 18mm, so that photocoverage at the CCD is approximately 1/90th that of large format cameras for the same ground pixel resolution. For small areas the digital format is less expensive, for example, Wright (1998) reported the comparative costs of a digital survey and a conventional survey of Exmoor national Park, UK, as £8971 for digital and £18400 for analogue with a further £12,800 to £17,232 for scanning the colour prints at 70µm (≈300 dpi).

For the production of orthorectified photographs, however, a threshold is reached where it becomes uneconomical to use small format cameras. Typical area threshold limits for orthorectified photographs for 0.5m and 1.0m ground pixel resolutions are presented in Tables 5.1 and 5.2 and Figures 5.4 and 5.5 respectively. The summary costings are derived from a survey of current (December 1999) charges in Europe. For corridor survey such as pipelines, roads and coastlines that can be photographed in a single flight line, digital is always cheaper.

The cost of collecting ground control contributes significantly to the overall cost of the production of orthorectified photographs, since at least 6 control points are required for each stereo pair (model). As the photocoverage is so much greater for the analogue survey the number of control points needed is considerably less for the entire block than is needed for the digital survey.

survey block area (km ²)	460 CIR cost (£)	9 X 9 film cost (£)
1 x 1	2814	22385
10 x 10	28802	44308
25 X 25	151872	85031

Table 5.1 Digital / analogue costings for orthophoto production at 0.5m pixel resolution for 3 survey block sizes

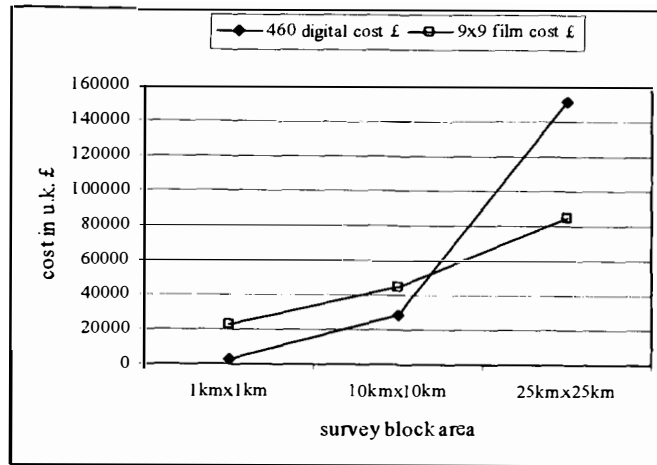


Figure 5.4 Digital / analogue costings for orthophoto production at 0.5m pixel resolution for 3 survey block sizes

survey block area (km ²)	460 CIR cost (£)	9 X 9 film cost (£)
1 x 1	2460	15476
10 x 10	10473	25960
25 X 25	43399	47799
50 x 50	155989	85873

Table 5.2 Digital / analogue costings for orthophoto production at 1m pixel resolution for 4 survey block sizes

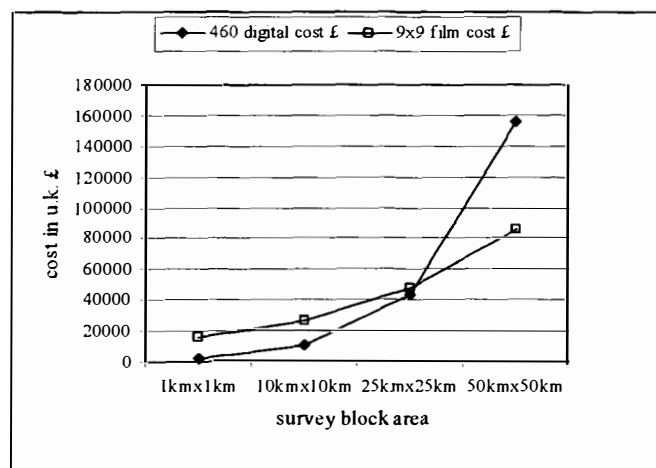


Figure 5.5 Digital / analogue costings for orthophoto production at 1m pixel resolution for 4 survey block sizes

5.4. TRUE COLOUR AND COLOUR INFRARED DIGITAL IMAGING

5.4.1. Digital image display

In true or natural colour digital imagery, blue, green and red wavelengths are sensed and recorded, and then displayed using the blue, green and red guns of a VDU display. In false colour infrared imagery, green, red and near infrared wavelengths are used, but near infrared energy is beyond the spectral response of the human retina.

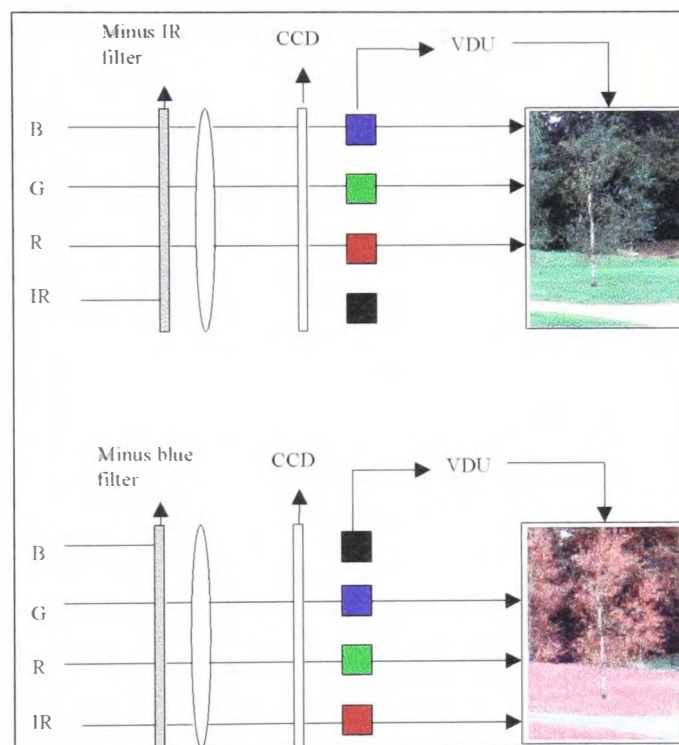


Figure 5.6 True colour and colour infrared image display

To enable human beings to see infrared radiation it is displayed in the red gun of a VDU display and by convention, red radiation is displayed in the green gun and green radiation is displayed in the blue gun. Figure 5.6 represents this schematically. In this way, objects, which have a high reflectance in the near infrared part of the spectrum, such as leafy vegetation, appear bright red, and objects with low near infrared response such as concrete, appear blue. In the Kodak digital science CIR cameras this is achieved through hardware and software.

5.4.2. Producing multiband images

The silicon sensor has a broadband response from 400 – 1100 nm as shown in Figure 6.4. To achieve a 'colour targeted' narrow band response, the wavelengths that reach the sensor must be limited in some way. This could be achieved relatively inexpensively and easily by placing a glass filter with the required characteristics in front of the sensor, either in front of or behind the lens. For example, a short pass filter would allow blue wavelengths to pass but would prevent any longer wavelengths reaching the sensor; a band pass would allow green wavelengths through but would filter shorter and longer wavelengths. This approach exposes the entire sensor array to the filtering mechanism so only allows one 'colour targeted' waveband to be imaged. To produce a three-band image using this technique with a single area-array camera such as the Kodak digital science series, three separate cameras are required. An alternative is to use a three-area array camera with a three-way beam splitter to allow radiation of the correct waveband to strike each array, this technology is common in professional video cameras.

To produce a multiband image using a single photoplane, multiple variations of the narrow band response must be devised. A filter wheel system exists which rotates in front of the sensor so that three successive images must be captured to produce a multiband image. This system presents difficulties for moving targets, or conversely, moving cameras, because of misalignment of the three bands (Lane, 1996). Another technology using the same philosophy as the filter wheel involves a tuneable liquid crystal filter which can cycle through the RGB filters during a single exposure such as the Dicomed Big Shot, but this suffered the same disadvantages as the filter wheel cameras. To overcome the cost implications of multiple cameras and the problems associated with producing colour photography using a single photoplane, Kodak devised a different approach using a colour filter array and this will be discussed in detail in 6.3.4.

5.5. CONTINUING DEVELOPMENTS

Five years ago in a critique of the state-of-the-art of airborne videography and digital camera sensor designs and their associated imaging and mapping methods, King (1995) observed that the digital photography approach often lacked the scientific rigour of method and techniques developed within the remote sensing community during the past 20 years. The vast majority of operational applications used qualitative visual analysis rather than quantitative work using automated computer based techniques, and only a few researchers had developed and applied calibration techniques.

As the use of digital photography for aerial survey gains momentum it is likely that research interest will concentrate more on the quantitative application of this imagery as in the case of the slightly more mature application of video as a remote sensing tool (Anderson *et al.*, 1997), where sensors have been radiometrically calibrated (Jensen *et al.*, 1995; Neale *et al.*, 1995), and geometric distortions due to changes in viewing geometry and interlacing have been addressed (Mitchell *et al.*, 1995; Pickup *et al.*, 1995).

Indeed, in the five years since King's critique, research has included investigations into the use of alternative platforms for air survey (Mills *et al.*, 1996; Koh, 1998a; Koh, 1998b), comparative assessments of film cameras and digital cameras, (Bobbe, 1997; Thompson & Houghton, 1999). There has been a spate of research into the geometric properties of digital cameras and the development of camera calibration models (Warner & Slaattelid, 1997; Clarke *et al.*, 1998; Clarke & Fryer, 1998; Shortis *et al.*, 1998; Walker, 1999). The photogrammetric capabilities of the Kodak Digital Science series has been investigated by Graham and Mills (1997), and in addition, Butler *et al.*, (1998), Robson and Shortis, (1998), Ahmad and Chandler (1999), and Walker (1999) have investigated the geometric and radiometric image quality of several digital camera systems.

Although the concept of using digital cameras for aerial photography is in its infancy, and therefore has not been tested extensively, several workers including Mills *et al.*, (1996); Bobbe & McKean (1995); King *et al.*, (1995); Copley *et al.*, (1997); Knapp *et al.*, (1997); Maas and Kersten (1997), Fraser (1998) are amongst a growing number of workers in the field who believe that low cost, off the shelf, multispectral cameras are suitable for a variety of applications including landcover analysis, satellite data validation, forest health monitoring and orthophoto production. In the past year several European national mapping and remote sensing centres have embraced the digital approach including: Euro-Mediterranean Centre for Insular and Coastal Dynamics (ICOD), Malta; IGN, France (Paparoditis, 1999 *pers com.*) and NRSC, U.K.

In a comprehensive review of digital and film cameras Light (1996), concluded that although there are several difficulties, including aircraft attitude and positioning, which must be addressed before digital cameras can supplant film cameras, once these problems are overcome there is a very real possibility that this new technology may ultimately emerge as the imaging system for the future providing the final link in the transition to an all digital environment.

This chapter has given a general overview of the stages in the development of digital photography and has highlighted some of the differences between analogue and digital photography. Brief mention of the Kodak Digital Science has been made, and, as these cameras have become an integral part of the Aerial Digital Photographic System (ADPS) used for this research, they are described in some detail in the context of the ADPS in Chapter 6.

THE AERIAL DIGITAL PHOTOGRAPHIC SYSTEM [ADPS]

6.1. DEVELOPMENT OF THE SYSTEM

The Aerial Digital Photographic System used for this research was developed at Bath Spa University College to address the increasing demand for rapid delivery, stereo, multispectral imagery with relatively high spatial resolution. The imagery is compatible with images acquired from current earth observation satellites, since the spectral sensitivity spans the entire range of visible light and extends well into the near infrared. The system is easy to use because it can be operated like a film based small format camera and is capable of capturing vertical aerial photographs below cloud cover.

6.1.1. The choice of sensor

Making the choice between video and full frame CCD digital cameras at the outset of this research project was driven by a number of factors, some of which were related to the desire to improve the practicalities of operation of the equipment and others to improvement in quality of the product itself.

In the first place, multispectral video using two 732 (H) x 290 (V) CCD video cameras fitted with red and near infra-red narrow band filters had already been used for coastal sand dune monitoring with limited success (Koh *et al.*, 1996). Digitisation of the data resulted in image frames with 699 (H) x 576 (V) pixels which gave a photo coverage of 350 m x 300 m for a 50cm pixel. Digitisation of image frames in both spectral bands and image co-registration were time consuming and tedious with the hardware and software available at the time. 'Grabbing' exactly corresponding frames in both spectral bands was tricky and any misalignment between the frames caused an effective decrease in photocoverage. The intrinsic quality of the imagery was moderate,

partly because of the effects of interlacing and forward motion (5.2.1.2) and also because there were large spectral variations from scene to scene. The spectral variations were due in large part to the fact that the automatic level control was designed to meter the entire bandwidth of the sensor (400 - 1100nm) and the cameras were fitted with very narrow bandwidth filters. The automatic level control was unable to cope with the reduced energy levels incident on the sensor so that the aperture was opened wide resulting in saturation in brighter parts of the scene. The video system was bulky and awkward to transport and to fit into the aircraft and relied on the aircraft power supply to drive the cameras and video recorders. The nature of the research meant that all types of light aircraft should be potential platforms, consequently most would not be fitted for air survey work. Generally speaking, pilots are wary of external devices drawing power from the aircraft and this factor alone caused difficulties in locating suitable aircraft with a willing pilot.

In the second place, full frame CCD cameras with infrared capabilities (Kodak Digital Science 420) became available off the shelf at relatively low cost due to the work pioneered by the USDA Forest Service in 1994 (Bobbe, 1997). The sensor size in these cameras is 1524 x 1012 pixels resulting in a ground coverage of 762 m x 506 m for a 50cm pixel, a significant improvement over the video image, with a consequent reduction in image processing time. In addition, the problem of pixel jitter is eliminated since the A to D converter is matched to the CCD and is driven by the same timing generator (Walker, 1999). The images are written directly to removable hard disks in digital form for direct computer analysis. The dynamic range of the digital camera sensor is superior (12 bit, 4096 greyscales) to that of video (8 bit, 256 greyscales) giving increased spectral resolution in the image. In addition, the camera is independent of the aircraft power supply, inspiring pilot confidence in the operation. Subsequent developments in digital camera technology resulted in the availability of cameras with larger arrays, for example, the Kodak DS 460 series with an array size of 3060(H) x 2036 (V).

The new system using full frame digital cameras not only overcomes some of the problems associated with video technology such as brightness control and compliance with TV standards

(5.2.1.2) but also provides a much more compact system for transportation and deployment in a small aircraft, where space is at a premium, and is schematically represented in Figure 6.1.

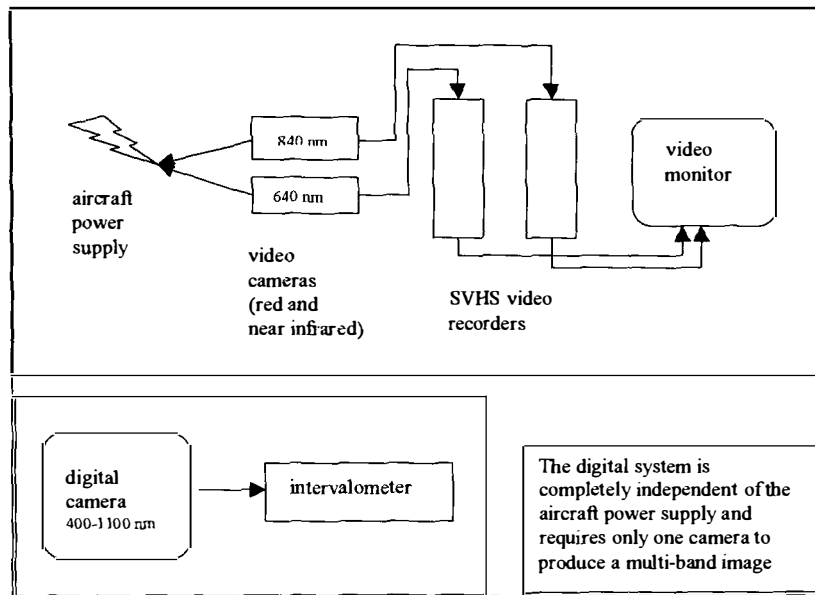


Figure 6.1 Image capture components of the video system and ADPS

6.1.2. Evolution of the ADPS

The original version of the ADPS was designed around the Kodak Digital Science 420 panchromatic IR camera, which has a silicon photodiode sensor matrix of 1524[H] by 1012[V] pixels, producing 1.5 million pixels in monochrome mode (the M5 chip). The ADPS was updated on production of the 420 CIR camera, which has the same size array as the panchromatic camera, but is capable of sensing in true colour mode or colour infrared mode and produces a three-band image. The current version of the ADPS uses the Kodak Digital Science 460 CIR camera. This camera differs from the 420 CIR in the array size of the CCD, having a 3060[H] by 2036[V] array (the M6 chip) producing 6 million pixels and giving a photocoverage four times larger than that of the Digital Science 420. A fuller description of the Digital Science cameras is given in section 6.3.1.

6.2. GENERAL SYSTEM SPECIFICATIONS

The system comprises 3 principal hardware components and one software component. These are a digital camera, an aircraft mounting plate and an intervalometer to manage the framing sequence (the hardware) and an interactive mission planner (the software) running in Microsoft Excel.

The ADPS weighs approximately 2.5kg and has overall dimensions of 25cm by 25cm by 25cm. The assembly, (Plate 6.1), is aircraft independent and can be installed within minutes. A variety of non-pressurised aircraft have been used for air survey with this system including the Cessna 150 series, 170 series, 180 series, 200 series, the De Havilland Beaver, Partanavia, Thruster Microlight, Piper Warrior, Super Cub and Bell, Hughes and Robinson helicopters.

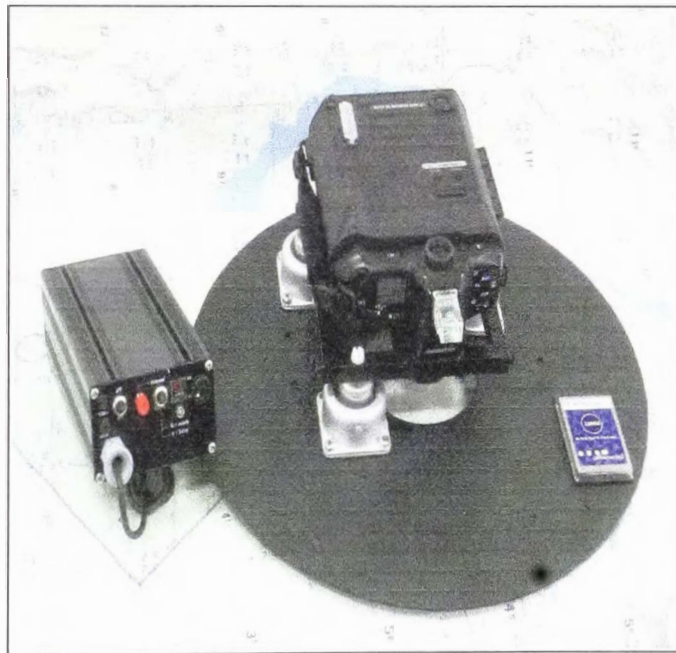


Plate 6.1. The ADPS comprising a Kodak DS 460 CIR camera, aircraft mounting plate, intervalometer and PCMCIA type III card

In all cases a 70mm diameter hole is required that looks vertically down. Most non-pressurised aircraft have inspection ports larger than 70mm diameter that look vertically down through floor and fuselage skin, and these have been used successfully.

6.3. THE ADPS CAMERAS

6.3.1. The Kodak Digital Science 420 and 460 series

There are many digital cameras available off the shelf, but there are few that have adequate spatial resolution and spectral sensitivity for aerial survey work. At the outset of this research the Kodak series of digital cameras with infrared capability were the only full frame CCD cameras available at relatively low price, potentially suitable for natural resource imaging. Considerable improvements have been achieved with each new camera in the series.

The Kodak Digital Science 420 panchromatic IR camera, which has a silicon photodiode sensor matrix of 1524[H] by 1012[V] pixels, producing 1.5 million pixels in monochrome mode (the M5 chip) was the first in the series. This camera is capable of producing a single band, grey scale image and if colour imagery is required it is necessary to use a series of cameras each fitted with a filter appropriate to the waveband required. The images must be co-registered and then composited to produce a colour image. This is a time consuming operation and detracts from the 'portability' of the system since more than one camera must be deployed. Never-the-less, this system has proved very useful when used with very narrow band filters, 640 ± 10.4 nm (red) and 840 ± 11.4 nm (very near infrared), and has been used by the Land Management Group, Cranfield University at Silsoe, to predict crop yield in the UK, (Taylor, J. 1998, pers. com.). The advantages of using this camera over later versions include: lower cost, smaller file size (each image is only one third that of the 420 CIR camera), and full spatial and spectral resolution.

A colour version of the 420 panchromatic camera was developed which has the same size array as the panchromatic camera but which produces a three-band RGB image. Production of the 420 CIR camera was accomplished through modification of the colour camera sensor and software development. The arrival of the CIR camera, which was designed for the United States Forest Department (Bobbe and Zigaldo, 1995), was an exciting step forward as it could be used to collect either true colour or false colour infrared images using only one camera. Post flight, band

alignment procedures are eliminated because there is only one optical axis for the three image bands, and in addition, the bands can be separated and processed individually and then used to produce vegetation indices.

The Kodak Digital Science 460 CIR camera differs from the 420 CIR in the array size of the CCD, having a 3060[H] by 2036[V] array (the M6 chip) and producing 6 million pixels. This gives a photocoverage four times larger than that of the Digital Science 420, making the field of view almost identical to that of 35mm film and offers considerable savings in processing time. Figure 6.2 demonstrates the comparative sensor size of a 35mm film camera, the DS 420 camera and the DS 460 camera for a given flying height and focal length lens.

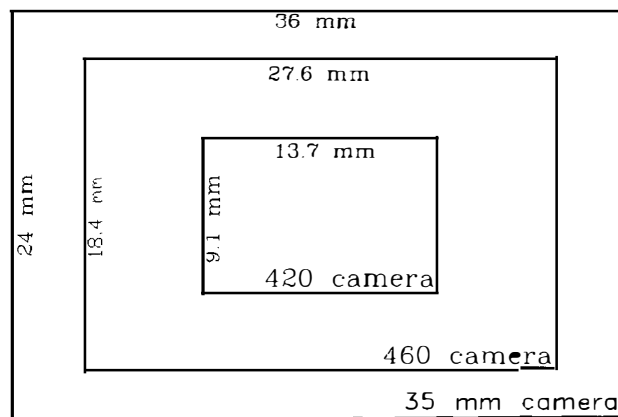


Figure 6.2 Comparative sensor sizes of a 35mm film camera, the 420 and 460 cameras

Graham and Mills (1997) have observed that although the nominal spatial resolution of the Digital Science 460 is the same as that of the Digital Science 420, the image quality is far superior due to the improved CFA interpolation algorithm incorporated within the Digital Science 460.

The most recent digital camera from Kodak is the Kodak Digital Science 660 Colour camera. This camera does not have near infrared capability since the sensor is not silicon based but is

indium tin oxide, which is not sensitive in the near infrared part of the spectrum The array size of this camera is 3040 [H] x 2008 [V].

6.3.2. Digital file formats and data storage in the Kodak DS series

The images are captured in TIF-EP (Tagged Interchange File Format for Electronic Photography) format using a colour filter array (CFA) technique. This produces a file size of 1.5 Mb for the 420 CIR camera and 6.2 Mb for the 460 CIR camera, which are stored in this format on PCMCIA cards. TIF-EP is an intermediate image file that maximises the number and quality of the images stored in memory. TIFF-EP allows image attribute data, such as date and time, aperture setting and shutter speed, as well as other types of digital data including GPS position data, to be stored along with the image data. This is shown in Figure 6.3.

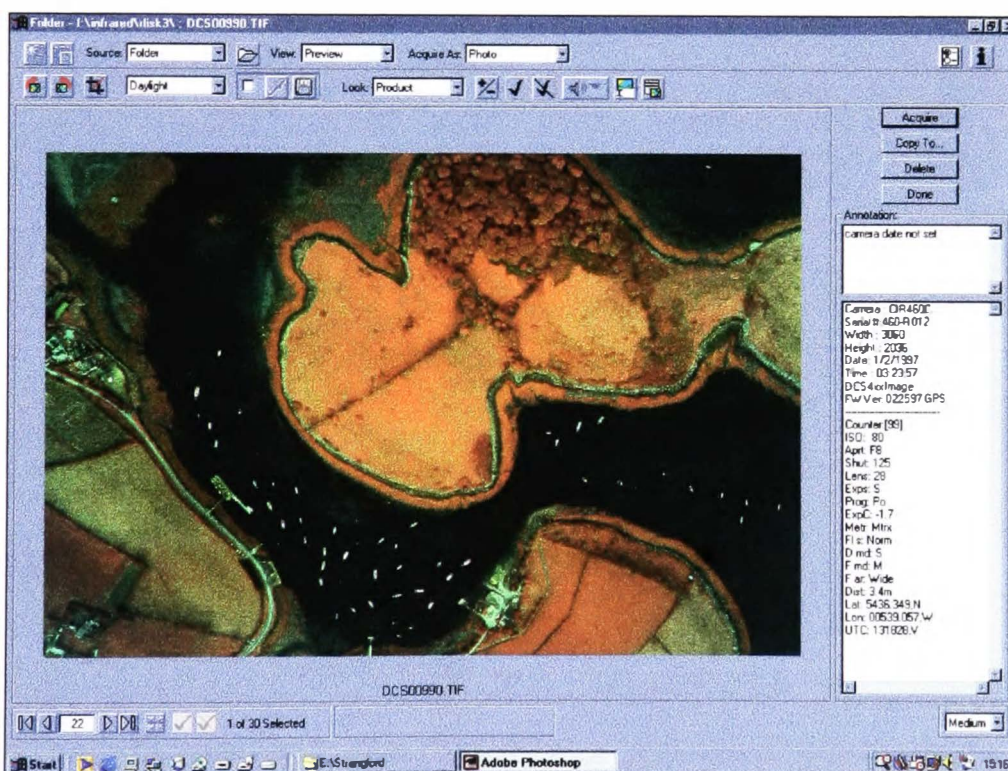


Figure 6.3 Screen grab of import window showing TIF-EP and image attribute data

When acquired using a PC or Macintosh, the file is extrapolated into a full colour image, with 12 bits per channel. This 36 bit image is resampled to a 24 bit colour image using the best 8 bits from each channel, producing a 4.6 Mb image or an 18.6 Mb image, for the 420 CIR and 460 CIR cameras respectively, in standard TIF format.

The improvements in array size and multispectral capability involve a cost in terms of increased file size. This is of particular importance for air survey, (6.6) as it extends the data writing time at the camera / PCMCIA card interface (maximum framing rate) and the download time at the PCMCIA card / PC interface; it also increases the storage space per image on the PCMCIA card, as shown in Table 6.1.

SPECIFICATION	CIR 420	CIR 460
CCD array size	1012 x 1524	2036 x 3060
Pixel size	9.013 μm	9.013 μm
Spectral sensitivity (nm)		
Unfiltered	400 - 1000	400 - 1000
Visible filter	400 - 700	400 - 700
Infrared filter	500 - 800	500 - 800
Sensor size (mm)	9.121 x 13.735	18.350 x 27.579
Burst rate	5 images in 2.3 s	2 images in 2 s
Minimum framing rate (s)	2.75	8.5
File size raw / interpolated (Mb)	1.6 / 6.5	6.2 / 18.5

Table 6.1 Framing Rates and File Sizes of the Kodak Digital Science Camera Series

PCMCIA cards are available in several sizes ranging from 171 Mb to 1Gb. The capacity of the card controls the number of compressed image files that can be stored and this has important implications for air survey management (6.6.4). The number of compressed files per PCMCIA card for the 420CIR and for the 460CIR is shown in Table 6.2

camera	No. of images per PCMCIA card				
	171 Mb	260 Mb	340 Mb	512 Mb	1 Gb
420 CIR	106	162	212	320	625
460 CIR	27	41	54	82	160

Table 6.2 Storage capacity of PCMCIA type III cards

6.3.3. Spectral Sensitivity

6.3.3.1. Spectral range and quantum efficiency

The spectral sensitivity of the sensor in the CIR versions of the cameras was designed to mimic the spectral sensitivity of Kodak 2443 colour IR film (King, 1997). The range is governed by the quality and sensitivity of the silicon based CCD detectors (Anderson, *et al.*, 1997) and spans the entire spectrum of visible light, extending well into the near infrared (400 nm to 1000 nm).

Silicon is the most commonly used 'chip' material as it is relatively cheap to manufacture and provides good quantum efficiency (the efficiency in conversion of incident photons to image signal) in the near infrared wavelengths. For CCDs the quantum efficiency is typically 10% in the blue (380 - 430 nm), 40% - 60% in the far red / very near infrared (680 - 800 nm) and 10% in the near infrared (900 - 1000 nm) - almost 50% of the response is in the near infrared, providing excellent potential for CIR imaging (King, 1995). Figure 6.4 shows the quantum efficiency of the spectral response curve for the Kodak Digital Science CIR cameras.

Figure 6.4 has been removed from the digitized thesis for copyright reasons.

Figure 6.4 Spectral sensitivity of the sensor (Eastman Kodak Company)

6.3.3.2. Survey altitude and poor light levels

The difference in sensor type between conventional large format film and digital small-format cameras dictates the focal length of the lens that is acceptable, and for similar ground pixel resolutions, the use of large format cameras require significantly higher survey flying altitudes because they use 150mm or 210mm focal length lenses. This geometry-induced requirement may limit survey flying to clear-sky conditions and often renders the large format unsuitable for disaster management roles when low-cloud cover often accompanies the disaster scene.

Under mission critical conditions digital small format systems are able to operate below cloud cover because of the short focal length (24mm or 28mm) of the lenses used. Furthermore, digital cameras appear to suffer less from inadequate light levels than film cameras. For example, Bobbe, (1997), demonstrated that the Kodak Digital Science CIR digital camera performed better under adverse lighting conditions than a Hasselblad 70mm camera which failed to expose the CIR film, owing to the higher sensitivities inherent in digital sensors to record images under low light conditions (because of the extensive dynamic range of the 12 bits per channel sensor allowing 4096 grey scales in each channel). Similar results were reported by Knapp *et al.*, (1997) when comparing data obtained from a DS 420CIR, a 35mm film camera and a 70mm film camera. This can significantly expand

the window of opportunity for data capture, especially in regions where cloud cover is frequent or in areas that are turbulence free only in early morning / late afternoon when light levels are less than perfect. Plate 6.2 is a digital CIR photograph of a difficult subject taken in early morning (7.30 am local time) where the low sun angle cast deep shadow in the excavation pit of an open cast mine.



Plate 6.2 Digital Science colour infrared image of an open cast mine

The image was captured at 16200 ft ASL from a Bell helicopter, giving a nominal ground pixel resolution of 25cm. Only rudimentary image processing was necessary (contrast stretch and edge enhancement) to reveal some detail in the image even where the benches of the mine are in shadow and this photograph provides evidence of the potential of aerial digital photography in an exacting environment.

6.3.4. The Kodak Colour Filter Array

The Kodak camera senses the blue, green, red and near-infrared (NIR) parts of the spectrum using different elements of the CCD array, known as the colour filter array or CFA. Multiband imaging is achieved by coating the individual photosites with waveband specific filters. There are three

types of filter; one which allows green and near infrared wavelengths to pass, one which allows red and near infrared wavelengths to pass, and finally one which allows blue and near infrared wavelengths to pass. The pattern of the coated photosites within the matrix is shown in Figure 6.5.

	G+IR	R+IR	G+IR
	B+IR	G+IR	B+IR
	G+IR	R+IR	G+IR

Figure 6.5 Colour Filter Array (CFA)

It can be seen that each photosite is sensitive to just one waveband pair (i.e. blue+NIR, green+NIR or red+NIR), and that there are twice as many green+NIR photosites as red+NIR or blue+NIR. The greater proportion of green sensitive pixels corresponds with the maximum sensitivity of the human eye to green wavelengths thus giving the image improved fidelity. Once an image has been captured using this arrangement, three separate images have to be created using the *adjacent pixel colour interpolation technique*. Since only one in two photosites record information for the green channel, interpolation is used to fill in the remainder of the array. Just one in four photosites collect information in the red channel, and so interpolation is used to fill the remaining three-quarters of the array. Likewise, interpolation is required to fill three quarters of the array to produce the blue channel image. This interpolation is achieved using a procedure known as “acquire” in TWAIN compliant software. The quality of the individual bands is determined by the sophistication of the interpolation algorithm. This procedure allows multiband imaging but at this stage each photocentre is sensitive to one primary colour plus near infrared wavelengths, to produce true colour or colour infrared imagery an optical filter is required.

For true colour imaging, an infrared cut filter is placed in front of the camera lens, to ensure that only visible wavelengths strike the photosites, as shown in Figure 6.6. The energy received at each photosite is converted to a digital number (DN) which in turn controls the brightness of the corresponding channel or gun (blue, green or red) of a visual display unit (VDU).

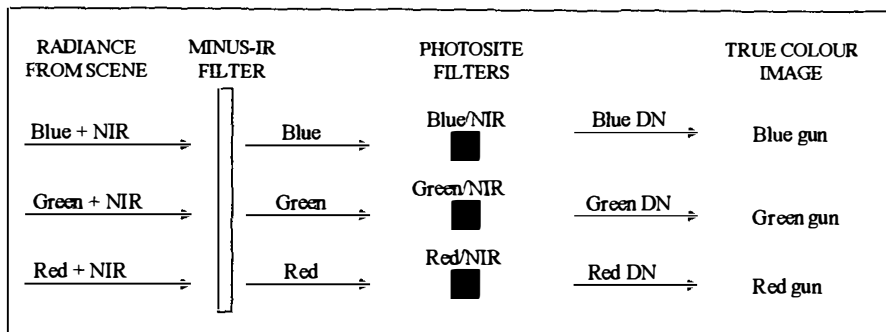


Figure 6.6 True colour image production using CFA and infrared cut filter

For false colour infrared imaging, a minus-blue filter is placed in front of the lens to ensure that only near infrared wavelengths reach the blue/near infrared photosites, (*i.e.* the infrared signal occupies the blue photosites). This enables the near infrared radiance to be measured, and this amount is subtracted from the total radiance received at the green/near infrared and at the red/near infrared photosites respectively as shown in Figure 6.7

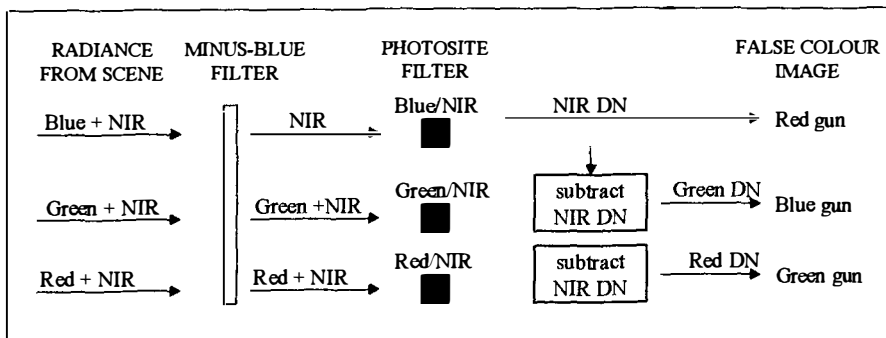


Figure 6.7. False colour infrared image production using CFA and minus blue filter

6.3.5. CIR AND TRUE COLOUR FILTERS

Although the response of the CCD allows the use of filters of very narrow bandwidth (10nm), (except in the blue region where the signal to noise ratio is low, and a minimum of 25 nm bandwidth is required for acceptable results), to produce customised images for specialist applications, the two filters supplied with the 420 and 460 cameras are relatively broadband. These are, the 650BP300, a broadband filter in the 500-800 nm spectral band enabling the CIR cameras to record false colour infrared and the VIS 550 BP 300 a filter in the 400-700 nm spectral band enabling the CIR cameras to record natural colour.

Figure 6.8 describes a number of spectral characteristics of the CIR camera and the 650BP300 filter, a band-pass filter allowing wavelengths between 500 nm and 810 nm only to reach the CCD. The general CCD response in the 400 - 900 nanometre bandwidth is indicated, as well as the range and response of the 650BP300 filter, superimposed on the general CCD curve. The response at the individual 'blue', green and red photosites is shown with peaks at 760, 540 and 650 nm respectively. The apparently anomalous 'blue' response which peaks well beyond the blue part of the electromagnetic spectrum at 750 nm with the 650BP300 filter in place is explained by the fact that the blue photosites are occupied by near infrared signals when the camera is operated in colour infrared mode (Figs.6.7 and 6.8).

Figure 6.8 Spectral response of the 650BP300 filter (Eastman Kodak Company)

Figure 6.9 shows the range and response of the 500BP300 filter at the individual blue, green and red photosites with peaks at 450, 540 and 680 nm respectively.

Figures 6.8 and 6.9 have been removed from the digitized thesis for copyright reasons.

Figure 6.9. Spectral response of the vis filter (Eastman Kodak Company)

6.3.6. Spatial resolution of the image in CIR mode and true colour mode

In Chapter 5: (5.3.4) attention was drawn to the difficulties arising from the intrinsic differences between analogue and digital photographs in trying to compare scale and resolutions. Defining the resolution of digital images produced by the Kodak DS 460 CIR camera requires further clarification.

Regardless of the stated GSD of the imagery, the amount of spatial detail which may be discerned appears to be greater for the true colour imagery than for the false colour imagery for the same pixel size. This probably arises from two factors, the first due to the physical properties of lenses and light and the second due to the CFA and the interpolation software. First, a slight de-focusing of near infrared wavelength occurs because the focal length of a lens at near infrared wavelengths is slightly greater than that at visible wavelengths giving a slightly out of focus image (Graham & Read, 1986). Second, loss of some spatial detail is a result of the noise effects in the green and red wavebands of the CIR as discussed below.

Plate 6.3 shows a colour infrared image (top left) and a true colour image (top right) of the same subject. These images were captured simultaneously using two DS 460 cameras, with the camera configured to colour mode mounted in front of that configured to CIR mode, in this way, ambient conditions in the field were as near identical as is possible. Both images have been split into their component R,G,B bands. Similar subsets of the red and green single band images were produced to allow a zoomed-in view to facilitate comparison of the images. (On a point of clarification: the bands used for comparison are the actual red wavelengths and green wavelengths responses and not the red and green VDU channel images).

Pairwise comparison of the red (centre) and green (bottom) waveband images reveals that the images obtained in CIR mode are of inferior quality to those obtained in true colour mode. The CIR images are more grainy and lack the spatial detail of the true colour mode images. This is most likely to have arisen from an amplification of noise introduced during the subtraction of the

near infrared component of the radiance incident on these photosites as illustrated in Figure 6.7. When used in true colour mode, with an infrared blocking filter, all of the energy incident on the photosites is recorded and converted to a digital number. When used in colour infrared mode, at the red and green photosites only part of the energy incident on the photosites is used to calculate the digital numbers (DNs), as the near infrared component has been subtracted. Thus the signal to noise ratio is reduced for the red and green wavebands in CIR mode.

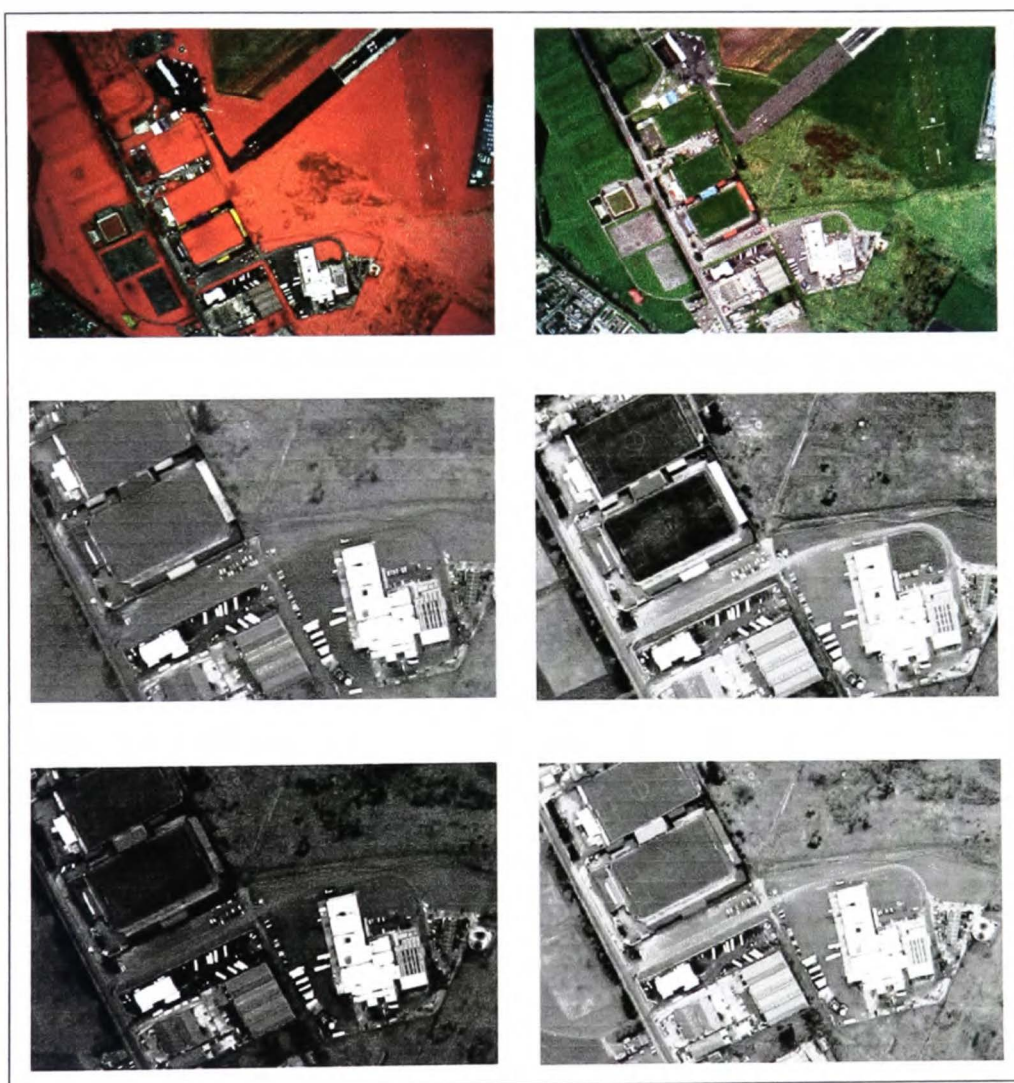


Plate 6.3 A visual comparison of the detail discernible in a colour infrared (left) and true colour image (right). Red response ($\approx 550 - 700\text{nm}$) centre and green response ($\approx 450 - 600\text{nm}$) bottom

In order to quantify this difference, Grant Thompson FRPS, FBIPP, of the Royal Photographic Society Aerial Imaging Group, carried out an independent investigation into the spatial resolution of DS 460 CIR camera, operated in both colour infrared and true colour modes with a 28mm lens. In November 1997 a hardcopy subsce of each of a CIR and a true colour image was provided for the investigation. These images were captured simultaneously in October 1997. The images were contrast stretched by autolevelling. The scale of each print was established by careful measurement of 6 control points on each image, the selected control points representing three lines being as near as possible at 120° to each other. The same points were then measured on a 1:50 000 map and the image scale was determined by the relationship:

$$Scale_{(image)} = Distance_{(map)} / Distance_{(image)} \times Map\ scale$$

The average image scales were :

CIR 1:1065

Vis 1:1056

Twenty measurements of Image Spread Function (ISF) were made from each of the prints and the mean value was calculated for each of the prints, together with the standard deviation and the coefficient of variation. The results are shown in Table 6.3 The image spread function is a measure of the resolving power of a system (including camera, computer and printer) and is used as a measure of the smallest discernible image patch in a hardcopy image (Thompson. 1997).

Image Type	ISF (avg.)	S.D.	CoVar.
DS 460 CIR	0.443	0.62	14.0%
DS 460 VIS	0.373	0.54	14.4%

Table 6.3 A comparison of the mean image spread function in a CIR and a True Colour digital image captured simultaneously

From the relationship $GSD = ISF \times \text{Image Scale}$ it was possible to calculate the GSD (ground sampled distance) since ISF and Image Scale were known, and in addition, from a flying height of 948m above mean ground level recorded for the images, the GSD values indicate an angular resolving power for each camera, plus computer and hardcopy system. The results are shown in Table 6.4

Camera type & mode	GSD	$\angle ar$ resolving power
DS 460 CIR, CIR	0.47m	0.50 milli-rad.
DS 460 CIR, vis	0.39m	0.41 milli-rad.

Table 6.4 The ground sampled distance (GSD) and angular ($\angle ar$) resolving power for each camera, computer and hardcopy image.

These findings might suggest that the camera should only be used in true colour mode, but this would mean that near infrared imagery would not be available and for studies involving the assessment of vegetation this would be disadvantageous. The near infrared waveband provides information on vegetation cover that is not available at visible wavelengths because near infrared wavelengths are reflected strongly by cell walls within leaves, and the denser and healthier the leaf canopy, the stronger the NIR reflectivity.

6.4. THE INTERVALOMETER

6.4.1. Power supply to the camera

Driving the camera and maintaining the storage devices places a heavy drain on batteries and this proved to be a tricky problem when the cameras were used towards the 'stated' limit of their batteries. The early cameras supplied by Kodak were prone to battery failure when used for aerial survey work. In addition, the batteries were not 'user replaceable' in the sense that the battery pack

was housed within the camera, requiring removal of the base plate for access and were certainly not replaceable in flight, and besides, Kodak would not accept liability for cameras that had been tampered with.

Up to 1997 the cameras were fitted with 900mAh NiCad batteries. All NiCad batteries suffer a memory effect, so that incomplete discharge before recharge caused an effective decrease in the capacity of the battery over successive charge cycles. This alone caused difficulties for aerial survey work but was only one of several problems encountered during the early camera trials. The nominal life of the battery was 1000 cycles and for the 420 and 460 cameras one complete charge allowed the capture of 400 and 300 images respectively (Eastman Kodak, no date). Using the camera for continuous firing placed a high demand on the battery and did not allow recovery after firing. Rapid deterioration ensued, and by halfway through the life cycle only about half of the stated number of frames could be captured on one full charge. Clearly this was inadequate for aerial survey as the following simple example illustrates:

To capture full stereo imagery, at 50cm pixel resolution, of a block of 10km length, on flat terrain, using the 460 camera orientated with its long axis along track would require 22 frames per line. With a compromised battery allowing the capture of 150 frames only 6 complete flight lines could be photographed on one charge cycle, representing a block width of only 4 km. Furthermore, the most efficient way to fly a survey is to maximise the actual survey time relative to aircraft costs such as relocation time, landing fees etc. The time for this actual survey, flown at 80 kts, is only 1.8 hours and with typical flight durations between refuelling in the region of 4 hours, for many light aircraft this would be a punitive way to operate in terms of both time and money.

In March 1997, Kodak recalled all the NiCad batteries and replaced them with 1100mAh nickel metal hydride batteries which do not suffer a memory effect, but these still proved inadequate for

prolonged use. In addition, problems were encountered in charging these batteries as they were found to overheat if they were left charging for more than two hours and Kodak was obliged to issue a supplement to the camera manual advising on this.

In response to these problems, an integrated external power management unit (using a gel-lead-acid battery) and intervalometer, housed in an electrically shielded and fireproof box, was developed specifically for the ADPS, by Alexander Koh at GeoTechnologies, Bath Spa University College, to enable the use of the Kodak cameras for air survey. This power supply continuously charges and supplements the internal battery so that continuous firing is no longer a problem. Moreover, this external DC supply is an improvement over using the AC transformer in the laboratory as it delivers 13.8V maximum whereas the mains transformer runs at 15V. In this way operation is maintained at a lower temperature with benefits to the internal battery (and with possible implications for dark current noise suppression).

The new generation cameras from Kodak, (including the DS660) are fitted with rechargeable and replaceable lithium polymer cells. These allow 100 frames per complete charge (optimum) but this camera has not been investigated yet for air survey. Since the time of writing, trials have been conducted by GeoTechnologies at Bath Spa University College and the University of Newcastle. Results of this trial are pending.

6.4.2. Firing the camera

The design of the digital camera using a modified Nikon camera is such that the communication port for the remote firing mechanism is occupied by the cable that connects the sensor to the PCMCIA card – (a facility which is not necessary in the film version of the camera). Firing the camera remotely by the usual means is therefore impossible, and in the early trials Bobbe *et al.*, (1997) manually fired the camera. This is not a sensible option for large surveys, so to address this problem the intervalometer was developed and was designed to fire the camera at a range of intervals to allow for different mission scenarios.

6.5. THE CAMERA MOUNT

Aside from any CAA regulations regarding modification and/or attachment of equipment to an aircraft, the design of any camera mount must take into consideration the type of aircraft, the dimensions and weight of the camera, the number of cameras required and the accessibility of the camera controls. It is preferable to mount the camera inside the aircraft for a number of reasons including shelter for the camera from wind buffet and engine exhaust and ease of access for the operator, although it is not always possible to do so and some camera mounts have been designed to sit outside the aircraft, either as an extension to the luggage compartment or with a door removed.

The versatility of aircraft type that might be used for the ADPS posed a problem for the mount design, if manufacture of a new mount for each new aircraft was to be avoided. Accordingly, the mount was designed to be near universal with only minor modifications to allow its use in a variety of aircraft. Designing the mount for this system presented additional problems unique to digital cameras.

First, unlike cameras that have been designed specifically for aerial work such as the Vinten 360, (a military camera engineered with a very reliable film transport system to withstand high G loadings and therefore also withstanding turbulence, vibration and shock (Warner *et al.*, 1996), the Kodak digital camera has no such design brief, but a write protection facility, designed to prevent damage is incorporated into the electronics of the PCMCIA card. In the event of the camera being subjected to excessive vibration or shock the disk is automatically parked. To enable the hard drive to spin-up again it must be removed from the camera which must then be reset, with a consequent loss of expensive time whilst airborne. To prevent this, the camera is mounted on a chassis supported on shock and vibration tolerant mounts to damp out excessive movement.

The mount has been developed through a series of prototypes and evolved into an aluminium quadrilateral chassis supported on four shock mounts, two fore and two aft as shown in Plate 6.4. The loadings on each shock mount have been specified to enable operation of the camera even in turbulent conditions because although it would be unusual to capture photography for photogrammetric purposes under such conditions it is important to be able to operate in adverse conditions for critical situations such as disaster reconnaissance or hazard mapping. Since the time of writing the mount has been redesigned to be even more lightweight and is now supported on only three shock mounts. This mount has performed to expectation and allowed the camera to continue firing even in extremely turbulent conditions when mounted in the floor of a Cessna 152, flying in the Cordillera Orientalis, Columbia (pers. obs.).

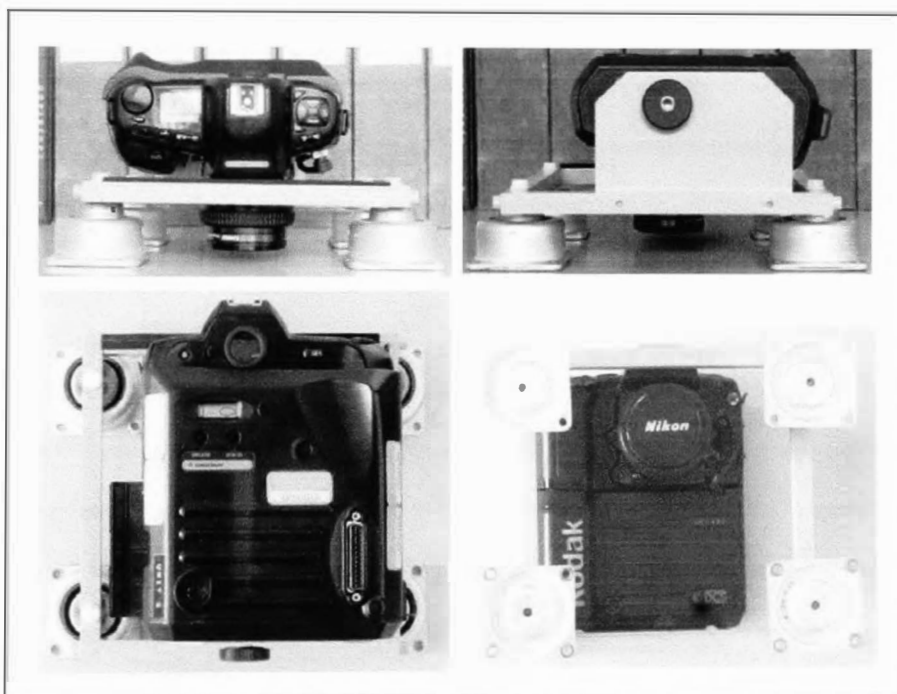


Plate 6.4 The ADPS universal mount: from the front (TL) from the back (TR) from above (BL) and from below (BR)

Second, whereas large format film cameras regularly carry 76m film magazines (allowing 250 photographs per can) they may also use 150m magazines (500 photographs) for large surveys, and 35mm cameras can be adapted to carry 500 exposures, the 460CIR camera is limited to 160

frames using the largest capacity (1Gb) PCMCIA card. Therefore, it must be possible to access the PCMCIA card slot to change the card when full and so an external mount is not ideal. All of these problems were demonstrated during a trial to evaluate the use of microlights as an operational platform for the ADPS when the operator resorted to hand-holding the camera in a near vertical position to photograph the subject (Graham and Mills, 1997; Koh, 1998b).

6.6. THE MISSION PLANNER

6.6.1. Flight track planning

Rigorous mission planning is the key to success with any aerial survey and an interactive mission planner has been designed to effect flight track planning, mission and processing costs and flight line navigation. The mission planner allows the user to select the resolution required, the dimensions of the survey block, the maximum and minimum elevations of the landscape and the forward and side overlaps that are required. The number of frames required for each flight line, the flight line spacing, the number of storage cards required and the number of flying hours are then calculated.

Table 6.5 shows the flight track planning component of the mission planner for a hypothetical survey. In this case the user selected pixel resolution is 50cm and the block size is 20km x 15km. The imagery must be captured with 70% forward overlap and 30% side lap. This specification would require 52 images per line and 24 lines per block. The simplest way to achieve this would be to store 3 full lines of data to a single 1Gb PCMCIA card. Thus the entire survey would require 8 PCMCIA cards each of 1Gb.

It is not possible to survey such an area in one sortie, even in ideal weather conditions, as the flying time required to survey the flight lines alone is in the region of 6 hours. The mission planner builds in a maximum of 3 hrs survey per day plus two extra days, one for planning and one contingency day. When a survey is scheduled over more than one day, the PCMCIA cards are

downloaded to a large capacity removable disk such as a 10 Gb Flip disk, or the files are written to CD, before the next survey day so that the cards may be cleared for the next sortie. This ensures that backup copies of the data can be made and is a more economical way to operate in that fewer, expensive PCMCIA cards are required.

Table 6.5 has been removed from the digitized thesis for copyright reasons.

Table 6.5 The flight track component of the ADPS mission and flight track planner

Planning for a digital survey requires a different approach to that for traditional survey using large format cameras. Important differences arise from three major areas, the array size of the sensor, the download time at the sensor / storage interface and the maximum capacity of the storage media. Although all of these things are closely interrelated they are discussed briefly under separate headings below. Other factors of note will be discussed in 6.6.5.

6.6.2. Issues related to the array size of the sensor

For any given flying height and focal length of lens the array size of the sensor controls the area on the ground that is imaged, and in the case of the DS 460 camera the array size is 3060 (H) x 2036 (V) pixels. An important consideration for flight planning is the required scale or spatial resolution of the imagery.

The number of frames needed to cover a study area is determined by the desired spatial resolution of the imagery. The finer the resolution required (i.e. the larger the scale), the smaller the area coverage of the image and the larger the number of frames required. For example, a pixel size of 10 cm would give overall image coverage using the Digital Science 460 of just 306m x 203m, whereas a pixel size of 1m would provide coverage of an area of 3.06km x 2.03km. Although it is difficult to make a direct comparison between large scale analogue photography and digital photography, commonly used aerial photo scales are between 1:10 000 and 1:25 000. The area on the ground covered by a 1:10 000 scale 23cm photograph is 2.3km x 2.3km and for a 1:25 000 scale photograph the coverage is 5.75km x 5.75km.

The small across track dimension of the digital photograph has implications for the required accuracy of navigation of the flight lines and there is very little tolerance for excursions from the planned line if the required sidelap is to be achieved. To address this problem, navigation is by autonomous GPS using the cross track error report to maintain the correct heading, and a safety margin which accounts for selective availability and small excursions is built into the mission planner, in effect bringing the flight lines closer together. (Since the removal of selective

availability by the Clinton administration earlier this year it should be possible to reduce the margin for error built into the planner.)

6.6.3. Issues related to the download time

A further important factor that must be considered is the download time, that is, the time taken for the image to be downloaded to the PCMCIA card. The download interval controls the maximum rate at which the camera can fire successive shots, as each frame must be downloaded to the removable hard disk before the next frame may be imaged. This in turn controls the percentage overlap that can be achieved. In the case of the DS 460 the stated download time is 12 seconds (although in reality the camera can be fired at a slightly faster rate). To ensure stereo coverage the aircraft must advance by no more than 40% of the image coverage between exposures. Flying at 50ms^{-1} (180kmh^{-1} or 95kts) the aircraft would advance by 600m in 12s. Since 600m is 40% of 1500m, the smallest pixel resolution that may be achieved with stereo cover is 50 cm with the camera mounted with its long axis (3060 cells) parallel to the flight line. The mission planner has a built in safety factor which does not accept requested pixel resolutions finer than 50cm. Mounting the camera in this orientation reduces the across track ground cover to 1.02km

6.6.4. Issues related to the maximum storage capacity of the storage medium

The number of images that can be stored to a single PCMCIA card depends on the camera type and the capacity of the card (Table 6.2). The survey must be flown so as to maximise the number of images stored to each card but is important to avoid changing cards partway along a flight line as the card changing operation takes more than the 12 seconds available between frames, causing a loss of stereo overlap. Using the DS 460 camera to capture stereo imagery with a 50cm pixel resolution, the maximum length of line possible using 512 Mb and 1Gb cards is approximately 50 km and 100 km respectively.

6.6.5. Other Issues

6.6.5.1. Exposure compensation

Exposure compensation is required when the camera is used in infrared mode because the camera metering is designed for use with an IR cut filter, since the camera was originally designed for true colour mode. When the IR filter (minus blue) is fitted only the red and green energy can be used for metering, but the sensor is also receiving infrared energy. Without exposure compensation the sensor can receive too much energy, and although the chip has antiblooming properties the image appears over-exposed even in only moderately bright conditions.

Experience has shown that an exposure compensation of -2.3 is the optimal initial setting for air survey work. It is important to maintain observation of the landscape so that if any features appear which would be likely to cause saturation in the near infrared, the exposure compensation can be adjusted accordingly. For example, very thin films of water return a high NIR response as do corrugated steel roofing and glass houses. Plate 6.5 shows the effect of exposure compensation on a series of photographs captured with the DS 420 CIR camera. This terrestrial scene was imaged at exposure compensations from 0 to -3.3, the subject matter and lighting conditions were as close to identical as is possible under field conditions, for each shot. Although terrestrial photography is not strictly comparable with aerial photography this set of photographs serves to illustrate the point in question.

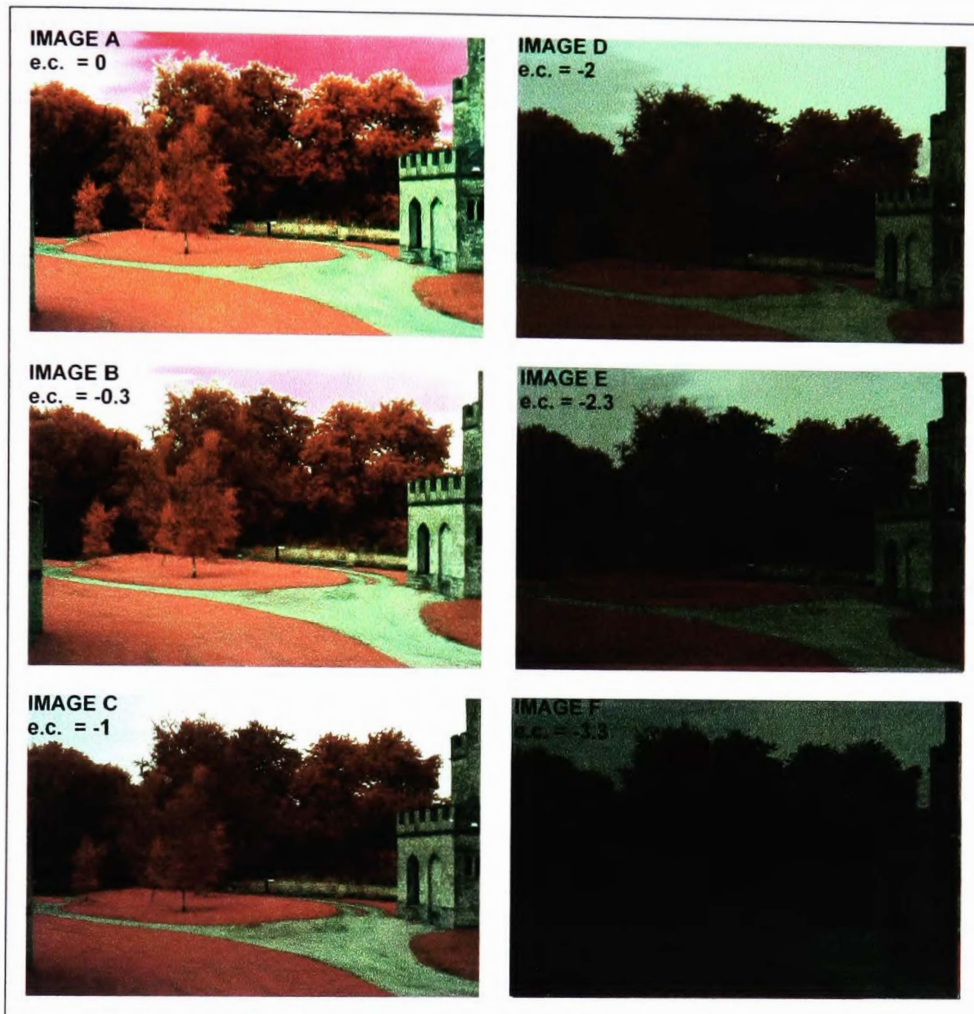


Plate 6.5 Series of photographs captured with the DS 420 CIR camera with exposure compensation set between 0 and -3.3

In this series of photographs it can be seen that exposure compensation settings from 0 to -1 (images A, B and C) suffer some degree of saturation and this means that there is a loss of data at the high end of the image histogram. With a decrease in exposure compensation less energy reaches the sensor and the photographs appear very dark, and, if the exposure compensation is set too low the result is a loss of data at the low end of the image histogram. A particular range of exposure compensation allows the optimum amount of energy to strike the sensor without causing data loss at either end of the image histogram. The images D, E and F appear very dark but when image E is autolevelled it produces an image with a good dynamic range as shown in Plate 6.6.



Plate 6.6 DS 460 CIR image captured with exposure compensation set at -2.3 and autolevelled to produce an image with a full dynamic range

6.6.5.2. *Pixel translation*

Pixel translation is related to the distance that the sensor moves forward in the time it takes for the shutter to open and close. At $1/500$ s the translation is 16% or 8cm for this survey. Translation causes smearing of the image because although each pixel in the array is imaging 50cm on the ground there is 50cm + 8cm worth of information in each pixel. This problem is overcome using forward motion compensation (FMC) in some high specification large format cameras but experience has shown that using this system (without FMC) care must be taken not to exceed 50% translation, otherwise smear becomes discernible.

6.6.6. **Navigation**

Because of the particular strictures imposed by the ADPS, the margins for error are very small and navigation must be very tightly controlled. Issues related to the array size and download time have already been dealt with but there are other factors that give rise to problems, which must be

considered to ensure complete coverage of the survey block. Navigation by autonomous GPS has overcome these particular problems and has been well received by pilots, once they are instructed in its use for the demanding regime required for narrow flight line navigation. For example, unlike large format survey, the aircraft is flying close to stall speed and at these low speeds the effect of a tail wind can cause the aircraft to travel faster than is permissible to ensure stereo overlap, even though the indicated air speed might be below the required speed. The converse is true, and if the aircraft is flying into wind it is necessary to decrease the framing rate. The GPS is used to calculate the true ground speed, that is the relative speed between the aircraft and the ground. In addition, to overcome the problem of drift and to ensure that the aircraft stays on track, the GPS is used to calculate the cross track error (deviation from the planned track) at one second intervals and the pilot is instructed accordingly.

Table 6.6 is an extract of the navigation section of the mission planner and the same hypothetical survey parameters as in 6.6.1 are used to demonstrate navigation planning. Once the bottom left hand corner co-ordinates of the survey block are identified in UTM projection WGS84 datum, the planner calculates the waypoints for the start and end of the flight lines which are projected 5km beyond the actual survey block. This 5km lead in and lead out allows the pilot room to turn the aircraft onto the next line, on track, at the survey speed and at the survey altitude. The planner takes into account the orientation of the flight lines and makes the 5km lead in / lead out adjustment in the correct direction. Figure 6.10 is a diagrammatic representation of the parameters in Table 6.6 and this illustration assumes that the bottom left hand corner of the block is specified to take account of the required overlaps for stereo coverage.

Map projection [m]:	UTM	
Map datum:	WGS 1984	
Grid direction of block North / East:	North	
Lead in [m] & lead out distance [m]:	5000	5000
Datum coordinate BLHC of block, x [m] & y [m]:	0	0
Start line 1, x [m] & y [m]:	314	-5000
End line 1, x [m] & y [m]:	314	15000
DTG to camera ON [km] & to camera OFF [km]:	15.2	4.8
Start line 2, x [m] & y [m]:	943	15000
End line 2, x [m] & y [m]:	943	-5000
DTG to camera ON [km] & to camera OFF [km]:	15.2	4.8
Start line 3, x [m] & y [m]:	1572	-5000
End line 3, x [m] & y [m]:	1572	15000
DTG to camera ON [km] & to camera OFF [km]:	15.2	4.8
Start line 4, x [m] & y [m]:	2201	15000
End line 4, x [m] & y [m]:	2201	-5000
DTG to camera ON [km] & to camera OFF [km]:	15.2	4.8

Table 6.6 Navigation section of the mission planner

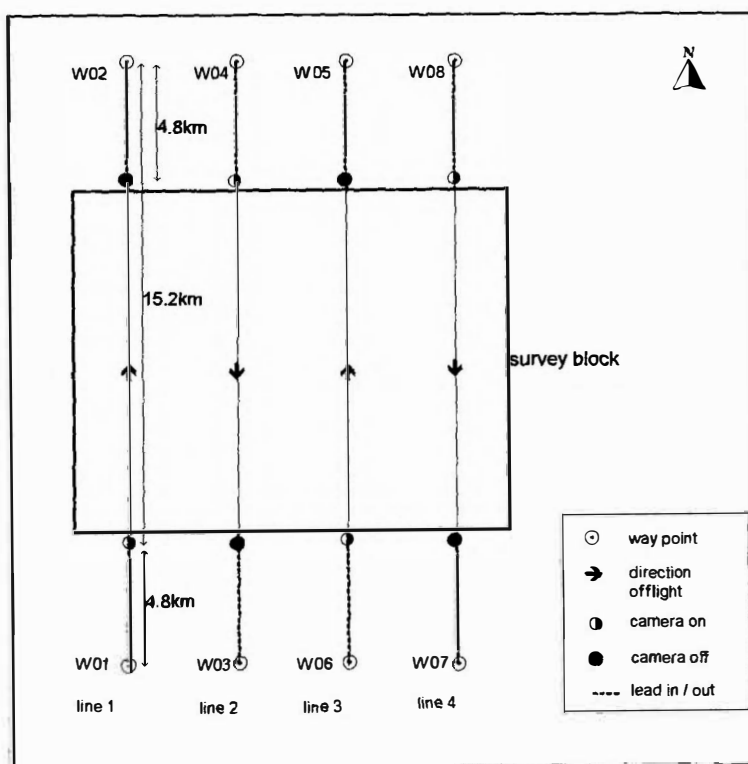


Figure 6.10 Flight line planning using the mission planner and GPS

One additional feature to note in Table 6.6 is the distance to go (DTG) for camera on and off. This instruction allows for full forward overlap on the first and last frames, but at the same time

ensures that the planned number of frames is not exceeded as this can compromise data storage for subsequent lines.

6.7. THE FUTURE

The ADPS has proved to be a very successful tool for data capture for many applications but it is limited in its application by its sensor dimensions. Current research and development has produced a new 12 bit colour camera with a larger array. The CCD, produced by Loral Fairchild, is on a silicon chip and is therefore sensitive across the full spectral range from 400 – 1100nm as shown in Figure 6.3. The full array size is 4096 x 4096 with a 15µm square pixel, but the imaging area is limited to 3900 x 3900 with a border of pixels giving an imaging area of 57mm. The border of pixels return a true black response of the sensor. This enables the digital signal processor to subtract any noise generated in the system, such as dark current, from all other pixels. This will produce a higher fidelity image with 130% greater photocoverage than is possible with the current cameras. In addition, the square dimensions of the array will significantly decrease the number of flight lines required to survey a block. The sensor is housed in a Hasselblad camera and currently this is supplied with an infrared cut filter allowing true colour photography.

AERIAL PHOTOGRAPHS AND PHOTOGRAMMETRY

The following account is not intended to be a comprehensive discourse, either on the intricate geometry of aerial photographs or on the minutiae of photogrammetric ideology but is designed to draw attention to some of the fundamental principles that affect a pragmatic approach to data collection, processing and analysis for the purpose of this research.

7.1. GEOMETRY OF AN AERIAL PHOTOGRAPH

7.1.1. Types of aerial photographs

There are two types of aerial photograph: vertical and oblique. A vertical photograph is one whose optical axis is in a vertical position, although unintentional and unavoidable inclination does occur for a variety of reasons. Obliques are photographs taken with the optical axis inclined from the vertical and they may be low or high obliques, depending on the angle of inclination as illustrated in Figure 7.1

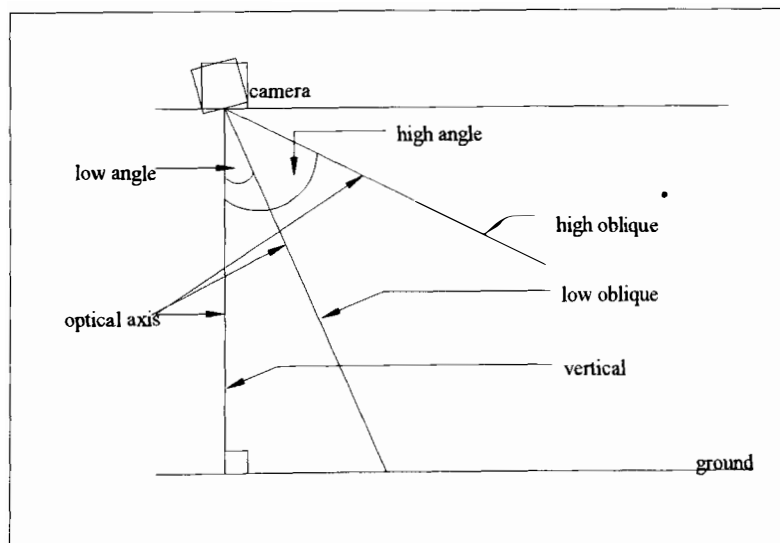


Figure 7.1 Classification of aerial photographs

Regardless of the classification, all photographs are central or perspective projections because the light rays are brought to focus through a central focal point, and this in itself gives rise to scale changes throughout the photograph which become increasingly large towards the edges of the photograph. For a perfect lens, the perspective centre of the lens which gives the geometric centre of the aerial photograph, is the principal point (PP). By convention the PP is taken as the origin of the photo-co-ordinate system (0,0), where PPx is parallel to the direction of flight and PPy is normal to the direction of flight. Nadir is defined as the point vertically beneath the camera and co-incides with the PP only if the photograph is perfectly vertical. The isocentre of a photograph is the point that falls halfway along a line between the PP and nadir.

7.1.2. Scale

The scale of a photograph is a ratio of the distance between corresponding points on the photograph and on the ground, so that in a 1: 10 000 scale photograph, a feature that measures 10mm on the photo actually measures 100m on the ground. The scale is related to the focal length of the camera and the distance from the target, and in the case of aerial photography this is the flying height above ground level, such that:

$$\text{Scale number} = f / H_g$$

Where f is the focal length of the lens and H_g is the flying height above ground level.

The focal length of the camera is the distance between the focal plane (film or CCD) and the centre of the lens. The focal length not only influences the scale of the photograph but also the field of view, both of which govern the ground coverage. Figure 7.2 shows how for a given height above the ground, a short focal length lens has a much wider field of view than a longer focal length lens and an object of length AB is imaged at a larger scale. This simple optical premise is of great significance in mission planning when choosing the type of lens to use for a particular survey.

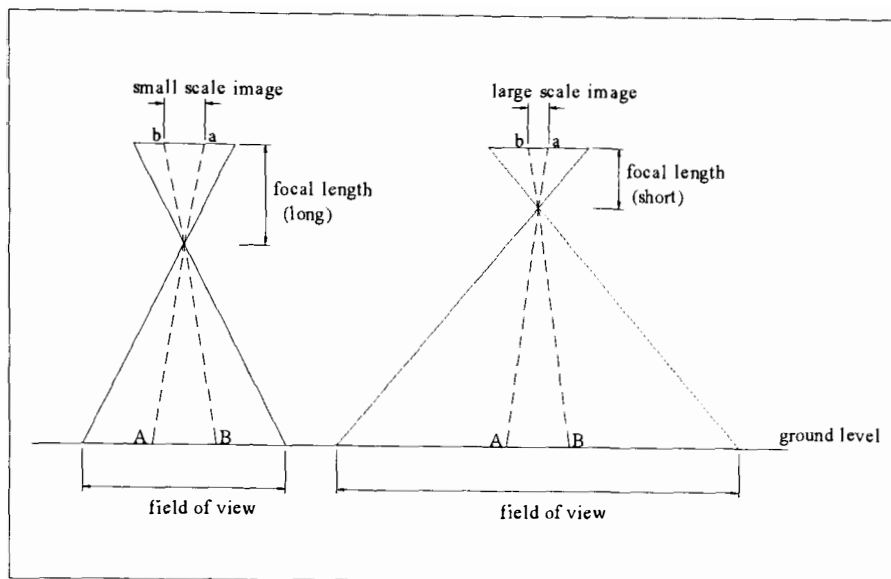


Figure 7.2 The relationship between focal length, field of view and scale of an object

This scenario holds good for a perfectly vertical photograph taken over perfectly flat terrain, but in the real world such a scenario is almost impossible to achieve. The scale of a photograph is variable across the entire photograph due to changes in viewing geometry caused by aircraft attitude and altitude and by terrain variation, and so is an average scale. In addition there can be considerable changes in average scale from photograph to photograph in a block survey

7.1.3. Image displacement and distortion

There are a number of factors that can affect the position of an object on a photograph. A shift in object position may be due either to distortion or to displacement. Distortions such as lens distortion and image motion alter the perspective characteristics of the image, whereas displacements due to topography or camera orientation do not.

7.1.3.1. Topographic displacement

The relief of the terrain influences the scale of the photography such that an object at a higher elevation will appear larger (i.e. smaller scale) than a same-sized object at a lower elevation. This is illustrated in Figure 7.3. Furthermore, high relief causes an apparent shift away from nadir whilst low relief causes an apparent shift towards nadir as shown in figure 7.4.

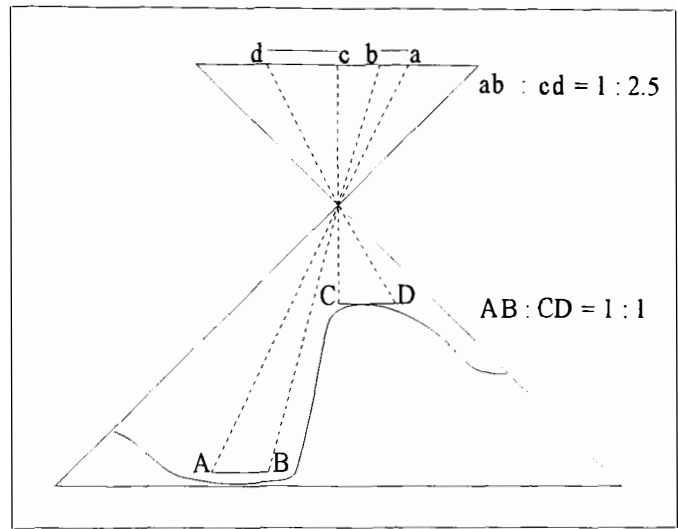


Figure 7.3 The effect of topography on scale

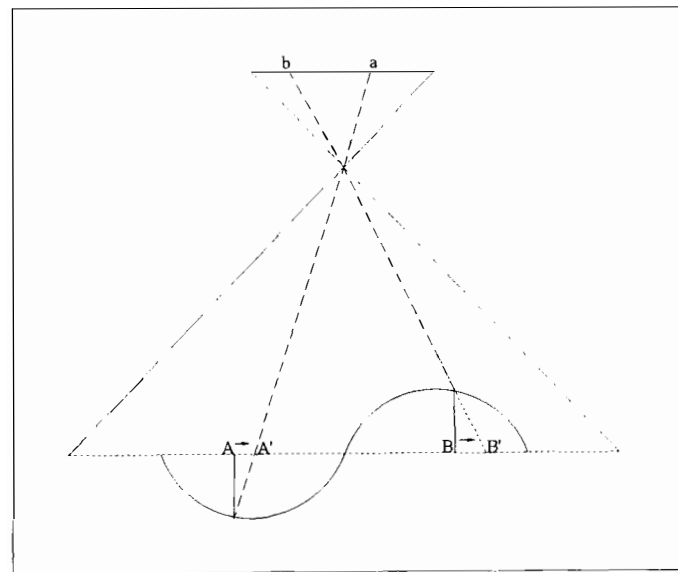


Figure 7.4 relief displacement of an object in a vertical photograph

7.1.3.2. Tilt displacement

Tilt displacement occurs when the aircraft is not completely horizontal at the moment of exposure. The camera can rotate around three axes, X, Y and Z, where X is the direction of flight and Y is perpendicular to X as shown in Figure 7.5.

- If the aircraft rotates about the Y axis the aircraft is said to pitch and the rotation by convention is ϕ .
- If the aircraft rotates about the X axis the aircraft is said to roll and the rotation is ω .
- If the aircraft rotates about the Z axis the aircraft is said to yaw and the rotation is κ .

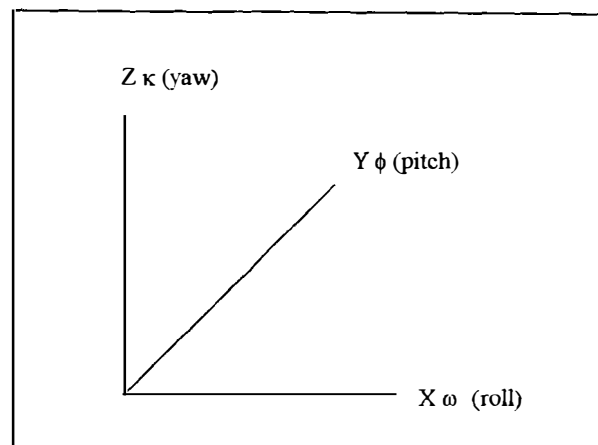


Figure 7.5 The three rotations of a camera: ω (roll); ϕ (pitch); κ (yaw)

Scalar changes occur across a photograph with ω or ϕ rotation, but κ rotation does not cause any scalar change. For example if the aircraft rolls to port then the scale of the photograph on the left hand side is larger than on the right hand side. Similarly, if the aircraft pitches nose up, the scale at the top of the photograph is smaller than the scale at the bottom of the photograph. Kappa rotation or yaw occurs in a plane parallel to the ground so there is no scalar effect but the relative orientation of the photograph to the flight line is altered. The changes in scale and orientation of the photograph caused by these rotations are illustrated in 7.6. The scenario presented here represents a perfectly flat terrain, where the terrain is uneven the scalar changes across the image become very complex.

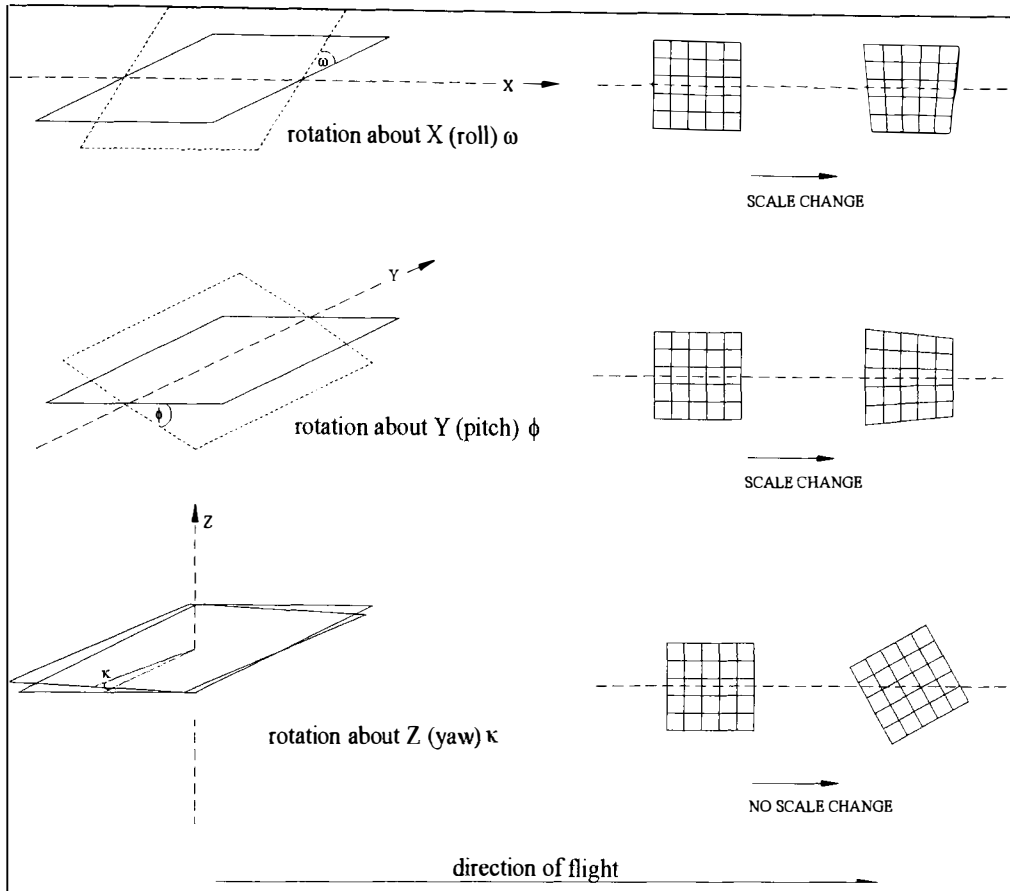


Figure 7.6 the effects of rotations in ω (roll); ϕ (pitch); κ (yaw) on scale and orientation of a vertical aerial photograph over flat terrain

7.2. ORTHOPHOTOGRAPHS

7.2.1. Introduction

The off-the-camera vertical digital aerial photograph has often been used inappropriately for the same purpose as its topographic map counterpart. Use of these unrectified vertical digital photographs as maps is common practice and may be attributed to the obvious spatial relationships between map and photograph, and to the often practiced method of fitting and matching consecutive photographs using digital image processing software to form a mosaic. Such uncontrolled mosaics do not have the metric or geodetic accuracy of the cartographer's map

giving a perspective view of the landscape, in contrast to the strictly orthogonal view of a map, and should not be used as maps.

The orthogonal view can be derived from a digital photograph by correcting for the attitude of the camera at the instant of image capture and by removing displacement errors resulting from the height of objects within the photo scene, collectively known as exterior orientation parameters. In addition, distortions due to camera parameters, known as interior orientation parameters, must be accounted for.

There are nine orientation elements of a near-vertical photograph to be addressed using photogrammetric techniques to produce an orthorectified photograph. The nine orientation elements are made up of six outer-orientation elements and three inner-orientation elements. Outer-orientation elements include three translations of the camera in cartographic space, represented by the eastings [X], northings [Y] and height [Z] of the camera above a datum plane, and three rotations of the camera, represented by the roll [ω], pitch [ϕ] and yaw [κ] of the aircraft. The inner-orientation elements which are known to a high degree of accuracy, upon camera calibration, include the calibrated focal length or Principal distance [f] of the lens and the location of the principal point as represented by the shifts in the x direction [PPx] and y direction [PPy].

The applied science of digital photogrammetry corrects for these errors, accounts for the distortions and derives reliable 3-dimensional measurements from the photograph supported by quality assurance reports. The fundamental premise upon which orthorectification is based is the derivation of height information using differential parallax in a stereo pair of (almost) vertical photographs.

7.2.2. Measurement of height from stereo photography

Human beings are able to perceive objects in three dimensions through a complex process in the brain that integrates two images of the same scene, viewed from slightly different positions because the eyes are approximately 6cm apart. If the same object is viewed first by one eye and

then by the other there is a change in appearance of the object. This difference in appearances of objects due to change in perspective is called 'stereo parallax' and is the basis of 3D stereo viewing and height measurement from stereo photography. Stereo photography emulates human 3D vision but unlike binocular vision where an object is viewed from 2 different positions simultaneously, a pair of photographs is taken from 2 different camera positions. A stereo pair of photographs consists of 2 adjacent overlapping photographs in the same flight line. The amount of parallax of a point is directly related to the elevation of the point and to the distance between the two exposures. This phenomenon can be used for the measurement of distance and height following a simple procedure represented diagrammatically in Figure 7.7. This procedure is summarised as follows.

- *The Principal Point (PP) is identified in both photographs.*
- *The conjugate principal point (CPP) is identified in both photographs – this is the relative location of the principal point in the one photograph, on the other photograph in the pair.*
- *The distance between the PP and the CPP is measured in both photographs, $Pb1$ and $Pb2$.*
- *The photographs are aligned with the PP and CPP on both photographs in a straight line.*
- *The distance between the top of the object in both photographs (dT) and between the base of the objects (dB) is measured.*
- *The average photobase (P) is calculated from: $P = (Pb1 + Pb2)/2$.*
- *The differential parallax (dP) is calculated from: $dP = dB - dT$*

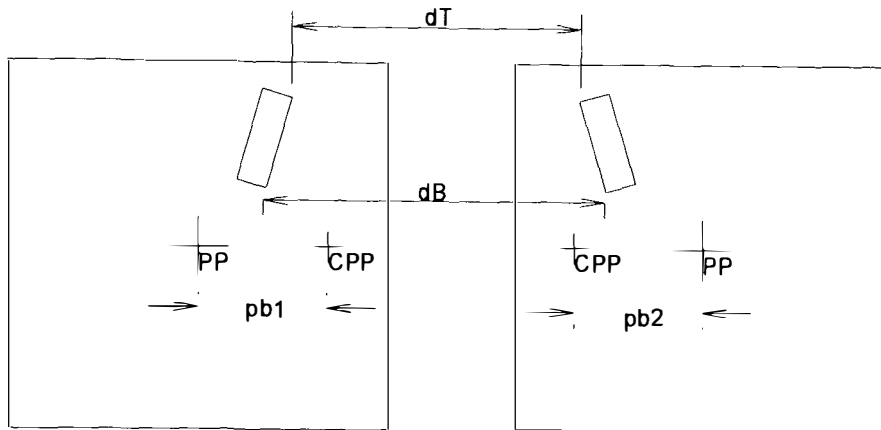


Figure 7.7 Height measurement from a stereo pair of photographs using differential parallax

The height may be calculated from:

$$H = A \times (dP / (P + dP))$$

Where: H is the difference in height between the top and base of the object. A is the altitude of the aircraft above the ground datum. dP is the differential parallax. P is the average base length. For accurate measurement absolute parallax should be used, this is the x coordinate of the object to be measured on the left image minus the x coordinate of the same object on the right image.

7.2.3. Stereo cover in a block survey

To capture photography with stereo coverage of a block requiring more than one flight line, sequential photographs must have at least 60% forward overlap and there must be about 20% side overlap to ensure complete coverage without gaps. Figure 7.8a shows the overlap for a single flightline and Figure 7.8b shows the overlaps for 2 flight lines. The degree of side lap can be varied and if a very high accuracy mosaic is required suffering the minimum effects of tilt and terrain distortion possible, the overlapping area can be increased so that a smaller central part of the individual models that are used to produce the mosaic is used.

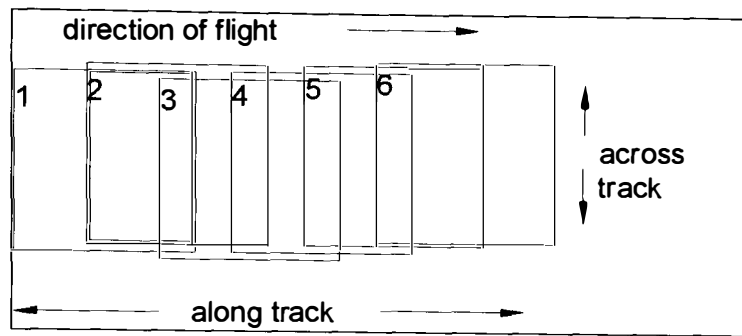


Figure 7.8a Forward overlap in a single flightline

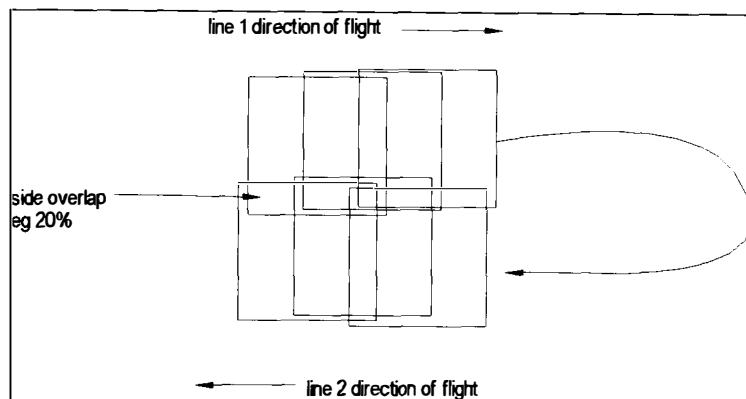


Figure 7.8b Side overlap in two flight lines

7.2.4. Digital photogrammetry

Until recently photogrammetric techniques for the extraction of elevation data from stereo pairs of photographs required expensive analytical stereo plotters (Welch, 1992) but softcopy photogrammetry is now becoming increasingly available on low cost PCs and Workstations. Walker (1999, p. 469) has remarked that (presently) the great majority of the imagery used in digital photogrammetry is not inherently digital but is obtained from digitising film images from metric aerial cameras using photogrammetric scanners. Recently there has been an upsurge in interest in the photogrammetric capabilities of digital cameras within the photogrammetric community (Mills *et al.*, 1996; Ahmad & Chandler, 1998; Robson & Shortis, 1998; Clarke *et al.*, 1998; Shortis *et al.*, 1998) and whereas the both the smaller array size cameras (such as the Kodak DS 200 and DS 420) and the larger array size (DS 460) have proved useful for close range

photogrammetry, Ahmad and Chandler have suggested that the DS 460 camera might also have potential where higher accuracy is not required and where the budget is minimal.

The increasing availability of digital cameras with larger array sizes is likely to give rise to a proliferation of the totally digital approach and in these early days of application of these new technologies it is important to push back the boundaries and develop new application areas and methodologies. even if the preliminary investigations do not yield such accurate results as the well established methods using metric photography and analytical stereoplotters. In this way, incremental progress can be achieved and in addition, advances in the technology can be implemented expediently as and when they become available.

This ideology is not without its critics, for example, Gooch *et al.*, (1999) believe that as digital photogrammetric systems become more sophisticated and the level of automation increases, the technical gap between the user and the system grows, leading to compromise and diminished benefits from the system. These types of concerns notwithstanding, one of the objectives of this study is to ascertain whether colour infrared digital imagery can be used to produce affordable, digital terrain models (DTMs) and orthophotography on a regular basis, that could be of use to the dune manager. The rationale for implementing this investigation is based on the premise that this is just the type of scenario that answers Ahmad and Chandler's description, where the budget is usually very small and there is no need for very high accuracy elevation models, as typically very little contemporaneous data exists and that some data is better than none, provided that a quality assurance report can be made available along with the data.

The particular photogrammetric software used here is VirtuoZo 2.0 running on a Silicon Graphics O2 workstation running under Irix, although a PC version also exists running under Windows 98 and NT. This will not be described in this chapter since the photogrammetric workflow will be described in the methodology in Chapter 8.

METHODOLOGY

8.1. INTRODUCTION

This chapter will document the methodology used for a totally digital approach to data collection for orthophoto map production using the ADPS since this has not been previously documented and has become an important aspect of this research in its own right. This methodology is not limited to use for this particular application so it has been written with the broader context of its application to digital aerial survey in mind.

To avoid tedium and for clarity, the details of the methods of analysis are better explained in chapters that will deal with individual case studies and particular analytical techniques. A general description of the data will be given here, but individual site descriptions will be included in the appropriate case studies. In this way the relevance of the analytical techniques used for each scenario will be readily apparent to the reader.

8.2. DATA DESCRIPTION

8.2.1. General description

The photographic data used in this research was acquired during the course of the 'DUNES' project, one of 29 projects within the ELOISE (The European Land-Ocean Interaction Studies) project cluster, sponsored by the European Union within its Marine Science and Technology (MAST) and Environment and Climate programmes. The 'DUNES' project was conceived as identifying the condition and vulnerability of sand dune systems using a suite of innovative tools designed for ease of use by the dune manager. The Aerial Digital Photographic System was a major component of this suite of tools and aerial images were acquired for many of the dune sites of south-west U.K., western France, and the Gulf of Cadiz.

It is not uncommon for geomorphological studies to have recourse to aerial photography which was captured for a variety of reasons and almost certainly without consideration for the particular requirements of geomorphological investigation (Thornes & Brunsden, 1997). Such requirements include the temporal frequency with which the data is captured since short sequences of long time interval may provide unsound evidence of geomorphological processes and lead the investigator to make erroneous inferences, sometimes with dangerous consequences. The data used in this study was not primarily intended for mapping change but rather for reconnaissance purposes and was therefore not ideally suited to the task of monitoring change in space and time. However, it was readily available and seemed to provide the opportunity to evaluate the digital camera, because it was of good quality, and was captured at reasonable intervals (1yr. and 2yrs.), albeit each epoch of data was captured with successive prototypes of the ADPS. It has been used with the shortcomings borne in mind.

Images of the U.K. and France have been selected to assess the usefulness of colour infrared photography to detect and / or measure a number of key parameters of interest to the dune manager. These include, for example, detection of indicators of anthropogenic pressure such as campsites, roads, car parks and pathways through the dunes and measurement of changes in morphological features such as the retreat / advance of the dune front, areas of bare sand, areas of vegetation units and the volume of blowouts. Four sites, one from SW England and three from France, have been selected as case studies to investigate the use of CIR digital imagery for particular types of analysis. These are:

- Ile d'Oleron, Western France, to measure dune front recession.
- Dossen, Northern France, to detect sediment redistribution.
- Ile de Noirmoutier. Western France to measure areas of blowout development and dune accretion.
- Holywell bay, South-West England, to measure volumes of morphological features and to assess the aerial digital photography for orthophoto map production.

A small scale map showing the locations of the 4 case study sites is given in Figure 8.1. Large scale maps are provided with each case study.

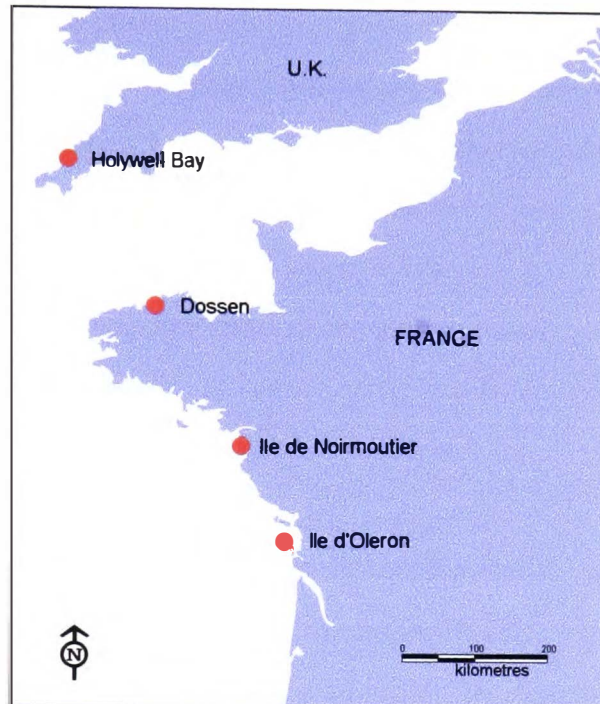


Figure 8.1 Map showing location of the 4 case study sites

Simple visual inspection of digital photographs can yield a wealth of information regarding the condition of dune systems and their hinterlands, but because the photographs are not rectified it is not possible to make absolute measurements of features on the ground. In the following 4 chapters, methods of analysis and measurement will be explored using 2D and 3D rectification and the results of different image analysis techniques will be presented.

For each of the case studies, brief site descriptions will be given, highlighting pertinent points, along with the results of the analysis and some discussion, and, although this might be an unconventional thesis format it is hoped that this approach will enable the reader to follow the thread of the work more easily.

8.3. DATA COLLECTION AND ANALYSIS

8.3.1. Organisation of the study

The cost of acquiring and processing aerial photography is relatively high, especially for cost-conscious research projects, so a methodology must be adopted which aims to achieve a maximum degree of accuracy as economically as possible. This remit requires an integrated approach to the process from planning to completion, and to this end a processing chain has been developed that provides a systematic approach enabling this aim to be achieved. It is convenient to divide the processing chain into 4 main elements, which follow logically from one to the next, although it is possible to enter or leave the chain at any one of the 4 main divisions depending on user requirements. These are shown in Figure 8.2 .

This processing chain has been developed and refined throughout the course of the research reflecting developments in computers and associated peripherals and in other new technologies as well as lessons learnt in the field and in the laboratory. The greatest driver has been the availability of new hardware and software such as new models of the digital camera, additional GPS receivers allowing differential post processing and real time satellite differential positioning, camera calibration software, photogrammetric software and image processing software .

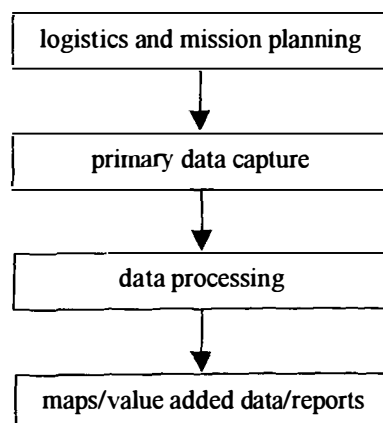


Figure 8.2 The 4 major elements of the processing chain

Each of these major divisions of the processing chain is subdivided into many parts and some of these are explained in sequence below.

8.3.2. Logistics and mission planning

Planning is an extremely important part of the data collection methodology since meticulous planning at the outset is the key to a successful operation. The first element of the processing chain is concerned with establishing a clearly defined purpose of use for the photography, planning the ground survey and planning the air survey. The major parameters that significantly affect quality, mission logistics and cost when adopting an all digital approach to map production are:

- the format of the camera
- the ground pixel resolution at point of capture
- the block area of the project site
- the survey altitude
- the required scale of the final map
- the compression method used for image data storage

Each of these parameters is addressed during logistics and mission planning. The components of the first major element of the processing chain for logistics and mission planning is shown in Figure 8.3.

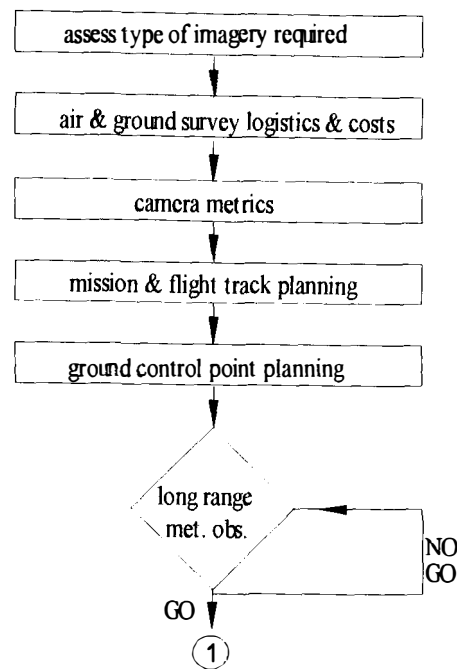


Figure 8.3 Logistics and mission planning

8.3.2.1. Assessing the type of imagery required

Defining application requirements to ensure that the imagery collected is fit for the purpose of use is not a trivial task because users are not usually familiar with specifying application requirements in digital terms (5.3.4). Ideally, the spatial resolution should be chosen so that the information needed can be acquired using the least data, because any oversights at this stage can result in inferior quality imagery and an exhausted budget. For example, the ground pixel resolution dictates the scale of the final map product, and it is of paramount importance that the digital photography is captured at a resolution that can satisfy the user's mapping requirements. An increase in the linear ground coverage of the pixel returns a reduction in the number of overlapping photographs and stereo models necessary to cover the project site. The number of ground control points required, storage and plotting media, data processing time and aircraft flying hours are all reduced with a corresponding cost benefit. This might at first seem to be attractive to the user, but results in a reduction in resolution of the digital photograph which diminishes the overall accuracy to which ground detail may be co-ordinated in both plan and height and may ultimately be unsuitable for the task in hand.

For some applications, e.g. vegetation mapping, colour infrared photography is required, but for other applications e.g. planning, the user may prefer true colour photography. In addition the user may need to comply with particular data standards or formats and may need to archive and distribute the data in a particular way. It is good practice to explore opportunities for 'added value' as this may affect the primary data acquisition parameters.

8.3.2.2. *Air and ground survey logistics and cost*

Air and ground survey logistics addresses issues such as relocation of the survey aircraft and crew from their base to the survey site. The type of terrain and ease of access are important considerations for ground control point collection planning and any photographic requirements which affect operations such as time of day, season or state of tide must be considered fully. All of these logistical factors influence the timing and the cost of the mission.

8.3.2.3. *Camera metrics*

Camera calibration allows interior orientation of the photographs during which process distortions due to camera geometry are removed (7.2.1). The principals of photogrammetry depend on the accuracy of the camera and in past few years there has been a wealth of research involving the metrics of both small format analogue and digital cameras (Short, 1992; Mills *et al.*, 1996; Mills & Newton, 1996; Fraser, 1997; Robson & Shortis, 1998; Clarke *et al.*, 1998) relying on self calibrating bundle adjustment to calculate the camera parameters.

The DS 460 camera, fitted with a 28mm lens, set at infinity, was calibrated from a test pattern projected onto a near planar laboratory wall. A multi-station convergent network of 8 images of the pattern were recorded and imported to 'EOS Systems Photomodeller Pro' camera calibration software which automatically calibrates the camera as shown in Figure 8.4.

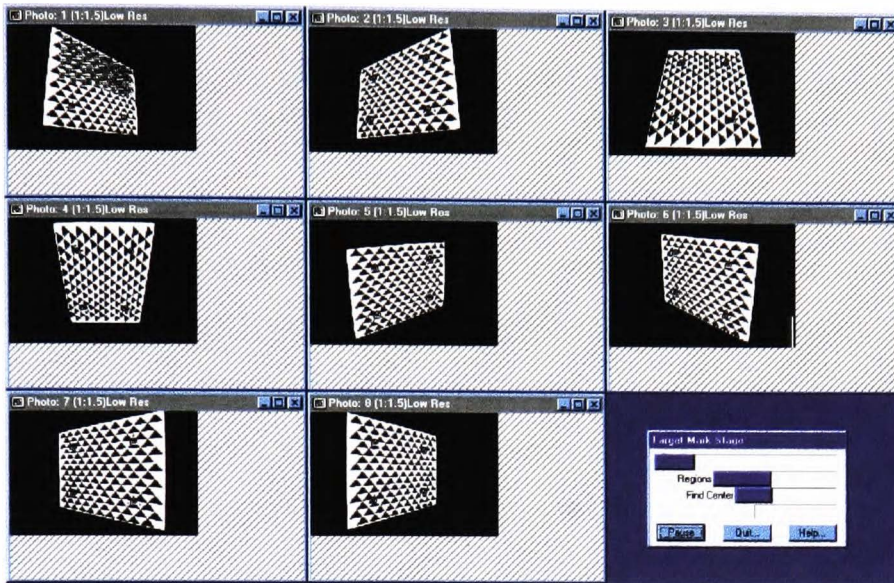


Figure 8.4 Convergent network of 8 images of the test pattern projected onto a near planar wall

In this way the principal distance (f), principal point offset from image centre (PP_x and PP_y) and the radial distortion (K_1) were calculated, these are shown in Table 8.1.

f (mm)	PP_x (mm)	PP_y (mm)	K_1
28.8458	14.5650	9.6553	0.00014600

Table 8.1 Camera calibration parameters for the DS 460 CIR camera with a 28mm focal length lens at infinity

Calibration should be repeated at regular intervals (air survey cameras are typically calibrated every six months or so) and because this is such a simple procedure it can be repeated before each survey if necessary.

8.3.2.4. Mission and flight track planning

Mission and flight track planning was achieved using the interactive mission planner described in detail in 6.6. Following consideration of the type of photography required, the dimensions of the survey block, the minimum and maximum elevations within the survey block and the desired ground pixel resolution of the imagery the number of images per line and the number of flight lines is calculated. From this, the required image data storage capacity as well as the density of ground control points that were needed for rectification is calculated. Navigation planning is all-important and it is the responsibility of the navigator to ascertain whether there are any flying restrictions in and around the survey block. Navigation is by autonomous GPS using the method described in 6.6.6.

8.3.2.5. Ground control point planning

Where accurate detailed maps are available it is often possible to plan the ground control point collection before the air survey has taken place. Where existing maps are poor, or in locations where there are no maps, but where there are many natural targets it may be necessary to plan control point collection after the photography has been collected when potential targets can be identified in the photographs. Where there are no maps and few or no natural targets, such as in the intertidal zone, location of artificial targets is planned and implemented immediately before the survey. In the latter case careful planning and team co-ordination is essential to ensure that the survey is scheduled for low tide with enough time for deployment of the targets so that they are in place and clearly visible when the aircraft passes overhead.

8.3.2.6. Meteorological constraints

Regardless of any human imposed conditions the ultimate controlling factor over an aerial survey is the weather and in particular, cloud cover. It is essential to consult a long-range (5 day) weather forecast before the decision to mobilise can be taken for an aerial photographic survey. The DS 460 camera has been shown to be capable of acquiring imagery even in overcast conditions and can often be flown below cloud cover when traditional film based survey cameras could not (6.3.3.2).

8.3.3. Primary data acquisition

The components of the primary data capture element of the processing chain are set out in Figure 8.5

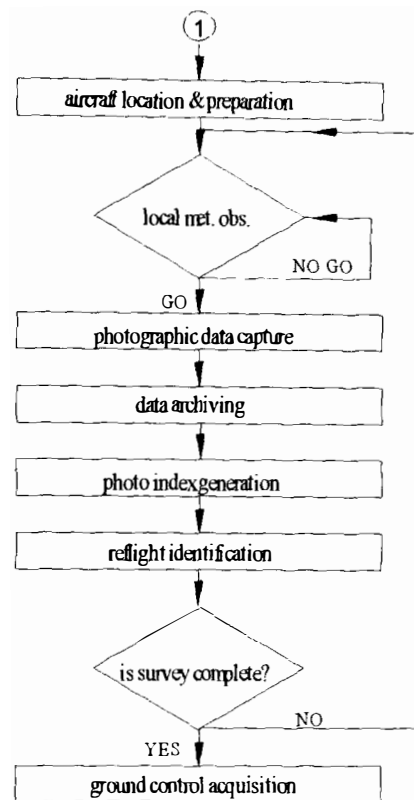


Figure 8.5 A processing chain for primary data acquisition

8.3.3.1. Digital image data

Three aerial photographic surveys were flown of the dune sites described above in June 1996, June 1997 and May 1999. In all cases the camera was mounted vertically in a light aircraft (Partanavia) and for each survey the camera was fitted with a 28 mm focal length lens and an Omega 650BP300 CIR filter to acquire colour infrared photography. To maintain continuity and comparability of the data sets each sortie was flown at a nominal 90 knots, 4,090 ft above ground level (AGL) resulting in a pixel resolution of approximately 40 cm. Photocoverage, flight line spacings, required survey ground speed, aircraft altitude, magnetic media requirements and camera framing rates were calculated using the flight planner (6.6). Flight track waypoints and aircraft altitude from the planner were uploaded to a GPS receiver and routes were constructed.

enabling the GPS to automatically compute the navigation information for use in flight. Table 8.2 details the date and type of imagery collected at each of the dune sites.

Dune site	June 1996	June 1997	May 1999
Holywell Bay	DCS 420 CIR	DCS 460 CIR	DCS 460 CIR
Dossen	DCS 420 CIR	DCS 460 CIR	DCS 460 CIR
Ile de Noirmoutier	DCS 420 CIR	DCS 460 CIR	DCS 460 CIR
Ile d'Oleron	DCS 420 CIR	DCS 460 CIR	DCS 460 CIR

Table 8.2 Camera series and filter type used for each survey at each site

8.3.3.2. Data archiving and photoindex generation

Data archiving is a very important part of digital air survey and again must be carried out in a disciplined manner if data loss is to be avoided. Unlike film based survey where the film is stored until it is processed, often at the end of a mission, digital data should be archived as soon as possible after landing. This approach ensures that the data are written to a read only medium eliminating the possibility of overwriting the files, the storage cards are cleared for the next sortie, and the data can be checked for missed frames. In addition the images are ready for use within hours of the survey. In this case the data were archived at the end of each sortie to CD-ROM in TIFF-ep format. A searchable photo index was produced in MapInfo for ease of retrieval of image frames. Each image is indexed by type, location, camera parameters and archive details as shown in the example from Ile d'Oleron, France, in Figure 8.6. Image centres are denoted as pink or red dots on the map for DS 420 or DS 460 respectively.

8.3.3.3. Reflight identification

One of the advantages of digital aerial survey over analogue is that the data can be quality controlled for reflight identification whilst the aircraft is still on site. Thumbnail images may be

accessed and viewed at the same time as data archiving so that any missed frames can be captured as soon as is convenient. When the air survey is complete ground control data can be collected.

Figure 8.6 has been removed from the digitized thesis for copyright reasons.

Figure 8.6 Image index in MapInfo for easy retrieval of image locations

8.3.3.4. *Ground control data*

Ground control for some of the imagery was acquired using post processed differential GPS with 2 Magellan ProMark X CP receivers for the 1996 and 1997 surveys and using real time differential GPS with the Omnistar system for the 1999 survey. In each case ground control data was collected after the survey was flown so that hard copy of the images was available for use in the field to ensure adequate distribution of ground control points. This method of ground control data collection limited control of the photographs to the landward side of the dune front as it was not practical to deploy targets in the intertidal zone owing to the geographic extent of the project area and the financial constraints of the project budget.

8.3.4. methodology for data analysis

8.3.4.1. Data processing and data analysis

The method chosen for data analysis is directly related to the the type of imagery, the available ground control and the intended purpose of use. Figure 8.7 is a simplified view of the likely routes taken depending on the type of imagery available. The actual routes chosen will be explained in more detail in the relevant case studies but an overview of image rectification and orthophoto production will be given, as digital photography presents a special case for image processing and photogrammetric software.

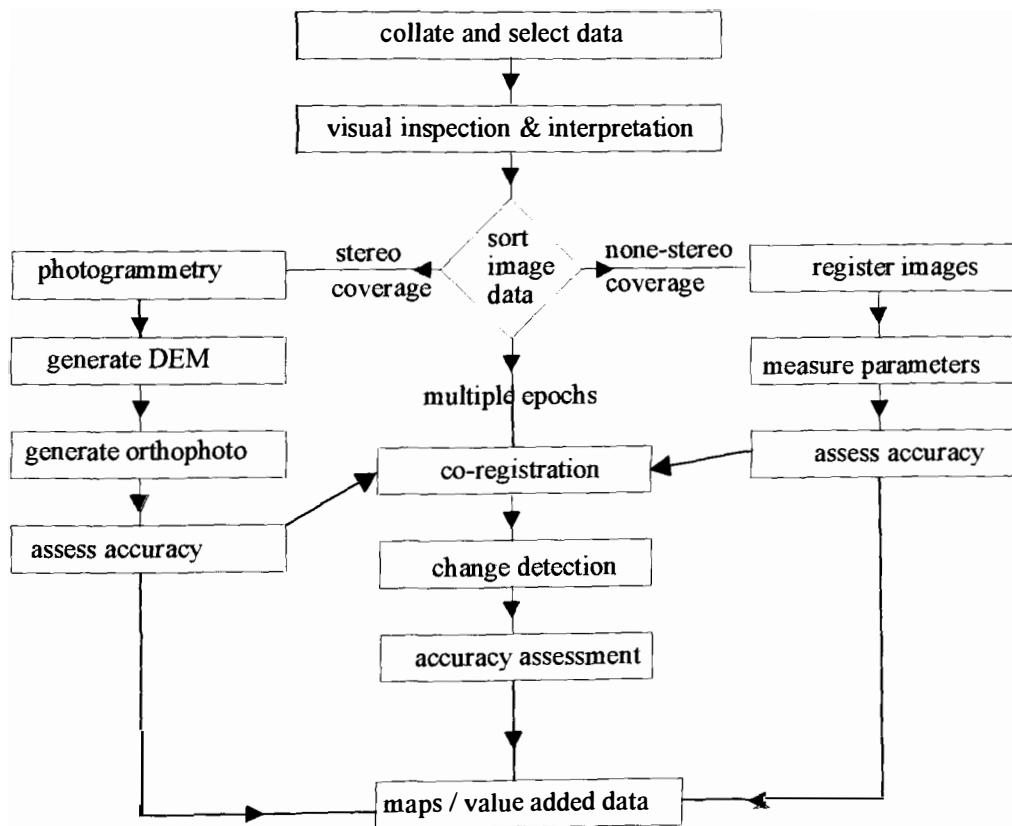


Figure 8.7 The image analysis routes for stereo and non-stereo digital photography

8.3.5. Geometric correction

Geometric correction rectifies the geometric errors inherent in imagery. There are a number of methods used to correct for geometric errors and the type of algorithm that is chosen and the

degree of accuracy of the the result depends largely on the type of imagery and control data that is available. The coordinate space of an image defines the location of the image in cartographic space, if it has been corrected using real world coordinate ground control. Without real world coordinates, an image may be corrected to another image, in which case its coordinate space is its location in relation to that other image. Both of these types of correction have been used in this study. In some sites adequate ground control was available for rectification to cartographic space but at other sites, ground control was impossible to achieve either because a GPS receiver was not available at the time and / or because the features on the photographs were not recorded on IGN maps.

Polynomial correction is usually used to transform an image from an unknown (raw) projection into a known projection where ground control is available in the x and y dimensions only (a 2D solution). Ground control points are located on the raw image and matched either with points on an image in the desired projection, or with coordinates taken from a map. The algorithm that is used models the distortions in the image by fitting a mathematical function through the ground control points. The image is then rectified using a best fit solution, often referred to as 'rubber matting' (Earth Resource Mapping Pty Ltd, 1999).

Of the three polynomial algorithms, namely linear, quadric and cubic, linear warping requires the least number of ground control points but delivers the least accurate solution. A quadratic solution requires more ground control and provides a better fit than the linear solution and the cubic polynomial which requires yet more ground control delivers the best solution of the three. Polynomial transforms reduce global distortions in the image but they do not resolve local distortions within an image. To remove the effects of camera distortions and displacements in an image a camera model and a digital elevation model (DEM) are required (to provide control in the z dimension) giving a 3D solution. Using stereo imagery and photogrammetric software it is possible to generate a DEM which can then be used to create an ortho-rectified image. This approach significantly improves the geometric rectification but also increases the cost. There is a clear need for both 2D and 3D rectification procedures, as the lower cost 2D solution is often

adequate for coarser resolution monitoring and mapping, whereas investigations requiring high accuracy measurements may have recourse to the more accurate 3D solution. One of the aims of this study is to develop an appreciation of the methodologies involved in digital photogrammetry for orthorectification and this is outlined in 8.3.6

8.3.6. Photogrammetric processing

8.3.6.1. Defining the input and output parameters

The production of orthophotos using softcopy photogrammetry involves a straightforward set of procedures where the computer is provided with the basic data needed to perform the calculations. In the first place the survey block is defined which establishes the number of lines, number of frames per line, imaging scale, the direction of flight, the magnitude of the overlaps and the required output resolution. Gooch and Chandler (1998) have advised that great care must be exercised in defining the strategy parameters which control the production of the digital elevation model (DEM) as the wrong specification can have a significant effect on the overall accuracy of the elevation model. Virtuozo, the software used to process ADPS imagery can generate the correct strategy parameters based on a set of facts identified in the block and model setup facilities where data input and output parameters are defined. Figure 8.8 is a screen grab of the block setup window showing the input and output parameters that are specified.

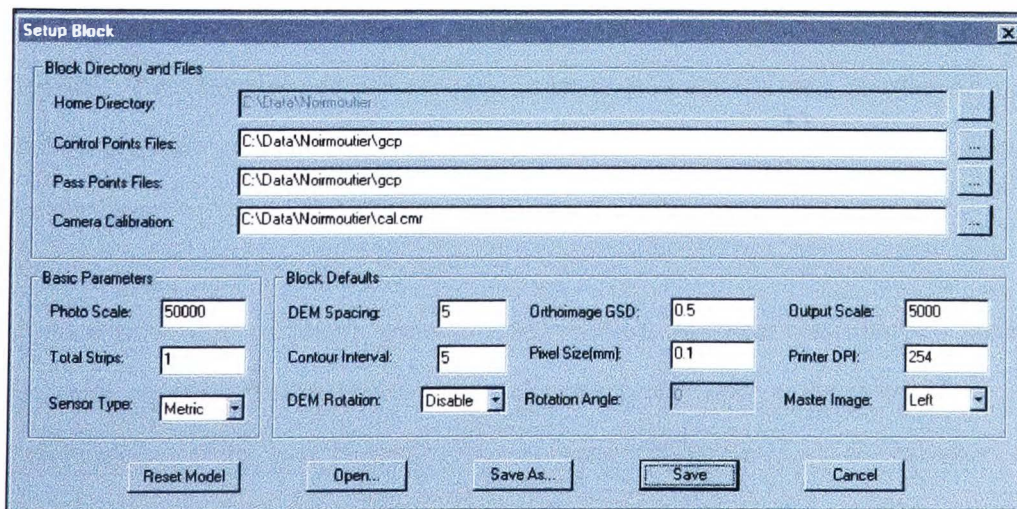


Figure 8.8 the block setup window showing input and output parameters

8.3.6.2. *Interior and exterior orientation*

Digital images present a special case for off the shelf photogrammetric software since most packages have not been designed with digital photographs in mind, rather they have been designed for large format photography where fiducial marks at the four corners of the photographs are at a known calibrated distance from the principal point, enabling an interior orientation to be calculated. The absence of fiducial marks is a potential problem, but digital images do not suffer from the problem reported by Short (1992) whereby small format film image negatives have rounded corners. Instead, digital images can be considered as metric since there is no appreciable distortion of the CCD under normal operational conditions, and the corners of the image are identified as fiducials. This information is recorded as an image mask in the camera parameter file along with the camera calibration details. The interior orientation of both the left and right images in each model is calculated using the camera calibration data and the image mask, this procedure removes distortions in the image due to camera distortions and relates the image coordinate system to the camera coordinate system, providing accurate mapping from ground space to image space.

8.3.6.3. *Relative and absolute orientation*

The ground control points are recorded in a GCP file to enable relative and absolute orientation of the image pairs. Ground control points are identified on both the left and right hand images for each model (conjugate points). Following the input of two or three points on both photographs in the model, Virtuozo is capable of finding the conjugate point in the second image with a good degree of precision when the remaining control points are identified in the first image, allowing a considerable saving in time over other software packages. Points can be edited by the user.

An automatic relative orientation operation which typically generates more than one hundred common points relates the overlapping areas of the left and right images. The entire overlap area of the image pair is displayed on screen to give an overview and a high zoom window allows the user to position the point correctly. Figure 8.9 shows the relative orientation window, matched points are numbered and depicted on the screen with red crosses.

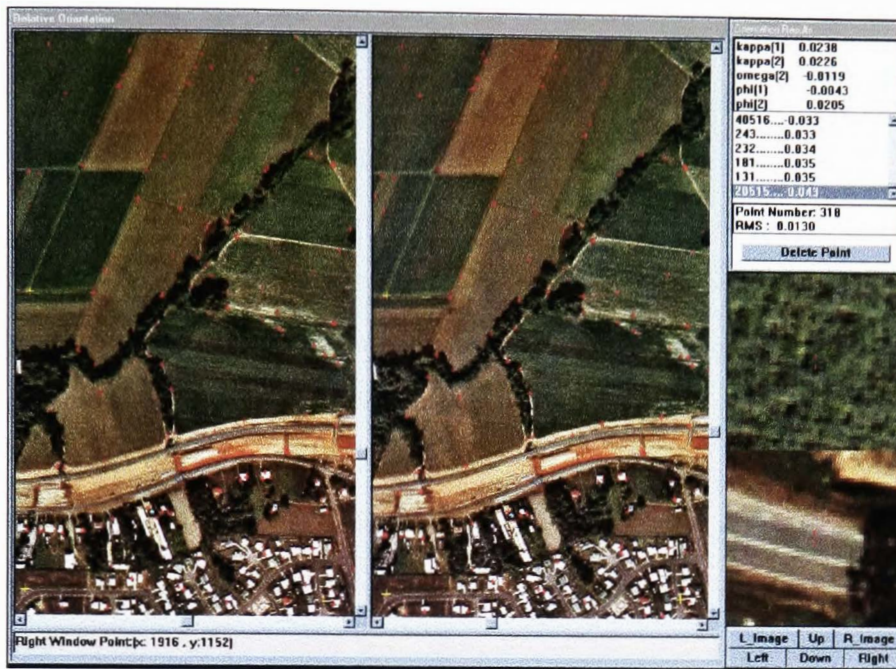


Figure 8.9 The relative orientation window in VirtuZo

The y-parallax residual errors for each related point is then calculated and the left and right portions of the stereo model are resampled to remove y-parallax so simplifying the calculations required to solve for elevation. The images are then matched so that x-parallax can be calculated and hence the elevation. In VirtuZo, image matching is accomplished by a set of algorithms that use probability relaxation and neural network techniques (Zhang *et al.*, 1996) and a full explanation of these may be found in the paper by Zhang *et al.* (*op. cit.*) The reliability factor for each conjugate pair describes the matching reliability giving the user guidance on editing unreliable points. The match editing window is a stereo view of the model that enables the user to edit points, lines and polygons by smoothing, interpolation, surface fitting and rematching. Absolute orientation using the ground control points allows the stereo model to be mapped into a real world co-ordinate system.

8.3.6.4. Generation of the DEM and orthoimage

There is sometimes confusion over the terms DEM and DTM and in VirtuZo both are used in the documentation to mean either one of two data sets. To some, a DEM is the unedited version of the

data set where, for example, the heights of buildings are included in the model and a DTM is the version of the data set where buildings, trees, telecom masts *etc.* have been edited out of the model and only the actual land elevations appear in the model. The definition put forward by Maune, (1996, p 131) states that “*The term DEM is the digital cartographic representation of the elevation of the land at regularly spaced intervals in x and y directions*”. The DTM as defined by Maune “*incorporates the elevation of significant topographic features on the land which are irregularly spaced so as to better characterise the shape of the land*”

In VirtuoZo, the DEM is created on a regular grid and the DTM is created on an irregular grid but either of these may or may not be edited to remove features and / or anomalies. Anomalous elevations or ‘spikes’ occur in the data due to matching problems areas such as the sea where the entire landscape is moving. The orthoimage is created based on the DTM and the corresponding original image.

Using conventional photography and photogrammetric techniques, the heights of well defined points can be obtained with a precision of 1/ 10 000 of the flying height (Slama, 1980; Wolf, 1983) and for a typical flying height of 1500m this corresponds to a vertical position of $\pm 0.15\text{m}$ (With a 150mm focal length lens this would capture photography at 1:10 000 scale). For softcopy photogrammetry vertical accuracies equivalent to 0.5 to 1 pixels have been reported by Brown & Arbogast, (1999). Manzer, (1996) has reported accuracy of 50 microns at the photo scale and to make a direct comparison with Slama’s and Wolf’s statement, this equates to an accuracy of 50cm for a 1:10000 image using a photogrammetric quality scanner.

8.3.6.5. Mosaicing

Mosaicing is the combination of several images into an image mosaic covering a (usually) large area (Afek & Brand, 1998). When the individual images are orthorectified, the mosaic may be used as a map. Mosaicing is a fully automated process in VirtuoZo and only requires the operator to select the area to be mosaiced.

8.4. SUMMARY

The advantages of using a system such as VirtuoZo is that much of the processing requires very little human interaction once the parameters have been defined. With the increasing availability of digital technologies, it is quite feasible that these tools will be within the reach of many environmental managers and that they will provide a cost effective way of monitoring the natural world, especially when the misgivings put forward by the experts in the various fields are addressed.

There have been a number of studies involving aerial photography of sand dune systems and photogrammetric processing (van der Hagen *et al.*, 1998; Droesen, 1999) and several studies investigating the use of digital photography for photogrammetric purposes (Mills *et al.*, 1996; Ahmad & Chandler, 1999). In addition, Eleveld *et al.*, (2000) have investigated the use of video to derive relief of sand dunes on the island of Ameland in the north of The Netherlands, and recently, Livingstone *et al.*, (1999) have compared aerial video and digital photography using a hand held Kodak DS 460 camera. for terrain modelling on a coastal spit, but this is perhaps the first investigation applying digital photography to measurement of change in sand dune systems and is an incremental step in the assessment of the utility of the cameras.

CASE STUDY 1 ~ measurement of recession at Ile d'Oleron

9.1. INTRODUCTION

Visual inspection of 3 epochs of digital photography acquired in 1996, 1997 and 1999 revealed what appeared to be substantial changes to the dune site at Ile d'Oleron, including evidence of overwash lobes and dune recession. This analysis will focus mainly on the dune recession between the beach-front car park on the D126E, and the distal end of the system around the Passe de Gatseau, but other changes such as the significant overwash deposits, particularly at the southern end of the system, will also be highlighted. Only limited GPS data for ground control was available for rectification, but sufficient path intersection points were available from a topographic map (IGN Ile d'Oleron, 1330 OT 1:25 000) to enable first order correction. In addition, a dune cliff recession map independently surveyed by the Office National des Forets (ONF) was available to provide an independent check on the recession rates obtained from the digital photographic surveys.

9.2. SITE DESCRIPTION

Ile d'Oleron lies equidistant between La Rochelle and the mouth of the R. Gironde. The island is about 27 km long and about 12 km at its widest, the long axis trending NW / SE. Figure 9.1 is an outline map of the island with an inset showing its relationship to the mainland.

Figure 9.1 has been removed from the digitized thesis for copyright reasons.

Figure 9.1 Outline map of Ile d'Oleron with inset showing La Rochelle to the north and the River Gironde and Bordeaux to the south

Much of the northern half of the island is underlain by a solid basement in the form of a rock platform, whereas south of the Plage de Vert Bois there is no solid geology exposed at the surface. A large west facing dune complex stretches almost the whole length of the island, although it is rather patchy in the north. The final 12.5 km south from La Perroche to the southern tip of the island consists of a massive dune complex of over 1700 ha in area, clothed in the planted Forêt Domaniale de St Trojan. The forest and the dune system are maintained by the ONF. Figure 9.2 shows the extent of the dune area, the distribution of campsites and car parks, the major paths and tracks through the dunes, the extent of the forest and the region of interest within the dune system outlined in red.

Figure 9.2 has been removed from the digitized thesis for copyright reasons.

Figure 9.2 Map of the southern end of Ile d'Oleron showing study area

In the past, a seaward growth of the dunes in this region of interest has been recorded, and between 1864 and the end of World War 2 just above 1 kilometre of accretion had occurred in a westerly direction (IGN TOP 25 1333 OT). Recent (1999) observations made in the field and in discussion with the local ONF manager confirmed that this coastline is now retreating.

Accounting for this erosion and coastal retreat is not the principal purpose of this case study but it is useful to have some understanding of the processes at work and although it is not possible to give a comprehensive analysis here, some of the factors and processes can be readily identified in the field and these are reported below.

- First, longshore drift of sand southwards along the west face of the island has been restricted by the construction of numerous groynes (few of which are marked on the topographic maps) and harbour installations as at La Perroche and Cotiniere (some 10 km to the north). These have undoubtedly interrupted sand supply to the south depriving the beach and hence the dunes of their primary sediment supply. Plate 9.1 is a CIR aerial view of the harbour at La Perroche with the harbour wall at top right, submerged pipeline and a substantial stone-block groyne on the beach at far left. This is the second in a series of five such groynes, the next three to the south of this one.

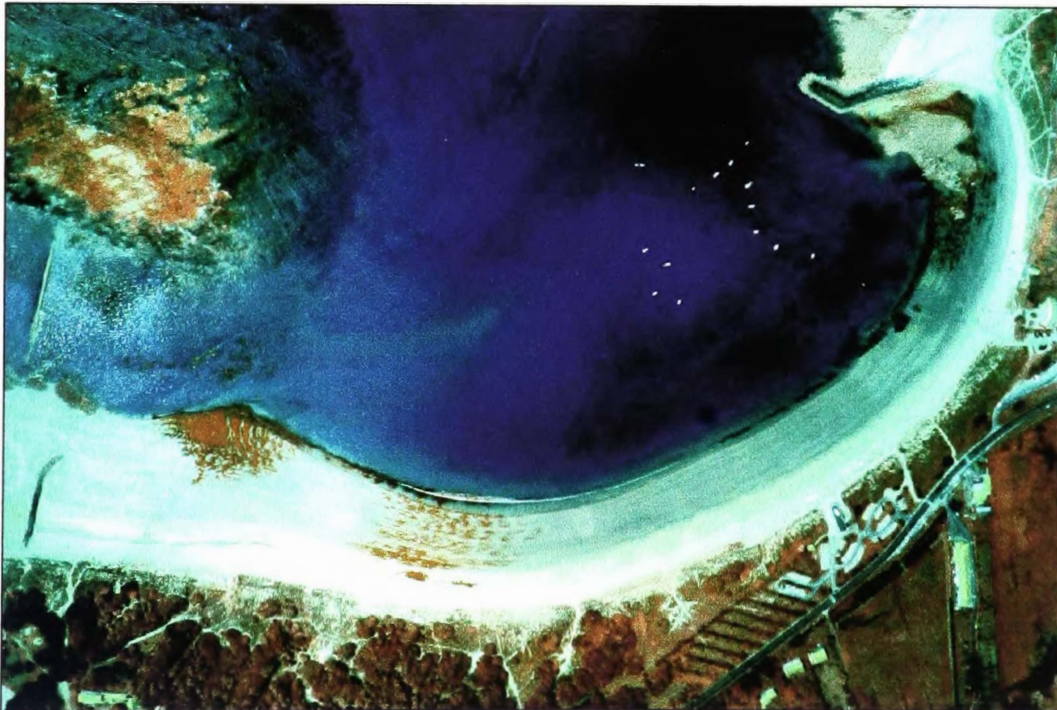


Plate 9.1 Aerial view of the harbour at La Perroche, Ile d'Oleron

The impact of these groynes on sediment supply to the dunes is exacerbated by the fact that they have been constructed so that they run out across the beach to meet a rocky outcrop, thus causing a much larger obstruction to sediment flow than would have resulted from the groynes alone, with sediment diverted a further kilometre or so off shore. The small town of la Perroche lies immediately behind the harbour.

- Second, the development of the forest cover on the dunes has reduced the (substantial) former exchange of sand between the dunes and the beach. Westerly winds still transport sand from the beaches and the bare dunes inland, but the forest cover now traps the sand and prevents the reverse flow, especially during winter when easterly winds would have returned sediment to the shore.
- Finally, whilst Ile d'Oleron has benefited economically from the growth in coastal recreation, some sites now show considerable wear from human pressure. The result of this sediment starvation and trampling pressure is manifested in erosion of the dune face to form sand cliffs, and devegetation of the leading edge of the dunes, exposing them to both wave and wind erosion. Plate 9.2 shows the cliffed dune around the mid-point of the region of interest where the cliff face is around 2 m high. Successive strand lines can be seen, the highest of these having reached the toe of the cliff, evidenced by the seaweed stranded on the beach. This photograph, taken in September 1998, shows how the dune is prone to very rapid erosion through wave attack, especially in stormy conditions.

According to a map of the dune front provided by the ONF, the rates of retreat of the dune face in the three years between 1995 and 1998 ranged from 15 m in the north of the system, to 70 m at the distal end of the system. This map was produced from measurements made at 100 m intervals along the dune, normal to the coastline.



Plate 9.2 Sand cliffs resulting from rapid erosion of the dune front, Ile d'Oleron, Sept. 1998

The changes in this dune complex detailed above, and in particular the rapid rates of retreat, provide an excellent opportunity to assess the usefulness and accuracy of digital photography in detecting linear change, namely in the retreating line of the dune cliff.

9.3. IMAGE REGISTRATION

9.3.1. Mosaicing and registration

Since the image data was captured using a photographic system which was continuously evolving and the data was primarily intended for reconnaissance purposes, the images were not ideally suited to the task of registration and mosaicing. For example, the forward overlap at 20% was inadequate for photogrammetric processing in the 1996 and 1997 data sets and in addition, the imagery had been captured following the coastline rather than following planned flight lines with the result that the relative orientation of adjacent photographs was sometimes well in excess of ten degrees. Plate 9.3 below shows the relative orientations of three frames from the 1996 epoch

demonstrating the fairly severe rotation as the aircraft followed the coastline and the small forward overlap that was achieved with the DS 420 camera mounted with the short axis parallel to the flight line. Accurate image registration, therefore, proved challenging for the various types of software available and so slightly unconventional techniques were required to achieve the desired results.

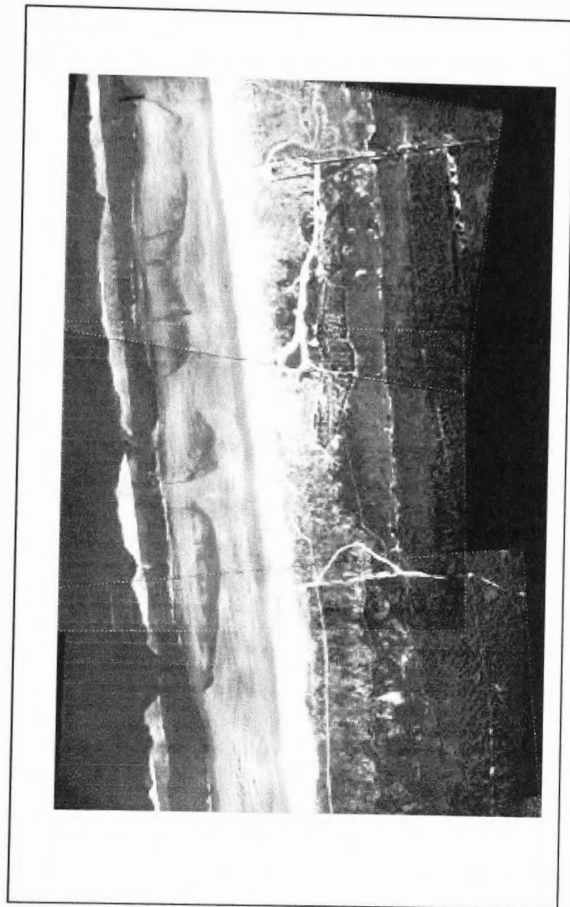


Plate 9.3 Relative orientation of the photographs of Ile d'Oleron from the 1996 epoch

During the 1999 survey the camera was mounted with its long axis parallel to the flight track, enabling stereo coverage of the dunes. This greater along track coverage, and the 60% overlap between photographs proved easier than the 1996 and 1997 photographs (which had been captured with the short axis parallel to the flight line) in producing a mosaic. The 1999 survey therefore became the base mosaic, registered to UTM projection, WGS84 datum, Zone 30 North. The 1996

and 1997 photographs were then registered to the 1999 mosaic. Registration and mosaicing were carried out in ER Mapper v. 6.1, and in the absence of elevation data, this was in 2D mode (8.3.5). This type of geo-correction yields less accurate measurements than orthophoto rectification but it is still a valuable source of information, and is a far more cost efficient option where very high accuracy is unnecessary. The net result was three co-registered mosaics, permitting an assessment of changes between 1996 - 1997 and 1996 - 1999 surveys.

Since this is a coastline in retreat, to avoid confusion the 1996 mosaic was declared the reference mosaic even though the 1999 images were used to produce the base mosaic. In this way the erosion rate of the dune front could be recorded in chronological order.

9.3.2. Error analysis

9.3.2.1. Determination of registration error

In investigations like this where much of the landscape is potentially mobile it can be difficult to say with certainty whether differences in location of features between epochs are due to error or due to change or to both. Never-the-less, it is important to try to quantify the error as erosion rates can only be as accurate as the data from which they are derived. Apart from any errors inherent in the data, errors introduced by the measurement methods must be accounted for and in this case the primary source of measurement error was thought to be in misregistration of the mosaics. Therefore, before the rate of coastal retreat could be measured co-registration errors between the mosaics were investigated. An example of misregistration can be seen in Plate 9.4 which shows part of the 1996 mosaic in red and the 1999 mosaic in green. Regions of misalignment of the path show clearly in either red or green. Care in interpreting such features must be exercised as this apparent misalignment could actually have been caused by erosion of the sides of the path rather than misalignment (although here the more likely cause is misregistration since other features in the image show similar red / green misalignment). For this reason, any measurements made involving paths should use the centre of alignment to minimise errors.

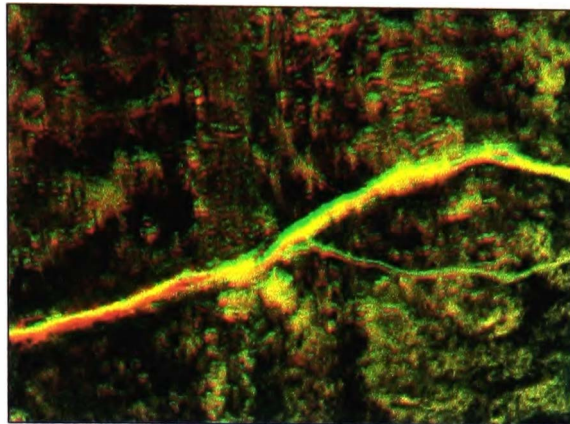


Plate 9.4 Composite image showing misregistration between images

To measure this misregistration the mosaics were imported to MapInfo Professional 5.5. Forty-six randomly distributed features occurring in all three epochs, including trees and vegetation units, path junctions, buildings and other human artefacts, were identified and digitised. The x and y coordinates of each individual feature were compared, and the relative registration errors between the 96 - 97 and 96 - 99 mosaics were determined. The results are recorded in Table 9.1. This error analysis also includes digitising errors but it was thought unnecessary to separate the two here.

	96x-97x	96y-97y	96x-99x	96y-99y
Minimum (m)	-3.21	-2.58	-2.85	-3.6
Maximum (m)	1.9	1.77	2.12	3.21
Mean (m)	0.06	-0.06	-0.12	0.4
Std. Deviation	1.13698	1.05456	1.2247	1.6159
Count	44	44	44	44
RMS (m)	1.1278	1.0445	1.2699	1.7671

Table 9.1 Summary statistics for misregistration between the 1996 mosaic and the 1997 and 1999 mosaics for Ile d'Oleron

Table 9.1 shows that for the 96 - 97 image, the RMS errors for both dimensions are of the order of 1 m indicating that, on average, the dune cliff could be located to within ± 1 m of its position relative to the 96 image. The errors for the 1999 mosaic are slightly larger at 1.26 m in x and 1.76 m in y. For this type of application this could be regarded as a reasonable level of accuracy (Moore, 2000; Anders & Byrnes, 1991) who have reported that on NOS-T sheets the shoreline is mapped to 0.5 mm accuracy at the map scale but that stable features are mapped with greater accuracy and commonly to ± 3 m)

9.3.2.2. Determination of the sample size

A number of observations were taken to determine the sample size required for the error estimation at the 95% confidence level. A sample size calculation based on standard statistical analysis using the formula:

$$2\sigma\bar{x} = 0.5 \quad \text{or} \quad 2\left(\frac{\sigma}{n}\right) = 0.5$$

(McClave & Sincich, 2000)

where σ is the standard deviation of the sample, \bar{x} is the sample mean, n is the number of observations required and 0.5m is the chosen confidence interval (tolerance) about the population mean.

The results of this calculation are given in Table 9.2. These results confirm that 42 samples were sufficient to satisfy the error estimation requirements of the worst case registration and since 44 observations had already been made no further observations were necessary.

	96x-97x	96y-97y	96x-99x	96y-99y
Min sample size	20.68386216	17.79367358	23.99875095	41.78261311
	(21)	(18)	(24)	(42)

Table 9.2 Minimum sample size required to assess the error in registration

The errors quoted here must be borne in mind where any measurements are discussed and a similar table of error estimation will be provided for each case study. To avoid tedium, the potential error will not be quoted alongside each measurement.

9.4. MEASUREMENT OF THE DUNE CLIFF RETREAT

The mosaics were opened in turn in MapInfo and the dune cliff crest lines were digitised. This enabled simultaneous display of the cliff crest in all three epochs. As well as the crest line, there were a number of other linear features on the photographs including: tide marks, strandlines, tyre tracks and the cliff base, therefore, to ensure that the correct line was chosen, a stereo viewer was used to scrutinise hard copy of pairs of images where they overlapped.

It is common practice in shoreline mapping from aerial photography to use the line between wet and dry sand as a proxy for shoreline position (Morton, 1991; Shoshany & Degani, 1992) and to make measurements from this line but this is well known to vary with tidal and seasonal changes (Dolan *et al.*, 1980; Smith & Zarillo, 1990) as well as with tidal range, beach slope, sediment size, wind and wave height (Dolan *et al.*, 1980). To avoid errors associated with measurements from an unreliable datum, a baseline coinciding with UTM 30N easting 635900 was established, running approximately 4000m from the north to the south of the area of interest. Using random number tables, 90 points were identified between the northern and southern limits of the baseline. Figure 9.3 shows the positions of the sample points numbered at every 10th point along the baseline, with points 1 and 90 at 55.25 m and 3971.19 m from the start of the baseline respectively.

Figure 9.3 has been removed from the digitized thesis for copyright reasons.

Figure 9.3 Sample point locations along the baseline, Ile d'Oleron

Orthogonal transects were then constructed from each random point located on the baseline to intersect the dune cliff line for each epoch. The location of the intersection in the x direction was recorded for each of the randomly generated y values and because the photographs were registered to a planar coordinate system, erosion of the dune front at each of the points was readily quantified by subtraction of the x coordinates. The digitised dune cliffs, base line and orthogonals are shown in Figure 9.4. This map shows part of the area of interest between sample points 50 and 71 where considerable erosion has occurred.

Figure 9.4 has been removed from the digitized thesis for copyright reasons.

Figure 9.4 Position of the dune cliff in 1996, 1997 and 1999, Ile d'Oleron

Table 9.3 gives the results of the analysis of the dune front positions with reference to the 1996 image at each of the 90 data points. Negative values occurring in 96-97 column denote accretion. From Table 9.3 it can be seen that between 1996 and 1997 the minimum and maximum values for retreat of the dune front were -5.17 m (accretion) and 28.12 m; for 1997 to 1999 these values were 0.46 and 48.14 and for 1996 – 1999 the minimum erosion measured was 2.58 m and the maximum 58.47 . These rates of erosion are in general agreement with the ground surveyed map provided by the OFN, and shown in Appendix 1, according to which, between 1990 and 1998 retreat of the distal end of the spit was of the order of 120 m, and between 1996 and 1998, retreat was of the order of 34 m.

sample point	dist along baseline (m)	erosion 96-97 (m)	erosion 97-99 (m)	erosion 96-99 (m)	sample point	dist along baseline (m)	erosion 96-97(m)	erosion 97-99 (m)	erosion 96-99 (m)
1	55.2477	2.45	6.54	8.99	46	2154.66	-0.48	25.99	25.51
2	111.939	3.79	6.19	9.98	47	2218.57	-0.75	22.02	21.27
3	140.941	0	12.35	12.35	48	2242.45	3.33	21.25	24.58
4	146.977	0	17.06	17.06	49	2254.39	3.81	19.06	22.87
5	180.703	10.52	0.46	10.98	50	2294.42	4.11	18.9	23.01
6	228.602	7.99	11.61	19.6	51	2543.49	5.84	23.73	29.57
7	270.202	5.3	5.02	10.32	52	2667.37	9.36	22.19	31.55
8	286.474	5.18	5	10.18	53	2755.17	14.35	17.18	31.53
9	293.692	5.04	5.07	10.11	54	2761.07	14.1	18.24	32.34
10	343.297	-0.56	11.12	10.56	55	2763.3	8.53	18.38	26.91
11	367.968	-2.68	11.05	8.37	56	2775.37	14.88	19.72	34.6
12	399.069	-5.17	7.75	2.58	57	2781.54	15.33	18.91	34.24
13	435.026	-1.4	11.04	9.64	58	2789.42	11.72	19.25	30.97
14	450.118	-1.21	11.11	9.9	59	2805.03	15.79	17.49	33.28
15	522.031	6.92	7.29	14.21	60	2806.48	16.16	17.4	33.56
16	530.168	7.09	6.69	13.78	61	2814.74	13.4	17.91	31.31
17	569.93	1.23	11.11	12.34	62	2820.39	13.07	19.07	32.14
18	575.967	0.41	11.29	11.7	63	2976.16	15.42	25.6	41.02
19	695.386	-1.96	7.47	5.51	64	2994	15.35	26.23	41.58
20	699.322	-2.38	7	4.62	65	3062.77	19.15	25.3	44.45
21	761.394	0.91	16.73	17.64	66	3068.67	16.76	30.11	46.87
22	771.236	0.28	15.72	16	67	3076.02	15.55	28.38	43.93
23	856.273	5.46	12.23	17.69	68	3113.16	19.56	26.73	46.29
24	864.803	6.02	9.7	15.72	69	3127.2	19.6	24.91	44.51
25	996.689	-2.01	15.66	13.65	70	3229.04	18.1	23.66	41.76
26	1011.12	-1.74	16.26	14.52	71	3327.72	23.46	26.93	50.39
27	1017.69	-1.15	13.99	12.84	72	3358.03	24.68	27.79	52.47
28	1065.45	-1.02	10.27	9.25	73	3419.84	25.54	26.63	52.17
29	1129.1	-0.27	7.86	7.59	74	3420.89	25.91	26.37	52.28
30	1220.04	-0.59	8.69	8.1	75	3435.85	23.66	24.79	48.45
31	1260.07	-1.41	10.69	9.28	76	3480.47	26.08	25.66	51.74
32	1262.04	-1.23	10.42	9.19	77	3535.46	28.12	26.97	55.09
33	1373.45	0.6	7.73	8.33	78	3555.4	26.9	25.99	52.89
34	1374.76	0.2	7.84	8.04	79	3586.77	24.43	23.81	48.24
35	1417.67	1.05	8.31	9.36	80	3626.79	19.77	24.68	44.45
36	1526.2	8.95	2.78	11.73	81	3639.52	20.86	23.65	44.51
37	1721.73	0.55	16.88	17.43	82	3645.82	21.04	24.24	45.28
38	1733.41	2.35	14.96	17.31	83	3648.84	22.05	23.38	45.43
39	1759.53	4.29	12.1	16.39	84	3650.54	20.84	24.56	45.4
40	1815.17	-3.57	24.73	21.16	85	3684.4	13.34	29.87	43.21
41	1849.55	-0.09	22.09	22	86	3831.38	20.15	29.52	49.67
42	1899.68	0.86	22.53	23.39	87	3869.96	19.14	33.69	52.83
43	1906.9	-1.54	22.28	20.74	88	3918.65	14.48	39.5	53.98
44	1991.8	0.64	22.66	23.3	89	3971.66	10.56	47.91	58.47
45	2125.66	-2.69	26.95	24.26	90	3972.19	10.14	48.14	58.28

Table 9.3. Erosion of the dune cliff at 90 sample points, Ile d'Oleron

9.5. OVERWASH DEPOSITS

Erosion of the first major dune ridge has resulted in overwash features with the sea penetrating the dune slack between the first two ridges. Field observations made in September 1998 at this site established that between the northernmost car park and the next (teardrop shaped) car park the dune crest was between 4 and 6 m in height. To the south of this, the first dune crest was around 1.5 m high, and there was evidence to suggest that at this time some relatively minor overwash had occurred where the crest was low. Plate 9.5 shows the typical lobe-shaped morphology of an overwash deposit at Ile d'Oleron, with the sand carried well back into the dune slack behind the dune ridge. Flotsam such as dead seaweed and driftwood can be seen on the sand and dune grasses have begun to re-emerge through the deposit. This photograph was taken from the dune ridge looking north-east across the dunes.

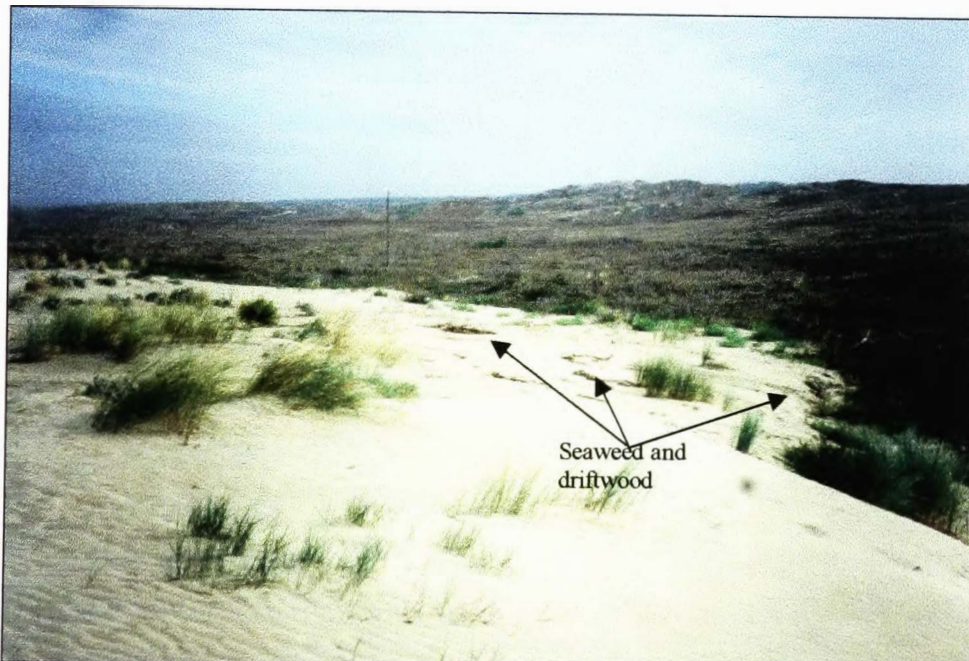


Plate 9.5 Lobe-shaped overwash deposit at Ile d'Oleron, Sept. 1998

The aerial survey in May 1999 showed that since the 1998 visit there had been major changes over a distance of several kilometres in this section of coast, with even the relatively high sand cliffs being overtopped by waves. Over-wash lobes extended up to 80 metres inland across the paths

behind the dune. Part of the site close to the Passe de Gatseau, at the southern end of the dunes, showing significant overwash is presented in Plate 9.6 - a CIR aerial view from the 1999 survey.



Plate 9.6 Aerial view of overwash deposits at southern end of Ile d'Oleron, May 1999

The changes that occurred between the 1997 and 1999 surveys are shown in Plate 9.7, where the 1997 mosaic is displayed as a greyscale image through the green channel and the 1999 mosaic is displayed as a greyscale image through the red channel. Loading the images in this way allows images from two epochs to be displayed simultaneously, and allows ready recognition of changes that have taken place. Most notable are the very large washover lobes on the 1999 image towards the south of the site which appear in red due to the fact that the dry bare sand returns a very high signal through the red channel. Had these features been present in the 1997 image there would have been a very high signal in the green channel also and the washover lobes would have appeared in the composite image in tones of yellow. This phenomenon can be seen in the dry bare sand where the dune has been denuded of vegetation prior to the 1997 photography and appears bright yellow.

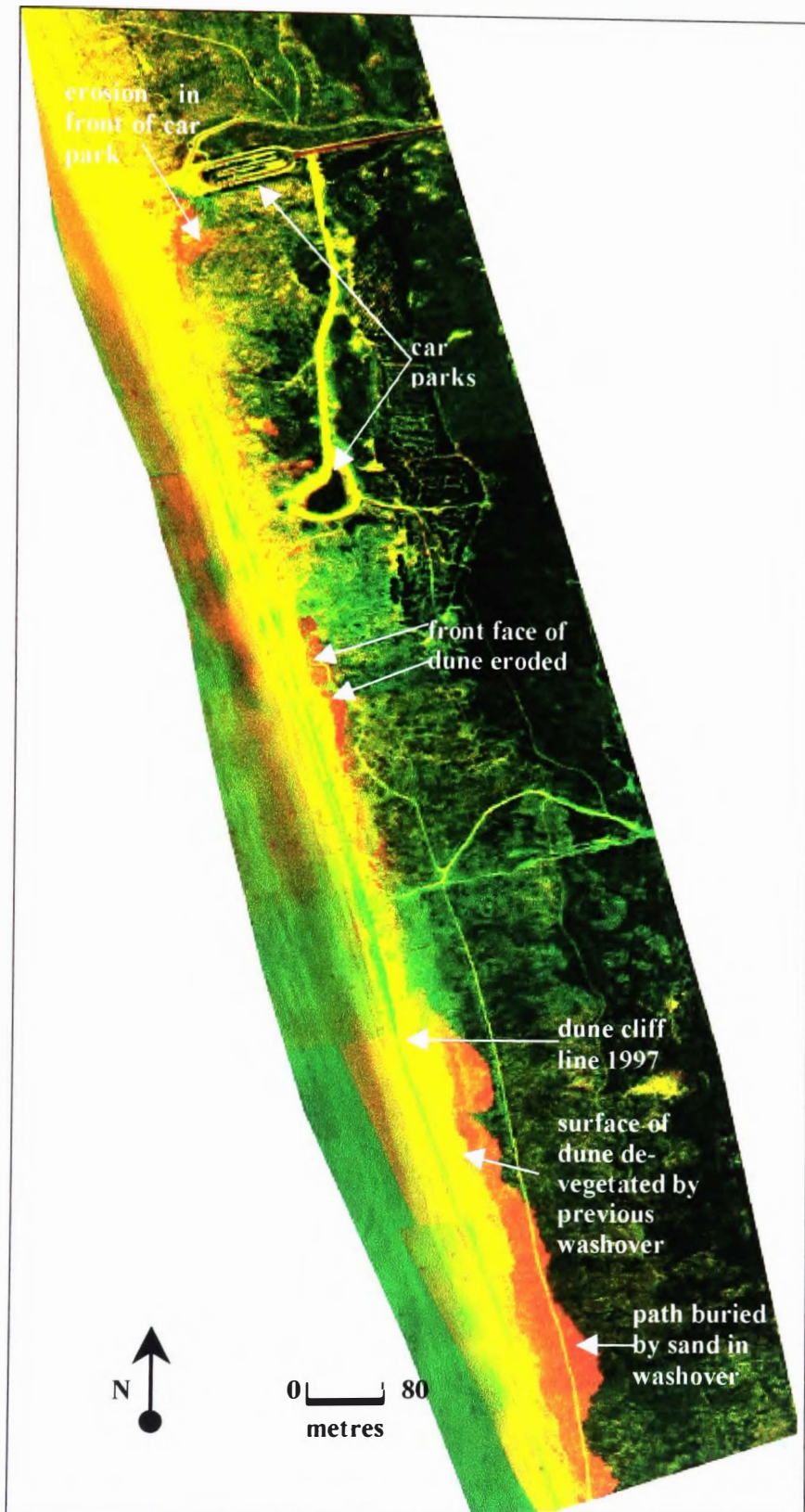


Plate 9.7 Ile d'Oleron, 1997 mosaic in green channel, 1999 mosaic in red channel.

Whilst it is not the intention of this work to interpret the mechanisms of coastal retreat in the various sites selected for evaluation of the aerial digital photography, analysis of the pattern of retreat has revealed interesting changes in the erosion and it is clear from Figure 9.5, which shows a plot of recession of the dune cliff at the sample points, that the greatest degree of retreat has been at the distal end of the system, with just under 60 m measured during the three year period.

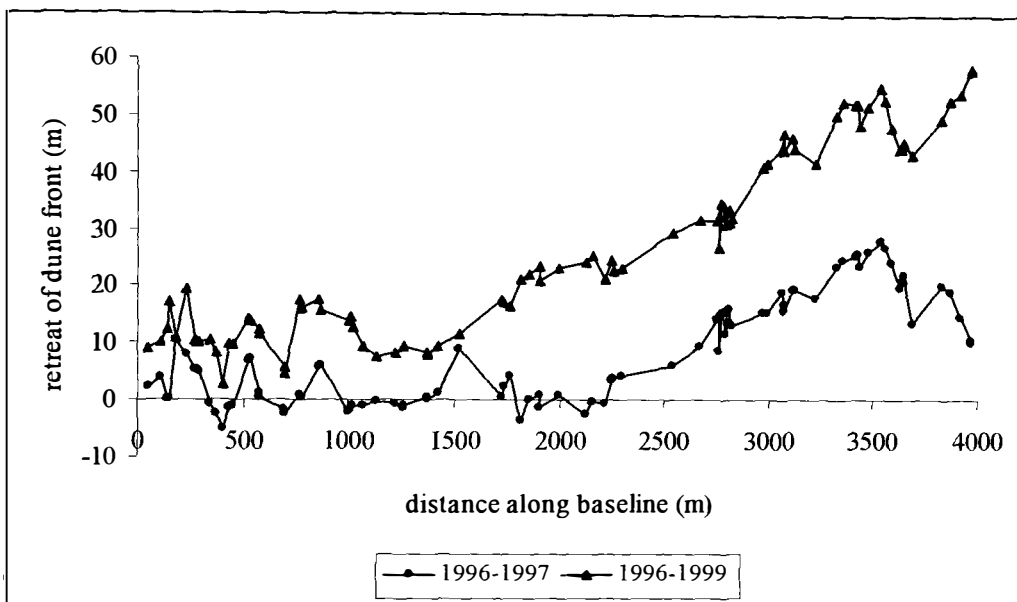


Figure 9.5 Retreat of the dune front 1996 –1997 ($\pm 1.12\text{m}$) and 1996 –1999 ($\pm 1.76\text{m}$)

In the period 1996 - 1997 there was little or no retreat for the first 2000 m south of the start of the survey baseline and in fact some accretion appears to have occurred here. At about 2200 m the plot reveals a sharp increase in recession as far as the 3500 m marker, with a slightly less marked recession to the end of the baseline. The changes between 1996 and 1999 show about 10 m of recession as far as 1500 m along the baseline, with marked recession again apparent to the south of that marker. The parallel trend of the two plots is very marked. There appears to be a pivot point on both plots, to the south of which marked erosion occurs, and that between 1997 and 1999 that pivot has shifted some 700 m to the north. Whether this observation is significant or not is impossible to say using such a short time series of data and analysis of this change is for future

work. What is important here is that although this data was not collected with this type of analysis in mind and was not ideally suited to this task, the results appear to be encouraging. The detailed plots of change in the position of the cliff crest line obtained from the analysis of the digital photography underscore the value of the ADPS and is an indication of the robustness of the data and the method.

CASE STUDY 2 ~ redistribution of sediment at Dossen

10.1. INTRODUCTION

Digital aerial surveys are available for the three epochs already listed at Ile d'Oleron, namely 1996, 1997 and 1999. The 1996 survey is incomplete, in that a small section of the seaward edge of the dune is missing on one image. This is not thought to be a major problem as the techniques used at this site can still be gainfully applied, and field knowledge of the site enabled an estimate of the small missing section.

The dune face is subject to both erosion and deposition of mobilised sand, and the digital photographs are used to map these changes in the distribution of sediment. A further complex change has enhanced the value of Dossen to this study. Simple inspection of the images from 1997 and 1999 reveal markedly increased deposition of sand in front of the west facing dune cliff, as well as lobes of sand deposited over vegetated areas behind the dune front (Plate 10.1 a & b). These new spreads of sand cover significant areas of the dunes, and the form and distribution of the deposits suggests that overwash is a possibility. The reality is somewhat different, and field evidence supports the view that sand driven ashore by wind and waves has been ramped against the sand cliff, eventually spilling over the cliff top as an advancing wind blown deposit, burying the existing vegetation. This highly dynamic environment makes this an ideal site to demonstrate the effectiveness of aerial digital photographs for monitoring changes in the area of the dune and in sand redistribution. and, as with Ile d'Oleron. the value of the rectified digital images lies in providing evidence of change and process.

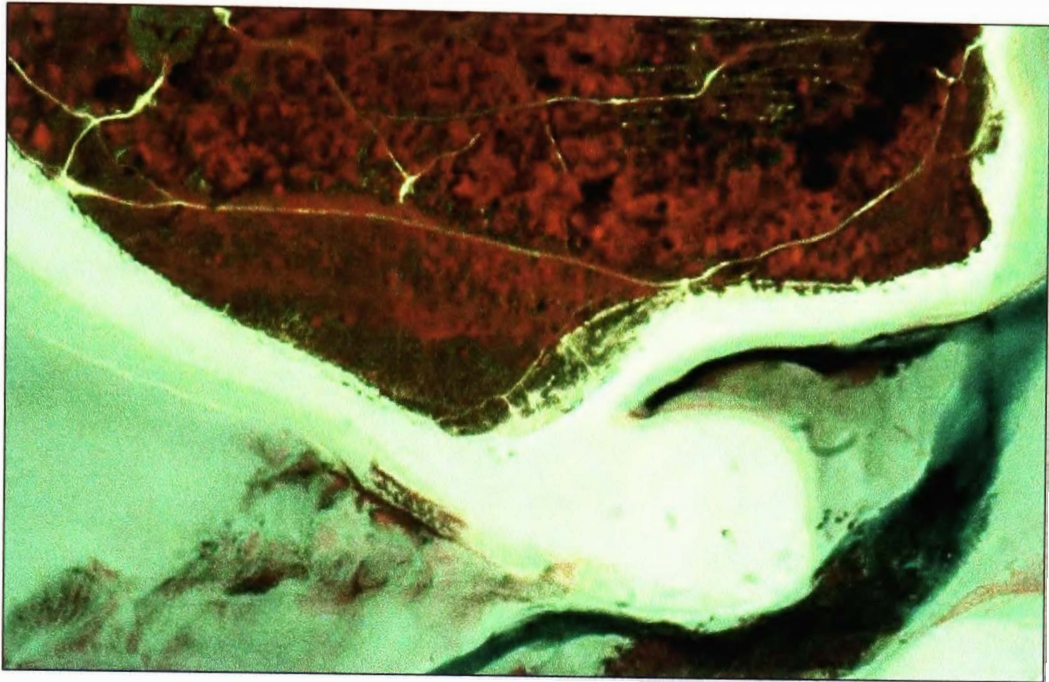


Plate 10.1 (a) DS 460 CIR photograph, May 1997, Dossen

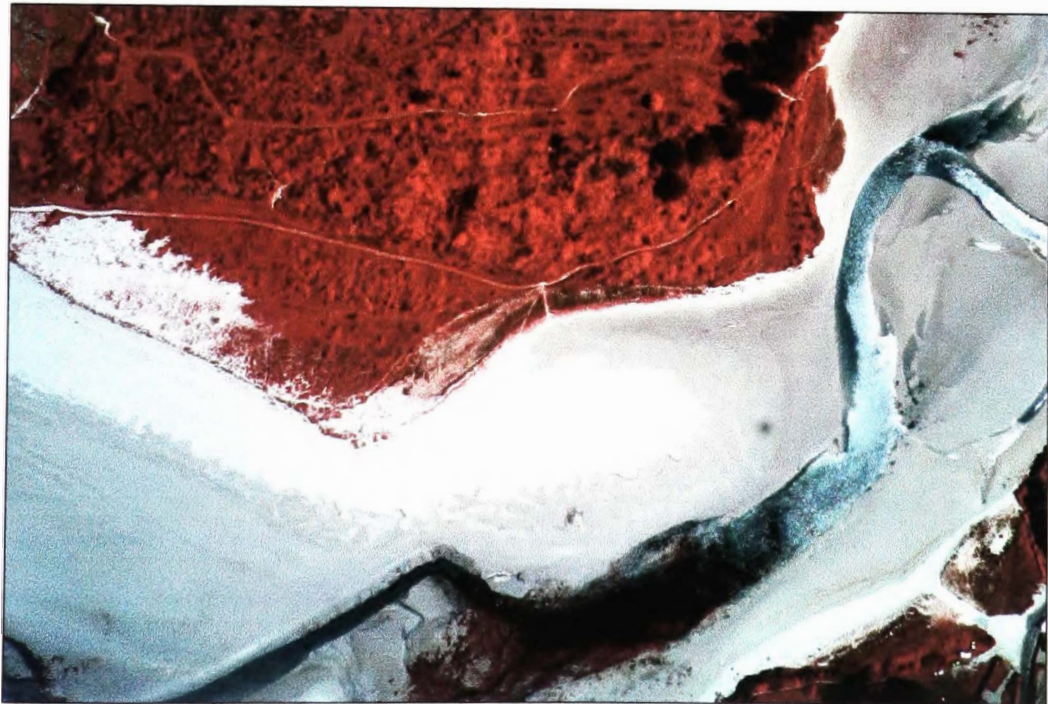


Plate 10.1 (b) DS 460 CIR photograph, May 1999, Dossen

10.2. SITE DESCRIPTION

The dune site of Dossen and the Foret de Santec is a relatively small site (125 ha) located immediately to the west of the ferry port of Roscoff on the north coast of France. The location of the site is marked with an arrow in Figure 10.1.

Figure 10.1 has been removed from the digitized thesis for copyright reasons.

Figure 10.1 Map showing the location of the dune site at Dossen to the west of Roscoff on the north coast of Brittany

The dunes and the related sediment supply have accumulated in the embayment formed by the Ile de Siec and the rocky headland at Tevenn and Figure 10.2 gives a more detailed map of the dune site and its immediate vicinity. The area of interest is marked with a red box and includes most of the dune front at this site extending into the estuary of the River Horn.

Figure 10.2 has been removed from the digitized thesis for copyright reasons.

Figure 10.2 The dune site at Dossen showing region of interest

The apron of sand exposed by extreme low tide is over 700 m wide within the embayment, and is derived from sand driven onshore by westerly winds and by waves, in addition to sediment delivered into the bay from two relatively small rivers, namely the Horn and the Guillec. The dune front trends north / south and is orthogonal to the prevailing wind and waves. The northern part of the sand dune complex is now covered by the small settlement of Dossen, whilst the southern portion of the dune complex is used as a campsite, set amongst the scrub and tree cover defined as the Foret de Santec.

Wave erosion of the dune face has been active for some time (pers. obs.) and enrochements have been necessary to protect the settlement in the northern part of the dune complex from attack; in this area almost the entire coast has been rock protected.



Plate 10.2 Enrochement in front of the dune at Dossen

The policy of enrochement has more recently been extended to the central complex where dune cliffing by the sea was active. Here, this management has proved ineffective, in that discontinuous rows of large stone blocks have been placed in front of the cliffed dune below the high water line, resulting in wave turbulence behind the blocks and consequently even more rapid excavation of the friable sand cliff. Plate 10.2 shows part of the enrochement in front of the central dune complex. The face of the dune displays typical symptoms of erosion with discrete clumps of vegetation sloughing off the dune and creeping down the face before removal by wave attack. Much of this eroded sand appears to have been driven southwards along the dune face into the estuary of the R. Horn, resulting in a net transfer of sand from the west facing sand cliff to the distal end of the complex. The southern section of the dune lying within the sheltered estuary of the Horn has grown considerably with attendant colonisation by dune grasses such as *Agropyron*

and Marram. Plate 10.3 shows numerous embryo dunes forming at the southern section of the dune site at Dossen, looking across the embayment, with the Ile de Sic in the background.

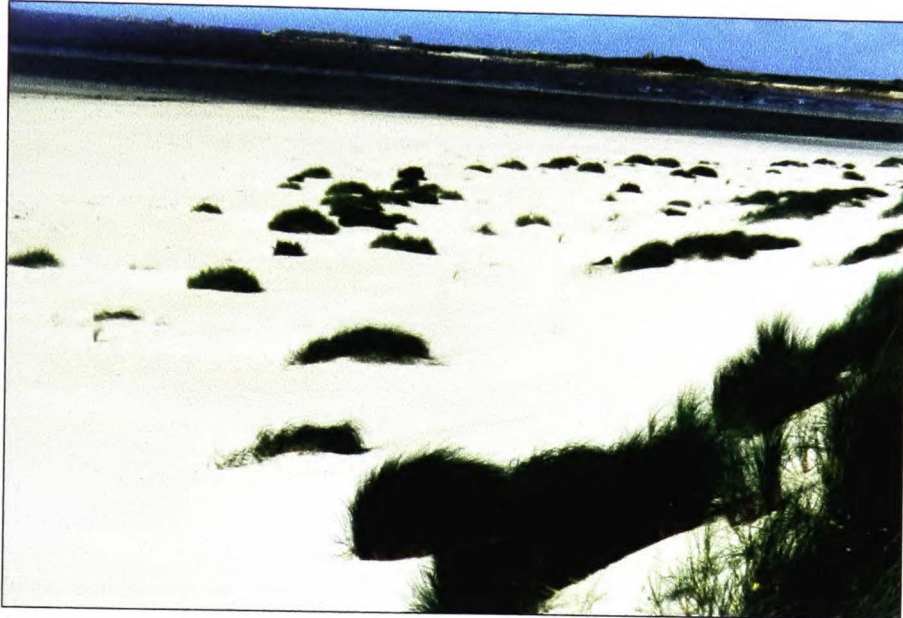


Plate 10.3 Clumps of dune building grasses forming embryo dunes at Dossen

10.3. IMAGE REGISTRATION AND ERROR ASSESSMENT

10.3.1. Image registration

Images from the three epochs were rectified, mosaiced and co-registered as detailed in section 9. (Ile d'Oleron). This is a standard technique and will not be further explained here, except to indicate that it was again carried out in ER Mapper without heighting data (2D) but this time the 1997 mosaic was chosen as the base mosaic because the orientation of the camera with the short axis parallel to the flight line gave more opportunities to select ground control points from those collected using GPS and from the IGN 1: 25000 map.

11.3.2 Error analysis

The accuracy of the mosaicing and co-registration processes is indicated in Table 10.1, as well as the required sample size of 37 observations derived from the formula given in 9.3.2.2. RMS data

suggest that the mean errors are less than 1.5 m. The sample size satisfies the sample size requirement for all calculations.

	96x-97x	96y-97y	97x-99x	97y-99y	96x-99x	96y-99y
Minimum (m)	-2.7	-2.8	-3.8	-2.8	-2.74	-2.74
Maximum (m)	2.8	2.6	3.01	2.9	1.42	3.22
Mean (m)	0.19	0.01	-0.3	0.03	-0.4	0.1
Std. Deviation	1.24	1.52	1.35	1.25	0.84	1.4
Count	37	37	37	37	37	37
RMS (m)	1.23	1.50	1.38	1.23	0.82	1.35
Required sample	25	37	30	26	12	32

Table 10.1 Summary statistics for registration errors between the three epochs, Dossen

10.4. CHANGE DETECTION

Mosaiced images were opened in MapInfo 5.5 and the beach / dune interface in each epoch was digitised. Figure10.3 shows part of the plot of the three dune fronts. It should be noted that the west facing section consists of eroded sand cliffs, whilst in the south, facing the estuary of the river Horn, some erosion - and latterly considerable deposition - has taken place.

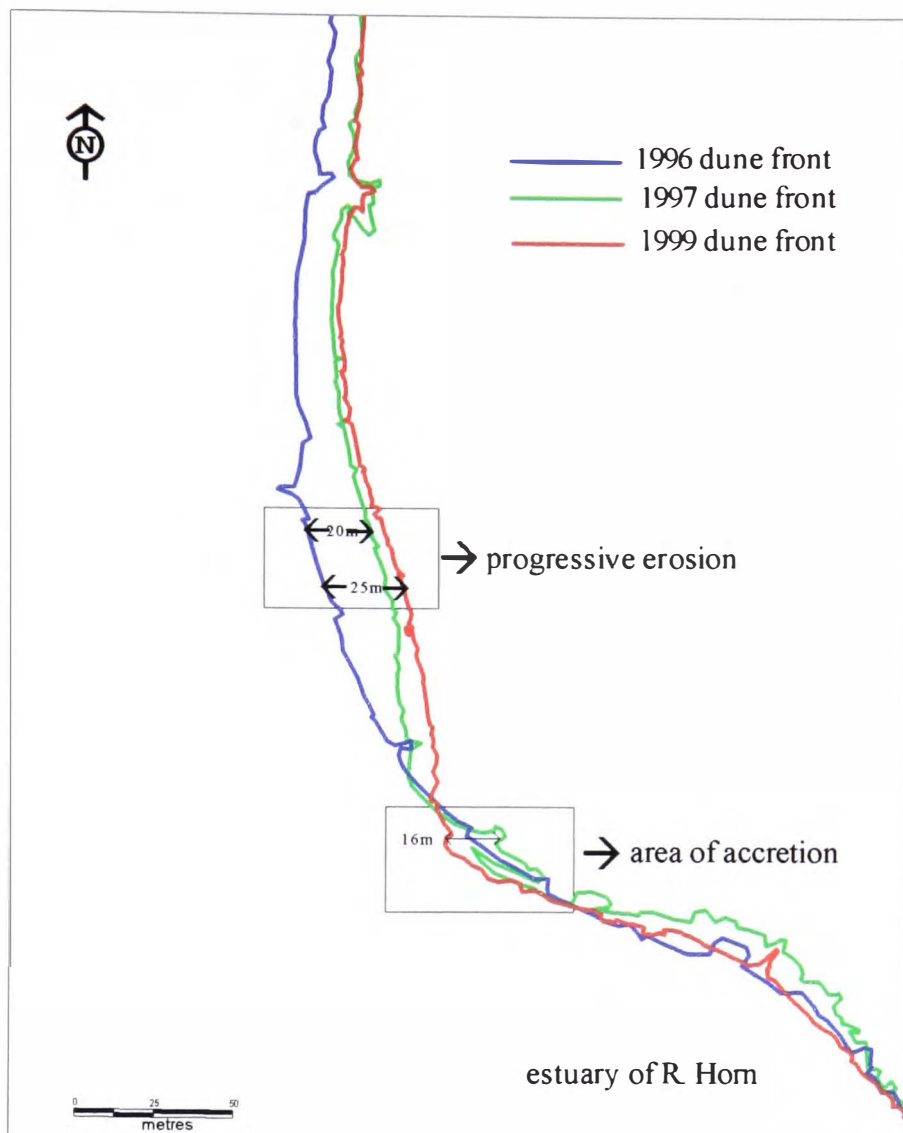


Figure 10.3 Part of the dune field with digitised dune fronts for three epochs showing areas of erosion and deposition.

Using these shoreline plots, areas of erosion and deposition as defined by the positions of the dune fronts in successive epochs were delimited as closed polygons. These are shown in Figure 10.4 a and b. The patterns and extent of deposition and accretion are quite different within and between epochs and whilst it is not the intention to account for these variations in either space or time, some discussion is essential in order to demonstrate the full value of the digital images in this context. The period between the 1996 and 1997 epochs saw erosion along the whole dune face

south of the main beach access point, the latter situated at the northern limits of the maps in Figure 10.4 a and b. In the northern zone, this was limited to just a few metres retreat of the sand cliff, but in the central zone the retreat in 1996 -1997 was up to 25 m at its widest point and between 5 and 15 m over much of the southern zone.

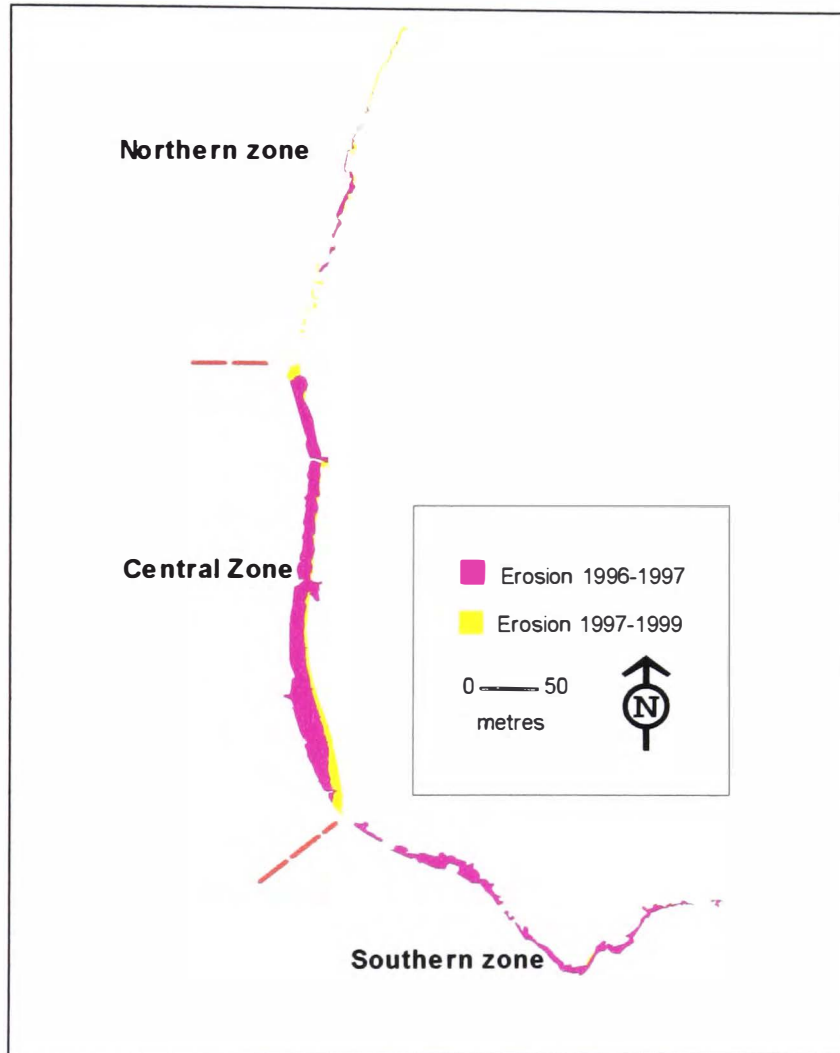


Figure 10.4 (a) Erosion 1997-1999 & 1996-1997 at Dossen, Foret de Santec, Brittany

Erosion in the two-year period 1997-1999 was rather less marked, with minor retreat in the northern zone, and continued - but much less pronounced retreat in the central zone (1m to 9 m). There was almost no erosion of the dune face in the southern zone during this two-year period.

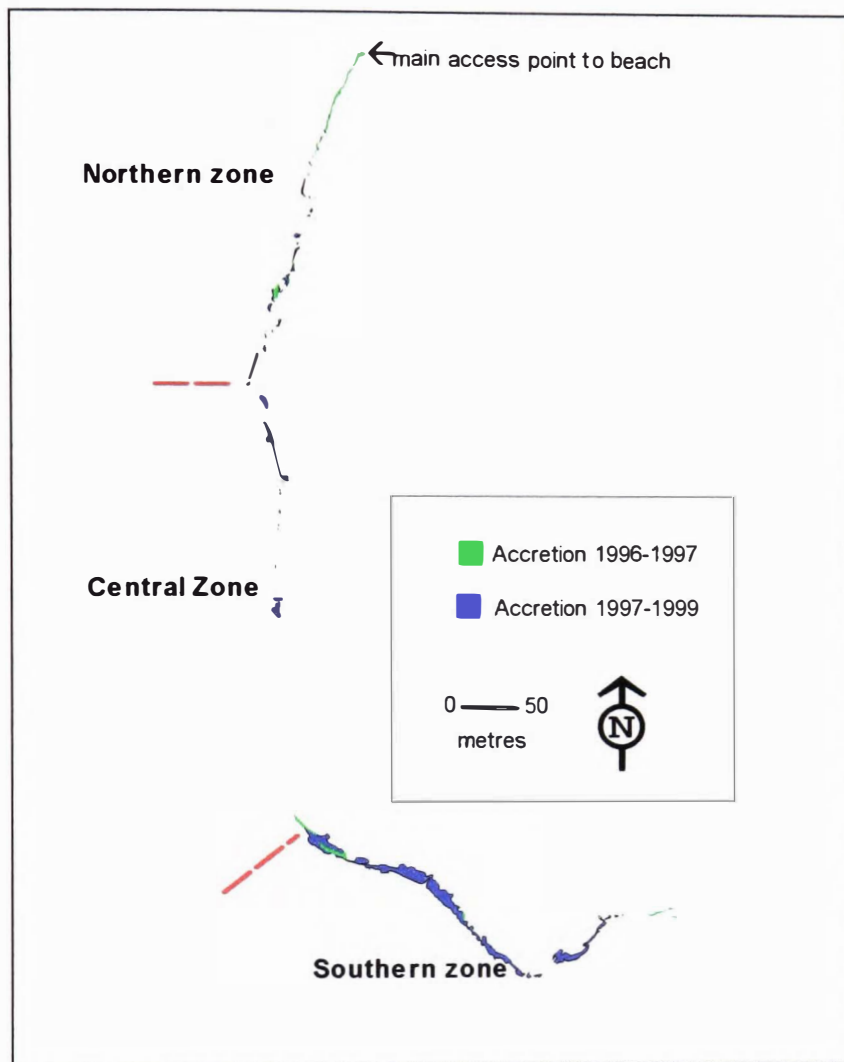


Figure 10.4 (b) Accretion 1997-1999 & 1996-1997 at Dossen, Foret de Santec, Brittany

The most striking comparison between the two plots is the relative areas eroded and accreted with far less accretion than erosion over the site as a whole. The area of accretion between 1996 and 1997 is small and almost absent from the central zone. The regime looks quite different in the two-year period between 1997 and 1999 with a large area of accretion in the southern zone and more minor deposits in the central and northern zones. These plots are useful for showing at a glance where the changes have occurred, and from them the actual areas of the zones of accretion and erosion have been calculated in MapInfo v5.5.

Table 10.2 records the surface area of the dune eroded in each of the three zones for each time interval and also records the total area eroded for each time interval. The gross erosion for 1996 – 1999 is also recorded for each zone and for the entire dune system. Similar results are recorded for accretion. The net erosion for each of the zones between 1996 and 1999 is recorded.

	Northern zone	Central zone	Southern zone	Entire system
Erosion 96-97 (m²)	185.84	4335.8	1620.66	6142.3
Erosion 97-99 (m²)	269.37	1071.76	42.82	1383.95
Erosion 96-99 (m²)	455.2	5407.56	1663.48	7526.24
Accretion 96-97 (m²)	111.7	3.8	137.43	252.95
Accretion 97-99 (m²)	150.8	210.2	1525.8	1886.8
Accretion 96-99 (m²)	262.5	214	1663.23	2139.73
Net erosion (m²)	192.7	5193.6	0.25	5386.51

Table 10.2. Erosion and deposition resulting in changes in the surface area of the dune between 1996 and 1999, Dossen.

These data emphasise the considerable variation between epochs, with 6142 m² eroded in 1996-1997 and only 1384 m² (22% of the 1996-1997 total) eroded in the two year period 1997-1999. It is worth emphasising that between 1997 and 1999 even the rapidly eroding central zone lost only 25% of the surface area eroded in the 1996-1997 period. Investigations might well centre on the record of storm activity and their coincidence with high tides during the 1996-1999 period, but equally, the influence of the poorly placed enrochement which was intended to protect the central zone should also be considered. The degree of turbulence caused by waves breaking over the enrochement, a discontinuous line of boulders placed at the foot of the sand cliff, is thought to have considerably aided the erosion of the sand dune cliff.

During the period 1996-1997 there was relatively little accretion around the dune massif, with only 253 m² of deposition recorded over the entire system. In the second period there was rather more accretion (1887 m²) with 80% of this occurring in the southern zone where nearly 1526 m² of sediment was deposited between the vegetated massif and the estuarine drainage channel of the river Horn. During this period, erosion in the southern zone was almost negligible with only 43m² recorded.

Over the course of the entire study, the whole system has suffered net erosion of some 5386 m² representing 0.4% of the entire dune system. Most of this erosion (96%) occurred in the central zone with 5194 m² lost. The areas of erosion and accretion in the southern part of the dune system were remarkably similar with 1663.5 m² eroded and 1663.2m² accreted. These extraordinarily closely matched values should not be taken too literally as they reflect the change in surface area and do not give any indication of the volumes of sediment involved, but they do provoke consideration of the dynamic dune / beach interchanges that are frequently cited in the literature (Carter, 1988; De Ruij, 1989; Arens & Weirsmas, 1994; Bennet & Olyphant, 1998) and it is a possibility that some of the sediment lost from the central eroding part of the dune has been redistributed to the southern zone by aeolian transport and longshore drift.

10.5. SEDIMENT REDISTRIBUTION

10.5.1. Sand deposited on the beach

The fate of the sand eroded from the central section is of considerable interest, given the large surface area liberated from the sediment sink of the dune. The colour infrared photography ensures a clear difference between the wet and dry sediment, and the rapid drainage and drying out of elevated sand features at low tide gives a ready appreciation of the relief of the beach sediment. Plate 10.4 illustrates this phenomenon where dry sand appears in brighter tones than wet sand.

The lobate feature at bottom centre of the photograph is a large accumulation of sand which appears to have tracked along the coast in an east-south-easterly direction by some 190m between 1996 and 1999 into the estuary of the Horn.

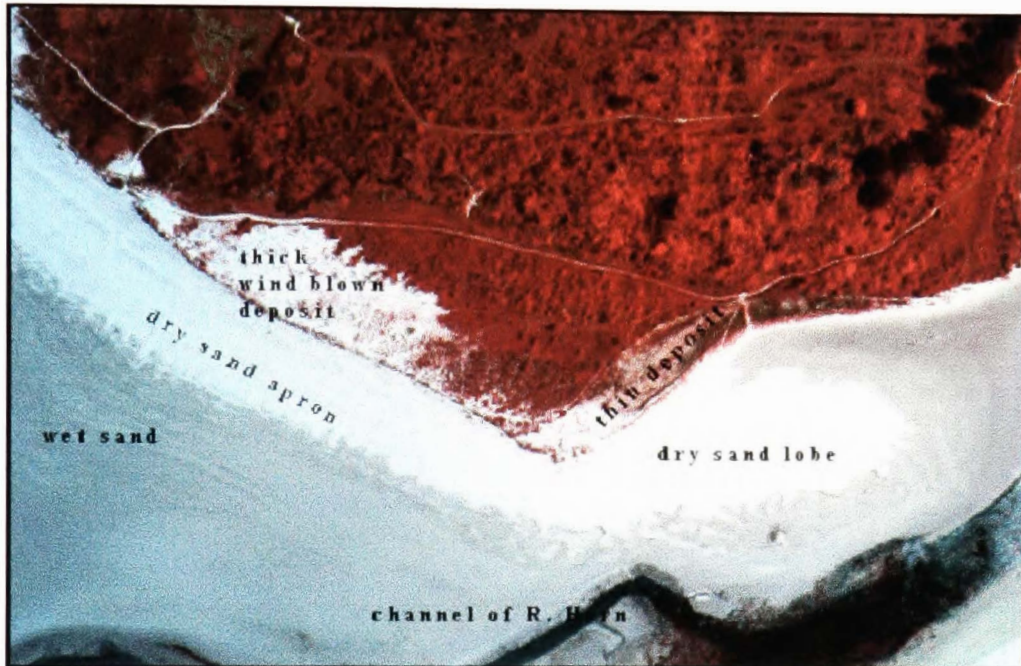


Plate 10.4 Colour infrared digital photograph showing sand deposit in the estuary of the R. Horn and wind blown sand on the dune at Dossen, May 1999

The extent and movement of this sand lobe has been traced using MapInfo and Figure 10.5 shows the relative positions of the sand lobe for each epoch as well as the extents of the dry sand, the wet sand, the river channel and the dune front during the three survey missions. As would be expected, the progression of the lobes towards the south and east has displaced the river channel, and this clearly establishes the physical existence of the lobes.

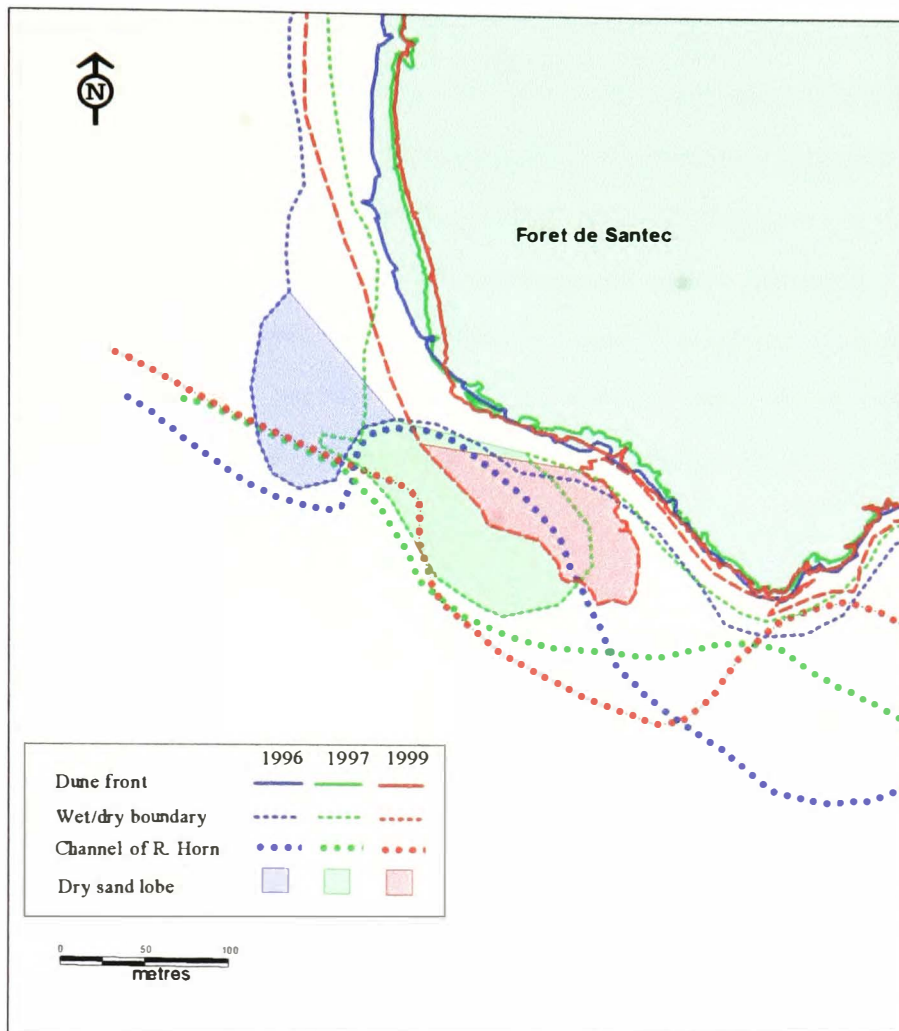


Figure 10.5 The progressive shift of sand lobes along the dune face and displacement of the estuarine channel of the River Horn, Dossen

The fate of this sand since June 1999 has not been further investigated in this assessment of the value of the digital photography, but could include attachment to the accreting southern section of the dune field, and /or, return to the bay via flood discharges from the rivers Horn and Guillec. This sand would then replenish the sediment cell in the bay, to eventually be delivered back to the beach and the dune. There are suggested examples of such closed cell sediment circulation at several other sites in Brittany - for example the Anse de Morgat, Crozon and Les Sables Blancs, Lesconil (J-CI Bodere *pers com.*). Further observations of future erosion and depositional trends at this site could be extremely informative.

10.5.2. Aeolian deposits on the dune

At most dune sites, during periods of strong onshore wind, there is transport of sand from the beach to the inland surfaces of the dune. Lag deposits of coarse sand, granule sized clasts or shell fragments on the bare seaward facing dune front bear witness to this process as the finest sand fractions are winnowed by the onshore winds and redeposited inland. Deposition from this process is sometimes almost imperceptible, especially on vegetated dunes, as the mobilised sand is trapped and concealed by the vegetation cover. Occasionally very strong onshore winds may drive discrete spreads of available sand onto the dune surface, and the 1999 image (Plate 10.4) shows the result of this process.

Deposition took place between June 1997 and May 1999. The relationship of the spreads of sand deposited on the vegetated dune surface to the sand mobilised by erosion in (especially) the central zone of the dune face is not clear from the photographs alone. In the field, the mechanism of this deposition is quite explicit, *i.e.* beach sand has been driven against the eroded sand cliff, and has built up as a wide ramp which has eventually overtopped the 4m cliff crest. Sand has then been driven up the ramp by the wind and has then either cascaded down the lee slope into the dune slack behind the dune front, or has been blown into the slack burying all but the tallest vegetation. In addition, paths normal to the beach have acted as conduits along which sand has been driven to the interior. Figure 10.6 maps the extent of the thick windblown deposit depicted in Plate 10.4 and shows a schematic representation of the process of aeolian deposition.

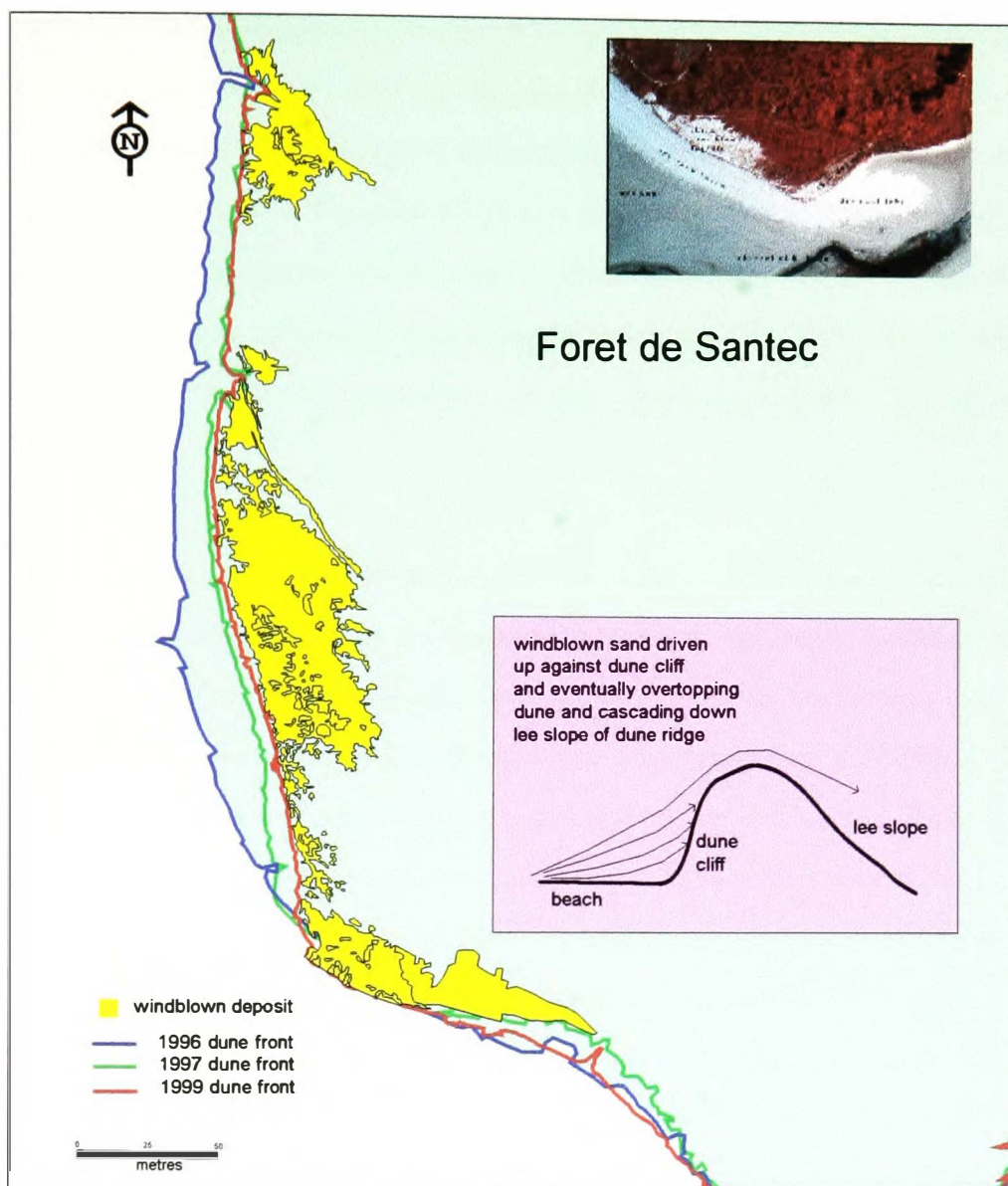


Figure 10.6 Extent of the wind blown deposit on the dune at the southern end of Dossen site, May 1999

Thick spreads of sand (little or no vegetation visible through the sand) deposited in this way cover approximately 5200 m² of the dune surface, with a further 850 m² covered by a rather thinner layer, with some vegetation showing through the overlying sand. Together these deposits account for around 0.5% of the surface area of the dune and this value almost certainly underestimates the area affected because much sand has been concealed by vegetation. Such processes are not

particularly unusual, but in this case the extent of the sand spreads is large and far exceeds other small-scale examples observed in the field. This suggests that the large amounts of sand available for this redistribution from beach to dune has been enabled by a particular factor, possibly sand mobilised by the erosion of the central zone of the dune, providing further illustration of the dynamic relationship between the beach and the dune. Monitoring this type of sediment mobilisation is of great interest to the dune manager as well as to the local population as it is just this kind of event that causes great concern to property holders now as it has in the past (see 3.1.2).

As illustrated above, images from the three epochs have provided detailed and relatively accurate information on sediment distribution and change within the Dossen dune site. The images also infer processes that are active, for example erosion and deposition along the dune front, but they also suggest other processes that could be investigated, such as the progressive movement of sand lobes towards the south east, and the redistribution of sand onto the dune surface. The value of these images is reduced by the lack of elevation data for ground control and that only one set of photographs was captured in stereo. The creation of digital elevation models for each epoch would have enabled orthophoto production and calculation of volumes of sediment mobilised by erosion, rather than the less useful measurements of surface area. This would have, in turn, assisted in tracking the redistribution of sediment following erosion. Never-the-less aerial digital photography lends itself to surveillance of this kind and the dune manager with modest computing skills can very rapidly create informative maps.

CASE STUDY 3 ~ measurement of surface change at Ile de Noirmoutier

11.1. INTRODUCTION

The southern part of the dune coast at Ile de Noirmoutier was surveyed in all three photographic missions i.e. 1996, 1997 and 1999. Preliminary inspection of the images has revealed a variety of features including settlements, campsites and sports facilities, as well as evidence of erosion and accretion. Field observations have substantiated photo-interpretation and confirmed progressive change from north to south of this linear dune, varying from marked erosion in the northerly section, south of Village de la Tresson, to marked accretion at the southern (distal) end of the spit. German blockhouses isolated on the beach 60 to 70 m in front of the dune readily testify to marine erosion and retreat of the dune front and in the north there is evidence of considerable erosion of the dunes in the form of large blowouts.

This investigation will centre on surface changes to the dunes from La Gueriniere to la Fosse (shown in Figure 11.2) and this site will be used to assess both erosion and accretion as well as the development of blowouts. The destruction of the vegetation cover in the northern section will be used as the vehicle to demonstrate the detection of erosion using aerial digital photography and in contrast the southern part of the dunes will be used to demonstrate the detection of colonisation by new vegetation. However, whilst it is relatively easy to demonstrate the sudden loss of vegetation cover around the margins of blowouts because of the sharp change in surface cover, it is much more difficult to show the more gradual changes resulting from colonisation of newly prograded dune surfaces with sparse and patchy vegetation. One of the advantages of using multispectral digital imagery over its film counterpart is that image processing routines can often reveal information that is otherwise inaccessible in hard copy (5.3.2). Even so, the distal end of the spit near Pointe de la Fosse provides a severe test of the usefulness of the ADPS.

11.2. ILE DE NOIRMOUTIER - THE PHYSICAL CONTEXT

The Ile de Noirmoutier is approximately 18 km in length and lies some 23 km south of the mouth of the river Loire on the west coast of France. Figure 11.1 is an outline map of the site with an inset showing the relationship of the Ile de Noirmoutier to the mainland.

Figure 11.1 has been removed from the digitized thesis for copyright reasons.

Figure 11.1 Outline map of the Ile de Noirmoutier with inset showing its location south of the River Loire

The island can be considered to be in two sections; the bulbous northern section which is underlain by leucogranites of late Variscan age forming the Pointe de L'Herbaudiere (with minor lower Eocene deposits at the eastern extremity of that part of the island) and the southern section that extends south-eastwards from the Pointe de L'Herbaudiere as a narrow causeway to join the southern part of the island at le Devin. The southern part is a narrow Holocene sand spit some 15 km long with a maximum height above sea-level of 20m, although much of it is actually lower

than this. This ridge is backed by a very large and partially reclaimed marais with extensive salt pans and polders and the main road from the northern section is built across the marsh. The island terminates in the south at the Pointe de la Fosse and is separated from the mainland by the deep water channel known as the Goulet de Fromentine. The southern part of the island which affords the study site for this investigation is mapped in more detail in Figure 11.2.

Figure 11.2 has been removed from the digitized thesis for copyright reasons.

Figure 11.2 Southern section of Ile de Noirmoutier, showing the major settlements and dune sites

The sand dune coastline is generally orientated to the south-west facing the North Atlantic Ocean and is thus exposed to high winds and waves. The sand dune ridge that forms the western spine of

the island protects a series of linear settlements extending from La Bosse (off the map) through La Gueriniere, Les Sables d'Or, Le Midi, Barbatre to La Fosse near the southern extremity. In general the sediment supplied to the dunes is fluvio-marine in origin, and in particular is derived from the River Loire and the several small rivers that drain into the Baie de Bourgneuf, and from the products of coastal erosion in the north of the island.

11.3. SURFACE CHANGES BETWEEN VILLAGE DE LA TRESSON AND LE MIDI ~ EROSION

11.3.1. Site description

The dunes in the more northern part of this region of interest are badly damaged and this has prompted a variety of management strategies including the erection of notice boards of the type in Plate 11.1. These have been designed both to warn visitors that the dune protects the settlement and that the vegetation cover is crucial to the survival of the dunes and to inform visitors about dune flora and dune habitats.



Plate 11.1 Educational notice boards at Les Sables d'Or and La Tresson, Ile de Noirmoutier

Photographic evidence of the degraded dunes in the northern part of this region of interest at Village des Sables d'Or (also known as Village de la Tresson) includes severe cliffing of the dune front (Plate 11.2, September 1998) which has led to the installation of zig-zag shaped fences to encourage deposition at the cliff foot (Plate 11.3 May 1999 and Plate 11.4 September 1999).



Plate 11.2 Broken fencing and cliffing at Village de la Tresson, Ile de Noirmoutier, Sept. 1998



Plate 11.3 New zig-zag fencing at Village de la Tresson, Ile de Noirmoutier, May 1999



Plate 11.4 New zig-zag fencing on dune at Village de la Tresson, looking north-east, Sept. 1999

In addition, very large blowouts which open onto the beach have formed just south of Village de la Tresson, and these are illustrated in Plates 11.5 and 11.6. Plate 11.5 is an annotated 'off the camera' (raw) aerial digital photograph and has not been georegistered, and the dunes here face south-west into the prevailing south-westerly winds. Plate 11.6 is a view of the same part of the dunes and beach taken from the dunes. This section of beach is not immediately backed by housing, but numerous foot-paths and vehicle tracks are visible, and path development, as a result of human pressure, has played a role in the development of these large, active blowouts within this section. These blowouts have developed where destruction of the vegetation cover has resulted in deflation hollows with consequent loss of sand. In addition to trampling pressure caused by visitors on foot, there is evidence that these dunes have been subjected to on dune car driving – which is very destructive of the vegetation cover, and the most recent images display evidence of motorcycle activity.

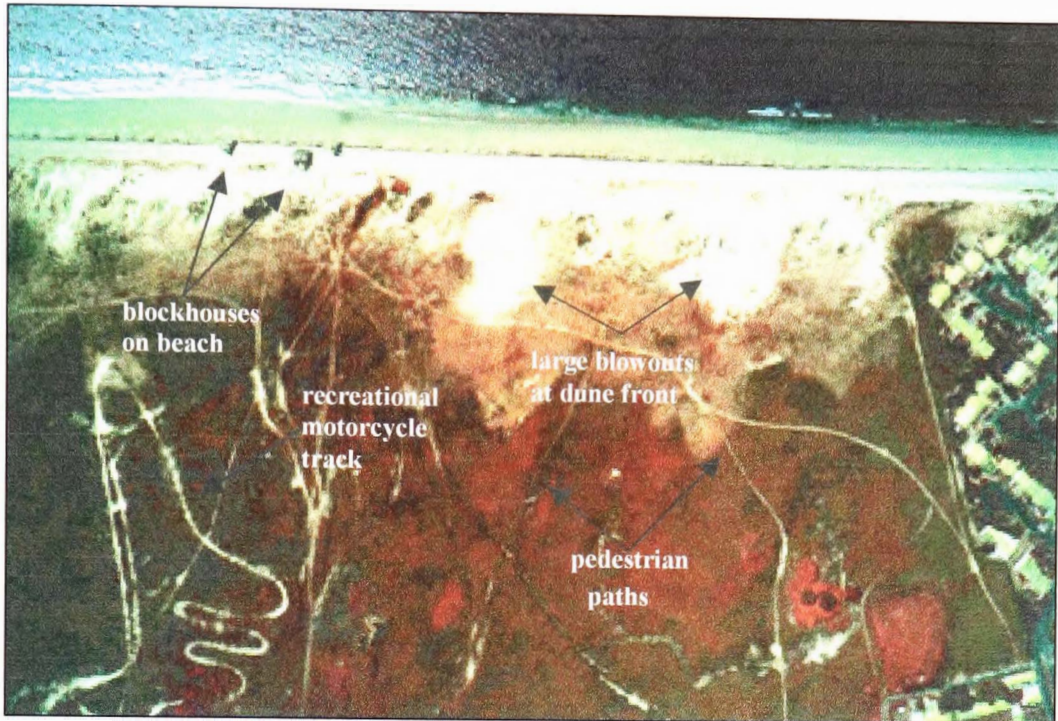


Plate 11.5 Aerial view of part of the dune between Village de la Tresson and le Midi, May 1999

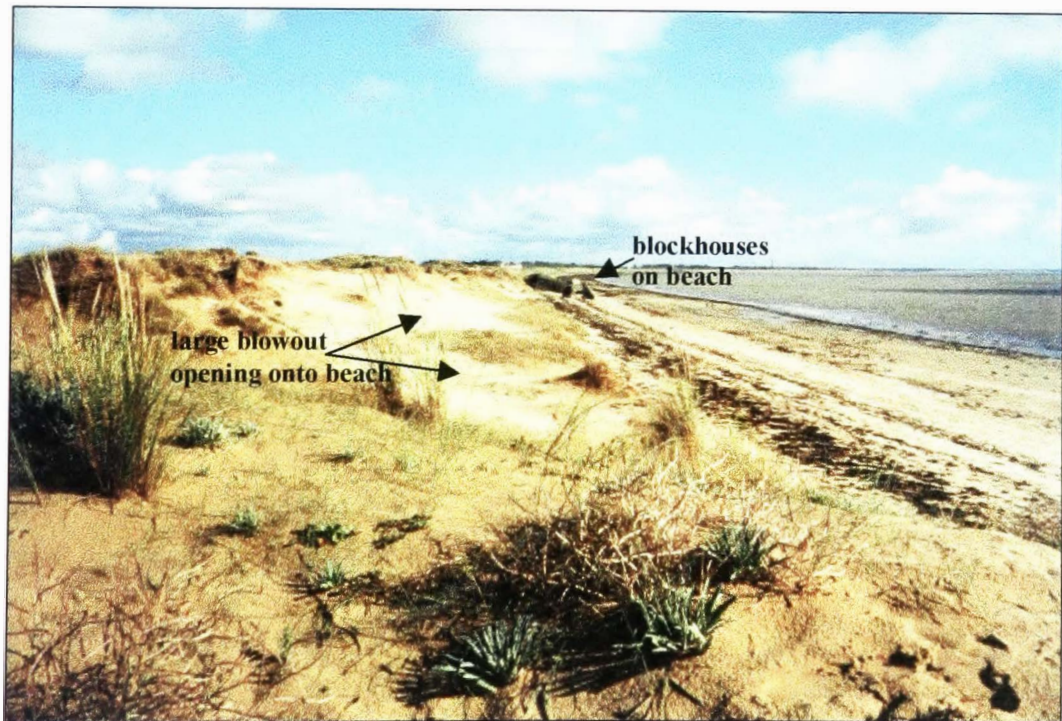


Plate 11.6 View of blowouts and blockhouses from the top of the first dune ridge, September 1999

In addition to the traffic which has destroyed the anchoring vegetation, resulting in the current degradation, erosion has also been facilitated by the relatively steep dune face presented to the prevailing westerly wind which drives the dry sand out of the hollows, mantling the grass sward behind the line of blowouts. In Plate 11.5 this appears as several light red lobate features immediately behind the blowouts. The process has also been exacerbated by a fall in the level of the beach which remains wet at low tide, reducing the supply of wind blown sand from the beach to the dune. This impoverishment reduces the potential to repair the effects of wind erosion. The drop in the beach level is probably the result of the installation of groynes and other structures to the north, interfering with the southerly longshore drift of sediment as at Ile d'Oleron. The sand cliffs that have developed in the dunes immediately in front of the houses in the Village de la Tresson represent a further, although adjacent threat, to this site.

The severely eroded dunes described above terminate in the south in a housing development known as Le Midi, which is constructed almost to the edge of the beach. At Plage du Midi the dune site is also under considerable pressure, both from this housing development and a major campsite immediately adjacent to the beach, built on what should naturally be mobile dune. This type of building activity undertaken without regard for the natural processes at the coast is expensive to defend and is distressing for the owners once the rate of erosion becomes apparent. In addition to the pressures exerted by the development here, the condition of the beach suggests that sand levels are falling here also, evidenced by the beach sand apron remaining wet at low tide, and it's becoming increasingly covered in pebbles.

With a reduced sand supply, there has been intensive wear of the very narrow dune belt separating the housing development and the campsite from the beach. In front of the houses, the dune has virtually disappeared, mostly replaced with an enrochement designed to protect the investment in housing. In front of the campsite, poor management has allowed a period of intensive wear, caused by free access across the dune to the beach. These features can be seen in Plate 11.7, a CIR

photograph from the 1999 survey, and the enrochement is indicated with arrows. Blowouts can be seen immediately to the north (photo left) of the housing development.



Plate 11.7 Blowouts, housing and camp site at Plage du Midi, Ile de Noirmoutier, May 1999

The camp site is relatively empty at this time, as the survey was flown at 'low season' and only the permanent caravans are in the site, whereas during the season the entire enclosure is packed with tents and mobile homes (pers. obs.). When the campsite is busy this narrow piece of remaining dune is subject to intense pressure. Plates 11.7 and 11.8 show the proximity of the campsite to the dune front and although there are fences between the campsite and the dune some are poorly maintained, and they are an inadequate deterrent to visitors. To counter this, a number of walkways have been laid down recently and a new substantial fence has been constructed between the beach and the foredune.



Plate 11.8 Campsite, dune and beach at Plage du Midi, Ile de Noirmoutier



Plate 11.9 Re colonisation of foredune immediately to south of campsite at Le Midi.

This more enlightened management policy has enabled some of the remaining dune surfaces to revegetate, and, not far to the south, as the balance between erosion and accretion changes, zig-zag sand traps have even begun to lead to accretion and colonisation by dune grasses in front of the eroded dunes (Plate 11.9).

11.3.2. Image Analysis of Blowouts between Village de la Tresson and Le Midi

Whereas blowouts are a natural phenomenon in sand dunes, and indeed desirable for ensuring the availability of free sand to sustain typical dune habitat, the location of these in particular, at the very front of the dune, makes them a hazard with regard to protection of the settlements behind the foredune. These morphological changes to the dune front look likely to continue for some time without management intervention and would therefore be classified as fragile components of the dune system (Rust & Illenberger, 1996). A simple technique which could be used by dune managers to monitor the progress of active blowouts is demonstrated in this analysis.

11.3.2.1. Image registration

Images from the three survey epochs have been used to monitor the growth of the blowouts in this area. Using the 1:25000 IGN map 1125OT topographic sheet, Ile de Noirmoutier, to derive control points, the 1997 CIR images were geocorrected and mosaiced in ER Mapper (2D mode) to UTM WGS84, 30N. This mosaic was used as the reference to which the 1996 and 1999 images were in turn rectified because in this case, the swath width of the 1997 images enabled the selection of more control points from the map than either of the 1996 or 1999 image sets. A complete mosaic of the study site showing relationship of settlements to the beach, major access paths and blowouts is shown in Plate 11.10.

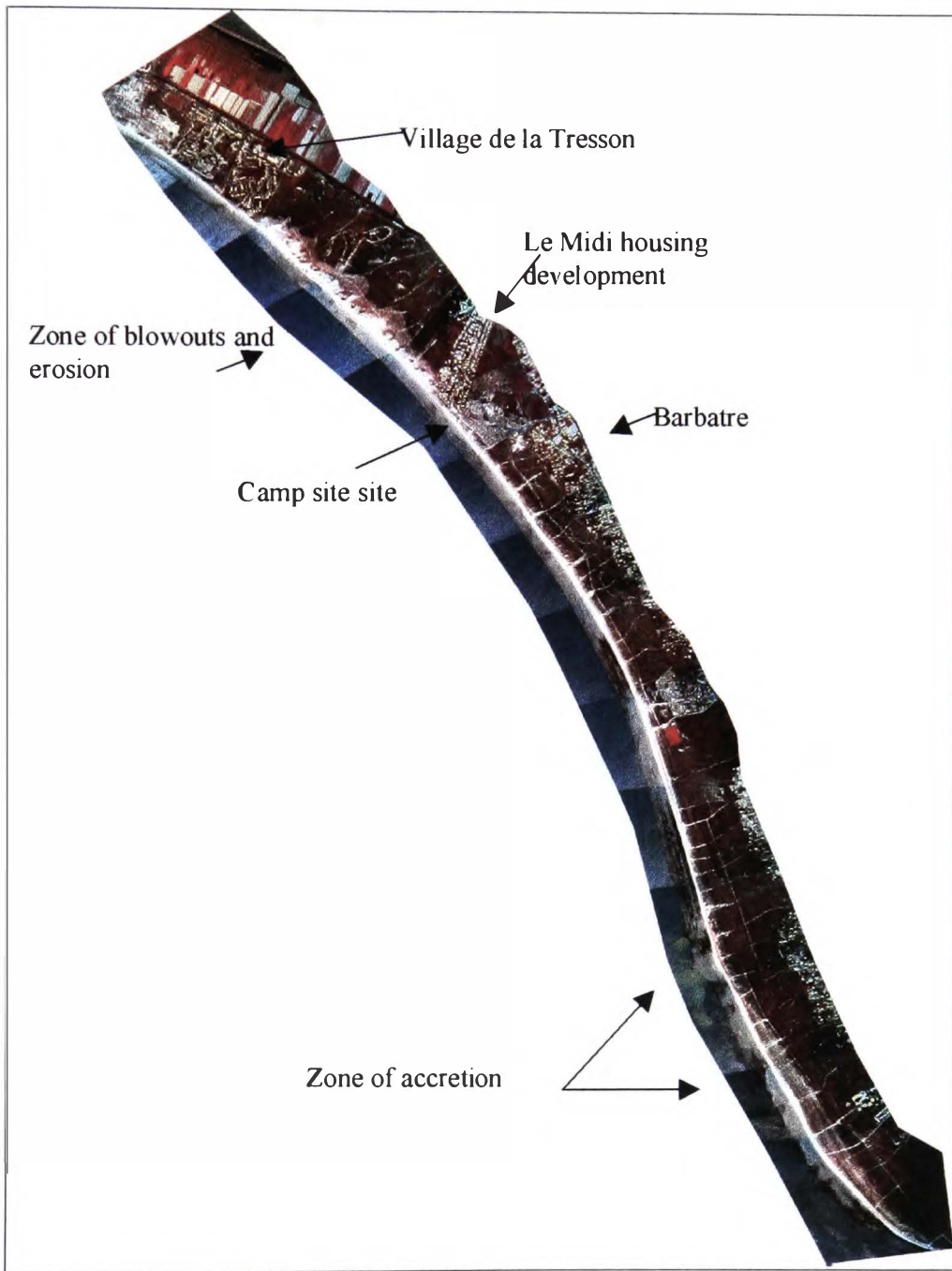


Plate 11.10 Georectified mosaic of the study area at Ile de Noirmoutier showing blowouts in the north and accretion in the south

The accuracy of the mosaicing and co-registration processes is indicated in Table 11.1, as well as the required sample size derived from the formula given in 9.3.2.2. The sample size satisfies the sample size requirement for all calculations, where 0.5m was again the chosen confidence interval about the population mean. RMS data suggest that the mean errors are less than 1.4 m.

	96X-97X	96Y-97Y	97X-99X	97Y-99Y
Minimum (m)	-1.51	-0.93	-0.53	-2.53
Maximum (m)	0.69	0.97	2.09	1.76
Mean (m)	-0.71	0.1	0.16	0.69
Std. Deviation	0.6	0.52	0.62	1.18
Count	23	23	23	23
RMS (m)	0.61	0.52	0.66	1.34
Required sample	8	5	7	23

Table 11.1 Summary statistics for registration errors between the three epochs.

11.3.2.2. Change detection

Each of the colour infra-red mosaics was converted to a single band, greyscale, image. Two of the mosaics were then displayed in ER Mapper, one in the green band and one in the red band producing a bi-temporal composite image. One band was made semi-transparent, allowing both bands to be viewed simultaneously so that differences between the two epochs could be seen.

Figure 11.3 illustrates this procedure.

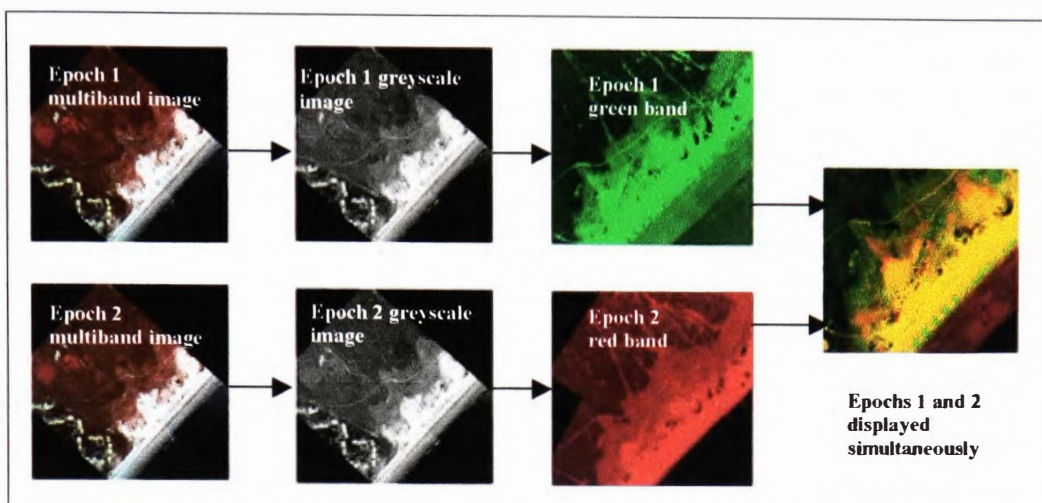


Figure 11.3 Stages in producing a red-green difference image

Displaying the images in this way allowed a comparison of areas of vegetation and bare sand between epochs. For simplicity of interpretation, images from just two epochs were compared each time, with the mosaic from the earlier epoch displayed in the green band, and that from the later epoch displayed in the red band.

To assist with interpretation of the bi-temporal composite images, digital values of three classes of feature namely, dry bare sand, dune vegetation and wind blown deposits were interrogated. Ten thousand pixels were sampled for each class in the 1997 CIR image for red, green and blue values. The mean values are recorded in Table 11.2

class of feature	red (700 -950 μm) mean DN	green(500-700 μm) mean DN	Blue (350-500 μm) Mean DN
Bare dry sand	236	253	184
Dune vegetation	63	28	5
Windblown sand	96	74	39

Table 11.2 Mean digital value for dry bare sand, dune vegetation and windblown deposit on the dune

In Table 11.2 it can be seen that dry bare sand returns the brightest signal in each waveband. Dune vegetation returns the least bright signal in all bands and sand deposited in the dunes returns values in between the other two classes in all bands. This can be used to determine where areas of change exist and this is best explained using the bi-temporal images produced for this case study.

Plate 11.11 shows a subset of the bi-temporal composite of 1996 and 1997 mosaics. The 1996 image is displayed in the green band and the 1997 mosaic is displayed in the red band.

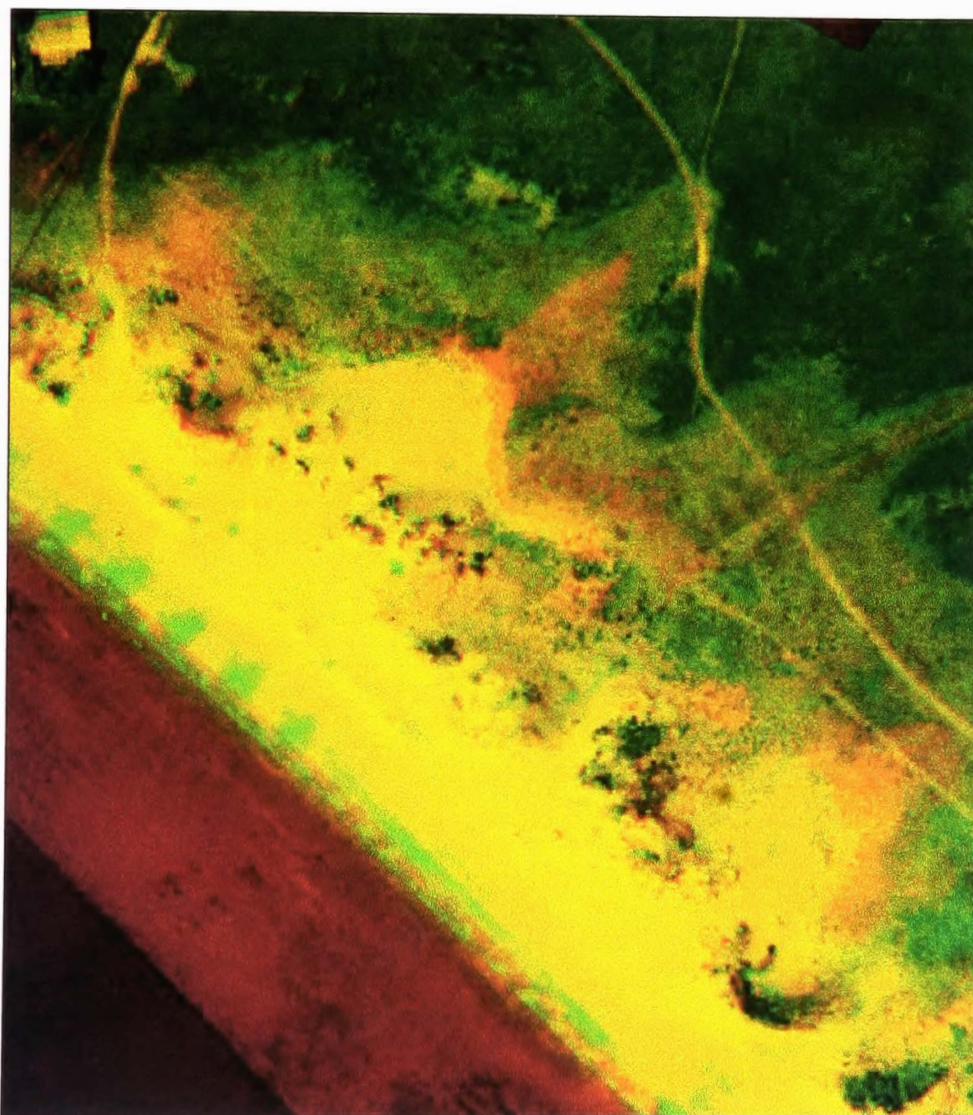


Plate 11.11 Bi-temporal image (1996 green, 1997 red) showing active blowouts south of the Village de la Tresson , Ile de Noirmoutier, France

Where identical features occur at the same pixel locations in two images the digital values at those locations are equal. Since equal amounts of red and green produce yellow, pixels with equal value in both bands in a two-band, red-green image are yellow and this must indicate no change. In this 1996 -1997 composite image much of the beach is unchanged, although the extent of dry sand is different with more dry sand in the 1997 image indicating a lower state of tide. Red areas around the edge of the blowouts show where new areas of bare sand have developed, since dry bare sand returns a high signal, especially in the near infrared. The extent of the wind blown sand is clearly visible and shows as mottled pink and green plumes extending inland from the blowouts.

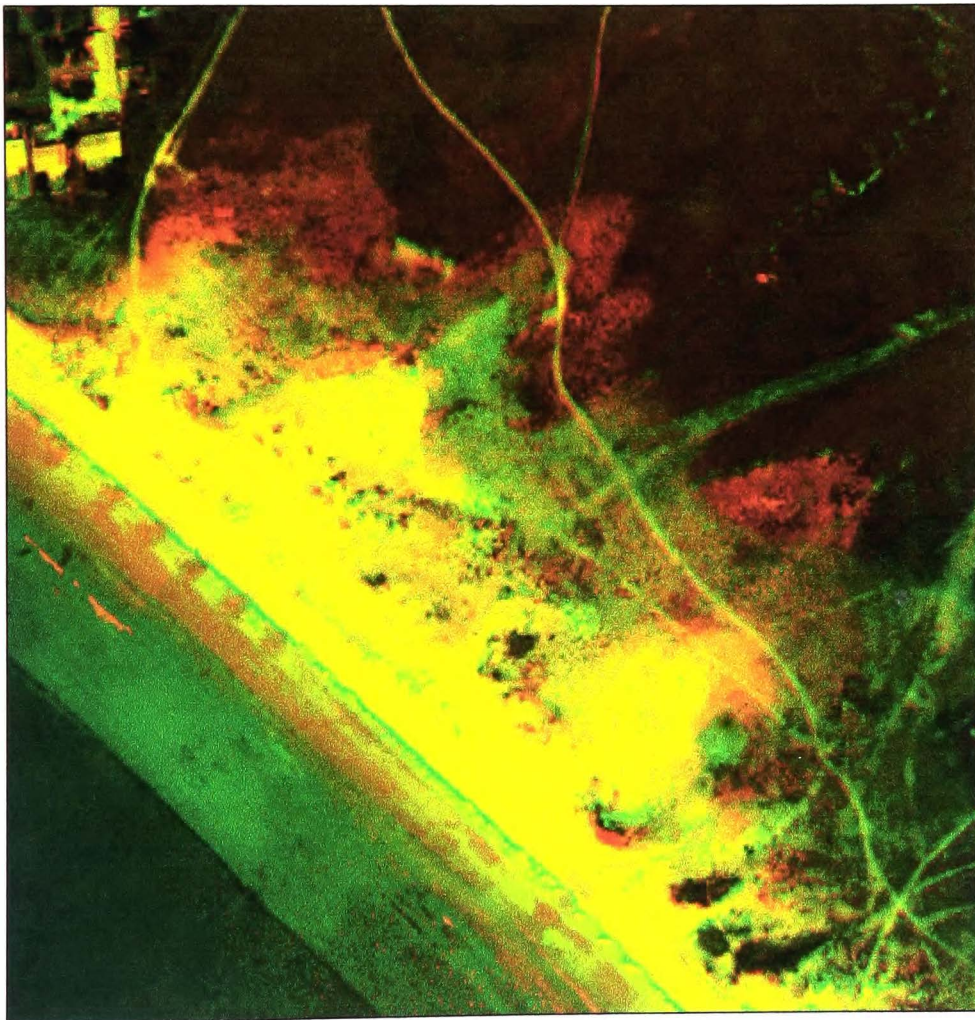


Plate 11.12 Bi-temporal image (1997 green, 1999 red) showing active blowouts south of the Village de la Tresson , Ile de Noirmoutier, France

Plate 11.12 is a bi-temporal image constructed from the 1997 and 1999 epochs, and shows further erosion of the blowouts and also loss of some isolated dune fragments on the foreshore. Green plumes behind the blowouts are wind blown sand deposits on the 1997 image and the red mottled plumes are those on the 1999 image.

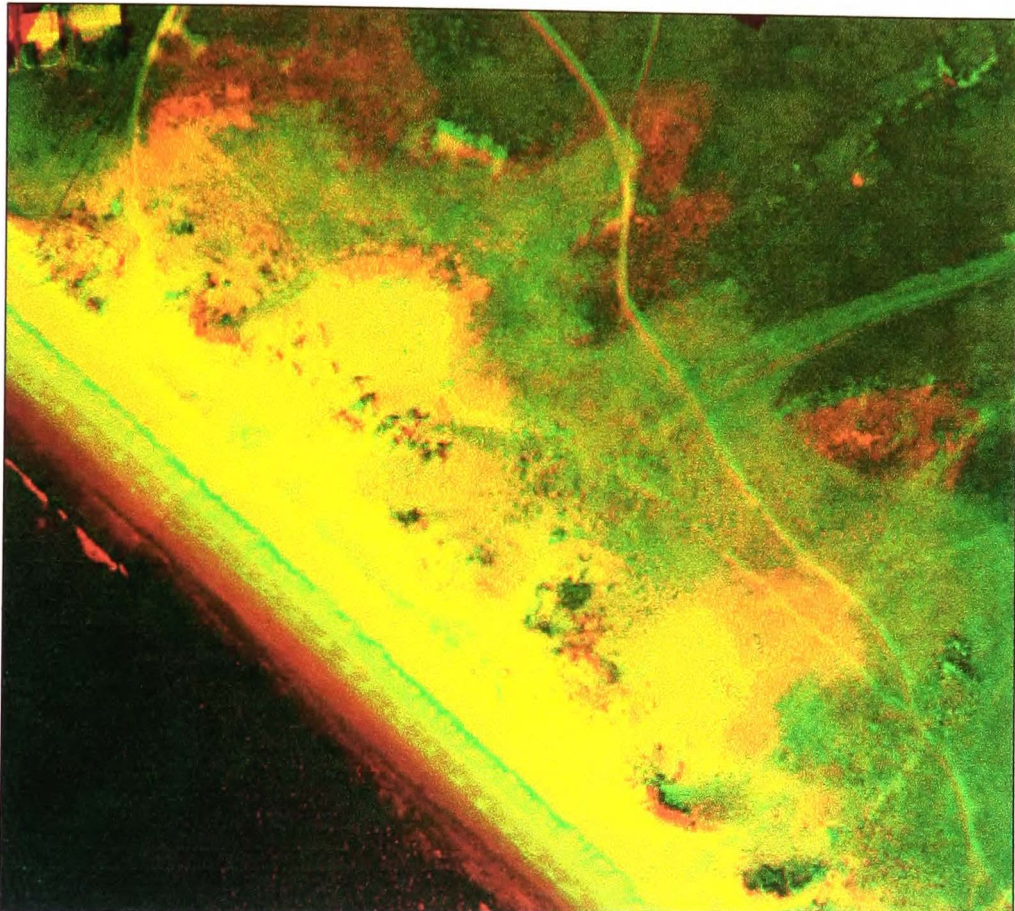


Plate 11.13 Bi-temporal image (1996 green, 1999 red) showing active blowouts south of the Village de la Tresson , Ile de Noirmoutier, France

The full extent of the change in the blowouts is demonstrated in Plate 11.13. Tonal values are as already described in Plates 11.11 and 11.12. Whilst Plate 11.13 shows an apparent overall increase in the erosion around the upper rim of the blowouts, especially in the central blowout, inspection of Plates 11.11 and 11.12 in sequence reveals that there has been spatial variation in the intensity of the erosion, first concentrated on the northern face and then on the eastern face.

These images are very effective in demonstrating change detection, but to quantify the extent of the change in surface area, the rim of the blowouts in each epoch have been digitised in MapInfo v 6.0 and are shown in Figure 11.4.

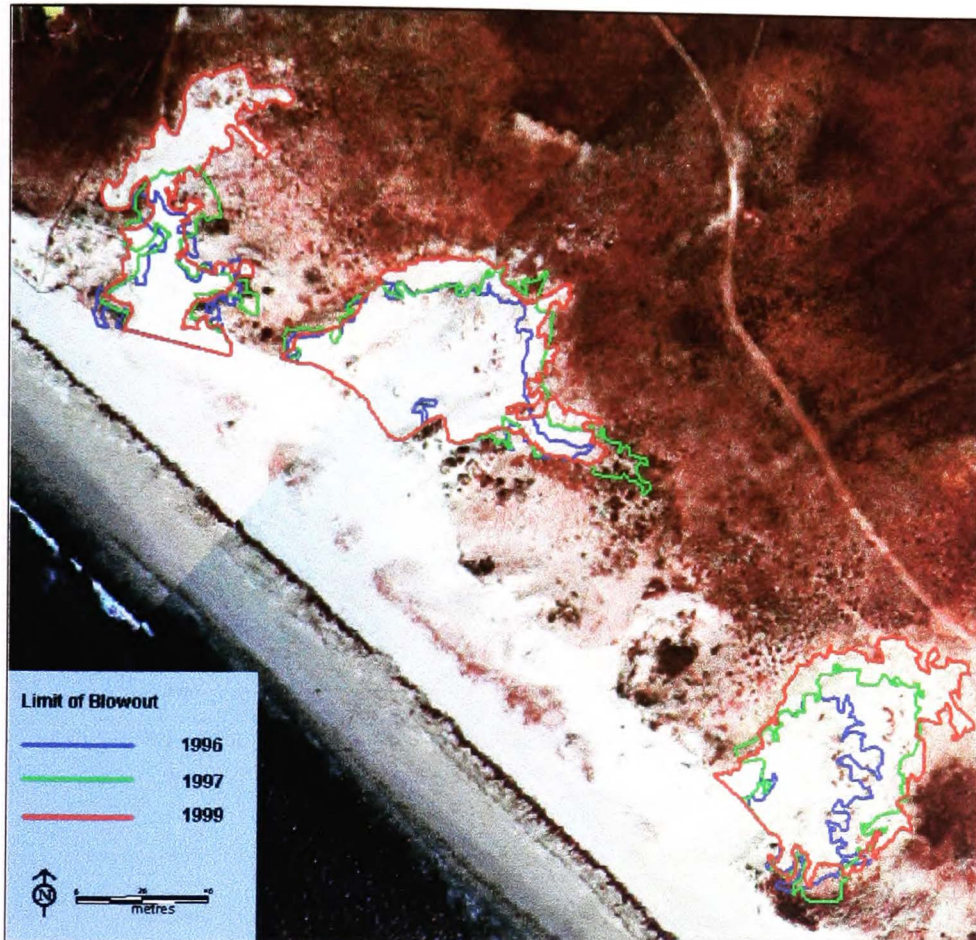


Figure 11.4 Digitised blowouts as source data for Tables 11.3 and 11.4, and relate to change detection shown in Plates 11.11, 11.12 and 11.13

The area of each blowout for each epoch is recorded in Table 11.3 and Figure 11.5 is a graphical representation of this data showing an increase in the area of all blowouts year on year although the largest of the three, blowout 2, appears to have changed least.

	Blowout 1 area (m ²)	Blowout 2 area (m ²)	Blowout 3 area (m ²)
1996-1997	976.25	2512.97	1455.71
1997-1999	1213.49	3168.54	2447.10
1996-1999	1870.92	3249.84	3226.50

Table 11.3 Areas of blowouts south of Village de la Tresson June 1996 to June 1999

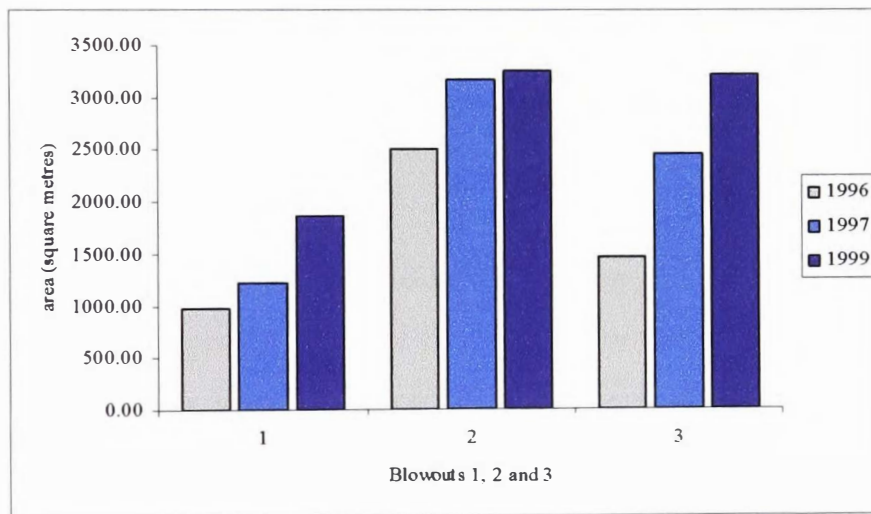


Figure 11.5 Chart showing increase in area of the three blowouts 1996 to 1999

In Table 11.4 the number of square metres eroded from each blowout for each epoch and the percentage increase in the surface area of each blowout is recorded. The total area of increase in each blowout over the entire study period is also recorded as is the percentage increase in area over the entire period.

increase in blowout area	Blowout 1	Blowout 2	Blowout 3
area eroded 1996-1997 (m ²)	237.24	655.57	991.39
area eroded 1997-1999 (m ²)	657.43	81.30	779.4
area eroded 1996-1999 (m ²)	894.67	736.87	1770.79
% increase 1996-1997	24.30	26.09	68.10
% increase 1997-1999	54.18	2.57	31.85
% increase 1996-1999	91.64	29.32	121.64

Table 11.4 Increase in the area of the blowouts 1996–1997, 1997-1999 & 1996-1999 and percentage increase over the same periods.

These values recorded in Tables 11.3 And 11.4 indicate the very rapid changes that are occurring along this stretch of the Ile de Noirmoutier coast. Over the three year period between 1996 and 1999 blowout 1 has increased by just under 92%, blowout 2 has increased by almost 30% and blowout 3 has more than doubled in size with a 121% increase in area. In total close to 3 400 square metres of dune vegetation have been destroyed by the advance of these very active deflation hollows. It is quite probable that large volumes of sand have been lost from the dune, since blowouts tend to deepen as they increase in surface area but without elevation data it is not possible to quantify this and this remains a limitation of this method.

One other interesting change has been detected in the development of the blowouts. Figure 11.6 shows changes in the perimeters of the blowouts relative to the increase in area. Two of the blowouts (1 and 3) show a small decrease in perimeter against an increase in area followed by an increase in both parameters. Blowout 2 shows a concordant increase in perimeter with area, followed by a decrease in perimeter against a further increase in area. In a sense, these patterns are consistent, and suggest that a period of expansion in area can leave irregular or crenulated

edges to the blowouts, with relatively long perimeters, and that these irregularities are likely to be eliminated in the next phase of growth, possibly through subsequent collapse of turf rolls.

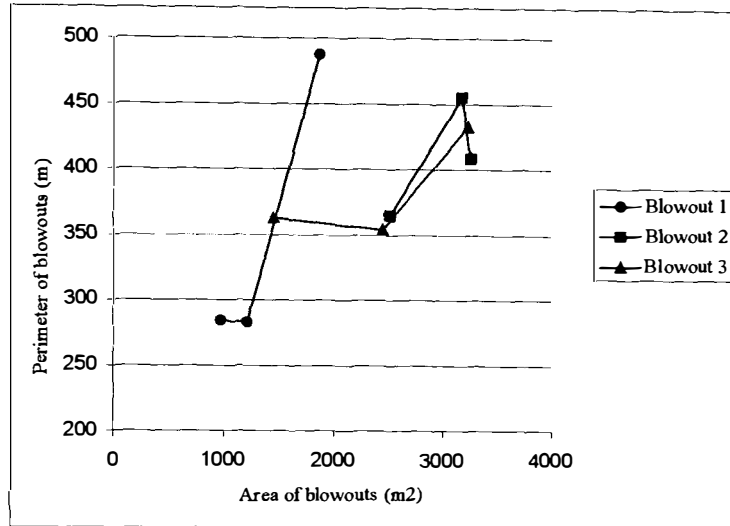


Figure 11.6. Relationship between blowout area and perimeter, Village de la Tresson.

Using such a small data set as this (both in space and time) the explanation put forward might be considered to be merely conjectural and the information itself may be of little value. However, the type of information here, which seems to be indicating the process of growth in the blowouts could be very useful for substantiating this (and other different inferences), if sufficient observations at a high enough frequency were available, and this could be a further advantage of the digital approach to change analysis in natural environments.

11.4. SURFACE CHANGES BETWEEN LA FRANDIERE AND POINTE DE LA FOSSE ~ ACCRETION

11.4.1. Site description

At the distal end of the spit, the dunes are backed by woodland enclosed by substantial wire fences, which separate housing at La Fosse from the beach and dune by several hundred metres. This system is administered by the Office National des Forets (ONF) and although some tracks link the spinal road of the island to the beaches, access for vehicles in this section is limited by

barriers, and because of this, public pressure on these dunes is relatively light with the few visitors well distributed along the shoreline. In general the tourist industry is at a low level with many visitors arriving on foot from the local community.

The sand supply to these dunes is good, witnessed by the large sand banks immediately offshore, and the southerly longshore drift, and as a result, these dunes are prograding. These sand banks are shown in Plate 11.14 and the newly accreting dune appears as small light red patches seaward of the dune front. The following photograph, Plate 11.15 is a view of the same stretch of coast looking south towards Pointe de la Fosse, and here the very light green band of vegetation at the dune front is newly colonising dune grasses, growing seaward of the original fence line which can be seen in the foreground of the picture. This photograph also shows large quantities of seaweed on the beach and this is another important factor in the development of embryo dunes because decaying organic matter provides nutrients and a microclimate for vegetation growth as well as trapping wind blown sand.

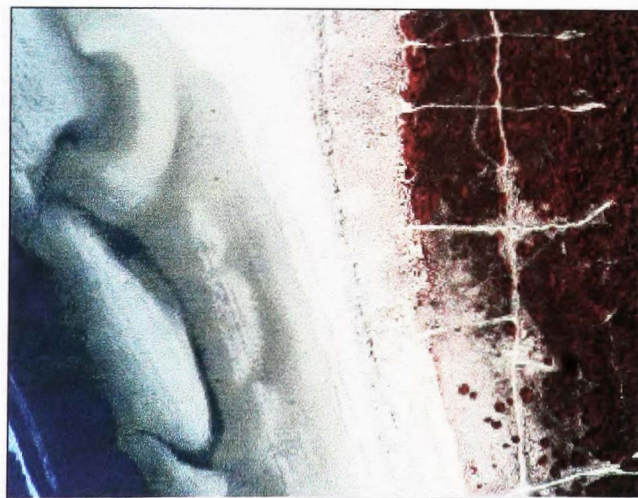


Plate 11.14 Large deposits of sand offshore at the southern end of the dunes at La Fosse, Ile de Noirmoutier, May 1997



Plate 11.15 Prograding dune at La Fosse, Ile de Noirmoutier, September 1998

11.4.2. Image Analysis of accretion between La Frandiere and La Fosse

Erosion of features such as blowouts can, as demonstrated above, be very rapid, and there is little problem in detecting such change using the ADPS. The colonisation of accreting dunes is much more subtle however, and attempts to monitor these changes are detailed in this section.

For this technique to be useful, the quality of the image to image registration must be very high, because of the small changes involved. On this type of terrain dGPS data is ideal as there are usually no previously recorded control points available. In this case, there was no dGPS data available for this southern part of the dunes and inadequate control point data on the available map. In order to demonstrate the effectiveness of the technique, unregistered images were co-registered in ER Mapper in 2D mode and the 1997 image was co-registered with the 1999 image. Table 11.5 records the errors in co-registration of the images but the values given are in pixels and not metres. The nominal ground pixel resolution for these images is 32cm so with error values of approximately 1 pixel, errors are in the region of 0.3 metres.

	97x-99x	97y-99y
Minimum (pixels)	-1.9	-2.86
Maximum (pixels)	1.91	1.9
Mean (pixels)	-0.05	-0.44
Std. Deviation	0.944	1.072
Count	32	32
RMS (pixels)	0.93	1.14
Required sample	23	29

Table 11.5 Co-registration of the CIR images of the southern part of Noirmoutier. Note units are in pixels and not metres.

Detection of change following the same procedure used to detect change in the blowouts was difficult to interpret. This was because the signal from bare dry sand was very bright, whereas the response of the vegetation (especially the dune grasses) was much lower, and the change in the vegetation in the two images could not be discerned. To overcome this problem, the images were inverted so that bright pixels with high values were assigned new low values and vice versa. In this way the low value vegetation pixels were assigned high values whilst the beach sand pixels were assigned low values. The new inverted images were then displayed as two-band, green-red images with the 1997 image in the green channel and the 1999 image in the red channel. The results are shown in Plate 11.16.

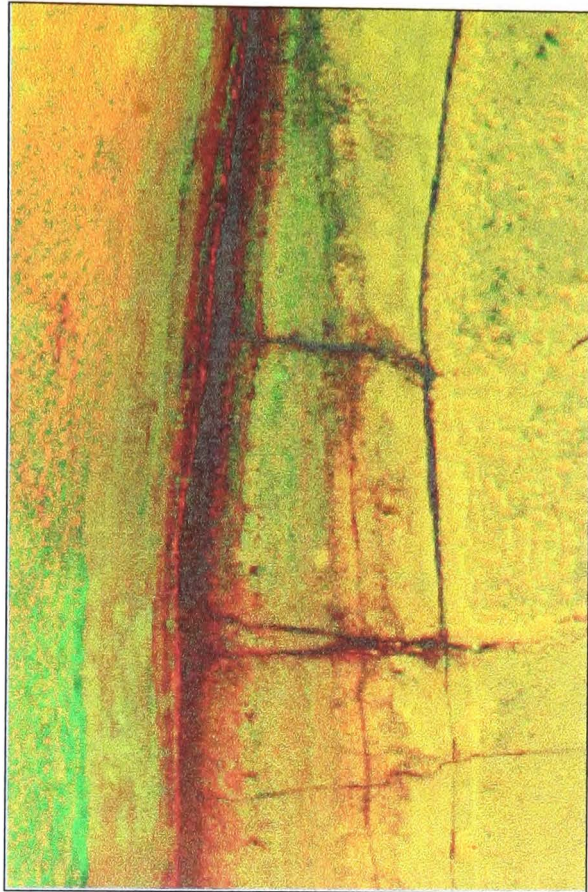


Plate 11.16 Inverted NIR responses of the 1997 image (green channel) and 1999 image (red channel) displayed as a bi-temporal composite image showing vegetation colonisation of the accreting dune coast near La Fosse, Ile de Noirmoutier, France

The key to interpreting this image lies in identifying the beach, which is displayed as a very dark toned strip running from top to bottom of the image, slightly left of centre. To the image left of the beach bright red tones mark the dead seaweed on the beach, and given that this is a bi-temporal image, changes on the beach other than sand redistribution must be expected and will show as red tones. To the photo right of the beach, the newly colonising vegetation is again shown in bright red tones, identifying the increase in vegetation cover between 1997 and 1999. Not only are the changes at the accreting dune front clear, but recolonisation of the paths and de-vegetated areas at the back of the dune can be seen.

Although this image is not geocorrected and therefore is not in true cartographic space it still provides useful information to the dune manager and whilst it is not possible to make absolute measurements of change, it is possible to make relative measurements of change from one epoch to another giving the dune manager a good guide to trends in changes over time.

In Chapter 12 a more rigorous approach to image correction, orthorectification, will be demonstrated using stereo digital photographs with more accurate ground control and softcopy photogrammetry. Orthorectification allows more reliable measurement from aerial photographs than is possible using the techniques demonstrated in Chapters 9, 10 and 11.

CASE STUDY 4 ~ measurement of volume at Holywell Bay

12.1.INTRODUCTION

Continual monitoring of dune sites can be used to measure the response of the landscape to environmental change, regardless of the agents of that change, and these measurements could include the amount of sediment moved, the direction of the movement and the timing and magnitude of the events (Brown & Arbogast, 1999). Measurement of the timing of events will depend on the frequency of the monitoring programme and often the interval between successive surveys using traditional methods has been too long to measure high frequency events at the coast. Using new technologies such as digital imaging and digital photogrammetry it should be possible to increase the monitoring frequency to an appropriate level at a palatable cost.

The techniques that have been used in the previous 3 case studies can all be regarded as 2 dimensional, and these have revealed some useful information, regarding coastline retreat, the extent of sediment redistribution (that is the surface areas of change), the direction of movement (erosion and accretion at Dossen, movement of the sand lobe at Dossen) and to some extent the timing and magnitude of the events (the retreat of the dune face between epochs at Ile d'Oleron).

To fully exploit the spatial data contained within a stereo pair of photographs digital terrain modelling techniques must be used which provides three dimensional data that can be used either graphically or statistically to extract information. The elevation model may be used to measure volume, and if a time series is available a DEM of change can be created to measure historical topographic change. In addition, once the photographs are orthorectified they are planimetrically correct and can be used to make accurate measurements of point, line and polygon data. If these techniques produce reliable products that are 'fit for the purpose of use' then they may well be

used to elicit new information from previously under exploited archived photography that can often be found in coastal dune managers' offices, for as far back as photography of acceptable quality is available. Although the accuracy of data is of prime importance, the main purpose of this analysis is to assess whether colour infrared digital photography can be used to produce orthorectified imagery that can be of use to the dune manager with acceptable accuracy of the results.

The photographs from the 1997 survey of this small dune site were captured in stereo mode. Unfortunately neither of the other two surveys provided useful data with stereo cover, in 1996 the overlap was insufficient and in 1999 the data was of poor quality owing to cloud cover and very turbulent conditions causing tilt displacements (7.1.3.2) well in excess of those acceptable for stereo correlation. Never-the-less the 1997 imagery was used to produce a DEM and from this orthorectified imagery and an orthophoto mosaic. Ground control data was collected using differential GPS and further control was available from the OS 1:2 500 map sheet, Plan SW 7659 – 7759, 1972.

12.2.SITE DESCRIPTION

Holywell Bay is situated on the north coast of Cornwall, SW England, 5 km south-west of Newquay. This is a small dune system of approximately 20 hectares and it faces north west to the Celtic Sea. Figure 12.1 is a map showing the location of the site. A more detailed view of the dune site is given in Plate 12.1. This is an uncontrolled photomosaic made from 10 individual DS 460 CIR frames, mosaiced together in Adobe Photoshop. This type of mosaic does not have the geometric integrity of an orthophoto mosaic but never-the-less it is a very useful product showing the dune site in context of the surrounding area and giving guidance on the extent and condition of the dunes. It is important to note that this mosaic is not orientated in cartographic space.

Figure 12.1 Map of Holywell Bay, Cornwall.

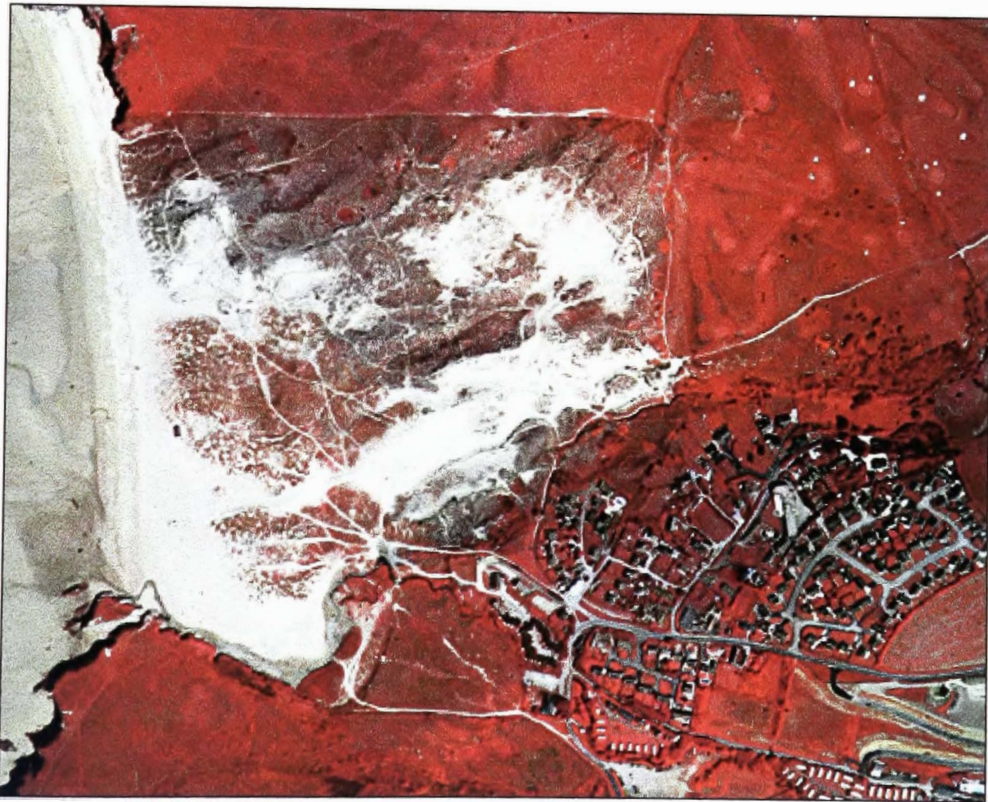


Plate 12.1 Uncontrolled mosaic of Holywell Bay showing the dunes, golf course and town of Holywell, Cornwall

There are several camp-sites to the south east of the dunes and there is a large military camp nearby. The village of Holywell provides modest tourist facilities and there are good road access and car parking facilities for the beach. The south-west coastal path runs through the dunes and part of the hind dune system, the Kelseys, is a golf course. The site appeals both to families and the surfing fraternity as the beach is gently sloping and the surf on this stretch of coast is particularly good.

The site is in both private and public ownership and is divided by a broad pathway running from the back of the dunes to the beach. The northern part is owned and managed by the National Trust and the southern part is owned and managed by the local council. Management strategies differ in the two parts and this is reflected in the difference in status of the two sides of the dune system.

In the past, the southern part has been badly eroded by public pressure and there has been little attempt to restrict access to vulnerable parts of the dune, although wooden walkways have been constructed on major paths through to the beach to encourage visitors to use them. This strategy has not protected the dunes here with the result that there are many paths criss-crossing the dunes, some of which are deeply incised. More recently, the owners have adopted a more active management strategy with fenced paths and planting schemes on badly eroded parts of the dune.

In contrast, the northern part has been more effectively managed and the general public has been denied access to a large part of the system. In this part of the system the dune front is much less eroded than in the southern part, although there are several very large active blowouts and numerous former blowouts which have become recolonised by marram grass. Where the terrain is suitable, areas have been enclosed and grazing by cattle has been re-introduced by the National Trust in order to restore species diversity in the dune vegetation (S.Crummay, Cornwall C.C., pers. com.).

A further management strategy that possibly contributes to the unevenness of visitor impact on the two parts of this dune is that imposed by the very stringent life-guard protocol observed during the summer vacation period. Bathers and surfers are actively encouraged to stay within the safe bathing flags and these are located at the southern end of the beach. Consequently visitors tend to confine themselves to this southern section and in so doing, tread the shortest path to this part of the beach through the dunes.

12.3. GROUND CONTROL

At the time of the survey, real time differential collection was not an option because although several service providers, including Racal Landstar and Fugro Omnistar, were operational they were beyond the budget of this research. Instead, a subscription was made to Focus FM (C & MT), a Real Time Correction Mode (RTCM) service provider, transmitting correction data between 87.5 and 108 Mhz, alongside Classic FM, a commercial radio station. Unfortunately, the service was newly commissioned and the dune site at Holywell Bay was out of range of the nearest transmitter. Since then relay transmitters have been installed and coverage is much improved.

Post processed differential positioning was used to collect ground control data using 2 Magellan ProMark X CP GPS receivers. Two flight lines each of 5 individual frames were sufficient for coverage of the dune system. The photographs were mosaiced rapidly in Adobe Photoshop and the uncontrolled mosaic, overlaid with a clear plastic sheet, was taken into the field to assist with the ground control survey. Points were chosen on the ground that were clearly visible in the image and these were marked on the plastic overlay. In addition, detailed diagrams were hand drawn to give descriptions of each point to assist with identification of the points in the images at the time of relative and absolute orientation. The points were well dispersed throughout the area ensuring that each model (stereo pair) had at least 6 control points in common, for rectification. The ground control was collected in UTM projection, referenced to the WGS84 datum. The base

station was set up on top of a rocky outcrop on the beach with an unobstructed view of the satellite constellation. This is shown in Plate 12.2

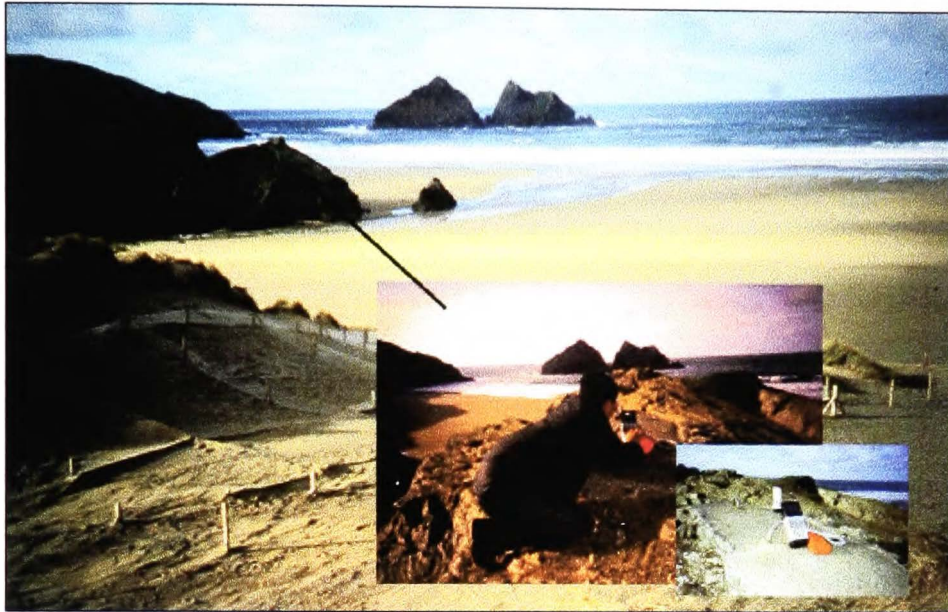


Plate 12.2 Setting up the GPS base station on a prominent outcrop with an open view of the sky

Between 100 and 700 data points were collected at one second intervals at each of the remote stations, the number of points depending on the dwell time at the remote station and on the satellite sets used. The location of the remote points and the base station (marked with a yellow spot) is shown in Plate 12.3.

The data was post processed using Magellan proprietary software. The statistics report provides accuracy assessment of the differential correction and from this the mean standard deviation was calculated and this result is recorded in Table 12.1.

mean sd in x (m)	mean sd in y (m)	mean sd in z (m)
2.74	1.51	2.28

Table 12.1 The mean standard deviation for differential correction of the GCPs

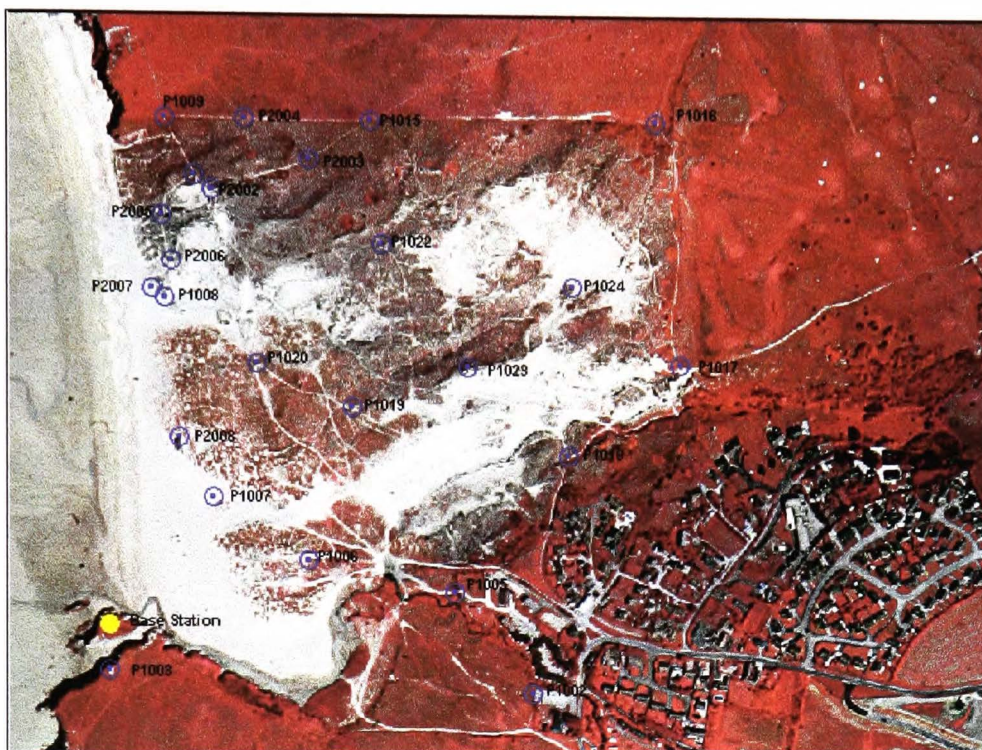


Plate 12.3 The location of the GCPs and the base station at Holywell Bay

12.4. PHOTOGRAMMETRIC PROCESSING

12.4.1. Data input

The images from both flight lines were inspected for overlaps and at this stage line 2 was found to have incomplete stereo cover. Line one was complete and was processed accordingly. The 5 TIFF format images were imported to Virtuoso and converted to 24 bit BIP (band interleaved by pixel) images. The header information is stored in ASCII format in a separate support file detailing the number of rows and columns, whether the file is greyscale or colour, if the image is metric or non-metric and the pixel size *etc.* The results of the camera calibration were input to the camera parameter file so that interior orientation of the images could be calculated. The ground control data was uploaded from Excel to the GCP file to enable absolute orientation and elevation extraction.

12.4.2. Block and model setup

The input and output parameters were specified during block and model setup as described in 8.3.6.1. The DEM interval was set to 2m and the contour interval was set to 5m. The output scale was specified at 1 : 5 000. Of the 4 models (stereo pairs) only three were required to provide orthorectified photographs of the entire dune front. Model number 1 is at the northern end of the system and includes the golf course and pasture to the north-east of the dunes, as well as the northern part of the dunes. Model number 2 is the central model and is mostly dune. Model number 3 is at the southern end of the system and includes the southern part of the dune, part of the town and cliff-top grassland above and to the south of the dune system.

12.4.3. Interior, relative and absolute orientations

Interior, relative and absolute orientations were run on each of the three models. During relative orientation Virtuoso generates common points identifiable on the overlapping area of both images in the model. These are measured relative to the fiducial marks in the camera mask and are influenced by such factors as the type of terrain, the amount of vegetation in the image and the texture of the surface. The beach area presents difficulties because it is relatively featureless and textureless. The sea presents a different problem in that it is constantly moving so it is impossible for the software to generate sensible common points. Absolute orientation maps the model to real world coordinates and it is possible to optimise this calculation by viewing the control point location in stereo mode and repositioning if necessary, by incremental shifts of one fifth of a pixel.

12.4.4. DEM / DTM extraction

The image matching procedure calculates the statistics for a defined window around a given pixel in the first image. The second image is searched for the window that best matches the window in the first image and the difference in the location of the centre pixels in both windows is used to calculate the elevation at that point. The calculation is based on the projection of the pixel location of the centre of each match window onto the ground coordinate system. The image match parameters were set to 5 as this gave a window large enough to produce a reasonable result in a

relatively short time. According to Gooch *et al.*, (1999) the right balance has to be struck between allowing the system to find sufficient matched points and allowing it to create 'false fixes'. A large window size increases the chance of success but also increases the chance of false fixes. Furthermore, it has the effect of generalising the terrain and potentially lowers the accuracy (peaks are lowered and troughs are raised). A large window is usually needed where the image content is low, and it may be for this reason that the software struggled to give a good result on the beach. The match parameters have a direct influence on the number of points generated in the DTM.

Before the DTM / DEM were created the image match was edited to remove spurious information such as spikes and troughs around the edges caused by edge effects. Editing allows the elevation 'postings' superimposed on a triangulated stereo pair to be changed using the stereo view. It is possible to edit individual postings or groups of postings by enclosing those areas where there are obvious anomalies, within a polygon. Anomalies are then removed by smoothing or interpolation between chosen points. In these images, spikes in the sea were removed by applying a constant level of zero elevation to all areas below the tidemark and small troughs and spikes on the beach were removed by smoothing. Each entire model was smoothed once using the gentle smooth facility to improve the representation of the shape of the landscape. Giles and Franklin (1996) demonstrated significant improvements in slope angle, incidence angle and curvature on smoothing, and that the accuracy of the elevation of control points did not suffer substantially during the process.

After match editing the DTM was created. During this process a height is calculated for each of the match points in the image (on an irregular grid). The DEM is generated from the DTM on a regular grid. The grid spacing was specified at 5m intervals. The grid file can be used to produce perspective and isometric plots and can be used to provide cross sections and profiles of the study area. An example of perspective and isometric plots will be give in sections 12.4.6 and an example of the structure of the DEM is shown in section Table 12.3. The contour file generated from the DEM is discussed in 12.4.5.

12.4.5. Contoured orthophoto

Contour plots can give a reasonable representation of the general site morphology and can indicate steep slopes and breaks of slope. The orthophotographs and contour image files were created for each model and the contoured orthophotographs of Models 1, 2 and 3 are shown in Plates 12.4 a, 12.5 and 12.6 respectively. The orthophotos are orientated north with a contour interval at 5m. These photographs have been clipped in the interest of decreasing the file size for display purposes, but still contain the dune which is the most important feature in this investigation. It is important to note that because these images have been clipped they are not displayed at the same scale. Plates 12.4b and 12.4c show detailed views of the othophoto of Model 1. These two extracts show contrasting areas in the contour image, although the maximum and minimum elevations are similar in both extracts, the morphology of the contour plots is markedly different reflecting the different types of landscape in the two plots.

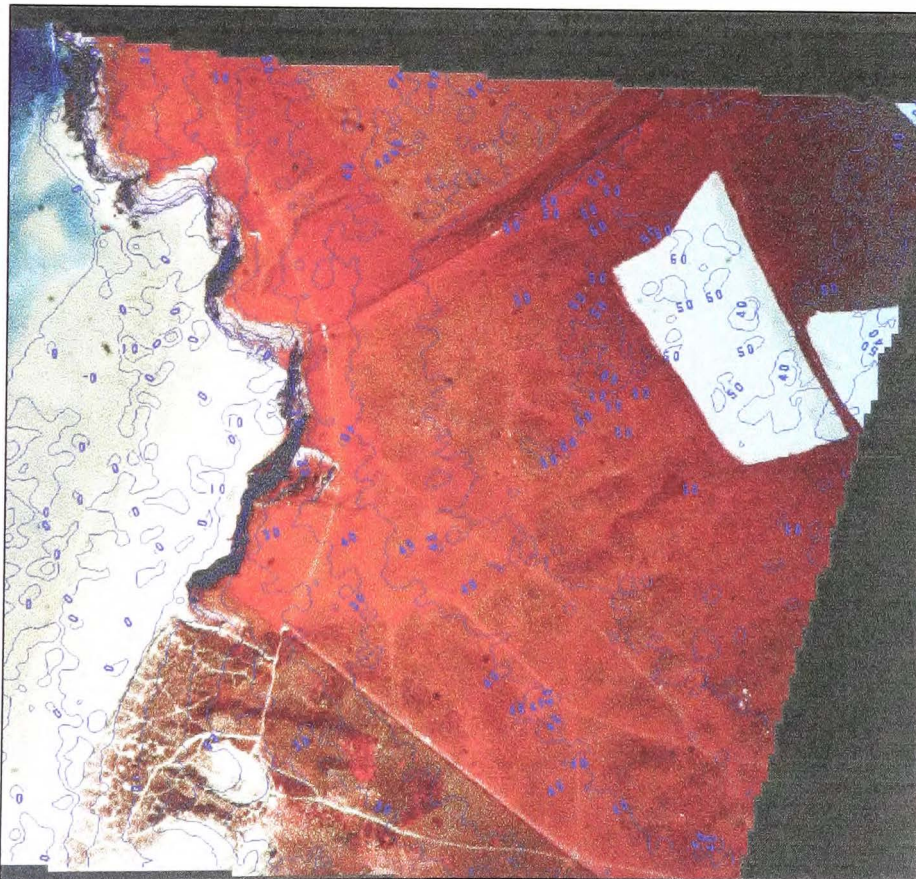


Plate 12.4a Contoured orthophoto created from Model 1

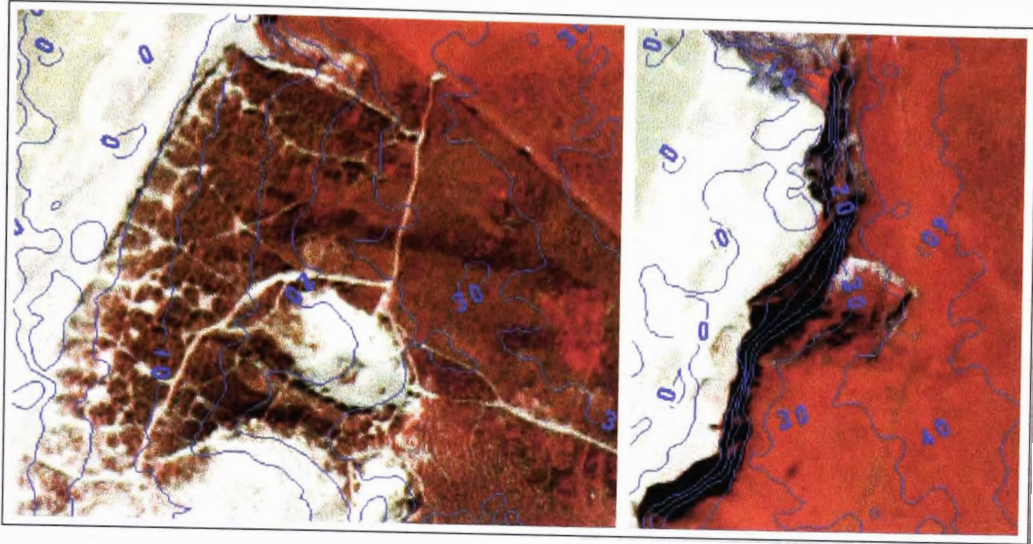


Plate 12.4b Detail of the dune front (left), and the headland north of the dune system (right)

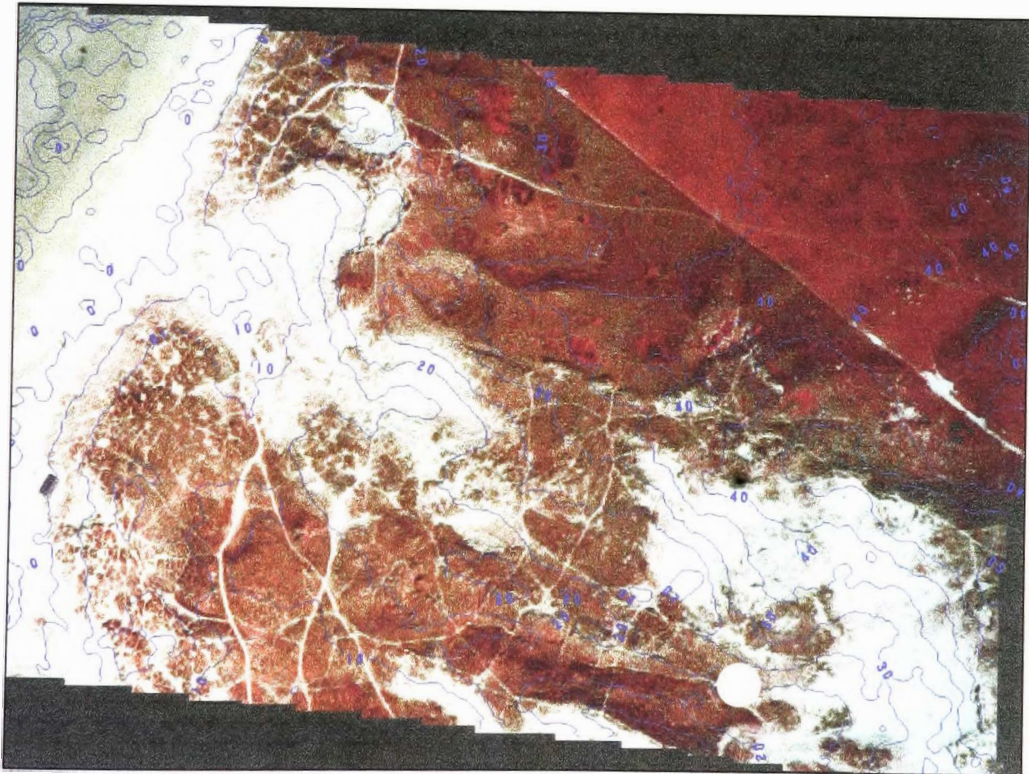


Plate 12.5 Contoured orthophoto created from Model 2



Plate 12.6 Contoured orthophoto created from model number 3

12.4.6. Perspective views

Once the orthophotos have been created it is possible to display them from different perspectives using the drape function. This allows the orthophoto to be draped over the elevation model to give a 3D representation in 2D space. Displaying the images in this way assists the user with further verification of the DEM such that any obvious anomalies that were missed during the match edit process on the planform stereo view become obvious when viewed from a different perspective. Perspective views also assist with photo-interpretation giving the user a better understanding of the morphology of the site, and give a different perspective on the spatial relationships of geomorphic features. For example digitising drainage networks and crest lines and assessing slope aspect can be significantly improved with reference to the perspective view (Welch & Remillard, 1996). Plate 12.7a shows an orthophoto draped over the DEM (top) and the isometric view of the DEM grid (bottom) of Model 2 looking east from the beach. Plates 12.7 b and c show different perspective views of the same orthophoto drape.

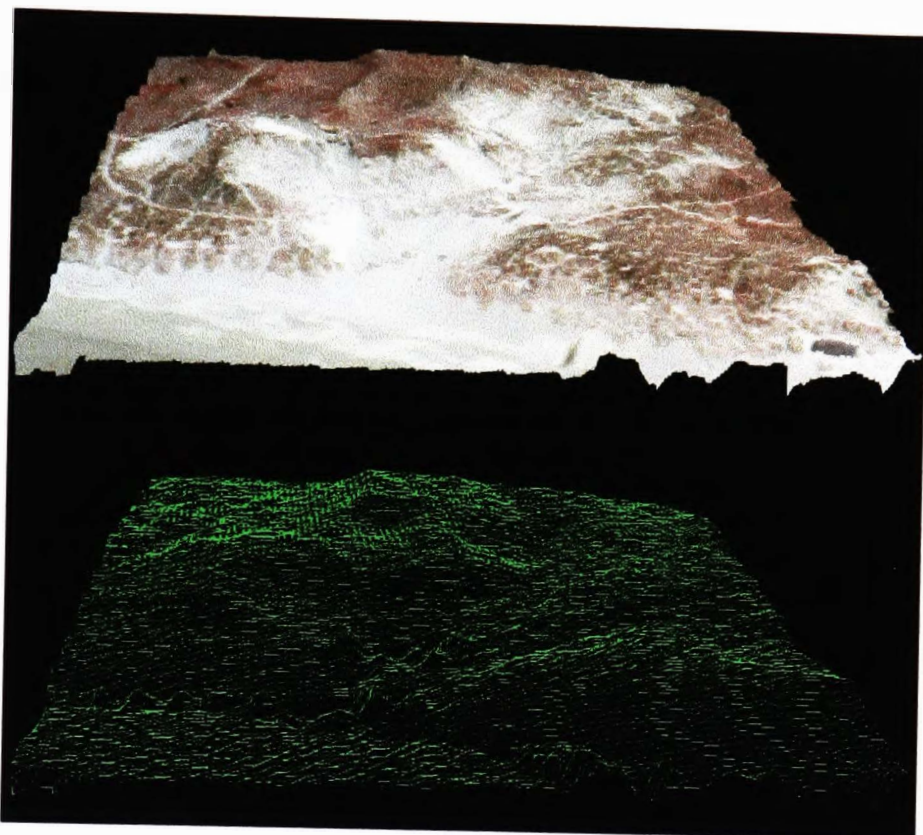


Plate 12.7a Draped orthophoto and isometric view of the DEM grid looking east

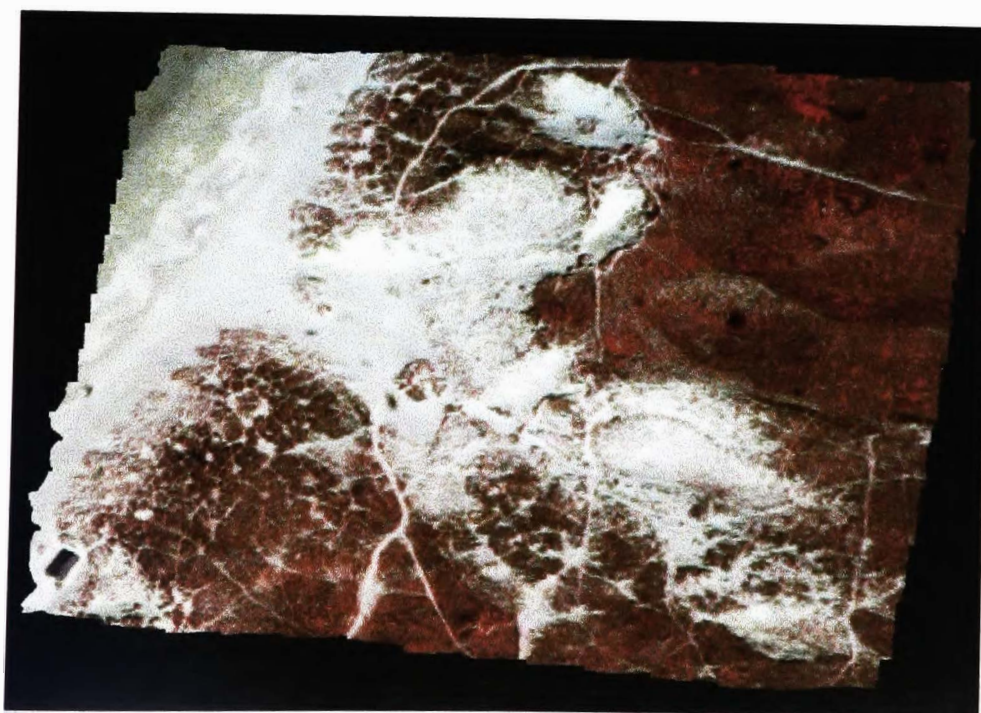


Plate 12.7b Perspective view of a subset of Model 2 looking north

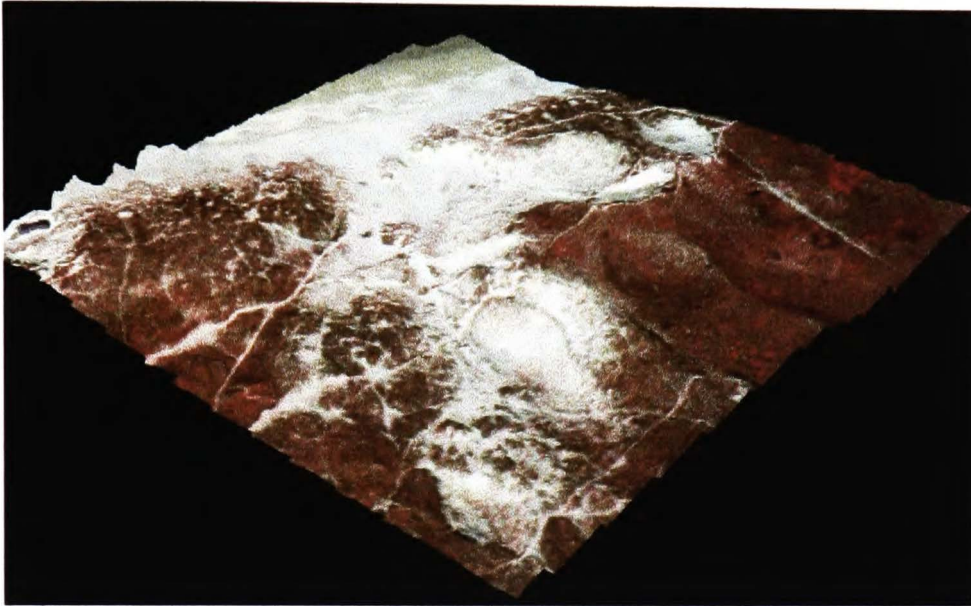


Plate 12.7c Perspective view of Model 2 looking north west

These particular perspective views have been included to enable visualisation in the form and spatial relationships of the blowouts within this study site. As can be seen, the blowouts are located within or on the margins of a deflation corridor leading inland from the beach. For the dune manager, line of sight information enhances decision making on such entities as placement and replacement of fences and paths *etc.* For example, routing a path through the large relict blowout revealed in (particularly) Plate 12.7c would certainly be a imprudent decision, risking reactivation of this feature.

The types of information in particular that can be assessed from these photographs is related to the nature of colour infrared imagery and the spectral response of vegetation. Checking the relationship between spatial location and vegetation type provides further evidence to support the verification of the DEM. This facility is not available to the same extent using either colour or greyscale photography. At this particular site the vegetation structure is relatively homogeneous but there are a few patches of shrubby vegetation which appear on the high ground. This point is worthy of mention, because although it is not very well demonstrated here it is potentially very

useful in dunescapes and other landscapes where there is greater differentiation between foredune and hind-dune species.

12.4.7. Orthophotomosaic

An orthophotomosaic was created in Virtuoso from the individual orthorectified images by merging the DEMs from each model forming a single continuous image. Such an orthorectified mosaic may be used as a map. Plate 12.8 is the contoured orthophoto map of the dune site at Holywell Bay. Unfortunately the mosaic is incomplete due to insufficient forward overlap in the second flight line. Plates 12.9 a, b and c are perspective views of the mosaic.

12.4.8. Quality assurance report

The Quality Assurance (QA) report file contains a list of the results of all the processes that have been performed and provides the user with a means of checking the quality of the georeferencing of the photographs and the output products such as the DEM, DTM and contoured orthophotograph. A summary of the QA data for the absolute orientation of each of the models is provided in Table 12.2. The full QA reports are provided Appendix 2.

Absolute orientation residual values RMS (m)				
	mx	my	mxy	mz
Model 1	1.4395	1.1742	1.8577	1.90
Model 2	2.1067	1.6767	2.6925	1.5511
Model 3	0.7714	1.0991	1.3427	6.6092

Table 12.2 Absolute orientation residual values for models 1,2 and 3

The mean xy values for models 1, 2 and 3 are mostly within or close to those stated for the National mapping accuracy standards (NMAS) that requires well defined horizontal features to be within ± 0.3 mm of their correct position at the 68% confidence level at the map scale. For this

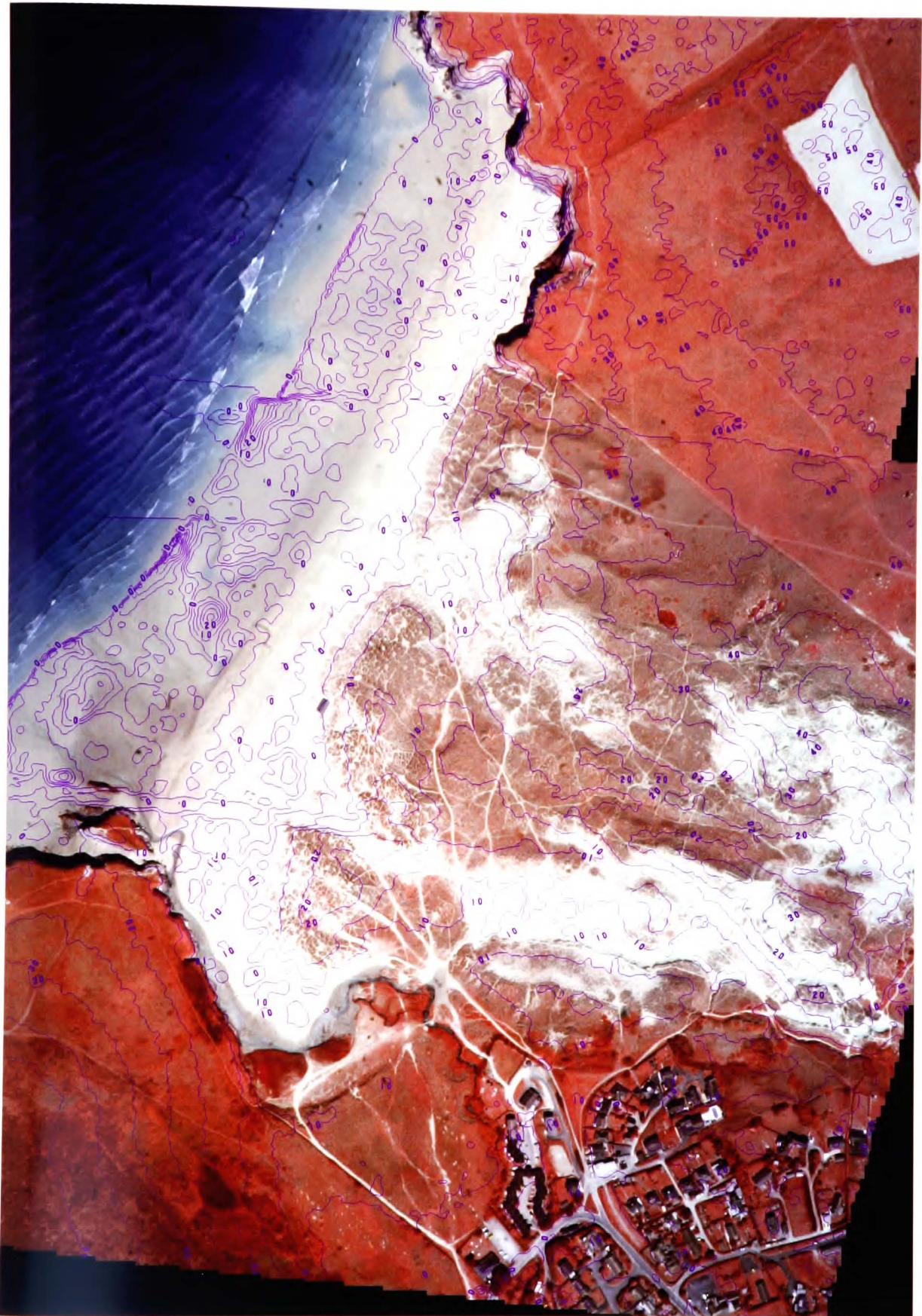


Plate 12.8 Contoured orthophoto mosaic of the dune front at Holywell Bay



Plate 12.9a Perspective view of the dune system at Holywell Bay looking east



Plate 12.9b Perspective view of the dune system at Holywell Bay looking north west

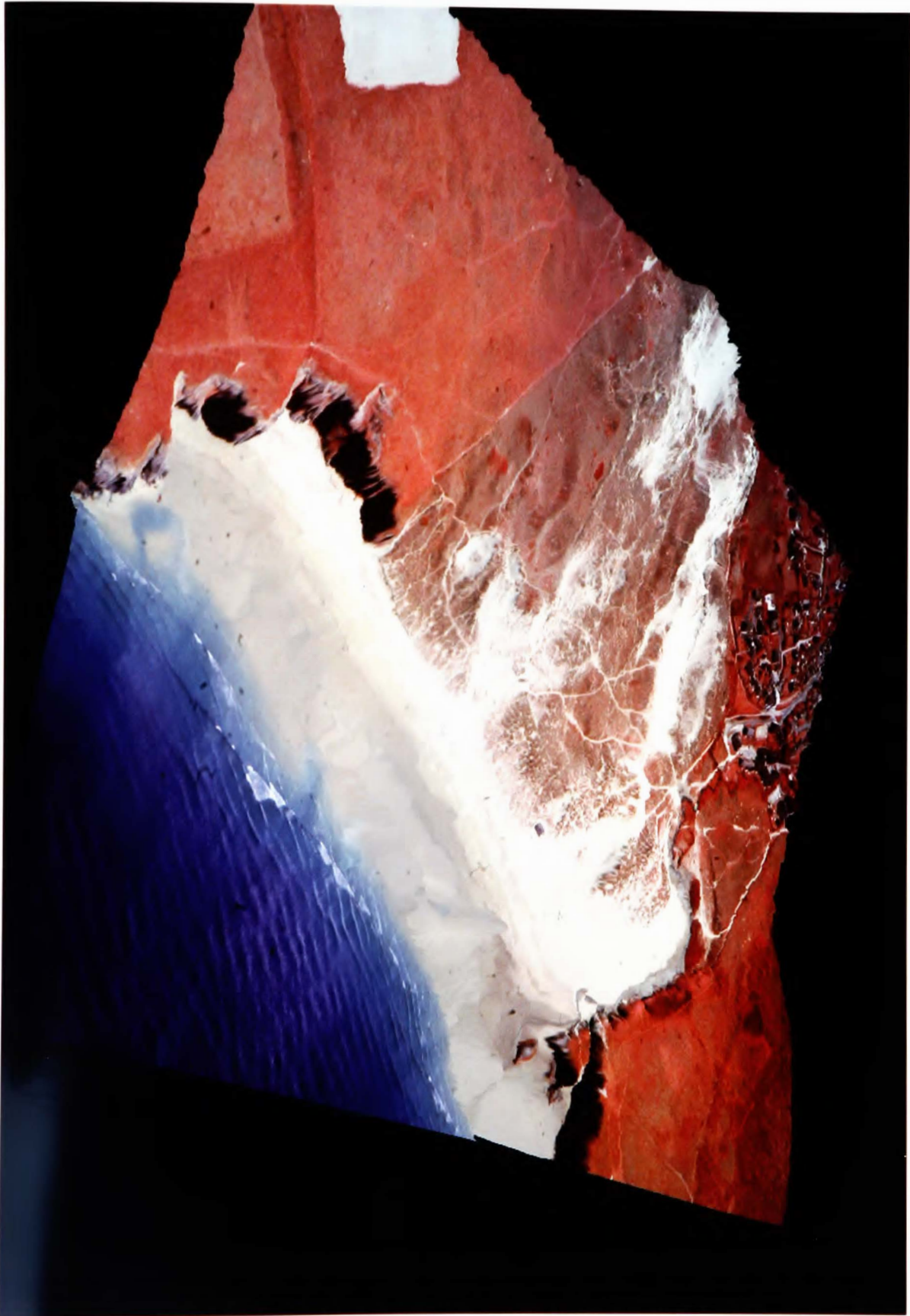


Plate 12.9c Perspective view of the dune system at Holywell Bay looking south east

imagery, captured with a nominal 40cm ground pixel, the best map scale achievable at 0.1mm output is around 1:4000. The models were processed at 1:5000 and this would equate to a NMAS mapping accuracy standard requirement of 1.5 m. This result also shows that if the imagery was truly captured with a ground sampled distance of 40cm the error is in the region of between 1.9 and 5.25 pixels in x, 2.7 and 4.1 pixels in y and 4 and 16 pixels in Z dimensions. The results are less accurate than was anticipated but there could be several reasons for this. First, the photography was not collected for photogrammetric purposes but for reconnaissance, and the relative orientations between the photographs in the models was greater than is ideal. Second, softcopy photogrammetry has been designed for black and white and true colour photography, and these images are CIR. The CIR photographs captured using the ADPS have been shown by Thompson (pers. com.) (6.3.6, Table 6.4) to be of inferior resolution (by approximately 20%) as compared with the true colour imagery so the pixel resolution would be degraded to approximately 50cm resolution and the accuracy would then be within 1.5 to 4.2 pixels in x, 2.1 – 3.3 pixels in y and 3.1 to 13 pixels in Z. Third, the errors are compared against the NMAS requirement; the RMS values are given at the 95% confidence level and the NMAS requirement is stated for the 68% confidence level. The elevation values at 3.1 to 13 pixels are well beyond those quoted by Welch (1989) for vertical accuracies equivalent to 0.5 to 1 pixel, but this was for scanned aerial film photography and processed by an experienced photogrammetrist.

Regardless of the shortcomings of the photogrammetric processing here, model 2 was further processed to extract higher resolution (2m) elevation data in the DEM so that measurements of volume could be made. Reprocessing the data does not improve the accuracy (mean xy 2.7m, mean z 1.5m) but produces elevations at a higher frequency. The errors inherent in the data were not felt to be a problem since they were not to be compared with data from any other source as the intention is to use one data set, edited to simulate several different scenarios. In this way, the relative errors between the data sets is zero.

12.5.DETERMINATION OF BLOWOUT VOLUME

12.5.1.Introduction

Volumetric analysis is an important technique in studies involving geomorphological considerations such as sediment budgets, landform analysis etc. Indicators of the condition of sand dune systems are often expressed by vegetation changes and morphological changes, and many are readily identified using digital imagery. For example, blowout development can be symptomatic of a dune system in danger, hence the extent and distribution of blowouts is of great interest to the manager. In Chapter 11, it was established that it is possible to track the progress of blowouts in the dune, in terms of their planimetric area, using georeferenced data from different epochs of digital photographs. Contoured orthophotographs provide information regarding the morphology of a site, and maps produced from two or more different epochs should provide contour plots that show changes in morphology where they have occurred, but it is difficult to quantify the changes objectively by sight. One of the greatest advantages of using a DEM is the possibility of calculating volumes of materials that have been added to, lost from or redistributed within the system for areas contained within the file. Using orthorectified digital imagery and a DEM it should be possible to extract volumetric data, and with a time series, differences in volume might be calculated by subtracting the grid from one epoch from that of another epoch. The result is a grid surface that shows areas of net change. Areas that return a zero value show either no change or areas where outputs are equal to inputs over the time series of the elevation models.

12.5.2.Photogrammetric processing at a higher resolution

To investigate whether these data are useful for producing measurements of volume, Model 2 was revisited and processed at a higher resolution, to extract a DEM with 2m grid spacing and 2m contour interval named DEM(0). To economise on time and disc space only that part of the model containing the dune system was processed and this higher resolution orthophoto is shown in Plate 12.10.

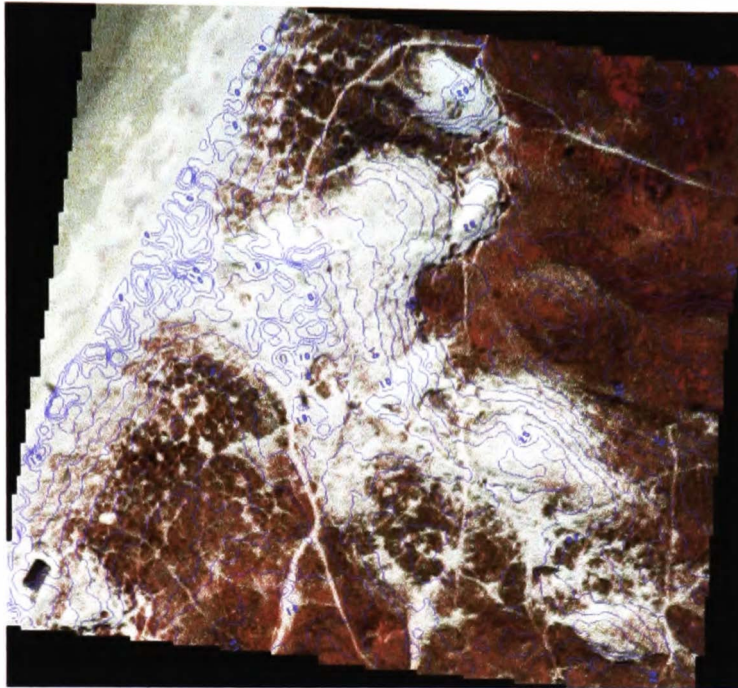


Plate 12.10 Contoured orthophoto with 2m contour interval of a subset of Model 2.

12.5.3. Calculating the volume of the blowouts

Since a time series of digital data was not available, a DEM of change could not be calculated. To simulate this, a crude estimate of the pre-erosion surface was constructed using a planar interpolation to provide a datum with which the measurements of the contemporaneous surface could be compared. Figure 12.2 is a cross section of a stylised blowout with the estimated pre-erosion surface marked with a dotted line.

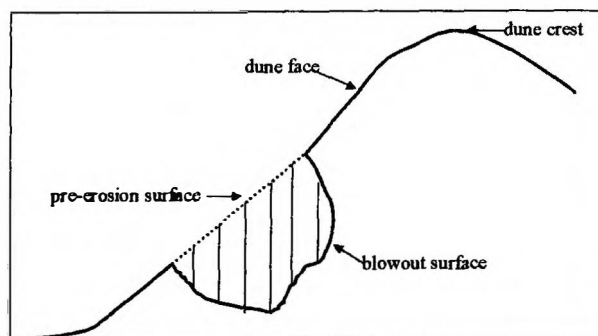


Figure 12.2 Cross section of a blowout in the dune with estimated pre-erosion surface

Three discrete blowouts (blowout 1, blowout 2 and blowout 3) were selected for the investigation as marked on Figure 12.4. and these were processed in a series of steps as shown in Figure 12.3, to extract the necessary information.

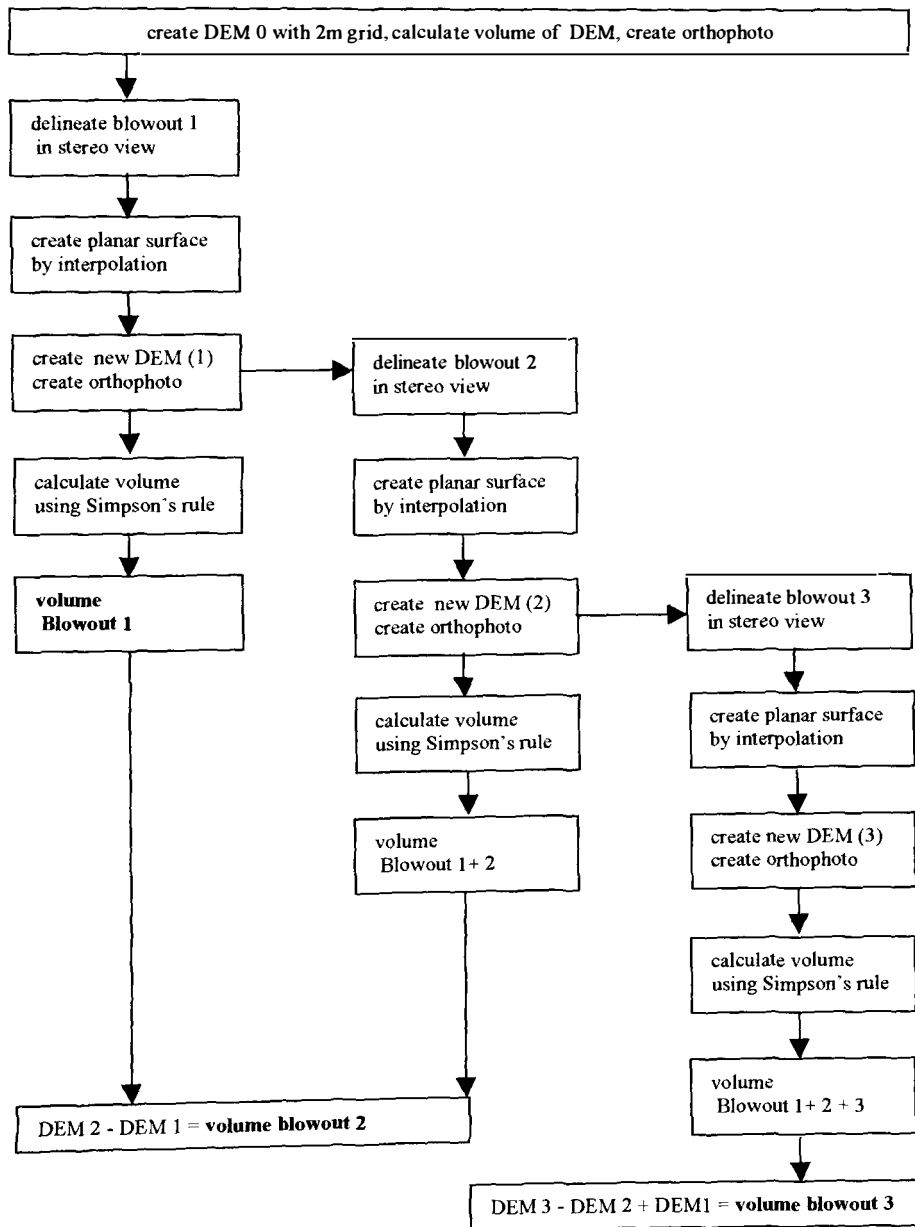


Figure 12.3 Workflow for calculation of blowout volumes using DEM of difference

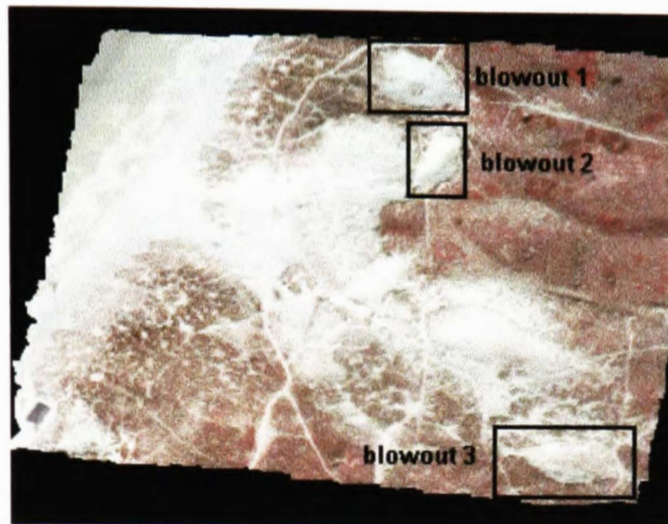


Figure 12.4 Orthophoto drupe showing selected blowouts

12.5.3.1. Editing the DEM

To create the estimated pre-erosion surface of blowout 1, the orthophoto created from DEM (0) was opened and the match edit facility was used to delineate the rim of the blowout in stereo mode. The elevation postings within the delineated polygon were selected and then edited by interpolation, to produce a planar surface. A new DEM was created, named DEM (1). The process was repeated for blowouts 2 and 3 and the results were saved as DEM (2) and DEM (3) so that DEM (2) contained edited surfaces for blowouts 1 and 2, and DEM (3) contained edited surfaces for all three blowouts.

The DEM of the unedited model (DEM 0) was exported to excel. The volume of the entire model was calculated using Simpson's rule (Appendix 3) to find the area under the curve for each row of the DEM. The volume was then calculated by multiplication of this area by the length of the side of the DEM grid, in this case 2m. The procedure was repeated for DEM (1). The volume of DEM (1) was subtracted from the volume of DEM (0) to give the DEM of difference. Since the only difference between the two DEMs was the reconstructed surface across the blowout, the result is the volume of the eroded mass (or the volume occupied by the blowout). The whole

procedure was repeated for DEM 2 (which contained blowouts 1 and 2), and DEM 3 (which contained blowouts 1,2 and 3). A small extract of the DEM (0) is shown in Table 12.3.

346950	5584194	0	2	2	564	233			
-32	-28	-13	10	21	20	13	3	-5	-13
-21	-25	-21	-14	-12	-16	-24	-29	-27	-17
1	25	63	89	96	91	77	59	43	32
27	25	21	15	10	13	19	35	47	50
50	47	50	55	61	68	76	84	87	91
96	101	108	114	119	124	128	134	140	143
143	144	145	149	152	151	148	143	138	133
129	125	121	117	112	108	105	104	103	104
104	116	123	123	121	120	117	114	111	108
108	114	125	134	139	139	138	137	136	134
134	138	141	141	142	151	157	156	155	161
168	170	169	170	170	172	176	178	176	176
223	225	225	224	223	226	232	236	234	232
228	226	226	224	223	222	226	231	232	232
232	230	231	233	234	233	232	234	241	247
254	258	266	276	284	286	284	287	292	296
304	316	327	328	327	328	332	335	336	342
350	354	356	362	367	372	375	379	389	395
393	390	388	391	397	400	400	399	399	398
396	392	387	384	381	380	379	379	379	382
385	387	389	394	402	401	405	412	421	426
427	427	435	446	447	448	447	448	446	451
460	469	478	480	478	476	476	476	476	476
476	476	476	476	476	476	476	476	476	476
476	476	476	476	476	476	-99999	-99999	-99999	-99999
-99999	-99999	-99999	-99999						

Table 12.3 Extract of DEM (0)

The extract of DEM (0) is the native ASCII file produced in Virtuoso. The first line of the file is the descriptor giving the UTM x and y coordinates of the bottom left cell of the DEM. The value 0 refers to the offset height, and in this case it is zero. The DEM interval in x and y are denoted by the numbers 2, and 564 and 233 refer to the number of rows and columns respectively. The values in all of the other lines are the elevation values expressed in decimetres enabling efficient storage of the data, since a decimal point does not need to be stored in every entry in the grid but in effect allows the value to one decimal place to be recorded. This is a very small DEM but it occupies 1Mb of disk space and with a further 131412 bytes of data (the number of bytes occupied by the total number of decimal points required) the file size would increase to 1.13Mb. (For DEMs created from 1: 10 000 large format aerial photographs, processed to give high resolution

DEMs the file sizes can typically be in the order of 6Mb.) The value -99999 refers to areas where there is no data, that is the black edge around the elevation model.

To enable calculations from the data, the header (descriptor line) was stripped off and the file was reformatted so that it was readable in Excel. The UTM coordinates of each cell were then entered, and, because the DEM was read in from bottom to top (*i.e* the y values were in reverse order) the data set was sorted by y-coordinate value in descending order to invert the matrix. A small extract of the DEM in Excel is shown in table 12.4.

REFERENCE_DATA	UTM30Eastings											
		347580	347582	347584	347586	347588	347590	347592	347594	347596	347598	
UTM30Northings	5584494	0	0	0	0	0	29	24	20	16	17	
	5584492	0	0	0	0	2	23	28	22	18	14	
	5584490	0	0	18	15	21	31	30	28	24	16	
	5584488	11	38	55	58	58	43	32	30	29	24	
	5584486	73	76	65	60	59	49	33	32	31	31	
	5584484	99	95	80	62	55	39	34	33	34	37	
	5584482	112	98	54	4	12	38	33	34	38	40	
	5584480	55	43	0	0	0	26	36	36	38	44	
	5584478	0	0	0	0	0	23	32	35	40	47	
	5584476	13	0	0	0	0	27	41	44	41	45	
	5584474	6	4	9	7	6	14	34	41	44	43	
	5584472	8	22	30	26	22	21	29	45	45	43	
	5584470	16	34	36	35	32	31	49	50	47	45	
	5584468	29	39	38	37	35	34	41	50	47	45	
	5584466	37	41	40	39	38	28	18	24	35	47	
	5584464	36	40	42	41	39	29	22	27	35	49	
	5584462	39	40	44	43	41	40	42	44	49	51	
	5584460	45	48	50	47	44	45	51	53	54	54	
	5584458	54	56	56	54	57	57	56	56	56	56	
	5584456	58	60	60	63	66	64	61	59	56	55	
	5584454	61	61	62	67	69	68	67	64	59	57	
	5584452	68	67	66	68	72	70	68	67	64	61	
	5584450	72	70	70	71	72	71	69	68	67	65	
	5584448	74	76	77	76	74	74	72	70	70	67	
	5584446	77	83	83	81	78	75	73	72	71	69	

Table 12.4 Extract of DEM (0) reformatted in Excel and with UTM northings and eastings

12.5.4. Results of the calculation of the volume of the blowouts

A full description of the DEMs of difference are given in Appendix 4. Table 12.5 is an extract of the calculation to find the volume of blowouts 1 and 2 using the results of the DEM of difference between DEM2 and DEM1.

S/3	F+L	Even	Odd	Area_UC_[M^2]	Volume_[M^3]
0.67	0	0	0	0	0
0.67	0	0	0	0	0
0.67	0	0	0	0	0
0.67	0	0	0	0	0
0.67	0	0	0	0	0
0.67	0	0	0	0	0
0.67	0	0	0	0	0
0.67	0	0	0	0	0
0.67	0	4	-4	1	1
0.67	0	60	56	23	47
0.67	0	73	81	30	61
0.67	0	41	42	17	33
0.67	0	-14	-14	-6	-11
0.67	0	-112	-116	-45	-91
0.67	0	-182	-184	-73	-146
0.67	0	-225	-222	-90	-179
0.67	0	-215	-208	-85	-170
0.67	0	-220	-230	-89	-179
0.67	0	-279	-281	-112	-224
0.67	0	-317	-319	-127	-254
0.67	0	-295	-299	-119	-237
0.67	0	-272	-273	-109	-218
0.67	0	-225	-229	-91	-181
0.67	0	-136	-143	-55	-111
0.67	0	-62	-68	-26	-51
0.67	0	20	21	8	16
0.67	0	35	36	14	28
0.67	0	43	43	17	34
0.67	0	42	35	16	32
0.67	0	2	0	1	1
0.67	0	0	0	0	0
0.67	0	0	0	0	0
0.67	0	0	0	0	0
0.67	0	-2	-2	-1	-2
0.67	0	25	29	11	21
0.67	0	51	55	21	42
0.67	0	18	27	8	17
0.67	0	-29	-24	-11	-22
0.67	0	-52	-59	-22	-43
0.67	0	-59	-63	-24	-48
0.67	0	-96	-100	-39	-78
0.67	0	-110	-112	-44	-89
0.67	0	-121	-122	-49	-97
0.67	0	-110	-119	-45	-90
0.67	0	-102	-101	-41	-81
0.67	0	-99	-91	-39	-77
0.67	0	-105	-103	-42	-83
0.67	0	-84	-88	-34	-68
0.67	0	-24	-28	-10	-20
0.67	0	5	8	2	5
0.67	0	22	19	8	17
0.67	0	30	26	11	23
0.67	0	27	38	12	25
0.67	0	1	3	1	1
0.67	0	0	0	0	0
0.67	0	0	0	0	0

Table 12.5 Calculation of the volume of Blowouts 1 and 2 from the DEM of difference.

This table shows the structure of spreadsheet for the calculations of 61 rows of data and 159 columns. This represents an area on the ground of 38796 m² or 3.87 ha and contains the DEM of difference for the blowouts signified by an interger in all but the first column (S/3) in the table. Null values represent no change and therefore the 0 either side of the group of intergers represents

the rim of the blowout. Each row in the table relates to one line of the DEM of difference and is 1 strip for Simpson's calculation of the area under a curve.

The results of the volume calculations are summarised in Table 12.6. The estimated mass of sand is also given, assuming a bulk density of 1.8 tm^{-3} (Powrie, 1997).

	Total vol (m^3)	Total mass (kg)
Blowout 1	1798	3237120
Blowout 2	649	1168800
Blowout 3	1471	2648640

Table 12.6 The estimated mass and volume of material eroded from blowouts 1, 2 and 3

12.5.5. Estimation of the error

These results of the volume calculations appear to give a reasonable representation of the actual geomorphic features on the ground but the volumes calculated are only as accurate as the least accurate element of the data permits, and this DEM has a vertical accuracy of $\pm 1.5\text{m}$. For the purpose of this investigation the errors in absolute position of the data in terms of the absolute orientation residuals and the GPS derived control data are not considered, nor is the GPS error in Z. This is because the investigation is using data with a relative positional error of zero. To understand the effect that the vertical error might have, the volumes were recalculated with all DEM values adjusted to -1.5m of the DEM of difference value. This gave the maximum error value (values in the DEM of difference are $-ve$ because the calculation was made with reference to the reconstructed surface). The recalculated values for volume and mass are recorded in Table 12.7.

	BLOWOUT 1	BLOWOUT 2	BLOWOUT 3
Volume (m ³)	1798	649	1471
Volume max (m ³)	2034	769	1662
Volume min (m ³)	1568	529	1280
Difference ± (m ³)	236	120	191

Table 12.7 The impact of the elevation accuracy on volume calculation

An elevation accuracy of ± 1.5 metres results in an error band of $\pm 13\%$ of the estimated volume of these relatively small blowouts.

12.6. SUMMARY

The results of this investigation have shown how digital small format colour infrared photography can be used to produce orthophoto mosaics. In addition, it has been possible to use the elevation data extracted from a stereo model to calculate the volumes of three small blowouts. The results were less accurate than had been anticipated but there are several reasons why this might be so. If the accuracy of the results are acceptable then these techniques could be used to provide very high density data for numerous epochs of photography which could then be used to map areas of negative, positive and negligible elevation change. With additional data such as the elevations of the substrate, such calculations of volume could be used to estimate the sediment volume of the entire site.

The most likely source of error was probably due to the fact that the photography was actually collected for reconnaissance purposes without due consideration for photogrammetric requirements. The photography was captured in fairly turbulent conditions and this in itself led to scalar changes between (and probably within) images, as well as tilt displacements. Capturing the

photography with photogrammetric processing in mind would probably have yielded better results. In addition the data was captured in CIR mode where the effects of slight defocussing of NIR wavelengths and effects of the CFA add to the difficulties. The next most important element lay in the collection of ground control. One of the difficulties encountered was in finding a reasonable collection of ground control points that were relatively stable across the site and easily recognised on both photographs in the model. In the period since the field work took place, real time differential GPS became available and this would have significantly increased the number of control points that could have been collected in one episode.

The products of this investigation show that the methodology used and the data captured by the ADPS are robust and that with an improvement in the accuracy of the primary data it could provide a very useful tool for the dune manager.

SUMMARY**13.1. INTRODUCTION**

Conclusions drawn from the individual case studies that comprise this study are already discussed in the relevant chapters. It would, however, be useful to draw the conclusions from the individual parts together in a brief synthesis to give an overview of the major findings of the study. In addition this gives the opportunity to evaluate both the data and the methodology adopted as the two are inextricably linked in the context of this research.

The need for a robust method of data collection for coastal mapping has been well established, and where time and money are no object traditional film based aerial photography and photogrammetry would be the ideal choice. Whilst coastal managers may sometimes have access to photographs from regional surveys, they almost certainly do not have sufficient funding to commission surveys at a high enough frequency to map the changes of interest. Using archive aerial photography is often a compromise because of its scale, spectral properties and its coverage. In addition, because of the intricacies of the changes at the coastal zone operating at a variety of different spatial and temporal scales, standard mapping products are unlikely to answer all of the needs of the coastal manager. A pragmatic approach to aerial survey is needed that can provide imagery which can satisfy as many as possible of the conditions dictated by the complexity of the coastal zone. This study has investigated a number of issues associated with the use of digital aerial photography for sand dune management including the methodologies for both capture and analysis of the imagery and the main conclusions are set out below.

13.2. THE MAIN CONCLUSIONS

13.2.1. Measurement of dune recession at Ile d' Oleron

Measurement of retreat at the coastal dunes (particularly in developed areas) is of prime importance for a number of reasons, including, scientific study, the determination of safe construction setback lines and for management decisions regarding future land use and existing property in the dune hinterland.

The dune site at Ile d' Oleron is characterised by retreat of the dune front as depicted in maps provided by the ONF. These maps were produced from ground survey techniques which necessarily involve deployment of personnel in the field. The CIR imagery of this site provided an opportunity for assessing the usefulness of the ADPS in mapping the changes remotely. Apart from a very small amount of accretion that occurred between 1996 and 1997 in the more northerly part of the study site, the results of this investigation showed that erosion occurred along the entire length of the dune front between 1996 and 1997 with up to 28.12 m of erosion at the southern end of the region of interest. Between 1997 and 1999 the maximum erosion was in the region of 48 m at the southern end of the site. The RMS errors for registration of the imagery were just above 1m (1.12, x and 1.04, y) for the 1996 – 1997 match and a little higher (1.26, x and 1.76, y) for the 1997 – 1999 match. The errors are well below many of the sampled data values recorded. One of the advantages of using multitemporal rectified photography to generate digital maps is that the measurements of retreat can be continuous along the entire length of the region of interest, giving a much clearer picture of the spatial dimension of the changes, unlike field methods of measurement that involve measurement at discrete intervals. Indeed the detailed plots of change in the position of the cliff crest line immediately revealed that the greatest degree of retreat occurred at the distal end of the system, with just under 60 m measured during the three year period.

13.2.2. Redistribution of sediment at Dossen

The site at Dossen is particularly suited to mapping changes in the spatial and temporal distributions of sediment because of the distinct physical character of the site. The colour infrared photography exhibits a clear difference between the wet and dry sediment and this is a very useful phenomenon because the rapid drainage and drying out of elevated sand features at low tide gives a ready appreciation of the relief of the beach sediment. The images infer processes that are active, for example erosion and deposition along the dune front, but they also suggest other processes that could be investigated, such as the progressive movement of sand lobes towards the south east, and the redistribution of sand onto the dune surface.

The changes occurring at the dune front at this site were more complex than those at Ile d'Oleron because they were characterised by both erosion and accretion that varied in both extent and distribution between epochs. Over the course of the entire study, the whole system suffered net erosion of some 5386 m² representing 0.4% of the entire dune system. Most of this erosion (96%) occurred in the central zone with 5194 m² lost. The fate of the sand eroded from the central section is of considerable interest, given the large surface area liberated from the sediment sink of the dune. The redistribution of sediment on the beach and on the dunes suggest that the large amounts of sand available for this redistribution from beach to dune has been enabled by a particular factor, possibly sand mobilised by the erosion of the central zone of the dune, which was then redistributed to the southern zone by aeolian transport and longshore drift, providing further illustration of the dynamic relationship between the beach and the dune.

13.2.3. Measurement of surface changes at Ile de Noirmoutier

The investigation at this site centred on the measurement of blowouts in the badly damaged dune front. A different technique for image analysis was used here to assess the progression of blowout enlargement. Bitemporal composite images were created allowing both images to be viewed simultaneously so that differences between any two epochs could be seen. These bitemporal images provide the dune manager with an excellent indicator of the location and rate of change

and of the processes occurring at the dune front. The value of this technique is the speed at which these images of difference can be produced, putting the information into the hands of the dune manager within a matter of hours of the photographs being captured. Mapping the changes revealed that over the three-year period between 1996 and 1999 two of the three blowouts investigated had more or less doubled in area. In total, close to 3 400 square metres of dune vegetation have been destroyed by the advance of these very active deflation hollows. It is quite probable that large volumes of sand have been lost from the dune, since blowouts tend to deepen as they increase in surface area but without elevation data it is not possible to quantify this and this remains a limitation of this method.

Monitoring accretion is also important for the dune manager since accretion is the goal of many management strategies and conversely, natural accretion indicates areas where minimal management effort needs to be expended. In this case, accretion is almost certainly due to natural factors rather than management intervention but the physical expression of accretion would be the same regardless of the agent concerned. One of the difficulties in monitoring accretion over short time intervals is that the vegetation is usually neither vigorous nor abundant and so the signal received at the sensor is relatively poor. For this reason, the registration of the multitemporal images must be very accurate, otherwise the errors are likely to mask or exaggerate the change. The technique used in the previous section of this case study for monitoring large erosional features was not appropriate, but the problems were overcome by the simple expedient of inverting the images. Although this analysis would almost certainly have benefited from using higher resolution imagery the results obtained showed potential for this method. The types of analyses that have been used at this site are completely unavailable to the dune manager who only has access to prints.

13.2.4. Measurement of volume at Holywell Bay

The previous three investigations provided image data that was rectified using 2D control because imagery was not available with enough forward overlap to enable parallax measurements between

the sequential images, nor was there adequate ground control data to allow a 3D correction. The results of this particular case study have shown how digital small format colour infrared photography can be used to produce orthophoto mosaics at 1:5000 scale when stereo coverage and 3D ground control is available. Photography at this scale is often used for coastal mapping and this in itself is a useful result in that it should be possible to compare archived photography with the new digital photography with the minimum of resampling in one or other of the photographs.

In 13.2.3 it was mooted that blowouts tend to deepen as they increase in surface area but that without elevation data it is not possible to quantify this. In this case study the extraction of a DEM has allowed the calculation of the volumes of three small blowouts using a simulated pre erosion surface which appear to give a reasonable representation of the actual geomorphic features on the ground and with additional data such as the elevations of the substrate, such calculations of volume could be used to estimate the sediment volume of the entire site.

13.3. EVALUATION OF THE METHODOLOGY AND THE DATA

A critical appraisal of the data and of the methodology used to capture the data and to process it will serve to explain many of the errors that have been associated with this study. The single most important factor probably lies in the digital photographic data which was intrinsically of high quality but which was captured for quite a different purpose. This meant that the data was not ideally suited even to 2D rectification because the overlaps were sometimes small and the angles of relative orientation were relatively large. In addition, the data was collected with a series of different types of digital camera such that the areas covered on the ground in each epoch were different, and, even when the same camera was used for more than one epoch the camera was rotated through 90 degrees in one epoch relative to the other creating further difficulties for the rectification routines. There were good reasons for all of these inconsistencies in the data and they reflect the continuous changes that must accompany any research into the use of new technologies, where each new development and experience brings greater understanding of the equipment and

the techniques best suited to its deployment and exploitation. These difficulties with the primary data however can be turned to advantage, since if the methodologies used do produce acceptable results using less than ideal data then it is highly likely that much better results could be obtained using data captured for the purpose of use. In a sense this data mimics many 'real world' scenarios where the photography that is available in a long time series is of variable quality, captured at a variety of scales and spectral resolutions and without reliable ground control data.

The methodology for data collection was improved with each mission so that although the data for this research was not ideal, refinement of the methodology put forward here, has in the light of experience gained during these and other aerial survey missions, resulted in a processing chain that has proved to be very reliable.

The availability of GPS data for ground control was limited, especially for the French dune sites and this was due to the remoteness of the sites and the limited budget for the research. The accuracy of the GPS data for those sites where it was collected was not as high as might have been expected and this was very probably due to inexperience in the field.

Some of the points of detail regarding the collection of ground control were not satisfied and this became apparent at the photogrammetric processing stage of the work. For example, points were chosen at inappropriate positions such as on steeply sloping ground and on moving targets such as swaying long grass. The decisive factor for image matching is a point's identifiability on the digital photogrammetric workstation and there were several areas on the dunes that presented difficulties with respect to this. Areas on the beach and on bare sand are difficult for image matching because they are relatively textureless. Areas that are constantly moving such as the sea and river are impossible to match. Improving the ground control would immediately allow a better rectification in all three dimensions and this would significantly improve the results of any measurements subsequently made from the photographs.

13.4. RECOMMENDATIONS FOR FUTURE RESEARCH

In common with most research projects this study has thrown up as many questions as it has answered. This study has been a severe test for the ADPS, but the products have shown both the data and the methodology to be robust and that the dune manager with modest computing skills could very rapidly create informative maps. Overall, the outcome is a positive one and has provided a deal of information where none previously existed. Now that the current ADPS and modus operandi have reached maturity, a time series of bespoke data would enable an investigation into some of the issues raised but not answered here, such as monitoring the progress of sediment stores and investigating processes such as the growth and development of blowouts. With an improvement in the integrity of the primary data it could provide a very useful tool for the dune manager. In addition, the image analysis techniques could well unlock valuable data which have been otherwise inaccessible due to their being held in analogue format and therefore not able to be registered one to another. Dune managers have expressed great interest in the system and its products and now that many of the issues have been investigated it is quite possible that this could become a well used resource for the wider coastal and indeed environmental community.

Further work could be taken along several different lines of enquiry such as comparison of the results achieved here with those from conventional aerial survey and / or the integration with archived film data. In each of the case studies the reasons put forward for the processes at work were speculative as there was no supporting data collected. Accessing data such as storm magnitude and frequency, tidal range and coincidence of high tide with storm activity and wind speed and direction data would add interesting dimensions to the results.

This type of imagery lends itself to integration with other types of digital data in a Geographic Information System (GIS) and this is a powerful tool for planning and management. A GIS provides continuity in dissemination of information between personnel on the inter and intra organisation levels. The maps that were created from the rectified images in this study were useful

for showing at a glance where the changes had occurred, and from them it was possible to measure features on the ground but integration with other data regarding, for example, ecological data, the population pressure at the site, tourist facilities, road access and parking *etc.* could provide the manager with comprehensive data base of information that could be readily retrieved and analysed.

In the near future, the ADPS will incorporate a new camera with a larger array size and faster download time and this will enable the capture of stereo photography at a higher resolution. This in turn should enable the production of elevation data and maps with higher accuracy.

These techniques need not be restricted to the management of sand dunes or indeed the coastal zone in general, but could be applicable in many environmental resource management and mapping situations.

REFERENCES

1. Afek Y. and Brand A., 1998. Mosaicking of orthorectified aerial images. *Photogrammetric Engineering & Remote Sensing*, 16 (2), February 1998, 115-125.
2. Ahmad, A., and Chandler, J.H., 1999. Photogrammetric capabilities of the Kodak DC40, DCS420 and DCS460 digital cameras. *Photogrammetric Record*, 16 (94),601-617.
3. Albanese, F., 1996, The Council of Europe Action for a Sustainable Integrated Management of Coastlines. *Studies in European Coastal Management*. eds. Jones, P.S., Healy, M.G., & Williams A.T.W., Samara Publishing Limited. 12-19.
4. Alveirinho-Dias, J. M., Curr, R. H. F., Davies, P., Pereira A. R., Williams A. T., 1994. Dune vulnerability and management: Portugal and North West Europe. *Littoral* 94, 837-848. Eds. Soares de Carvalho G. & Gomes F., Instituto de Hidraulica e Recursos Hidricos, Universidade do Porto, Portugal.
5. Anders F.J. and Byrnes M.R., 1991. Accuracy of shoreline change rates as determined from maps and aerial photographs. *Shore and Beach*, 59 (1), 17-26.
6. Anderson, J.E., Desmond G.B., Lemeshefsky, G.P., and Morgan, D.R., 1997. Reflectance calibrated multispectral video: a test bed for high spectral and spatial resolution remote sensing. *PE & RS*, vol. 63 (3), 224-229.
7. Ardagh, J., 1982, *France in the 1980's*. Penguin, London. 256Pp.
8. Arens, S.M., 1992. Transport of sand into the foredunes of Schiermonnikoog. *Report on the field measurements, 1990-1991. Dept. of Physical Geography and Soil Science, University of Amsterdam*. 6 lpp.
9. Arens S.M. and Wiersma, J., 1994. The Dutch foredunes: inventory and classification. *Journal of Coastal Research*, 10, (1), 189-202.
10. Atkinson, P. and Curran, P., 1997. Choosing an appropriate spatial resolution for remote sensing investigations. *PE & RS*, vol. 63 (12), 1345-1351.
11. Avis, A.M., 1989. A review of coastal dune stabilisation in Cape Province, South Africa. *Landscape and Urban Planning*, 18, 55-68.

12. Bagnold, R., 1936. The movement of desert sand. Proceedings of the Royal Society, Series A, 157, 594-620.
13. Baker, J., 1998. Military use, sand dunes and nature conservation in the U.K. Coastal dune management: shared experience of European conservation practice. Proceedings of the European Symposium: Coastal Dunes of the Atlantic Biogeographical Region, Southport, England, September 1998. Eds. J.A. Houston, S.E. Edmondson, and P.J. Rooney. In press.
14. Bakker, H.C., and van Kootwijk, E.J., 1993. Vegetation mapping in a Dutch tidal area using a combination of visual and digital analysis. Remote Sensing for monitoring the changing environment of Europe, Winkler (Ed.), Balkema, Rotterdam. 27-44.
15. Band, W.T., 1979. Beach management for recreation in Scotland. In: Les cotes Atlantiques de l'Europe, evolution, aménagement, protection - Brest, France. Ed. A. Guilcher, 261-268. (Acts de Colloques no.9 Brest: CNEXO
16. Band, W.T., 1981. Machairs for recreation. In: Sand dune Machair 3, 3-6. ed. D.S. Ranwell, Cambridge: Institute of Terrestrial Ecology.
17. Barron P. and Dalton G., 1996. Direct seeding of native trees and shrubs in coastal environments. Journal of Coastal Research, 12, (4), 1006-1008.
18. Bate, G. and Ferguson, M., 1996. Blowouts in coastal foredunes. Landscape and Urban Planning, 34, 215-224.
19. Bayfield, N.G., 1979. Recovery of four heath communities on Cairngorm, Scotland, from disturbance by trampling. Biological Conservation, 15, 165-179.
20. Bennet, S.W., and Olyphant, G.A., 1998. Temporal and spatial variability in rates of aeolian transport determined from automated sand traps: Indiana Dunes National Lakeshore, U.S.A. Journal of Coastal Research, 14, (1), 283-290.
21. Bobbe, T., 1997. Applications of a colour infrared digital camera system as a remote sensing tool for natural resource management. Proceedings of The First North American Symposium on Small Format Aerial Photography, Octobr 14-17, Minnesota, USA. 71-79.
22. Bobbe T., McKean J., 1995. Evaluation of a digital camera system for natural resource management. Earth Observation Magazine, vol. 4, (4), 46 - 48.

23. Bobbe, T., and Zigaldo, 1995. Colour Infrared Digital Camera System used for Natural Resource Aerial Surveys. Earth Observation Magazine, vol. 4, 6, pp. 60-62.
24. Boerboom, J.H.A., 1957. Duinlandschap Scheveningen Wassenaar 1300 – heden. Laboratorium voor plantensystematiek en geografie, Landbouwhogeschool, Wageningen.
25. Boorman, L.A., 1976. Dune management. A management report. Institute of Terrestrial Ecology, Cambridge.
26. Boorman, L.A., 1977. Sand Dunes in: The Coastline, ed. Barnes R.S.K.,161-197. Wiley, London
27. Boorman L.A., and Fuller, R.M., 1977. Studies on the impact of paths on the dune vegetation at Winterton, Norfolk, England. Biol. Conservation, 12, 203-216.
28. Booyesen, P de V., 1994. The Effect of stabilisation of the Bushman's River beach sand dunes with rooikrans. Report of the Boesmans Kariega Trust. May, 1994 15 pp.
29. Bowles, J.M. and Maun, M.A., 1982. Biol. Conservation, 24, 273-283
30. Bray, M., Hook J., and Carter D., 1997. Planning for sea-level rise on the south coast of England: advising the decision-makers. Trans Inst Br Geogr NS 22, 13-30.
31. Brivio, P.A., and Zilioli, E., 1996. Assessing wetland changes in the Venice Lagoon by means of satellite remote sensing data. Journal of Coastal Conservation, 2, 23-32.
32. Brown, D.G., and Arbogast, A.F., 1999. Digital photogrammetric change analysis as applied to active coastal dunes in Michigan. Photogrammetric Engineering and Remote Sensing, 69 (4), 467-474.
33. Brunn, P., 1988. The Brunn rule of erosion by sea-level rise: a discussion on large scale two and three dimensional usages. Journal of Coastal Research 4 4, 627 – 648
34. Brunnsden, D., and Moore, R., 1999. Engineering geomorphology on the coast: lessons from west Dorset. Geomorphology, 31, 391-409.
35. Brunnsden, D., 1992. Coastal and landslide problems in west Dorset. In: Papers and Proceedings of the SCOPAC conference: coastal instability and development planning, October 1991, Portsmouth, 29-44.

36. Burden, R.F., and Randerson, P.F., 1972. Quantitative studies of the effects of human trampling on vegetation as an aid to the management of semi-natural areas. Journal of Applied Ecology, 9, 439-457.
37. Burger, B., 1996. The airborne advantage, Earth Observation Magazine, September 1996, Vol 5, (9), 46-49.
38. Burton, P., 1998. Grazing as a management tool and the constraints of the agricultural system: a case study of grazing on Sandscale Haws Nature Reserve in Cumbria. Coastal Dune Management: Shared Experience of European Conservation Practice. Proceedings of the European Symposium: Coastal Dunes of the Atlantic Biogeographical Region, Southport, England, September 1998. Eds. J.A. Houston, S.E. Edmondson, and P.J. Rooney. In press.
39. Campbell, J. B., 1987. Introduction to remote sensing. Guilford, 551 pp.
40. Carter, R.W.G., 1980. Human activities and geomorphic processes: the example of recreation pressure on the Northern Ireland coast. Zeitschrift fur Geomorphologie, Supplementband 34, 155-164.
41. Carter, R.W.G., 1988. Coastal environments. Academic Press.
42. Carter, R.W.G., 1991. Near future sea level impacts on coastal dune landscapes. Landscape Ecology, 6 (1/2), 29-39.
43. Carter, R.W.G., Nordstrom, K.F., and Psuty, N.P., 1990. The study of coastal dunes. In: Coastal dunes, form and process, ed. Carter, R.W.G., Nordstrom, K.F., and Psuty, N.P., Wiley, 1-14.
44. Cartright, R., 1987. Foredune Development on a Developed Shoreline: Nedonna Beach, Oregon. Coastal Zone '87, 1343-1356.
45. CCIRG [Climate Change Impacts Review Group], 1996. Review of the potential effects of climate change in the United Kingdom, Second Report. Prepared at the request of the Department of the Environment. London: HMSO.
46. Chapman, D.M., 1989. Coastal dunes of New South Wales: status and management. Technical Report 893, Sydney, University of Sydney Coastal Studies Unit.
47. Chapman, D.M., Berghs, M., Wickham, G. and Strike, T., 1987. Coastal dune status and management conflicts, New South Wales, Australia. Coastal Zone 87, 4778-4793.

48. Charlier, R.H., and Charlier, C.C.P., 1995. Sustainable multiple use and management of the coastal zone. Environmental management and Health, Vol. 6 (No.1), 14-24.
49. Chauvaud, S., Bouchon, C., and Maniere, R., 1998. Remote sensing techniques adapted to high resolution mapping of tropical marine ecosystems (coral reefs, seagrass beds and mangrove). Int. J. Remote Sensing, 19 (18), 3625-3639.
50. Ciavola, P., Mantovani, F., Simeoni, U., and Tessari, U., 1999. Relation between river dynamics and coastal changes in Albania: an assessment integrating satellite imagery with historical data. Int. J. Remote Sensing, 20, (3), 561-584.
51. Clarke, T.A. and Fryer, J.G., 1998. The development of camera calibration methods and models. Photogrammetric Record, 16 (91), 51-66.
52. Clarke, T.A., Wang, X., and Fryer, J.G., 1998. The Principal Point and CCD cameras, Photogrammetric Record, 16 (92), 293-312.
53. Comer, R.P., Kinn, G., Light, D., and Mondello, C., 1998. Talking Digital, Photogrammetric Engineering and Remote Sensing, 64, (2) 1139-1142.
54. Coops, A., 1953. Vegetatie en vegetatiekartering van der Bierlap, een duinvallie bij wassenaar. Duinwaterleiding van s'Gravenhage, the Hague.
55. Copley V. R., Flasse S. P., Navarro, P., Ceccato P. and Koh, A., 1997. Validation of satellite data by airborne digital photographic data for estimating low vegetation cover. In Press
56. Correia, F., Dias, J.A., Boski, T. and Ferreira, O., 1996. The retreat of the Eastern Quarteira cliffed coast (Portugal) and its possible causes. Studies in European Coastal Zone Management, 129-136. eds. Jones, P.S., Healy, M.G., & Williams A.T.W., Samara Publishing Limited.
57. Costanza . R., Perrings C. and Cleveland, C.J., (eds) 1997. The Development of Ecological Economics. Cheltenham: Edward Elgar.
58. Council of the European Communities. 1992. Council Resolution 92/C59/01 on the Future Community policy concerning the European coastal zone. 25th February 1992. Official Journal of the European Communities.

59. Cousin, F.M.H., Geelen, L.H.W.T., Olsthoorn, T.N., 1998. Amsterdam water supply, implementation of eco-hydrological research. Coastline, EUCC quarterly magazine, 1998, 3, 13-20. Eds. Drees, M.J., Buissink, F., Goddijn, H., Houston, J., and Jimenez, J.A.
60. Cracknell, A.P., 1999. Remote sensing techniques in in estuaries and coastal zones- an update. International Journal of Remote Sensing, 20, 3, 485-496.
61. Crawley, G., 1981. The solid state still camera and the future. B. J. Phot., in: Graham, R., 1998, Digital Imaging. Whittles Publishing, 77pp.
62. Creed, C.G., BodgeK.R., Suter, C.L., 2000. Construction slopes for beach nourishment projects. Journal of Waterway, Port and Coastal Engineering, vol 126, (1), 57-62.
63. Curr, R.H.F., Koh, A., Edwards, E., Williams, A.T. and Davies, P., 2000. Assessing anthropogenic impact on Mediterranean sand dunes from aerial digital photography. Journal of Coastal Conservation, 6, 15-22.
64. Dahl B.E., Fall, B.A., and Ottens, L.C., 1975. In Estuarine Research, ed. Cronin, L.E., Vol 2, 457-483, in Carter, R.W.G., 1988, Coastal Environments, Academic Press.
65. Davies, P., Curr, R.H.F., Williams A.T.W., Hallegouet, B., Bodere, J-C. and Koh A., 1995. Dune management strategies: a semi-quantitative assessment of the interrelationship between coastal dune vulnerability and protection measures. Coastal management and habitat conservation: (eds) A.H.P.M. Salman, H. Berends and M. Bonazountas. EUCC, Leiden, The Netherlands.
66. Davis, D., 1992 Issues in Coastal Zone Management, International Journal of Environmental Education and Information, published by Environmental Resources Unit, University of Salford. Pp. 46
67. de Bonte, A.J., Boosten, A., van der Hagen, H.G.J.M., and Sykora, K.V., 1999. Vegetation development influenced by grazing in the coastal dunes near The Hague, The Netherlands. Journal of Coastal Conservation, 5, pp. 59-68.
68. de Ruij, J.H.M., 1989. The sediment balance along the Holland coast 1963-1986. Rijkswaterstaat, Dienst Getijdewateren, 's-Gravenhage/Directie Zeeland, Middleburg. Nota GWA089.016/ZL-NLX-89.42. pp.43. In: Arens S.M. and Wiersma, J., 1994. The Dutch foredunes: inventory and classification. Journal of Coastal Research, 10, (1), 189-202.

69. de Ruig, J.H.M., 1995. The Dutch experience: four years of dynamic preservation of the coastline. Directions in European Coastal Zone Management, eds. Healy, M.G., & Doody, J.P., Samara Publishing Limited, Cardigan. 253-266.
70. Dixon, K.L., and Pilkey, O.H., 1991. Summary of beach nourishment on the U.S. Gulf of Mexico shoreline, Journal of Coastal Research, 7, (1), 249-256.
71. Dolan, R., Hayden, B.P., May, P. and May, S., 1980. The reliability of shoreline change measurements from aerial photographs. Shore and Beach 48 (4), 22-29.
72. Doody, P., 1985. The conservation of sand dunes in Great Britain - A review. Focus on Nature Conservation, No. 13, Sand Dunes and their Management, Nature Conservancy Council. Pp 56
73. Doody, P., 1989. Conservation and development of the coastal dunes of Great Britain. In: van der Meulen, F., Jungerius P.D. and Visser J.H. eds. Perspectives in Coastal Dune Management. The Hague: SPB Academic Publishing. 279-285.
74. Doody, J.P., 1991. Sand dune inventory of Europe. European Union for Coastal Conservation / Joint Nature Conservation Committee. Pp.73
75. Doody, J.P., 1993. The coastal dunes of Europe. In: Danske Klitter-overvagning, forvaltning og forskning. Skov- og Naturstyrelsen. Copenhagen.
76. Doyle, B., 1999. DV Cassette: The new wave of digital camcorders (25 Jan 1999), <http://www.dvtgroup.com/DigVideo/DVC/DVC.html>.
77. Droesen, W., 1999. Spatial modelling and monitoring of natural landscapes. Published Thesis, Wageningen Agricultural University. Pp. 163.
78. Earth Resource Mapping Pty Ltd, 1999. Version 6.1 Help Files. Copyright © 1988, 1989, 1990, 1991, 1993, 1994, 1995, 1996, 1997, 1998, 1999.
79. Eastman Kodak Company, no date. Kodak Professional DCS 420 digital camera fact sheet. Kodak Eastman Company, 343 State Street, Rochester, New York.
80. Edirisinghe, A., Louis, J.P., and Chapman, G.E., 1999. Radiometric calibration of multispectral airborne video systems. Int. J. Remote Sensing, 20, (14), 2855-2870.

81. Eke F., 1997. Coastal legislation and implementation in Turkey - prospects for co-operation. Proceedings of the third International Conference on the Mediterranean Coastal Environment, Medcoast '97, November 11 - 14, 1997, Qawra, Malta. E. Ozhan ed. 665-677.
82. Eleveld, M.A., Blok, S.T., and Bakx, J.P.G., 2000. Deriving relief of a coastal landscape with aerial video data. *International Journal of Remote Sensing*, 21 (1) 189-195.
83. English Nature 1992. Campaign for a Living Coast, Coastal Zone Conservation, English Nature's Rationale, Objectives and Practical Recommendations.
84. European Golf Association Ecology Unit, 1995. An Environmental Strategy for Golf in Europe. Pisces Publications, Newbury.
85. European Golf Association Ecology Unit, 1997. The Committed to Green Handbook for Golf Courses. Pisces Publications, Newbury.
86. Everitt, J.H., Escobar, D.E., Cavazos, I., Noriega, J.R., and Davis, M.R., 1995. A three-camera multispectral video imaging system. Remote Sensing of the Environment, 54, 333-337.
87. Everitt, J.H., Escobar, D.E., Cavazos, I., Noriega, J.R., Davis, M.R., 1996. A three camera, multispectral digital video imaging system. Proceedings of the 15th Biennial Workshop on videography and colour photography in resource assessment, ASPRS, Indiana State University, Terre Haute, Indiana, 1-3 May, 1995, 244-252.
88. Everitt, J.H., Alaniz, M.A., Escobar, D.E., Lonard, R.I., and Davis, M.R., 1999(a). Reflectance characteristics and film image relations among important plant species on South Padre Island, Texas. Journal of Coastal Research, 15, (3), 789-795.
89. Everitt, J.H., Escobar, D.E., Yang, C., Lonard, R.I., Judd, F.W., Alaniz, M.A., Cavazos, I., Davis, M.R., and Hockaday, D.L., 1999(b). Distinguishing ecological parameters in a coastal area using a video system with visible / near infrared / mid infrared sensitivity. Journal of Coastal Research, 15, (4), 1145-1150.
90. Favennec, J., 1996. Coastal management by the French National Forestry Service in Aquitaine, France, Studies in European Coastal Zone Management, 191-196. eds. Jones, P.S., Healy, M.G., & Williams A.T.W., Samara Publishing Limited. 355 Pp.

91. Ferguson, R.L., Wood, L., and Graham, D.B., 1993. Monitoring spatial change in seagrass habitat with aerial photography. Photogrammetric Engineering and Remote Sensing, 59 (6) 1033-1038.
92. Flinn, D., 1997. The role of wave diffraction in the formation of St. Ninian's Ayre (tombolo) in Shetland, Scotland. Journal of Coastal Research, 13, (1), 202-208.
93. Frame, J., 1971. Fundamentals of grassland management. 10: The Grazing Animal. Scott. Agric., 50, 28-44.
94. Fraser, C.S., 1997. Digital camera self calibration. ISPRS journal of Photogrammetry and Remote Sensing, 52, 149-159.
95. Fraser, C.S., 1998. Some thoughts on the emergence of digital close range photogrammetry. Photogrammetric Record, 16, (91), 37-50.
96. Fryer, J.G., Chandler J. H., and Cooper, M.A.R., 1994. On the accuracy of heighting from aerial photographs and maps: implications to process modellers. Earth Surface Processes and Landforms. 19, 557-583.
97. Gares P.A., and Nordstrom, K.F., 1991. Coastal dune blowouts - dynamics and management implications. Coastal Zone '91, New York: American Society of Civil Engineers, 2851-2862.
98. Gehu, M., 1985. European dune and shoreline vegetation. Nature and Environment Series No. 32, Council of Europe, Strasbourg, 59. ISBN 92-871-0778-5.
99. Gillham, M., 1987. Sand Dunes. Heritage Coast Joint Management Committee, 111pp.
100. Goldberg, E.D., 1994. Coastal zone space - prelude to conflict? UNESCO, Paris.
101. Goldsmith, V., 1978. Coastal Dunes. In: Cosatal Sedimentary Environments. Ed. Davies R. A., Jr., New York. Springer 171-236
102. Gooch M.J., Chandler, J.H., and Stojic, M., 1999. Accuracy assessment of digital elevation models generated using the Erdas Imagine Orthomax digital photogrammetric system, Photogrammetric Record, 16, (93) 519-531.
103. Goodpasture, A. V., 1996. Digital imaging and GPS technology for resource management. Earth Observation Magazine, October 1996, vol.5, (10), 45-47.

104. Gorman, L., Morang, A., and Larson, R., 1998. Monitoring the coastal environment; part IV: mapping shoreline changes and bathymetric analysis. Journal of Coastal Research, 14, (1) 62-92.
105. Gornitz, V., 1995. Sea Level Rise: a review of recent past and near future trends. Earth Surface Processes and Landforms, 20, 7 – 20.
106. Gornitz, V. and Seeber, L., 1990. Vertical crustal motions along the east coast, North America, from historic and Holocene sea level data. Tectonophysics, 178, 127-150.
107. Goudie, A., 2000. The Human Impact on the Natural Environment. Blackwell. Pp511.
108. Graham, R., 1998. Digital Imaging. Whittles Publishing. Pp. 212.
109. Graham, R., and Mills J., 1997. Experiences with Airborne Digital Photography for Photogrammetry and GIS. Proceedings of the First North American Symposium on Small Format Aerial Photography, October 14-17, Minnesota, USA, 17-36.
110. Graham, R. and Read, R. 1986, Manual of Aerial Photography, London: Focal press 346pp.
111. Green, E.P., Clark, C.D., Mumby, P.J., Edwards, A.J., and Ellis, A.C., 1998. Remote sensing techniques for mangrove mapping. Int. J. Remote Sensing, 19, (5), 935-956.
112. Greve, C.W, (editor) 1996. Digital photogrammetry: an addendum to the manual of aerial photography. American Society of Photogrammetry and Remote Sensing. 213-226
113. Guilcher, A. and Hallegouet, B., 1991. Coastal dunes in Brittany and their management. Journal of Coastal Research, 7, (2), 517-533
114. Harvey, N., Barnett, E.J., Bourman, R.P., and Belperio, A.P., 1999. Holocene sea level change at Port Pirie, South Australia: a contribution to global sea level rise estimates from tide gauges. Journal of Coastal Research, 15, (3), 607-615.
115. Haslett, S., Davies, P and Curr, R.H.F., 2000. Geomorphologic and paleoenvironmental development of Holocene perched coastal dune systems in Brittany, France. Geografiska Annaler, Series A, 82, 79-88
116. Hauerbach, P. 1992. Skagen Odde-Skaw spit: an area of land created between two seas. Folia Geographica Danica, TOM XX, Copenhagen, 66-68, 81-82, in Jensen, F., 1994, Dune Management in Denmark: Application of the Nature Protection Act of 1992, Journal of Coastal Research, 10, (2), 263-269.

117. Healy, M.G., 1995. European coastal management: an introduction. Directions in European Coastal Zone Management, eds. Healy, M.G., & Doody, J.P., Samara Publishing Limited, Cardigan. 556pp.
118. Heathershaw, A.D., Carr, A.P., Blackly, M.W.L., and Hammond, F.D.C., 1978. Swansea Bay (Sker). (Report 74) Taunton: Institute of Oceanographic Sciences (Unpublished). In: Ranwell, D., & Boar, R., 1986, Coast Dune Management Guide. Institute of Terrestrial Ecology, Natural Environment Research Council, 105 pp.
119. Heitschmidt, J., Gress, T., Ritz, H., and Seal, M., 1996. Classifying land cover of a barrier island using high resolution multispectral imagery. Proceedings of the 15th Biennial Workshop on videography and colour photography in resource assessment, ASPRS, Indiana State University, Terre Haute, Indiana, 1-3 May, 1995, 260-269.
120. Helmer, W., Vellinga, P., Litjens, G., Goosen, H., Ruijgrok, E., and Overmars, W., 1996. Growing with the sea - creating a resilient coastline. Zeist: World Wide Fund for Nature (WWF).
121. Hellstrom, G.B., & Lubke, R.A., 1993. Recent changes to a climbing-falling dune system on the Robberg Peninsula Southern Cape coast, South Africa. Journal of Coastal Research, 9 (3) 647-653.
122. Hesp, P., 1984. Fore-dune formation in southeast Australia. In: Coastal Geomorphology in Australia. Ed. Thom, B., G. Sydney: Academic, 69-97.
123. Hesp, P., and Short A.D., 1980. Dune forms of the Younghusband Peninsula, S.E. South Australia. In: Proceedings, conference. Aeolian landscapes in the semi-arid of South Eastern Australia. Riverina Branch, Australian Society of Soil Science, 65-66.
124. Higgins, L.S., 1939. An investigation into the problem of the sand dune areas of the South Wales Coast, In: Davis, H.R.J., and Toft, L.A., 1971. The Parish and Church of St. Mary. Pennard, Gower. Pennard Parochial Church Council.
125. Hodgeson, R., Cady, F., and Pairman, D., 1981. A solid state airborne sensing system for remote sensing. Photogrammetric Engineering and Remote Sensing, Vol 47, pp. 177-182.
126. Hoffman, M., Cosyns, E., Deconinck, M., and Zwaenepoel, 1998. Donkey diet in a Flemish dune area: do they eat what they were supposed to eat? Coastal Dune Management: Shared

- Experience of European Conservation Practice. Proceedings of the European Symposium: Coastal Dunes of the Atlantic Biogeographical Region, Southport, England, September 1998.
Eds. J.A. Houston, S.E. Edmondson, and P.J. Rooney.
127. Hohle, J., 1996. Experiences with the production of digital orthophotos, PE & RS, vol. 64, (10), 1189- 1194.
128. Horikawa, K. & Shen, W., 1960. Sand movements by wind action (on the characteristics of sand traps). U.S. Army, Corps of Engineers, BIE.B. Tech. Memo., No. 119.
129. Houston, J., 1992a. Blowing in the wind. Landscape Design, Dec./Jan 1991/1992, 25-28
130. Houston, J., 1992b. Sands of time. Geographical magazine, March 1992, 1-5.
131. Hylgaard T. and Liddle, M.J., 1981. The effect of trampling on a sand dune ecosystem dominated by *Empetrum nigrum*. Journal of Applied Ecology, 18, 559-569.
132. Illenberger, W., 1993. Variations of sediment dynamics in Algoa Bay during the Holocene. Suid-Afrikaanse Tydskrif vir Wetenskap, vol. 89, 187 - 196.
133. Illenberger, W. & Burkinshaw, J., 1996. Coastal dunes and dunefields, 71-86. In: The geomorphology of the Eastern Cape, South Africa. Groatt & Sherrin, Grahamstown; Ed: C.A. Lewis, 138 pp.
134. Illenberger, W. & Rust, I., 1986. Venturi-compensated eolian sand trap for field uses. J. Sedim. Petrol., 56, 541-543.
135. Inter-American Development Bank, 1997 (draft). Coastal and marine resources management – a strategy paper. 50pp. In: Galloway, J.S., and Barragan Munoz, J.M., 1998. Recent ICZM Programme developments in Latin America, Proceedings of the fourth international Conference of the European Coastal Association for Science and Technology. Littoral 98, September 1998, Barcelona. Ed. J.L. Monso de Prat, 169-175.
136. Intergovernmental Panel on Climate change (IPCC), 1992. Global climate change and the rising challenge of the sea. Report prepared for the IPCC by working group 3, The coastal zone management subgroup, Rijkwaterstaat, The Hague. 124 pp.
137. Intergovernmental Panel on Climate Change (IPCC), 1995. Climate change 1995: the science of climate change (contribution of working group 1 to the second assessment report of the

- intergovernmental panel on climate change). Houghton, J.T., Meira Filho, L.G., Callander, B.A., Harris, N., Kattenberg, A. and Maskell, K. Cambridge University Press.
138. Janssen, M.P., 1995. Coastal management: restoration of natural processes in foredunes. Directions in European coastal zone management. eds. Healy, M.G., & Doody, J.P., Samara Publishing Limited, 195-198.
139. Jensen, F., 1994. Dune management in Denmark: application of the Nature Protection Act of 1992. Journal of Coastal Research, 10, (2), 263-269.
140. Jensen, J.R., Rutchey, K., Koch, M.S., and Narumalani, S., 1995. Inland wetland change detection in the Everglades water conservation area 2A, using a time series of normalised remotely sensed data. PE & RS, vol. 61, 199-209.
141. Jimenez, J.A., Sanchez-Arcilla, Bou, J., and Ortiz, M. A., 1997. Journal of Coastal Research, 13, 4, 1256 – 1266.
142. Kassas, M., 1971. The River Nile ecological system: a study towards an international programme. Biological Conservation, 4, 19 - 25.
143. Kay, R., and Alder, J., 1999. Coastal Planning and management. E & FN Spon, an imprint of Routledge. 375pp.
144. Kelletat, D., 1992. Coastal erosion and protection measures at the German North Sea Coast. Journal of Coastal Research, 8, (3), 699-711.
145. Ketchum, B.H., 1972. The water's edge: critical problems of the coastal zone. In: Proceedings of the Coastal Zone Workshop, Wood's Hole, Massachusetts, 22 May – 3 June 1972. MIT Press, Cambridge, MA.
146. Khalil, S., 1997. Critical problems of the Egyptian Mediterranean coastal zones. Proceedings of the third International Conference on the Mediterranean Coastal Environment, Medcoast '97, November 11 - 14, 1997, Qawra, Malta. E. Ozhan ed, 513-521.
147. Khedr, A-H.A., 1998. Vegetation zonation and management in the Damietta Estuary of the River Nile. Journal of Coastal Conservation, 4, 79-86.
148. Killemaes, I., and Herrier, J.L., 1998. Synopsis of the Flemish coastal dune conservation policy. Coastal Dune Management: Shared Experience of European Conservation Practice. Proceedings of the European Symposium: Coastal Dunes of the Atlantic Biogeographical

- Region, Southport, England, September 1998. Eds. J.A. Houston, S.E. Edmondson, and P.J. Rooney. In press.
149. King, C.A.M., 1973. Dynamics of beach accretion in south Lincolnshire, England. In: Coastal Geomorphology, Coates, D.R., (ed.) (1973). 73-98.
150. King, D.J., 1991. Determination and reduction of cover type brightness variations with view angle in airborne multispectral video imagery. Photogrammetric Engineering and Remote Sensing, 57, 1571-1577.
151. King, D.J. 1995. Airborne multispectral digital camera and video sensors: a critical review of system designs and applications. (HTML) Canadian Journal of Remote Sensing, Special Issue on Aerial Optical Remote Sensing 21 (3), 245-273.
152. King, D.J., 1997. Low Cost Multispectral Digital Camera Imaging For Forest Modelling and Topographic Mapping. Presentation at Third International Airborne Remote Sensing Conference and Exhibition, 7 - 10 July, 1997, Copenhagen, Denmark 8 Pp.
153. King, D.J. & Vlcek, J., 1990. Development of a multispectral video system and its application to forestry. Canadian Journal Remote Sensing, 16, 15-22.
154. Klein, R.J.T., Smit, M.J., Goosen, H., and Hulsbergen, C.H., 1998. Resilience and vulnerability: coastal dynamics or Dutch dykes. The Geographical Journal, 164, (3), 259-268.
155. Klijn, J.A., 1990a. The younger dunes in The Netherlands: chronology and causation. In: Dunes of the European coasts: geomorphology, hydrology, soils, Catena Supplement 18, 89-100. Eds. Bakker, Th. W., Jungerius, P.D., and Klijn, J.A.
156. Klijn, J.A., 1990b. Dune forming factors in a geographical context. In: Dunes of the European coasts: geomorphology, hydrology, soils, Catena Supplement 18, 1-13. Eds. Bakker, Th. W., Jungerius, P.D., and Klijn, J.A.
157. Knapp, K., A., Disperati, A., and Hoppus, M., 1997. Evaluation of a colour infrared digital camera system for forest health protection applications in the western United States and southern Brazil. Proceedings of the First North American Symposium on Small Format Aerial Photography, Octobr 14-17, Minnesota, USA, 80-90.
158. Knutson, P.L., 1980. Experimental dune restoration and stabilisation, Nauset Beach, Cape Cod, Massachusetts. TP 80-5, US Army Corps of Engineers, Coastal Engineers, Coastal

- Engineering Research Centre, Fort Belvoir, Virginia. In: Experimental Dune Building and Vegetative Stabiisation in Sand Deficient Barrier Island setting on the Louisiana Coast, USA. Journal of Coastal Research, 7, (1), 137-149. Eds. Mendelssohn, I.A., Hester, M.W., Monteferrante, F.J., and Talbot, F., 1991.
159. Koehler, H.H., Harder, H., Meyerdirks, J., and Voigt A., 1996. The effect of trampling on the microarthropod fauna of dune sediments. A Case Study from Jutland, Denmark. Studies in European Coastal Zone Management, 221-245. Eds. Jones, P.S., Healy, M.G., &, Williams A.T.W., Samara Publishing Limited.
160. Koh, A., 1996. The use of balloons and their suitability as imaging platforms for the colour infrared Aerial Digital Photographhic System. Report on the Peri-Urban Interface [PUI] Demonstration Programme on the use of cheap aerial digital photography for the Department for International development [DFID] formerly the U.K. Overseas Development Administration. 10Pp
161. Koh, A., 1998. An evaluation of the use of microlights as an operational platform for the colour infrared Aerial Digital Photographhic System. Report on the Peri-Urban Interface [PUI] Demonstration Programme on the use of cheap aerial digital photography for the Department for International development [DFID] formerly the U.K. Overseas Development Administration. 9Pp.
162. Koh, A., Edwards, E., Curr, R.H.F., and Strawbridge, F., 1996. Techniques in electronic imaging for natural resource monitoring. Remote sensing and GIS for natural resource management. Proceedings of a one day technical workshop jointly organised by the Natural Resources Institute and the University of Greenwich. Eds. C.H. Power, L.J. Rosenberg, and I Downey, 47-54.
163. Konecny, G., Schuche, W. and Wu, J., 1982. Investigations on the interpretability of images by different sensors and platforms for small scale mapping. Proceedings ISPRS, Comm. 1 Symposium, Canberra, 11-22. In: Graham, R., 1998, Digital Imaging. Whittles Publishing. 212 pp.

164. La Cock G. D., Lubke R. A., Wilken M., 1992. Dune movement in the Kwaihoek region of the Eastern Cape, South Africa, and its bearing on future developments of the region. Journal of Coastal Research, 8 (1), 210 - 217.
165. Lane, D., 1996. Solid state colour cameras: tradeoffs and costs now. Advanced Imaging, April 1996, 63-66.
166. Leatherman S.P., and Godfrey, P.J., 1979. The impact of off-road vehicles on coastal ecosystems in Cape Cod National Seashore. Amherst MA: National Park Service Cooperative Research Unit, University of Massachusetts, 65 pp.
167. Lee, C.K., and Faig, W., 1999. Dynamic monitoring with video systems. Photogrammetric Engineering and Remote Sensing, 65, (5), 589-595.
168. Leys, K.F. and Werritty, A., 1999. River Channel planform change: software for historical analysis. Geomorphology, 29 107-120.
169. Liddle, M., 1997. Recreation Ecology. Chapman and Hall, London.
170. Liddle, M.J. and Greig-Smith, P., 1975a, A survey of tracks and paths in a sand dune ecosystem. 1 Soils. Journal of Applied Ecology, 12, 893-908.
171. Liddle M.J. and Greig-Smith, P., 1975b, A Survey of Tracks and Paths in a Sand Dune Ecosystem. 2 Vegetation. Journal of Applied Ecology, 12, 909-930.
172. Light D. L., 1996. Film cameras or digital sensors? The challenge ahead for aerial imaging. Photogrammetric Engineering and Remote Sensing, 62 (3), 285 - 291.
173. Livingstone, D., Raper, J., and McCarthy, T., 1999. Integrating aerial videography and digital photography with terrain modelling: an application for coastal geomorphology. Geomorphology, 29, 77-92
174. Loffler, M., and Coosen, J., 1995. Ecological impact of sand replenishment. Directions in European Coastal Management. Eds. Healy and Doody Samara Publishing Limited. Cardigan. 556pp.
175. Loizidou, X.I. and Iacovou, N.G., 1997. Coastal zone management for Cyprus: finalisation and implementation. Proceedings of the third International Conference on the Mediterranean Coastal Environment, Medcoast '97, November 11 - 14, 1997, Qawra, Malta. Ed. E. Ozhan 533-545.

176. Louise, J., Lamb, D., McKenzie, G., Chapman G., Edirisinghe, A., McCloud, I and Pratley, J., 1995. Operational use and calibration of airborne video imagery for agricultural and environmental land management applications. Proceedings of the 15th Biennial Workshop on videography and colour photography in resource assessment, ASPRS, Indiana State University, Terre Haute, Indiana, 1-3 May, 1995, 326-333.
177. Louisse, C.J., and Van der Meulen, F., 1991. Future coastal defence in The Netherlands: strategies for protection and sustainable development. Journal of Coastal Research, 7, (4), 1027-1041.
178. Lyon, J. G., and Greene, R. G., 1990. Using aerial photographs to measure the historical aerial extent of lake Erie coastal wetlands. Photogrammetric Engineering and Remote Sensing, 58 (9), 1355 - 1360.
179. Maas, H-G., and Kersten, T., 1997. Aerotriangulation and DEM/Orthophoto generation from high-resolution still-video imagery. Photogrammetric Engineering and Remote Sensing, vol. 63, (9), 1079-1084.
180. Mao, C., & Howard, S., 1996. Pre-processing of airborne digital CCD digital camera image. Proceedings of the 15th Biennial Workshop on videography and colour photography in resource assessment, ASPRS, Indiana State University, Terre Haute, Indiana, 1-3 May, 1995, 106-128.
181. Mao, C., & Kettler, D., 1996. Digital CCD camera for airborne remote sensing. Proceedings of the 15th Biennial Workshop on videography and colour photography in resource assessment, ASPRS, Indiana State University, Terre Haute, Indiana, 1-3 May, 1995, 1-12.
182. Makarovic B. and Tempfil, K., 1997. Digitising images and automatic processing in photogrammetry. ITC Journal, 1, 107-126. In: Graham, R., 1998, Digital Imaging. Whittles Publishing, 212 pp.
183. Manzer, G., 1996. Avoiding digital orthophoto problems. 158-162. In: Digital Photogrammetry – an addendum to the manual of photogrammetry. Ed. Greve, C. Published by American Society for Photogrammetry and Remote Sensing. Pp.247.

184. Marsh, G.P., 1864. Man and nature. New York. Scribner. In: Man and nature, 1965. Ed. E. Lowenthal, Cambridge, Mass.: Belknap Press. In: Goudie. A., 2000. The Human Impact on the Natural Environment, Blackwell.
185. Marzloff, I., and Ries J.B., 1997. 33-mm photography taken from a hot air blimp: monitoring processes of land degradation in northern Spain. History of Small Format Aerial Photography: a Canadian View. Proceedings of the First North American Symposium on Small Format Aerial Photography, October 14-17, Minnesota, USA, 91-101.
186. Mather, A.S. and Ritchie, W., 1977. The beaches of the Highlands and Islands, Countryside Commission for Scotland, Perth.
187. Maune, D. F., 1996. DEM extraction, editing, matching and quality control techniques: introduction to digital elevation models. 131-134. In: Digital Photogrammetry – an addendum to the manual of photogrammetry. Ed. Greve, C. Published by American Society for Photogrammetry and Remote Sensing. Pp.247.
188. Mauriello, M.N., 1989. Dune maintenance and enhancement. a New Jersey example. Coastal Zone '89, 1023-1037.
189. May, V.J., 1985. The supply of sediments to sand dunes. Focus on Nature Conservation, No. 13, Sand Dunes and their Management, Nature Conservancy Council.
190. McInnes R.G., Jewell, S., and Roberts, H., 1998. Coastal management on the Isle of Wight, UK. The Geographical Journal, 164 (3), 291-306
191. McClave, J.T. and Sincich, T., 2000. Statistics. Prentice Hall, 848 pp.
192. McKie, R., 2000. Forgotten charts prove sea threat. The Observer, 30-01-2000, 28.
193. McLachlan A., Illenberger, W.K., Burkinshaw, J.R., & Burns, M.E.R., 1994. Management implications of tampering with littoral sand sources. Journal of Coastal Research, 12, 51-59.
194. McManus, J. and Soulsby, J.A., 1994. Macro and micro sediment forms and sequences using multi-platform remotely sensed imagery in the Eden Estuary, South East Scotland. In: Remote sensing - from research to applications in the New Europe. Proceedings of the 13th EARSel Symposium, Dundee. Ed. R. Vaughan. 353-356.
195. Meisner, D.E., 1986. Fundamentals of airborne video remote sensing. Remote Sensing of Environment, 19, 63-79.

196. Meisner, D.E., & Lindstrom, O.M., 1985. Design and operation of a colour aerial video system. Photogrammetric Engineering and Remote Sensing, 51, 555-560.
197. Mendelssohn, I.A., Hester, M.W., Monteferrante, F.J., and Talbot, F., 1991. Experimental dune building and vegetative stabilisation in sand deficient barrier island setting on the Louisiana Coast, USA. Journal of Coastal Research, 7, (1), 137-149.
198. Meur-Ferrec, C., and Ruz, M.H., 1998. Coastal dune re-establishment on an artificial rubble foundation, Dunkerque Port, France. Coastal Dune Management: Shared Experience of European Conservation Practice. Proceedings of the European Symposium: Coastal Dunes of the Atlantic Biogeographical Region, Southport, England, September 1998. Eds. J.A. Houston, S.E. Edmondson, and P.J. Rooney. In press.
199. Meyer, M.P., 1997. History of small format aerial photography - US view. Proceedings of the First North American Symposium on Small Format Aerial Photography, October 14-17, Minnesota, USA, 3-7.
200. Mills J.P and Newton, I., 1996, A new approach to the verification and revision of large scale mapping. Photogrammetry and Remote Sensing, 51, 17-27.
201. Mills J. P., Newton, I., Graham, R. W., 1996. Aerial photography for survey purposes with a high resolution small format digital camera. Photogrammetric Record, 15 (88), 575-587.
202. Mitchell, T.A., Qi, J., Clarke, T., Moran, M.S., Neale, C.M.U., and Schowengerdt, R.A., 1995, Geometric Rectification of Multi-temporal, Multiband Videographic Imagery. American Society for Photogrammetry and Remote Sensing. 15th Biennial Workshop on Videography and Colour Photography in Resource Assessment. Ed. Paul Mausel, ASPRS: Bethesda, MD.
203. Moller, J.T., 1992. Balanced coastal protection on a Danish North Sea Coast. Journal of Coastal Research, 8, (3), 712-718.
204. Moore, L. J., 2000. Shoreline Mapping Techniques, Journal of Coastal Research, 16, 1, 111-124.
205. Morgan, C., 1995. First digital camcorders to go on sale. Camcorder User, October, 6-7.

206. Mourik, J., Ehrenburg, A., and van Til, M., 1995. Dune landscapes near Zandvoort aan Zee, The Netherlands: use and management past and present. Directions in European Coastal Zone Management. Eds. Healy, M.G., & Doody, J.P., Samara Publishing Limited, 483-488.
207. Neale, C.M.U., Kuiper, J., Tarbet, K.L., and Qiu, X., 1994. Image enhancement and processing automation routine for digital multispectral video imagery. Proceedings of the 14th Biennial Workshop on Colour aerial Photography and Videography for Resource Monitoring. ASPRS, Utah State University, Logan, Utah, 25-29 May, 1993, 29-36.
208. Neale, C.M.U., Qiu, J., Moran, M.S., Pinter, P., Clarke, T., Mitchell, T.A., Sundararaman, S., and Ahmed, R., 1995. Methods of radiometric calibration and reflectance determinations from airborne multispectral digital imagery. American Society for Photogrammetry and Remote Sensing, 15th Biennial Workshop on Videography and Colour Photography in Resource Assessment. Ed. Paul Mausel ASPRS: Bethesda, MD.
209. Newman, D.E., 1976. Beach replenishment: sea defences and a review of the role of artificial beach replenishment. Proc. Inst. Civ. Engineers, 60, 445-460.
210. Nixon, P.R., Escobar, D.E., and Bowen, R.L., 1987. A multispectral false colour video imaging system for remote sensing applications. Proceedings 11th biennial workshop on colour photography and videography in the plant sciences. (America Society for Photogrammetry and Remote Sensing. Bethesda, Maryland), 295-305.
211. Nordstrom, K.F., 1994. Beaches and dunes of human altered coasts. Progress in Physical Geography, 18, (4), 497-516.
212. Nordstrom, K. F. and Lotstein, E. L., 1989. Perspectives on resource use of dynamic coastal dunes. Geog. Review. Vol. 79 (1), 1 - 12.
213. Nordstrom, K. F. and Psuty, N.B., 1980. Dune district management: a framework for shorefront protection and landuse control. Coastal Zone Management Journal. Vol. 7 (1), 1-23.
214. O'Brien, M.K., Valverde, H.R., Trembanis, A.C., and Haddad, T.C., 1999. Summary of beach nourishment activity along the Great Lakes' shoreline 1955-1966. Journal of Coastal Research, 15, (1), 206-219.

- 215.OECD [Organisation for Economic Cooperation and Development] 1993, Coastal Zone Management: Integrated Policies. OECD, Paris, 128 pp.
- 216.Oostwoud Wijdenes, D.J., Poesen, J., Vandekerckhove, L. and Ghesquiere, M., 2000, Spatial distribution of gully head activity and sediment supply along an ephemeral channel in a Mediterranean environment, Catena, 39 147-167.
- 217.Orford, J.D., Carter, R.W.G., McKenna. J. and Jennings S.C., 1995. The relationship between the rate of mesoscale sea-level rise and the rate of retreat of swash aligned gravel dominated barriers. Marine Geology, 124, 177 – 86.
- 218.OST [Office of Science and Technology], 1997. Foresight: progress through partnership. Report 16. The Marine Panel, Department of Trade and Industry. London OST.
- 219.Ovington, P., 1951. The afforestation of Tentsmuir Sands. Journal of Ecology, 39, 363-375.
- 220.Paraskevas. P.A., and Lekkas, T.D., 1997. Wastewater treatment strategies for the Mediteranean coastal areas. Proceedings of the third International Conference on the Mediterranean Coastal Environment. Medcoast '97, November 11 - 14, 1997, Qawra, Malta. Ed. E. Ozhan, 299-314.
- 221.Pearson. R., Grace, J., and May, G., 1994. Real-time airborne agricultural monitoring. Remote Sensing of Environment. 49, (3), 304-310.
- 222.Pethick, J., 1992. Saltmarsh geomorphology. In: Saltmarshes: morphodynamics conservation and engineering significance. Cambridge University Press. Eds. Allen, J.R.L. and Pye, K.
- 223.Pethick, J., 1993. Shoreline adjustments and coastal management: physical and biological processes under accelerated sea level rise. Geographical Journal, 159 (2), 162-8.
- 224.Pickup, G., Bastin, G.N., Chewings, V.H., and Jacobs, D.N., 1995. Correction and classification procedures for assessing rangeland vegetation cover with airborne video data. American Society for Photogrammetry and Remote Sensing. 15th Biennial Workshop on Videography and Colour Photography in Resource Assessment. Ed. Paul Mausel, ASPRS: Bethesda, MD.
- 225.Pickup, G., Chewings, V.H., and Pearce, G., 1995. Procedures for correcting high resolution airborne video imagery. Internation Journal of Remote Sensing, 16, (9), 1647-1662.

226. Peipe, J., and Schneider C-T., 1995. High resolution still video camera for industrial photogrammetry. Photogrammetric Record, 15 (85), 135 - 139.
227. Pilkey, O.H. and Wright, H.L., 1988. Seawalls versus beaches. Journal of Coastal Research, Special Issue No. 4, 44-66.
228. Pilkey O.H. & Thieler, 1992, in Scholle P.A., 1996. SEPM Photo CD 4, 1731 East 71st Street, Tulsa, OK 74136-5108 USA
229. Pirazzoli, P.A., 1993. Global sea level changes and their measurement. Global and Planetary Change, 8, 135-148.
230. Powrie, W., 1997. Soil mechanics: concepts and applications. E and FN Spon, 420pp.
231. Radley, G.P., 1992. The dunes of England, an example of a national inventory. In: Coastal Dunes, 1992. Eds. Carter, Curtis and Sheehy-Skeffington. Balkema, Rotterdam. 439-453.
232. Ramsey III, E.J., and Laine, S.C., 1997. Comparison of Landsat Thematic Mapper and high resolution photography to identify change in complex coastal wetlands. Journal of Coastal Research, 13, (2), 281-292.
233. Ranwell, D., 1975, Management of salt marsh and coastal dune vegetation. In: Estuarine Research, Vol 2, ed. L.E. Cronin, 471-483. London, Academic Press.
234. Ranwell, D., & Boar, R., 1986. Coast dune management guide. Institute of Terrestrial Ecology, Natural Environment Research Council, 105 pp.
235. Raynor, J.M., and Seitz, P., 1990. The technology and practical problems of pixel synchronous CCD data acquisition for optical metrology applications. International archives of Photogrammetry and Remote Sensing, 28, (5), 96-103.
236. R.E., 2000, The island hell that is The Beach. Geographical Magazine, January 2000, 11.
237. Reid, W., 1997, Coastal Change, What does it mean for our health? Plenary paper at: Coastal Zone 97, Boston, USA, 22 - 24 July 1997.
238. Reimers, M., 1998. How human traffic can revitalise the dunes: an example from the Danish Island of Romo. Coastal Dune Management: Shared Experience of European Conservation Practice. Proceedings of the European Symposium: Coastal Dunes of the Atlantic Biogeographical Region, Southport, England, September 1998. Eds. J.A. Houston, S.E. Edmondson, and P.J. Rooney. In press.

239. Rhind, P.M., Blackstock, T.H., Jones, R. and Sandison, W., 1998. The evolution of Newborough Warren dune system over the past four decades and its implication for future management. Coastal Dune Management: Shared Experience of European Conservation Practice. Proceedings of the European Symposium: Coastal Dunes of the Atlantic Biogeographical Region, Southport, England, September 1998. Eds. J.A. Houston, S.E. Edmondson, and P.J. Rooney. In press.
240. Richardson, A.J., Everitt, J.H., Escobar, D.E., 1993. Reflectance calibration of aerial video imagery with automatic gain compensation on and off. International Journal of Remote Sensing, 14, (15), 2791-2801.
241. Ricketts, P.J., 1992. Current approaches in Geographic Information Systems for coastal management. Marine Pollution Bulletin, 25 (1-4), 82-87.
242. Rijkswaterstaat, 1998. Te kust en te(r) keur. The Hague: Ministry of Transport. Public Works and Water Management.
243. Ritchie, W., 1981. Environmental aspects of oil and gas pipeline landfalls in northeast Scotland. Proceedings 17th International Coastal Engineering Conference, Sydney, Australia, 1980. American Society of Engineers. New York, 2938-2954.
244. Roberts, A. B. C., and Anderson, J. M., 1999. Shallow water bathymetry using integrated airborne multi-spectral remote sensing. International Journal of Remote Sensing, 19, (3), 497 - 510.
245. Robson, S and Shortis, M.R., 1998. Practical influences of geometric and radiometric image quality provided by different digital camera systems. Photogrammetric Record, 16 (92). 225-248.
246. Rowe, J.P., Warner, T.A., Dean, D.R., and Egan, A.F., 1999. A remote sensing strategy for measuring logging road system length from small format aerial photography. Photogrammetric Engineering and Remote Sensing, 65, (6), 697-703.
247. Rust, I.C., & Illenberger, W.K., 1996. Coastal dunes: sensitive or not?. Landscape and Urban Planning, 34, 165-169.
248. Sanderson P.G., Eliot, I., and Fuller, M., 1998. Historical development of a foredune plain at Desperate Bay, western Australia. Journal of Coastal Research, 14, (4). 1187-1201.

249. Savage, R.P., 1962, Proceedings 8th Conference of Coastal Engineering. 380-396.
250. Savage R.P., & Woodhouse, W.W., Jr., 1969. Creation and stabilisation of coastal dunes. Proceedings, 11th Congress on coastal engineering, London, Sept 1968, 672-700.
251. Scholle P.A., 1996. SEPM Photo CD 4, 1731 East 71st Street, Tulsa, OK 74136-5108 USA
252. Seabloom E.W. and Wiedemann A.M., 1994. Distribution and effects of *Ammophila breviligulata* Fern, (American Beachgrass) on the foredunes of the Washington Coast. Journal of Coastal Research, 10, (1), 178-188.
253. Selby, M.J., 1993. Hillslope Materials and Processes, Oxford University Press, 353-354.
254. Sharaf El Din, S.H., 1974. Longshore sand transport in the surf zone along the Mediterranean Egyptian coast. Limnol. Oceanogr. 19 (2), 182-189.
255. Shennan, I. and Woodworth, P.L., 1992. A comparison of late Holocene and twentieth century sea level trends from the UK and North Sea region. J. Geophys Int., 109, 96-105.
256. Sherman, D.J., 1990. Measuring Aeolian Transport Rates. Proceedings Canadian Symposium on Coastal Sand Dunes, 37-47.
257. Sherman, D.J., Bauer, B.O., Carter, R.W.G., Jackson, D., McCloskey, J., Davidson-Arnott, R.G.D., Gares, P.A., Jackson, N.L., & Nordstrom K.F, 1994. The Aeolus Project: Measuring Coastal Wind and Sediment Systems. Proceedings of Coastal Dynamics '94. Feb. 21-25 Barcelona, Spain, 476-487.
258. Short, T., 1992. The calibration of a 35mm non-metric camera and the investigation of its potential use in photogrammetry. Photogrammetric Record, 14 (80) 313-322.
259. Shortis, M. R., Robson, S., and Beyer, H.A., 1998. Principal point behaviour and calibration parameter models for Kodak DCS cameras. Photogrammetric Record, 16 (92), 165-186.
260. Shoshany, M. and Degani, A., 1992. Shoreline detection by digital image processing of aerial photography. Journal of Coastal Research, 8(1), pp.29-34.
261. Simeoni, U., Calderoni, G., Tessari, U., and Mazzini, E., 1999. A new application of system theory to foredunes intervention strategies. Journal of Coastal Research, 15, (2), 457-470.
262. Slama, C.C. 1980. Manual of Photogrammetry, American Society for Photogrammetry and Remote Sensing. Falls Church. In: Fryer, J.G., Chandler J. H., and Cooper, M.A.R., 1994. On

- the accuracy of heighting from aerial photographs and maps: implications to process modellers. Earth Surface Processes and Landforms. 19, 557-583.
263. Smith, G.L. and Zarillo, G.A., 1990. Calculating long term shoreline recession rates using aerial photographic and beach profiling techniques. Journal of Coastal Research 1, 111-120.
264. Sorensen, J., 1997, National and International Efforts at Integrated Coastal Management: Definitions, Achievements and Lessons. Coastal Management, 25: 3 - 41.
265. Sothorn, E.J., Randerson, P.F., Williams, A.T. and Dixon, J., 1985. Ecological effects of recreation at Merthyr Mawr dunes, South Wales. NCC Publication No. 30. Sand Dunes and Their Management. Ed. P Doody, 217-238.
266. Soulsby, R.L., 1998. Coastal study of three dimensional sand transport processes and morphodynamics. Proceedings of the third European Marine Science and technology Conference, Lisbon, 23-27 May 1998. Eds. K.-G. Barthel, H. Barth, M. Bohle-Carbonell. C. Fragakis, E. Lipiatou, P. Martin, G. Ollier, M. Waydert.
267. Stubbs, D., 1998. Golf courses as a catalyst for conservation of coastal habitats. Coastal Dune Management: Shared Experience of European Conservation Practice. Proceedings of the European Symposium: Coastal Dunes of the Atlantic Biogeographical Region, Southport, England, September 1998. Eds. J.A. Houston, S.E. Edmondson, and P.J. Rooney. In press.
268. Tallis, J., 1997. The southern Pennine experience: an overview of blanket mire degradation. Proceedings of the British Ecological Society (Mires Research Group) Conference on Blanket Mire Degradation, Causes, Consequences and Challenges, University of Manchester, 9-11 April, 1997.
269. Tekke, R., 1995. Ecoteams and greenteams: taking care of nature outside protected areas. Directions in European Coastal Zone Management, eds. Healy, M.G., & Doody, J.P., Samara Publishing Limited, 195-198.
270. Thompson, G. H., 1994. A practical method of determining the ground sampled distance in small scale aerospace photography. The Journal of Photographic Science, 42, 129-133.
271. Thompson, G.H., 1995. The image spread function as a practical guide to spatial resolution with aerospace technology. The Journal of Photographic Science, 43, 57-60.

272. Thompson, G.H., 1997. Assessing the resolving power of photographic systems used for terrestrial remote sensing. Photogrammetric Record, 15 (90), 937-944.
273. Thompson G.H., and Haughton, C., 1999. An evaluation of a Kodak DCS 460CIR camera for airborne remote sensing by comparison with photography using Kodak professional infrared EIR film. In press.
274. Thomes. J. B. and Brunsten, D., 1977. Geomorphology and Time. Methuen and Co. London, 442 pp.
275. Tinley, K.L., 1985. Coastal Dunes of south Africa. SA National Scientific Programmes, Report No. 109, FRD.
276. Tooley, M.J., & Shennon, I., 1987, Sea Level Changes. Basil Blackwell, Oxford, UK.
277. Turner, R.K., Lorenzoni, I., Beaumont, N., Bateman, I.J., Langford I.H., and McDonald, A.L., 1998. Coastal management for sustainable development: analysing environmental and socio-economic changes on the UK coast. The Geographical Journal, Vol.164, (No.3), November 1998, 269-281.
278. Um, J-S., & Wright, R., 1999a. Video strip mosaiking: a two dimensional approach by convergent image bridging. Int. J. Remote Sensing, 20, (10), 2015-2032.
279. Um, J-S., & Wright R., 1999b. The analogue to digital transition and implications for operational use of airborne videography. Photogrammetric Engineering and Remote Sensing, 65, (3), 269-275.
280. United Nations Conference on Environment and Development. 1992. Agenda 21, Programme of action for Sustainable development. United Nations Department of public Information, New York, USA.
281. Valverde, H.R., Trembanis, A.C., and Pilkey, O.H., 1999. Summary of beach nourishment episodes on the U.S. east coast barrier islands. Journal of Coastal Research, 15, (4), 1100-1118.
282. Van der Hagen. H.G.J.M., Van Til. M. and Drosen, W.J... 1998. Coastal Dune Management: Shared Experience of European Conservation Practice. Proceedings of the European Symposium: Coastal Dunes of the Atlantic Biogeographical Region, Southport, England, September 1998. Eds. J.A. Houston, S.E. Edmondson, and P.J. Rooney. (Still in press)

283. Van der Meulen, F., 1997. Dune water catchment in the Netherlands. In: Ecosystems of the World 2c, dry coastal ecosystems, general aspects. Elsevier, Amsterdam. Ed. E. Van der Maarel, 533-556,
284. Van der Meulen, F. and van der Maarel. 1989. Coastal defence alternatives and nature development perspectives. In: Perspectives in Coastal Dune Management. The Hague: SPB Academic Publications. Eds. Meulen F. van der, Jungerius, P.D. and Visser, J., 183-195.
285. Van Noortwijk, J.M., and Peerbolte, E.B., 2000. Optimal sand nourishment decisions. Journal of Waterway, Port and Coastal Engineering, vol 126, (1), pp. 30-38.
286. Van der Putten, W.H., 1990. Establishment of *Ammophia arenaria* (marram grass) from culms, seeds and rhizomes. Journal of Applied Ecology, 27, 188-199.
287. Van Stratten, L.M.J.U., 1961. Directional effects of winds, waves and currents along the Dutch North Sea coast. Geologie en Mijnbouw, 40, 333-346.
288. Van der Vegte, F.W., Faber, J., and Kuiters, L., 1985. Vegetation, land use and management of the inner dune zone in the North-Holland dune reserve, The Netherlands. Vegetatio, 62, 449-456.
289. Wainwright, M., 1999. Trails of destruction, The Guardian, Saturday June 19th 1999. 14
290. Walker, A.S., 1999. Responses to users: the continuing evolution of commercial digital photogrammetry. Photogrammetric Record, 16 (93), 469-483.
291. Warner, W.S. and Slaattelid, B.R., 1997. Multiplotting with images from the Kodak DCS420 digital camera. Photogrammetric Record, 15 (89), 665-672.
292. Warner, W.S., 1994. Measuring and mapping crop loss with 35 mm and 70 mm aerial photography. Norwegian Journal of Agricultural Sciences, 8 (1), 37-48.
293. Warner, W.S., Graham, R.W. and Read, R.E., 1996. Small Format Aerial Photography. Whittles Publishing, Caithness. 376pp.
294. Watson, J.J., Kerley, G.I.H., and McLachlan, A., 1997. Nesting habitat of birds breeding in a coastal dunefield, South Africa and management implications. Journal of Coastal Research, 13, (1), 36-45.
295. Welch, R., 1989. Desktop mapping with personal computers, Photogrammetric Engineering and Remote Sensing, 55, 11, 1651-1662.

296. Welch, R., and Remillard, M., 1996. GPS, photogrammetry and GIS for resource mapping applications. 183-191. Digital Photogrammetry, an addendum to the manual of photogrammetry. Ed. Greve, C., American Society for Photogrammetry and remote sensing, Bethesda Maryland. Pp. 247
297. Welch, R., Remillard, M., and Alberts J., 1992. Integration of GPS, remote sensing and GIS techniques for coastal resource management. Photogrammetric Engineering and Remote Sensing 58 (11), 1571 – 1578
298. Willets, B.B., and Phillips, C.J., 1978. Proc. Sixteenth Conf. Coast. Eng. 2020-2050.
299. Williams, A.T.W. and Randerson P.F., 1989. Nexus: ecology, recreation and management of a dune system in South Wales. Perspectives in Coastal Dune Management. Academic Publishing by, The Hague, The Netherlands. Eds. F Van der Meulen, P.D. Jungerius and J.H. Visser.
300. Willis, A.J., 1963. Braunton Burrows: The effects on the vegetation of the addition of mineral nutrients to the dune soils. Journal of Ecology, 51, 353-374.
301. Woodhouse, W.W., 1978. Dune Building and Stabilisation with Vegetation. SR-3, CERC, US Army Corps of Engineers, Fort Belvoir, Va.
302. World Bank, 1993. Noordwijk Guidelines for Integrated Coastal Zone Management. World Bank Environment Department, Land water and Natural Habitats Division, Washington DC.
303. Woolf, P.R., 1983. Elements of Photogrammetry, McGraw Hill, New York. 628pp.
304. Wright, D., 1998, title, Unpublished Msc Thesis, University of Greenwich, Chatham Maritime, Kent.
305. Zhang, J., Zhang, Z, Shen, W., and Wang, Z. 1996. VirtuoZo digital photogrammetry system and its theoretical foundation and key algorithms. International Archives of Photogrammetry and Remote Sensing. 31 part B2, Vienna, 424-429.
306. Zsilinszky V.G., Giannelia A.M. and Rafelson, M.J., 1979. A review of the supplementary aerial photography programme of the Ontario Ministry of Natural Resources. Proceedings, Remote Sensing Symposium, Canada - Ontario Joint Forest Research Committee. Canadian Forest Service, Great Lakes Forest Research Centre, Sault Ste. Marie, Ontario P6A 5M7, 115-123.

307.Zsilinszky, V.G., 1997. History of small format aerial photography: a Canadian view.
Proceedings of the First North American Symposium on Small Format Aerial Photography,
October 14-17, Minnesota, USA, 8-16.

PROTOCOLE

APPENDIX 1

Pour la carte 1:

Mesure de la variation du trait de côte à angle droit à partir de poteaux alignés et distants:

- de 500 m chacun pour les points 0 et 0.5.
- de 100 m chacun pour les points -0.1 à D.

Orientation par rapport au nord pour les points 0.5 à A1: 354 Gr.

Orientation par rapport au nord pour les points A2 à D: 54 Gr.

La mesure s'effectue tous les ans lors de la deuxième semaine de septembre.

Pour la carte 2:

Mesure de la variation du trait de côte à angle droit à partir de poteaux alignés et distants de 500 m chacun

Orientation par rapport au nord pour les points 0.5 à 2: 384 Gr.

Orientation par rapport au nord pour les points 2 à 4: 393 Gr.

La mesure s'effectue tous les ans lors de la deuxième semaine de septembre.

Pour la carte 3:

Mesure de la variation du trait de côte à angle droit à partir de poteaux alignés et distants de 500 m chacun

Orientation par rapport au nord pour les points 4.5 à 5.5: 393 Gr.

Orientation par rapport au nord pour les points 5.5 à 7.5: 384 Gr.

La mesure s'effectue tous les ans lors de la deuxième semaine de septembre.

Tableau des distances repère - bord de mer par année.

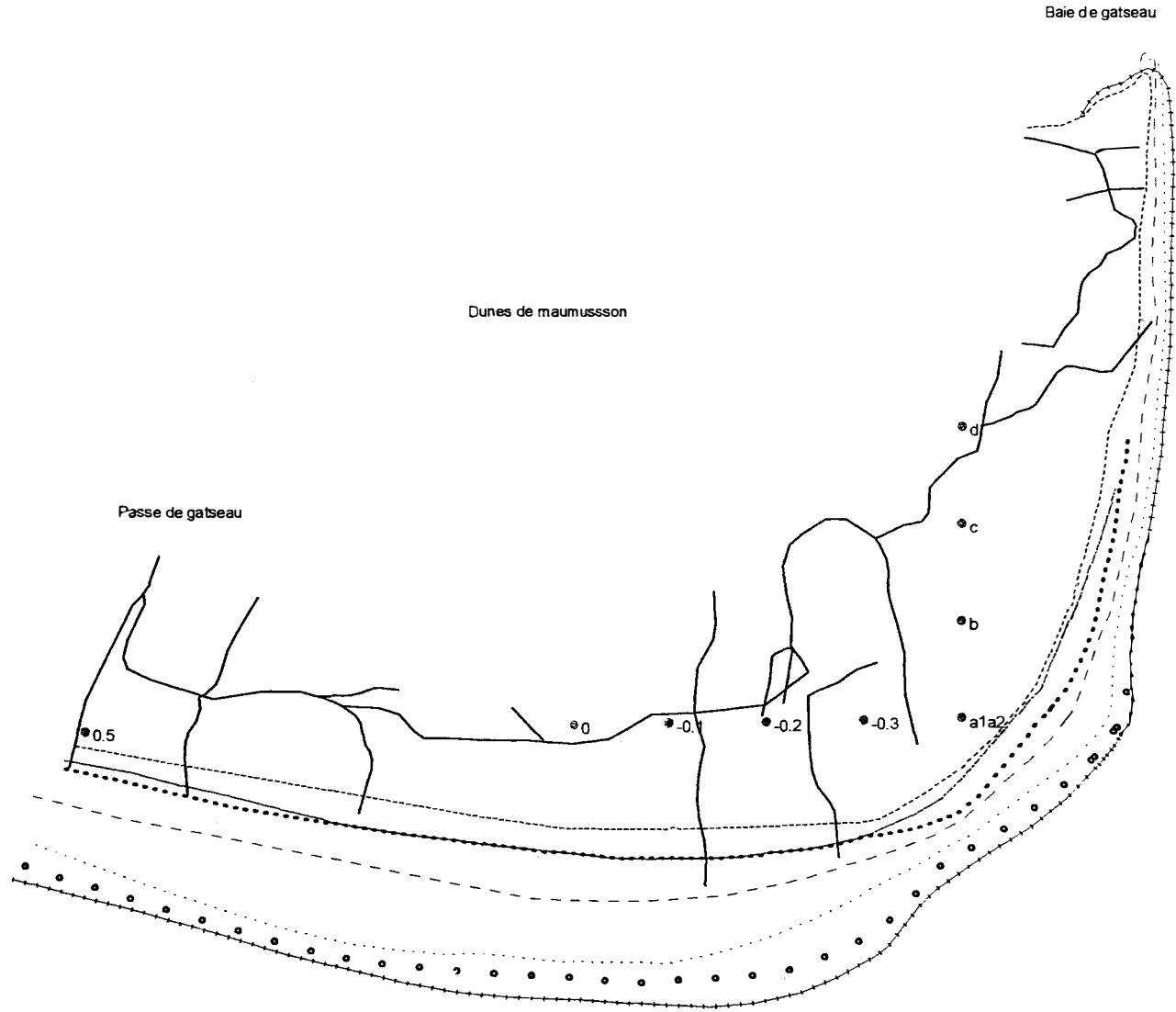
année	pt 0.5	pt 0	pt -0.1	pt -0.2	pt -0.3	pt A1	pt A2	pt B	pt C	pt D
1990	168	280	285	278	232	134	180	170	192	205
1992	155	258	260	250	215	128	166	162	192	198
1994	130	240	244	238	204	120	150	155	184	198
1995	80	178	178	176	153	95	108	145	172	184
1996	44	128	135	131	112	90	82	136	156	170
1997	37	128	135	131	112	62	55	110	144	170
1998	15	101	105	105	102	50	52	104	132	149

année	pt 1	pt 1.5	pt 2	pt 2.5	pt 3	pt 3.5	pt 4
1992	160	147	98	116	92	96	109
1994	141	120	84	94	78	78	95
1995	124	109	72	84	70	70	79
1996	110	100	60	68	62	57	65
1997	89	77	52	66	62	55	63
1998	76	68	42	51	56	49	59

année	pt 4.5	pt 5	pt 5.5	pt 6	pt 6.5	pt 7	pt 7.5
1996	84	105	133	105	91	83	94
1997	78	101	131	103	88	80	94
1998	72	100	129	101	85	80	94

Trait de côte Oléron

- Poteau
- 1990
- 1992
- 1994
- 1995
- 1996
- 1997
- 1998



APPENDIX 2

Virtuozo Processing Information Report File

Interior orientation information:
(/geot1/Holywell/f2_1_f1_1.ste)

Left image (/geot1/Holywell/Images/f2_1):

Principle Coord. [col X row]: 1016.253 1530.002
[x0 X y0]: 0.000 0.000

RMS: Mx = 0.000 My = 0.001
Residual: point NO. dx dy
 1 0.000 0.001
 2 0.000 -0.001
 3 0.000 0.001
 4 0.000 -0.001
 4 0.000 -0.001

Right image (/geot1/Holywell/Images/f1_1):

Principle Coord. [col X row]: 1016.253 1530.002
[x0 X y0]: 0.000 0.000

RMS: Mx = 0.000 My = 0.001
Residual: point NO. dx dy
 1 0.000 0.001
 2 0.000 -0.001
 3 0.000 0.001
 4 0.000 -0.001
 4 0.000 -0.001

relative orientation information:
(/geot1/Holywell/f2_1_f1_1.ste)

Relative orientation information:

Left rotation matrix:

/		\
	0.97797698 -0.14508900 0.15003601	
	0.14675000 0.98917401 0.00000000	
	-0.14841200 0.02201800 0.98868102	
\		/

Right rotation matrix:

/		\
	0.97599202 -0.14975600 0.15815200	
	0.14204700 0.98809803 0.05903700	
	-0.16511001 -0.03515400 0.98564798	
\		/

Right photo rotation angle (rad):

Phi = -0.15060499
Omega = 0.00000000
Kappa = 0.14728200

Left photo rotation angle (rad):

Phi = -0.15909800
Omega = -0.05907100
Kappa = 0.14278001

Residual:	point NO.	dq
	1	0.001000
	2	0.004000
	3	-0.008000
	4	-0.005000
	5	0.007000
	6	0.002000
	7	0.004000
	8	0.002000
	9	-0.004000
	10	-0.006000
	11	-0.004000
	12	-0.004000
	13	-0.003000
	14	-0.006000
	15	0.000000
	16	0.004000
	17	-0.002000
	18	0.002000
	19	0.008000
	20	-0.004000
	21	0.001000
	22	0.002000
	23	0.003000
	24	0.002000
	25	0.004000
	26	0.000000
	27	-0.004000
	28	0.007000
	2003	0.004000
	30	0.010000
	31	-0.001000
	32	0.001000
	33	0.007000
	34	-0.001000
	35	0.001000
	36	0.000000
	37	0.004000
	38	-0.005000
	39	0.006000
	40	-0.006000
	41	-0.002000
	42	0.000000
	43	-0.003000

1015	-0.007000
1010	0.005000
1011	0.001000
2001	0.003000
2002	-0.006000
2004	-0.001000
2005	0.000000
2006	0.009000
2007	-0.024000

RMS: Mq = 0.006000

Absolute orientation information:
(/geot1/Holywell/f2_1_f1_1.ste)

Absolute orientation information:

Left rotation matrix:

/				\
	0.04567809	-0.99895614	0.00034414	
	0.99820709	0.04563050	-0.03873530	
	0.03867916	0.00211288	0.99924946	
\				/

Right rotation matrix:

/				\
	0.05039242	-0.99715990	-0.05597137	
	0.99849004	0.05152829	-0.01903843	
	0.02186847	-0.05492746	0.99825084	
\				/

Left station coordinates:

Xs = 347507.824 Ys = 5584570.453 Zs = 1212.945

Right station coordinates:

Xs = 347568.493 Ys = 5584878.751 Zs = 1272.905

Left angle elements:

Phi = -0.000344 Omega = 0.038745 Kapa = 1.525116

Right angle elements:

Phi = 0.056011 Omega = 0.019040 Kapa = 1.519236

Residual:

No.	dX	dY	dZ
2003	1.071411	-0.270227	0.705188
1015	-0.463861	1.464538	0.306966
1010	-3.228061	0.143962	0.257767
1011	0.990182	-2.369516	-2.064780
2001	0.473661	-1.448706	2.655789

2002	0.857081	-0.309290	0.685659
2004	2.029926	0.296933	0.373663
2005	-0.724041	0.453232	2.272917
2006	0.458331	0.192827	-1.036106
2007	-1.464628	1.846246	-4.157061

RMS: mx = 1.439545 my = 1.174182
mxy = 1.857685 mz = 1.900134

Image matching information:
(/geot1/Holywell/f2_1_f1_1.ste)

Initial parameters

left image: rows =2473 columns =1288
right image: rows =2473 columns =1288

Match window width = 5
Match window length = 5
Searching range = 5
Match grid X_interval = 5
Match grid Y_interval = 5

MATCH_BLOCK == 1
MATCH_LEVEL == 3
MATCH_AREAS == 18 X 9

162 : 0 0.0 %
162 : 54 33.3 %
162 : 80 49.4 %
162 : 103 63.6 %
162 : 118 72.8 %
162 : 130 80.2 %
162 : 136 84.0 %
162 : 137 84.6 %
162 : 140 86.4 %

MATCH_BLOCK == 1
MATCH_LEVEL == 2
MATCH_AREAS == 54 X 28

1512 : 0 0.0 %
1512 : 580 38.4 %
1512 : 923 61.0 %
1512 : 1074 71.0 %
1512 : 1144 75.7 %

1512 : 1185 78.4 %
1512 : 1223 80.9 %
1512 : 1253 82.9 %
1512 : 1276 84.4 %
1512 : 1288 85.2 %
1512 : 1294 85.6 %
1512 : 1302 86.1 %
1512 : 1311 86.7 %

MATCH_BLOCK == 1
MATCH_LEVEL == 1
MATCH_AREAS == 164 X 85

13940 : 0 0.0 %
13940 : 3790 27.2 %
13940 : 5496 39.4 %
13940 : 6384 45.8 %
13940 : 6996 50.2 %
13940 : 7468 53.6 %
13940 : 7845 56.3 %
13940 : 8148 58.5 %
13940 : 8384 60.1 %
13940 : 8557 61.4 %
13940 : 8721 62.6 %
13940 : 8843 63.4 %
13940 : 8948 64.2 %
13940 : 9044 64.9 %
13940 : 9119 65.4 %
13940 : 9174 65.8 %
13940 : 9218 66.1 %
13940 : 9271 66.5 %
13940 : 9310 66.8 %
13940 : 9352 67.1 %
13940 : 9381 67.3 %
13940 : 9415 67.5 %
13940 : 9441 67.7 %
13940 : 9461 67.9 %
13940 : 9477 68.0 %
13940 : 9497 68.1 %
13940 : 9517 68.3 %
13940 : 9534 68.4 %
13940 : 9556 68.6 %
13940 : 9574 68.7 %
13940 : 9589 68.8 %
13940 : 9600 68.9 %
13940 : 9614 69.0 %
13940 : 9626 69.1 %
13940 : 9637 69.1 %
13940 : 9640 69.2 %

MATCH_BLOCK == 1
MATCH_LEVEL == 0
MATCH_AREAS == 494 X 257

126958 : 0 0.0 %
 126958 : 15794 12.4 %
 126958 : 23686 18.7 %
 126958 : 29759 23.4 %
 126958 : 35422 27.9 %
 126958 : 40305 31.7 %
 126958 : 44577 35.1 %
 126958 : 48265 38.0 %
 126958 : 51259 40.4 %
 126958 : 53670 42.3 %
 126958 : 55761 43.9 %
 126958 : 57503 45.3 %
 126958 : 58926 46.4 %
 126958 : 60112 47.3 %
 126958 : 61096 48.1 %
 126958 : 61948 48.8 %
 126958 : 62665 49.4 %
 126958 : 63301 49.9 %
 126958 : 63868 50.3 %
 126958 : 64371 50.7 %
 126958 : 64783 51.0 %
 126958 : 65175 51.3 %
 126958 : 65494 51.6 %
 126958 : 65800 51.8 %
 126958 : 66090 52.1 %
 126958 : 66318 52.2 %
 126958 : 66534 52.4 %
 126958 : 66745 52.6 %
 126958 : 66914 52.7 %
 126958 : 67095 52.8 %
 126958 : 67246 53.0 %
 126958 : 67390 53.1 %
 126958 : 67515 53.2 %
 126958 : 67625 53.3 %
 126958 : 67739 53.4 %

Residuals of Control Points from DEM:

DEM file: /geot1/Holywell/f2_1_f1_1/product/f2_1_f1_1.mde
 Control Point File: /geot1/Holywell/Holygcp

N0.	X	Y	Z	dZ	
1009	347721.315	5584646.493	23.021	4.917	
1010	347745.189	5584823.580	36.063	1.094	
1011	347993.247	5584746.976	48.401	-0.729	
1015	347894.877	5584507.708	34.609	0.673	
1021	347714.779	5584526.562	31.896	-4.241	
2023	347808.000	5584521.000	42.000	-10.900	
2001	347714.000	5584550.000	24.840	0.960	
2002	347740.500	5584545.000	24.140	1.272	
2003	347789.500	5584525.500	28.277	1.398	
2004	347762.000	5584537.000	25.940	0.860	

2005	347653.000	5584566.000	11.316	1.284
2006	347628.000	5584523.500	9.838	0.062
2009	347954.000	5584534.500	37.086	1.914

Number of points = 13
 Mean value = -0.1
 Absolute mean value= 2.3
 Mean square root = 3.7

	No.	Percent
dZ <= 1.0 :	5	38.5
1.0 < dZ <= 2.0 :	5	38.5
2.0 < dZ <= 3.0 :	0	0.0
3.0 < dZ <= 4.0 :	0	0.0
4.0 < dZ <= 5.0 :	2	15.4
5.0 < dZ <= 6.0 :	0	0.0
6.0 < dZ <= 10.0 :	0	0.0
10.0 < dZ <= 20.0 :	1	7.7
20.0 < dZ <= 100.0 :	0	0.0

 VirtuoZo image file information (Ortho Image):

Image name: /geot1/Holywell/f2_1_f1_1/product/f2_1_f1_1.orl
 Dimensions [row X col]: 1037 X 2157
 Color model: 24-bits Color Image
 X_Dimension PixelSize: 0.10000 mm
 Y_Dimension PixelSize: 0.10000 mm

Geographic informations:

Image Scale: 1 : 5000
 Rotate angle: 0.00000000 Rad (0.00000 Deg)
 X_Ground PixelSize: 0.50000
 Y_Ground PixelSize: 0.50000

Bottom_Left coordinate[x,y]: 347028.000 5584498.000
 Bottom_Right coordinate[x,y]: 348106.000 5584498.000
 Top_Left coordinate[x,y]: 347028.000 5585016.000
 Top_Right coordinate[x,y]: 348106.000 5585016.000

 VirtuoZo image file information (Contour Image):

Image name: /geot1/Holywell/f2_1_f1_1/product/f2_1_f1_1.cnt
 Dimensions [row X col]: 1037 X 2157
 Color model: 8-bits GrayScale Image
 X_Dimension PixelSize: 0.10000 mm
 Y_Dimension PixelSize: 0.10000 mm

Geographic informations:

Image Scale: 1 : 5000
 Rotate angle: 0.00000000 Rad (0.00000 Deg)
 X_Ground PixelSize: 0.50000
 Y_Ground PixelSize: 0.50000

Bottom_Left coordinate[x,y]: 347028.000 5584498.000
 Bottom_Right coordinate[x,y]: 348106.000 5584498.000
 Top_Left coordinate[x,y]: 347028.000 5585016.000
 Top_Right coordinate[x,y]: 348106.000 5585016.000

VirtuoZo image file information (Ortho+Contour Image):

Image name: /geot1/Holywell/f2_1_f1_1/product/f2_1_f1_1.orc
 Dimensions [row X col]: 1037 X 2157
 Color model: 24-bits Color Image
 X_Dimension PixelSize: 0.10000 mm
 Y_Dimension PixelSize: 0.10000 mm

Geographic informations:

Image Scale: 1 : 5000
 Rotate angle: 0.00000000 Rad (0.00000 Deg)
 X_Ground PixelSize: 0.50000
 Y_Ground PixelSize: 0.50000

Bottom_Left coordinate[x,y]: 347028.000 5584498.000
 Bottom_Right coordinate[x,y]: 348106.000 5584498.000
 Top_Left coordinate[x,y]: 347028.000 5585016.000
 Top_Right coordinate[x,y]: 348106.000 5585016.000

Virtuozo Processing Information Report File

Interior orientation information:
 (/geot1/Holywell/f3_1_f2_1.ste)

Left image (/geot1/Holywell/Images/f3_1):

Principle Coord. [col X row]: 1018.000 1530.000
 [x0 X y0]: 0.000 0.000

RMS: Mx = 1.000 My = 0.000
 Residual: point NO. dx dy
 8 1.000 0.000

Right image (/geot1/Holywell/Images/f2_1):

Principle Coord. [col X row]: 1018.000 1530.000
 [x0 X y0]: 0.000 0.000

RMS: Mx = 1.000 My = 0.000
 Residual: point NO. dx dy
 8 1.000 0.000

relative orientation information:
 (/geot1/Holywell/f3_1_f2_1.ste)

 Relative orientation information:

Left rotation matrix:

/				\
	0.99737400	-0.04992700	-0.05245500	
	0.04999500	0.99874902	0.00000000	
	0.05238900	-0.00262200	0.99862301	
\				/

Right rotation matrix:

/				\
	0.99472499	-0.10246600	0.00473100	
	0.10257300	0.99335700	-0.05217000	
	0.00064600	0.05238000	0.99862701	
\				/

Right photo rotation angle (rad):

Phi = 0.05247900
 Omega = 0.00000000
 Kappa = 0.05001600

Left photo rotation angle (rad):

Phi = -0.00473700
 Omega = 0.05219300
 Kappa = 0.10289400

Residual:	point NO.	dq
	1	-0.002000
	2	-0.002000
	3	0.000000
	4	0.003000
	5	0.002000
	6	0.005000
	7	0.005000
	8	0.000000
	9	-0.001000
	10	-0.003000
	11	-0.003000
	12	-0.002000
	13	0.004000
	14	0.002000
	15	-0.003000
	16	0.000000
	17	0.002000
	18	0.002000
	19	-0.003000
	20	0.002000
	21	0.004000
	22	0.003000
	23	-0.003000
	24	0.004000
	25	0.004000

26	0.004000
27	0.001000
28	0.002000
29	0.002000
30	0.003000
31	0.004000
32	0.005000
33	-0.002000
34	-0.002000
35	-0.006000
36	0.002000
37	0.000000
38	-0.002000
39	0.002000
40	-0.006000
41	-0.003000
42	0.000000
43	-0.002000
44	0.003000
45	-0.005000
46	-0.002000
47	0.002000
48	-0.002000
49	0.004000
50	-0.001000
51	0.003000
52	0.006000
53	0.001000
54	-0.005000
55	-0.005000
56	0.001000
57	-0.008000
58	-0.001000
59	0.001000
60	0.003000
61	-0.005000
62	0.005000
63	-0.002000
64	0.006000
65	-0.001000
66	-0.002000
67	0.000000
68	-0.002000
69	-0.004000
70	0.001000
71	0.005000
72	-0.005000
73	-0.006000
74	0.001000
75	0.002000
76	0.001000
77	-0.004000
78	-0.001000
79	0.006000
80	0.003000
81	0.000000

82	0.001000
83	-0.004000
84	0.000000
85	0.002000
86	0.001000
87	-0.005000
88	-0.006000
1015	-0.003000
1008	-0.021000
1020	0.006000
1019	-0.004000
1022	0.003000
1024	0.012000
1023	-0.008000
1007	0.005000

RMS: Mq = 0.004000

 Absolute orientation information:
 (/geot1/Holywell/f3_1_f2_1.ste)

 Absolute orientation information:

Left rotation matrix:

/				\
	0.11313859	-0.99106783	-0.07059938	
	0.98666060	0.10369606	0.12549081	
	-0.11704903	-0.08385548	0.98957962	
\				/

Right rotation matrix:

/				\
	0.06416041	-0.99789184	-0.00976155	
	0.98297882	0.06150811	0.17311670	
	-0.17215133	-0.02070263	0.98485297	
\				/

Left station coordinates:

Xs = 347429.027 Ys = 5584397.429 Zs = 1226.158

Right station coordinates:

Xs = 347501.049 Ys = 5584819.219 Zs = 1154.814

Left angle elements:

Phi = 0.071222 Omiga = -0.125823 Kapa = 1.466083

Right angle elements:

Phi = 0.009911 Omiga = -0.173993 Kapa = 1.508305

Residual:

No.	dX	dY	dZ
1015	-1.753101	-0.223402	-1.444377
1008	3.636185	-3.372003	-0.543976
1020	-2.226330	2.298586	2.709976
1019	0.659259	-0.720656	-2.480867
1022	-1.865890	0.859211	1.818646
1024	2.119795	-0.827773	0.142770
1023	1.400809	0.025058	-0.004015
1007	-1.970726	1.960979	-0.198157

RMS: mx = 2.106759 my = 1.676778
mxy = 2.692586 mz = 1.551126

Image matching information:
(/geot1/Holywell/f3_1_f2_1.ste)

Initial parameters

left image: rows = 767 columns = 754
right image: rows = 767 columns = 754

Match window width = 5
Match window length = 5
Searching range = 0
Match grid X_interval = 3
Match grid Y_interval = 3

MATCH_BLOCK == 1
MATCH_LEVEL == 3
MATCH_AREAS == 4 X 4

16 : 0 0.0 %
16 : 5 31.2 %
16 : 8 50.0 %
16 : 8 50.0 %

MATCH_BLOCK == 1
MATCH_LEVEL == 2
MATCH_AREAS == 16 X 15

240 : 0 0.0 %
240 : 194 80.8 %
240 : 216 90.0 %
240 : 216 90.0 %
240 : 216 90.0 %

240 : 216 90.0 %

MATCH_BLOCK == 1
MATCH_LEVEL == 1
MATCH_AREAS == 50 X 49

2450 : 0 0.0 %
2450 : 2135 87.1 %
2450 : 2274 92.8 %
2450 : 2320 94.7 %
2450 : 2335 95.3 %
2450 : 2345 95.7 %
2450 : 2352 96.0 %
2450 : 2364 96.5 %
2450 : 2370 96.7 %
2450 : 2372 96.8 %
2450 : 2376 97.0 %

MATCH_BLOCK == 1
MATCH_LEVEL == 0
MATCH_AREAS == 255 X 250

63750 : 0 0.0 %
63750 : 36122 56.7 %
63750 : 42941 67.4 %
63750 : 46076 72.3 %
63750 : 48277 75.7 %
63750 : 49792 78.1 %
63750 : 51007 80.0 %
63750 : 51927 81.5 %
63750 : 52711 82.7 %
63750 : 53361 83.7 %
63750 : 53839 84.5 %
63750 : 54207 85.0 %
63750 : 54505 85.5 %
63750 : 54818 86.0 %
63750 : 55075 86.4 %
63750 : 55253 86.7 %
63750 : 55425 86.9 %
63750 : 55568 87.2 %
63750 : 55693 87.4 %
63750 : 55796 87.5 %
63750 : 55895 87.7 %
63750 : 55965 87.8 %
63750 : 56037 87.9 %
63750 : 56094 88.0 %
63750 : 56143 88.1 %
63750 : 56196 88.2 %

Residuals of Control Points from DEM:

DEM file: /geot1/Holywell/f3_1_f2_1/product/f3_1_f2_1.dem
 Control Point File: /geot1/Holywell/Holygcp

No.	X	Y	Z	dZ	
1008	347592.915	5584477.839	1.653	1.770	
1020	347634.769	5584368.169	7.702	3.265	
1021	347714.779	5584526.562	31.896	-4.138	
2023	347808.000	5584521.000	42.000	-11.050	
2000	347787.000	5584399.500	27.774	-0.512	
2001	347714.000	5584550.000	24.840	-0.040	
2002	347740.500	5584545.000	24.140	0.060	
2003	347789.500	5584525.500	28.277	-0.121	
2004	347762.000	5584537.000	25.940	-0.540	
2005	347653.000	5584566.000	11.316	-0.216	
2006	347628.000	5584523.500	9.838	-0.313	
2007	347594.500	5584497.000	2.484	-0.034	

Number of points = 12
 Mean value = -1.0
 Absolute mean value = 1.8
 Mean square root = 3.6

dZ <=	No.	Percent
1.0 :	8	66.7
1.0 < dZ <= 2.0 :	1	8.3
2.0 < dZ <= 3.0 :	0	0.0
3.0 < dZ <= 4.0 :	1	8.3
4.0 < dZ <= 5.0 :	1	8.3
5.0 < dZ <= 6.0 :	0	0.0
6.0 < dZ <= 10.0 :	0	0.0
10.0 < dZ <= 20.0 :	1	8.3
20.0 < dZ <= 100.0 :	0	0.0

VirtuoZo image file information (Ortho Image):

Image name: /geot1/Holywell/f3_1_f2_1/product/f3_1_f2_1.orl
 Dimensions [row X col]: 1161 X 1265
 Color model: 24-bits Color Image
 X_Dimension PixelSize: 0.10000 mm
 Y_Dimension PixelSize: 0.10000 mm

Geographic informations:

Image Scale: 1 : 2500
 Rotate angle: 0.00000000 Rad (0.00000 Deg)
 X_Ground PixelSize: 0.25000
 Y_Ground PixelSize: 0.25000
 Bottom_Left coordinate[x,y]: 347502.000 5584306.000
 Bottom_Right coordinate[x,y]: 347818.000 5584306.000
 Top_Left coordinate[x,y]: 347502.000 5584596.000
 Top_Right coordinate[x,y]: 347818.000 5584596.000

VirtuoZo image file information (Contour Image):

Image name: /geot1/Holywell/f3_1_f2_1/product/f3_1_f2_1.cnt
Dimensions [row X col]: 1161 X 1265
Color model: 8-bits GrayScale Image
X_Dimension PixelSize: 0.10000 mm
Y_Dimension PixelSize: 0.10000 mm

Geographic informations:

Image Scale: 1 : 2500
Rotate angle: 0.00000000 Rad (0.00000 Deg)
X_Ground PixelSize: 0.25000
Y_Ground PixelSize: 0.25000

Bottom_Left coordinate[x,y]: 347502.000 5584306.000
Bottom_Right coordinate[x,y]: 347818.000 5584306.000
Top_Left coordinate[x,y]: 347502.000 5584596.000
Top_Right coordinate[x,y]: 347818.000 5584596.000

VirtuoZo image file information (Ortho+Contour Image):

Image name: /geot1/Holywell/f3_1_f2_1/product/f3_1_f2_1.orc
Dimensions [row X col]: 1161 X 1265
Color model: 24-bits Color Image
X_Dimension PixelSize: 0.10000 mm
Y_Dimension PixelSize: 0.10000 mm

Geographic informations:

Image Scale: 1 : 2500
Rotate angle: 0.00000000 Rad (0.00000 Deg)
X_Ground PixelSize: 0.25000
Y_Ground PixelSize: 0.25000

Bottom_Left coordinate[x,y]: 347502.000 5584306.000
Bottom_Right coordinate[x,y]: 347818.000 5584306.000
Top_Left coordinate[x,y]: 347502.000 5584596.000
Top_Right coordinate[x,y]: 347818.000 5584596.000

Interior orientation information:
(/geot1/Holywell/f3_1_f2_1.ste)

Left image (/geot1/Holywell/Images/f3_1):

Principle Coord. [col X row]: 1018.000 1530.000
[x0 X y0]: 0.000 0.000

RMS: Mx = 1.000 My = 0.000
Residual: point NO. dx dy
8 1.000 0.000

Right image (/geot1/Holywell/Images/f2_1):

Principle Coord. [col X row]: 1018.000 1530.000
 [x0 X y0]: 0.000 0.000

RMS: Mx = 1.000 My = 0.000
 Residual: point NO. dx dy
 8 1.000 0.000

relative orientation information:
 (/geot1/Holywell/f3_1_f2_1.ste)

Relative orientation information:

Left rotation matrix:

/				\
	0.99737400	-0.04992700	-0.05245500	
	0.04999500	0.99874902	0.00000000	
	0.05238900	-0.00262200	0.99862301	
\				/

Right rotation matrix:

/				\
	0.99472499	-0.10246600	0.00473100	
	0.10257300	0.99335700	-0.05217000	
	0.00064600	0.05238000	0.99862701	
\				/

Right photo rotation angle (rad):

Phi = 0.05247900
 Omega = 0.00000000
 Kappa = 0.05001600

Left photo rotation angle (rad):

Phi = -0.00473700
 Omega = 0.05219300
 Kappa = 0.10289400

Residual:	point NO.	dq
	1	-0.002000
	2	-0.002000
	3	0.000000
	4	0.003000
	5	0.002000
	6	0.005000
	7	0.005000
	8	0.000000
	9	-0.001000
	10	-0.003000
	11	-0.003000
	12	-0.002000
	13	0.004000
	14	0.002000
	15	-0.003000
	16	0.000000

17	0.002000
18	0.002000
19	-0.003000
20	0.002000
21	0.004000
22	0.003000
23	-0.003000
24	0.004000
25	0.004000
26	0.004000
27	0.001000
28	0.002000
29	0.002000
30	0.003000
31	0.004000
32	0.005000
33	-0.002000
34	-0.002000
35	-0.006000
36	0.002000
37	0.000000
38	-0.002000
39	0.002000
40	-0.006000
41	-0.003000
42	0.000000
43	-0.002000
44	0.003000
45	-0.005000
46	-0.002000
47	0.002000
48	-0.002000
49	0.004000
50	-0.001000
51	0.003000
52	0.006000
53	0.001000
54	-0.005000
55	-0.005000
56	0.001000
57	-0.008000
58	-0.001000
59	0.001000
60	0.003000
61	-0.005000
62	0.005000
63	-0.002000
64	0.006000
65	-0.001000
66	-0.002000
67	0.000000
68	-0.002000
69	-0.004000
70	0.001000
71	0.005000
72	-0.005000

73	-0.006000
74	0.001000
75	0.002000
76	0.001000
77	-0.004000
78	-0.001000
79	0.006000
80	0.003000
81	0.000000
82	0.001000
83	-0.004000
84	0.000000
85	0.002000
86	0.001000
87	-0.005000
88	-0.006000
1015	-0.003000
1008	-0.021000
1020	0.006000
1019	-0.004000
1022	0.003000
1024	0.012000
1023	-0.008000
1007	0.005000

RMS: Mq = 0.004000

Absolute orientation information:
(/geot1/Holywell/f3_1_f2_1.ste)

Absolute orientation information:

Left rotation matrix:

/				\
	0.11313859	-0.99106783	-0.07059938	
	0.98666060	0.10369606	0.12549081	
	-0.11704903	-0.08385548	0.98957962	
\				/

Right rotation matrix:

/				\
	0.06416041	-0.99789184	-0.00976155	
	0.98297882	0.06150811	0.17311670	
	-0.17215133	-0.02070263	0.98485297	
\				/

Left station coordinates:

Xs = 347429.027 Ys = 5584397.429 Zs = 1226.158

Right station coordinates:

Xs = 347501.049 Ys = 5584819.219 Zs = 1154.814

Left angle elements:

Phi = 0.071222 Omega = -0.125823 Kapa = 1.466083
 Right angle elements:
 Phi = 0.009911 Omega = -0.173993 Kapa = 1.508305

Residual:

No.	dX	dY	dZ
1015	-1.753101	-0.223402	-1.444377
I008	3.636185	-3.372003	-0.543976
I020	-2.226330	2.298586	2.709976
1019	0.659259	-0.720656	-2.480867
1022	-1.865890	0.859211	1.818646
1024	2.119795	-0.827773	0.142770
1023	1.400809	0.025058	-0.004015
1007	-1.970726	1.960979	-0.198157

RMS: mx = 2.106759 my = 1.676778
 mxy = 2.692586 mz = 1.551126

Image matching information:
 (/geot1/Holywell/f3_1_f2_1.ste)

Initial parameters

left image: rows =2891 columns =1037
 right image: rows =2891 columns =1037

Match window width = 5
 Match window length = 5
 Searching range = 5
 Match grid X_interval = 5
 Match grid Y_interval = 5

MATCH_BLOCK == 1
 MATCH_LEVEL == 3
 MATCH_AREAS == 21 X 7

147 : 0 0.0 %
 147 : 54 36.7 %
 147 : 75 51.0 %
 147 : 80 54.4 %
 147 : 85 57.8 %
 147 : 89 60.5 %

MATCH_BLOCK == 1
MATCH_LEVEL == 2
MATCH_AREAS == 64 X 23

1472 : 0 0.0 %
1472 : 658 44.7 %
1472 : 852 57.9 %
1472 : 938 63.7 %
1472 : 980 66.6 %
1472 : 1010 68.6 %
1472 : 1040 70.7 %
1472 : 1067 72.5 %
1472 : 1089 74.0 %
1472 : 1107 75.2 %
1472 : 1119 76.0 %
1472 : 1125 76.4 %
1472 : 1127 76.6 %
1472 : 1134 77.0 %

MATCH_BLOCK == 1
MATCH_LEVEL == 1
MATCH_AREAS == 192 X 69

13248 : 0 0.0 %
13248 : 5657 42.7 %
13248 : 6810 51.4 %
13248 : 7298 55.1 %
13248 : 7619 57.5 %
13248 : 7865 59.4 %
13248 : 8062 60.9 %
13248 : 8242 62.2 %
13248 : 8412 63.5 %
13248 : 8554 64.6 %
13248 : 8658 65.4 %
13248 : 8753 66.1 %
13248 : 8848 66.8 %
13248 : 8935 67.4 %
13248 : 9005 68.0 %
13248 : 9057 68.4 %
13248 : 9091 68.6 %
13248 : 9123 68.9 %
13248 : 9158 69.1 %
13248 : 9178 69.3 %
13248 : 9203 69.5 %
13248 : 9223 69.6 %
13248 : 9249 69.8 %
13248 : 9266 69.9 %
13248 : 9282 70.1 %
13248 : 9297 70.2 %
13248 : 9314 70.3 %
13248 : 9323 70.4 %
13248 : 9331 70.4 %

13248 : 9334 70.5 %

MATCH_BLOCK == 1
MATCH_LEVEL == 0
MATCH_AREAS == 578 X 207

119646 : 0 0.0 %
119646 : 29662 24.8 %
119646 : 38587 32.3 %
119646 : 43810 36.6 %
119646 : 47744 39.9 %
119646 : 50705 42.4 %
119646 : 53182 44.4 %
119646 : 55181 46.1 %
119646 : 57029 47.7 %
119646 : 58537 48.9 %
119646 : 59844 50.0 %
119646 : 60891 50.9 %
119646 : 61800 51.7 %
119646 : 62570 52.3 %
119646 : 63223 52.8 %
119646 : 63788 53.3 %
119646 : 64267 53.7 %
119646 : 64653 54.0 %
119646 : 65070 54.4 %
119646 : 65392 54.7 %
119646 : 65652 54.9 %
119646 : 65896 55.1 %
119646 : 66091 55.2 %
119646 : 66308 55.4 %
119646 : 66478 55.6 %
119646 : 66641 55.7 %
119646 : 66798 55.8 %
119646 : 66927 55.9 %
119646 : 67025 56.0 %
119646 : 67127 56.1 %
119646 : 67212 56.2 %

Residuals of Control Points from DEM:

DEM file: /geot1/Holywell/f3_1_f2_1/product/f3_1_f2_1.mde
Control Point File: /geot1/Holywell/Holygcp

NO.	X	Y	Z	dZ	
1007	347514.418	5584285.422	3.527	0.311	
1008	347592.915	5584477.839	1.653	1.302	
1015	347894.877	5584507.708	34.609	0.673	
1019	347686.899	5584273.047	12.327	-1.069	
1020	347634.769	5584368.169	7.702	3.167	
1021	347714.779	5584526.562	31.896	-4.241	
1022	347833.393	5584391.331	30.372	1.637	
1023	347829.335	5584227.228	25.964	-0.279	

1024	347973.643	5584222.220	19.506	0.711
2023	347808.000	5584521.000	42.000	-10.900
2000	347787.000	5584399.500	27.774	-0.036
2001	347714.000	5584550.000	24.840	0.960
2002	347740.500	5584545.000	24.140	1.272
2003	347789.500	5584525.500	28.277	1.398
2004	347762.000	5584537.000	25.940	0.860
2005	347653.000	5584566.000	11.316	1.284
2006	347628.000	5584523.500	9.838	0.062
2007	347594.500	5584497.000	2.484	-0.046
2008	348027.000	5584545.000	37.400	-0.325
2009	347954.000	5584534.500	37.086	1.914
2010	347914.500	5584445.500	36.240	-0.196

Number of points = 21
 Mean value = -0.1
 Absolute mean value = 1.6
 Mean square root = 2.8

	No.	Percent
dZ <= 1.0 :	11	52.4
1.0 < dZ <= 2.0 :	7	33.3
2.0 < dZ <= 3.0 :	0	0.0
3.0 < dZ <= 4.0 :	1	4.8
4.0 < dZ <= 5.0 :	1	4.8
5.0 < dZ <= 6.0 :	0	0.0
6.0 < dZ <= 10.0 :	0	0.0
10.0 < dZ <= 20.0 :	1	4.8
20.0 < dZ <= 100.0 :	0	0.0

 VirtuoZo image file information (Ortho Image):

Image name: /geot1/Holywell/f3_1_f2_1/product/f3_1_f2_1.orl
 Dimensions [row X col]: 929 X 2253
 Color model: 24-bits Color Image
 X_Dimension PixelSize: 0.10000 mm
 Y_Dimension PixelSize: 0.10000 mm

Geographic informations:

Image Scale: 1 : 5000
 Rotate angle: 0.00000000 Rad (0.00000 Deg)
 X_Ground PixelSize: 0.50000
 Y_Ground PixelSize: 0.50000

Bottom_Left coordinate[x,y]: 346950.000 5584194.000
 Bottom_Right coordinate[x,y]: 348076.000 5584194.000
 Top_Left coordinate[x,y]: 346950.000 5584658.000
 Top_Right coordinate[x,y]: 348076.000 5584658.000

 VirtuoZo image file information (Contour Image):

Image name: /geot1/Holywell/f3_1_f2_1/product/f3_1_f2_1.cnt
 Dimensions [row X col]: 929 X 2253

Color model: 8-bits GrayScale Image
X_Dimension PixelSize: 0.10000 mm
Y_Dimension PixelSize: 0.10000 mm

Geographic infomations:

Image Scale: 1 : 5000
Rotate angle: 0.00000000 Rad (0.00000 Deg)
X_Ground PixelSize: 0.50000
Y_Ground PixelSize: 0.50000

Bottom_Left coordinate[x,y]: 346950.000 5584194.000
Bottom_Right coordinate[x,y]: 348076.000 5584194.000
Top_Left coordinate[x,y]: 346950.000 5584658.000
Top_Right coordinate[x,y]: 348076.000 5584658.000

VirtuoZo image file infomation (Ortho+Contour Image):

Image name: /geot1/Holywell/f3_1_f2_1/product/f3_1_f2_1.orc
Dimensions [row X col]: 929 X 2253
Color model: 24-bits Color Image
X_Dimension PixelSize: 0.10000 mm
Y_Dimension PixelSize: 0.10000 mm

Geographic infomations:

Image Scale: 1 : 5000
Rotate angle: 0.00000000 Rad (0.00000 Deg)
X_Ground PixelSize: 0.50000
Y_Ground PixelSize: 0.50000

Bottom_Left coordinate[x,y]: 346950.000 5584194.000
Bottom_Right coordinate[x,y]: 348076.000 5584194.000
Top_Left coordinate[x,y]: 346950.000 5584658.000
Top_Right coordinate[x,y]: 348076.000 5584658.000

Virtuozo Processing Information Report File

Interior orientation information:
(/geot1/Holywell/f4_1_f3_1.ste)

Left image (/geot1/Holywell/Images/f4_1):

Principle Coord. [col X row]: 1018.000 1530.000
[x0 X y0]: 0.000 0.000

RMS: Mx = 1.000 My = 0.000
Residual: point NO. dx dy
8 1.000 0.000

Right image (/geot1/Holywell/Images/f3_1):

Principle Coord. [col X row]: 1018.000 1530.000
[x0 X y0]: 0.000 0.000

RMS: Mx = 1.000 My = 0.000
Residual: point NO. dx dy
8 1.000 0.000

relative orientation information:
(/geot1/Holywell/f4_1_f3_1.ste)

Relative orientation information:

Left rotation matrix:

```
 /
 | 0.99267602 -0.11787600 0.02643200 |
 | 0.11791700 0.99302298 0.00000000 |
 | -0.02624800 0.00311700 0.99965101 |
 \
```

Right rotation matrix:

```
 /
 | 0.98931003 -0.11989400 0.08300800 |
 | 0.11931200 0.99278498 0.01195100 |
 | -0.08384200 -0.00191900 0.99647701 |
 \
```

Right photo rotation angle (rad):

Phi = -0.02643500
Omega = 0.00000000
Kappa = 0.11819200

Left photo rotation angle (rad):

Phi = -0.08310900
Omega = -0.01195100
Kappa = 0.11960500

Residual: point NO. dq
1 -0.009000
2 0.001000
3 -0.002000
4 -0.006000
5 0.005000
6 -0.002000
7 -0.001000
8 -0.003000
9 -0.003000
10 0.001000
11 -0.003000
12 -0.003000
13 -0.007000
14 0.002000

15	-0.002000
16	-0.008000
17	-0.004000
18	-0.001000
19	-0.004000
20	-0.004000
21	-0.001000
22	-0.006000
23	-0.005000
24	-0.002000
25	0.003000
26	-0.005000
27	-0.001000
28	0.004000
29	0.004000
30	0.002000
31	-0.002000
32	0.000000
33	-0.001000
34	0.003000
35	-0.001000
36	-0.006000
37	0.003000
38	-0.003000
39	-0.001000
40	0.006000
41	-0.003000
42	-0.004000
43	0.005000
44	-0.001000
45	0.005000
46	-0.001000
47	0.006000
48	0.008000
49	0.001000
50	0.000000
51	0.002000
52	0.000000
53	0.003000
54	0.005000
55	0.001000
56	0.003000
57	0.008000
58	0.002000
59	0.006000
60	0.009000
61	0.003000
62	0.007000
63	0.003000
64	-0.003000
65	-0.007000
66	0.003000
67	0.000000
68	0.004000
69	0.000000
70	0.001000

71	0.001000
72	0.005000
73	-0.002000
74	0.009000
75	-0.002000
76	0.008000
77	0.002000
78	0.005000
79	0.005000
80	-0.002000
81	-0.001000
82	-0.006000
83	0.004000
84	0.007000
85	0.001000
86	0.000000
87	-0.001000
88	0.000000
89	0.003000
90	-0.006000
91	0.003000
92	0.003000
93	0.004000
94	0.001000
95	-0.007000
96	0.004000
97	-0.002000
98	0.004000
99	0.005000
100	0.003000
101	0.006000
102	0.000000
103	0.007000
104	-0.003000
105	-0.003000
106	0.000000
1003	-0.004000
1004	-0.024000
1017	-0.027000
1005	0.003000
1002	-0.001000
1018	0.002000

RMS: $M_q = 0.005000$

 Absolute orientation information:
 (/geot1/Holywell/f4_1_f3_1.ste)

 Absolute orientation information:

Left rotation matrix:

/				\
	0.10808170	-0.99392438	-0.02080076	

```

|      0.99412870    0.10816497    -0.00291724    |
|      0.00514943    -0.02036333    0.99977940    |
\

```

Right rotation matrix:

```

/
|      0.10749455    -0.99400997    -0.01972484    |
|      0.99281865    0.10627583    0.05492336    |
|      -0.05249810    -0.02548715    0.99829572    |
\

```

Left station coordinates:

Xs = 347394.263 Ys = 5583870.657 Zs = 1224.471

Right station coordinates:

Xs = 347495.131 Ys = 5584309.610 Zs = 1239.787

Left angle elements:

Phi = 0.020802 Omega = 0.002917 Kapa = 1.462419

Right angle elements:

Phi = 0.019756 Omega = -0.054951 Kapa = 1.464158

Residual:

No.	dX	dY	dZ
1003	0.454846	-0.446525	6.270758
1004	-1.269401	-0.557685	-8.281677
1017	-0.764386	-1.936236	-9.557571
1005	0.943953	0.764634	7.092204
1002	0.123786	1.223465	3.360729
1018	0.511203	0.952346	1.115557

RMS: mx = 0.771389 my = 1.099083
 mxy = 1.342768 mz = 6.609262

Image matching information:
 (/geotl/Holywell/f4_1_f3_1.ste)

Initial parameters

left image: rows =2804 columns =1067
 right image: rows =2804 columns =1067

Match window width = 5
 Match window length = 5
 Searching range = 5
 Match grid X_interval = 5
 Match grid Y_interval = 5

MATCH_BLOCK == 1
MATCH_LEVEL == 3
MATCH_AREAS == 20 X 7

140 : 0 0.0 %
140 : 62 44.3 %
140 : 79 56.4 %
140 : 84 60.0 %
140 : 85 60.7 %
140 : 85 60.7 %

MATCH_BLOCK == 1
MATCH_LEVEL == 2
MATCH_AREAS == 62 X 23

1426 : 0 0.0 %
1426 : 902 63.3 %
1426 : 1100 77.1 %
1426 : 1135 79.6 %
1426 : 1157 81.1 %
1426 : 1160 81.3 %
1426 : 1172 82.2 %
1426 : 1179 82.7 %
1426 : 1187 83.2 %
1426 : 1193 83.7 %

MATCH_BLOCK == 1
MATCH_LEVEL == 1
MATCH_AREAS == 186 X 71

13206 : 0 0.0 %
13206 : 9034 68.4 %
13206 : 10235 77.5 %
13206 : 10726 81.2 %
13206 : 10977 83.1 %
13206 : 11151 84.4 %
13206 : 11287 85.5 %
13206 : 11413 86.4 %
13206 : 11512 87.2 %
13206 : 11577 87.7 %
13206 : 11636 88.1 %
13206 : 11684 88.5 %
13206 : 11722 88.8 %
13206 : 11750 89.0 %
13206 : 11771 89.1 %
13206 : 11788 89.3 %
13206 : 11807 89.4 %

13206 : 11825 89.5 %
 13206 : 11842 89.7 %
 13206 : 11855 89.8 %
 13206 : 11872 89.9 %
 13206 : 11882 90.0 %
 13206 : 11890 90.0 %
 13206 : 11899 90.1 %

MATCH_BLOCK == 1
 MATCH_LEVEL == 0
 MATCH_AREAS == 560 X 213

119280 : 0 0.0 %
 119280 : 50144 42.0 %
 119280 : 63634 53.3 %
 119280 : 70941 59.5 %
 119280 : 76553 64.2 %
 119280 : 80483 67.5 %
 119280 : 83600 70.1 %
 119280 : 85929 72.0 %
 119280 : 87821 73.6 %
 119280 : 89308 74.9 %
 119280 : 90572 75.9 %
 119280 : 91513 76.7 %
 119280 : 92320 77.4 %
 119280 : 93012 78.0 %
 119280 : 93595 78.5 %
 119280 : 94109 78.9 %
 119280 : 94532 79.3 %
 119280 : 94878 79.5 %
 119280 : 95166 79.8 %
 119280 : 95421 80.0 %
 119280 : 95674 80.2 %
 119280 : 95883 80.4 %
 119280 : 96081 80.6 %
 119280 : 96228 80.7 %
 119280 : 96380 80.8 %
 119280 : 96523 80.9 %
 119280 : 96661 81.0 %
 119280 : 96758 81.1 %
 119280 : 96850 81.2 %
 119280 : 96938 81.3 %

Residuals of Control Points from DEM:

DEM file: /geot1/Holywell/f4_1_f3_1/product/f4_1_f3_1.dem
 Control Point File: /geot1/Holywell/Holygcp

N0.	X	Y	Z	dZ	
1002	347662.035	5583901.381	-1.710	2.881	
1003	347317.301	5584205.843	14.598	5.334	
1004	347024.907	5584073.743	47.236	-8.506	

1005	347657.932	5584047.018	-1.168	6.819
1006	347527.242	5584192.762	15.400	6.876
1017	348013.815	5584086.988	14.003	-1.760
1018	347853.691	5584081.770	5.135	1.527

Number of points = 7
 Mean value = 1.9
 Absolute mean value = 4.8
 Mean square root = 5.5

	No.	Percent
dZ <= 1.0 :	0	0.0
1.0 < dZ <= 2.0 :	2	28.6
2.0 < dZ <= 3.0 :	1	14.3
3.0 < dZ <= 4.0 :	0	0.0
4.0 < dZ <= 5.0 :	0	0.0
5.0 < dZ <= 6.0 :	1	14.3
6.0 < dZ <= 10.0 :	3	42.9
10.0 < dZ <= 20.0 :	0	0.0
20.0 < dZ <= 100.0 :	0	0.0

 VirtuoZo image file information (Ortho Image):

Image name: /geot1/Holywell/f4_1_f3_1/product/f4_1_f3_1.orr
 Dimensions [row X col]: 981 X 2273
 Color model: 24-bits Color Image
 X_Dimension PixelSize: 0.10000 mm
 Y_Dimension PixelSize: 0.10000 mm

Geographic informations:

Image Scale: 1 : 5000
 Rotate angle: 0.00000000 Rad (0.00000 Deg)
 X_Ground PixelSize: 0.50000
 Y_Ground PixelSize: 0.50000

Bottom_Left coordinate[x,y]: 346904.000 5583818.000
 Bottom_Right coordinate[x,y]: 348040.000 5583818.000
 Top_Left coordinate[x,y]: 346904.000 5584308.000
 Top_Right coordinate[x,y]: 348040.000 5584308.000

 VirtuoZo image file information (Contour Image):

Image name: /geot1/Holywell/f4_1_f3_1/product/f4_1_f3_1.cnt
 Dimensions [row X col]: 981 X 2273
 Color model: 8-bits GrayScale Image
 X_Dimension PixelSize: 0.10000 mm
 Y_Dimension PixelSize: 0.10000 mm

Geographic informations:

Image Scale: 1 : 5000
 Rotate angle: 0.00000000 Rad (0.00000 Deg)
 X_Ground PixelSize: 0.50000

Y_Ground PixelSize: 0.50000

Bottom_Left coordinate[x,y]: 346904.000 5583818.000

Bottom_Right coordinate[x,y]: 348040.000 5583818.000

Top_Left coordinate[x,y]: 346904.000 5584308.000

Top_Right coordinate[x,y]: 348040.000 5584308.000

VirtuoZo image file information (Ortho+Contour Image):

Image name: /geot1/Holywell/f4_1_f3_1/product/f4_1_f3_1.orc

Dimensions [row X col]: 981 X 2273

Color model: 24-bits Color Image

X_Dimension PixelSize: 0.10000 mm

Y_Dimension PixelSize: 0.10000 mm

Geographic informations:

Image Scale: 1 : 5000

Rotate angle: 0.00000000 Rad (0.00000 Deg)

X_Ground PixelSize: 0.50000

Y_Ground PixelSize: 0.50000

Bottom_Left coordinate[x,y]: 346904.000 5583818.000

Bottom_Right coordinate[x,y]: 348040.000 5583818.000

Top_Left coordinate[x,y]: 346904.000 5584308.000

Top_Right coordinate[x,y]: 348040.000 5584308.000

APPENDIX 3

SIMPSON'S RULE

The principle of Simpson's rule is illustrated in Figure 12.6.

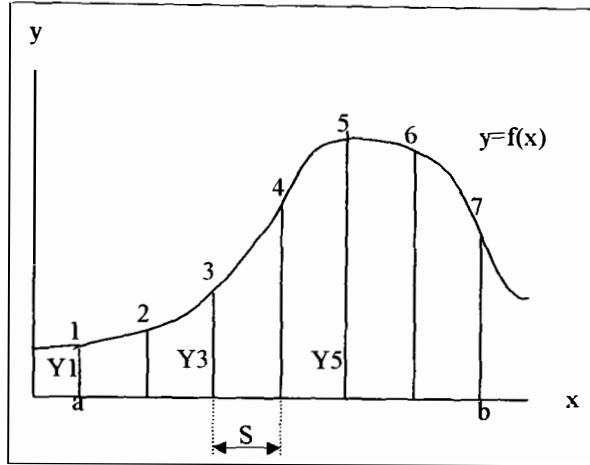


Figure 12.6 Simpson's rule for calculating the area under a curve

Integration between two points $x(a)$ and $x(b)$ can be used to calculate the area under a curve $y = f(x)$. Using Simpson's rule:

- the area under the curve is divided into an even number of strips (n) each of equal width (s).
- The ordinates are numbered y_1, y_2, \dots, y_{n+1} . The number of ordinates is one more than the number of strips.
- The area A is then given by $S/3 [(F+L) + 4E + 2R]$

Where: S = the width of each strip, $F + L$ = the sum of the first and last ordinates, $4E = 4 \times$ the sum of the even numbered ordinates, $2R = 2 \times$ the sum of the remaining odd numbered ordinates.

In this case each strip corresponds to one row in the DEM. The strip width S is $2m$, that is the specified DEM spacing. The number of ordinates corresponds to the number of columns in the DEM.

APPENDIX 4

DEM 1

S/3	F+L	Even	Odd	Area_UC_[M^2]	Volume_[M^3]
0.67	0	12	26	7	13
0.67	0	263	233	101	202
0.67	0	613	567	239	478
0.67	0	990	1066	406	812
0.67	0	1 856	1 766	730	1 461
0.67	0	2 779	2 665	1 096	2 193
0.67	0	4 239	4 102	1 677	3 355
0.67	0	5 562	5 418	2 206	4 411
0.67	0	5 633	5 494	2 235	4 469
0.67	0	7 095	7 229	2 856	5 712
0.67	0	8 269	8 430	3 329	6 658
0.67	307	9 720	9 568	3 888	7 776
0.67	306	9 681	9 535	3 873	7 747
0.67	305	9 679	9 516	3 870	7 740
0.67	307	9 705	9 547	3 881	7 763
0.67	312	9 799	9 632	3 918	7 836
0.67	316	9 975	9 802	3 988	7 976
0.67	314	9 937	9 745	3 970	7 940
0.67	312	9 876	9 710	3 949	7 898
0.67	314	9 972	9 806	3 988	7 975
0.67	314	10 116	9 951	4 045	8 091
0.67	311	10 238	10 070	4 094	8 187
0.67	310	10 434	10 235	4 168	8 335
0.67	310	10 661	10 506	4 264	8 529
0.67	324	10 837	10 680	4 335	8 671
0.67	329	10 990	10 834	4 397	8 794
0.67	313	11 103	10 933	4 439	8 879
0.67	315	11 245	11 110	4 501	9 002
0.67	319	11 444	11 288	4 578	9 156
0.67	315	11 569	11 442	4 632	9 263
0.67	309	11 619	11 475	4 649	9 298
0.67	312	11 612	11 434	4 642	9 284
0.67	312	11 573	11 403	4 627	9 255
0.67	306	11 541	11 388	4 616	9 233
0.67	319	11 444	11 294	4 579	9 158
0.67	321	11 305	11 146	4 522	9 044
0.67	308	11 266	11 104	4 505	9 011
0.67	301	11 211	11 074	4 486	8 972
0.67	300	11 127	10 938	4 446	8 891
0.67	298	11 009	10 860	4 404	8 807
0.67	295	10 909	10 753	4 362	8 725
0.67	297	10 826	10 682	4 331	8 662
0.67	295	10 814	10 668	4 326	8 652
0.67	288	10 806	10 684	4 325	8 651
0.67	304	10 800	10 664	4 322	8 644
0.67	298	10 744	10 612	4 300	8 600
0.67	301	10 697	10 559	4 280	8 561
0.67	301	10 720	10 589	4 291	8 581
0.67	305	10 649	10 694	4 339	8 679
0.67	303	10 948	10 793	4 379	8 757
0.67	297	11 039	10 910	4 418	8 836
0.67	293	11 096	10 991	4 444	8 888
0.67	293	11 276	11 132	4 511	9 021
0.67	291	11 276	11 107	4 507	9 015
0.67	292	11 254	11 123	4 504	9 007
0.67	0	11 277	11 151	4 494	8 988
0.67	0	11 344	11 174	4 515	9 030
0.67	0	11 307	11 192	4 507	9 015
0.67	0	11 221	11 099	4 472	8 944
0.67	0	11 226	11 098	4 473	8 947
0.67	0	11 309	11 165	4 504	9 009
0.67	0	11 295	11 140	4 497	8 995
0.67	0	11 338	11 179	4 514	9 028
0.67	0	11 527	11 371	4 590	9 180
0.67	0	11 747	11 550	4 673	9 345
0.67	0	11 435	11 609	4 597	9 194
0.67	0	11 448	11 631	4 604	9 207
0.67	0	11 521	11 694	4 631	9 263
0.67	0	11 538	11 729	4 641	9 281
0.67	0	11 642	11 836	4 683	9 365
0.67	0	11 762	11 943	4 729	9 458
0.67	0	11 904	12 084	4 786	9 571
0.67	0	12 066	12 266	4 853	9 706

	TOTAL VOLUME	1 200 194 [M^3]
TOTAL MASS AT BULK DENSITY OF MATERIAL OF	1800 [kg/M^3]	2 160 348 960 [kg]

DEM 2

S/3	F+L	Even	Odd	Area_UC [M^2]	Volume [M^3]
0.67	0	12	26	7	13
0.67	0	263	233	101	202
0.67	0	613	567	239	478
0.67	0	990	1066	406	812
0.67	0	1856	1766	730	1461
0.67	0	2779	2665	1096	2193
0.67	0	4239	4102	1677	3355
0.67	0	5562	5418	2206	4411
0.67	0	5629	5498	2234	4468
0.67	0	7035	7173	2832	5665
0.67	0	8196	8349	3299	6598
0.67	307	9679	9526	3872	7743
0.67	306	9695	9549	3879	7758
0.67	305	9791	9632	3916	7831
0.67	307	9887	9731	3954	7909
0.67	312	10024	9854	4008	8015
0.67	316	10190	10010	4073	8146
0.67	314	10157	9975	4069	8119
0.67	312	10155	9991	4061	8122
0.67	314	10289	10125	4115	8229
0.67	314	10411	10250	4164	8328
0.67	311	10510	10343	4202	8405
0.67	310	10659	10464	4258	8517
0.67	310	10797	10649	4320	8639
0.67	324	10899	10748	4361	8722
0.67	329	10970	10813	4389	8778
0.67	313	11068	10897	4425	8851
0.67	315	11202	11067	4484	8968
0.67	319	11402	11253	4562	9124
0.67	315	11567	11442	4631	9262
0.67	309	11619	11475	4649	9298
0.67	312	11612	11434	4642	9284
0.67	312	11573	11403	4627	9255
0.67	306	11543	11390	4617	9234
0.67	319	11419	11265	4568	9137
0.67	321	11254	11091	4501	9003
0.67	308	11248	11077	4497	8994
0.67	301	11240	11098	4497	8994
0.67	300	11179	10997	4467	8935
0.67	298	11068	10923	4428	8855
0.67	295	11005	10853	4401	8803
0.67	297	10936	10794	4375	8751
0.67	295	10935	10790	4374	8749
0.67	288	10916	10803	4371	8741
0.67	304	10902	10765	4363	8726
0.67	298	10843	10703	4338	8677
0.67	301	10802	10662	4322	8644
0.67	301	10804	10677	4325	8649
0.67	305	10873	10722	4349	8699
0.67	303	10943	10785	4376	8753
0.67	297	11017	10891	4410	8820
0.67	293	11066	10965	4432	8865
0.67	293	11249	11094	4498	8997
0.67	291	11275	11104	4507	9013
0.67	292	11254	11123	4504	9007
0.67	0	11277	11151	4494	8988
0.67	0	11344	11174	4515	9030
0.67	0	11307	11192	4507	9015
0.67	0	11221	11099	4472	8944
0.67	0	11226	11098	4473	8947
0.67	0	11309	11165	4504	9009
0.67	0	11295	11140	4497	8995
0.67	0	11338	11179	4514	9028
0.67	0	11527	11371	4590	9180
0.67	0	11747	11550	4673	9345
0.67	0	11435	11609	4597	9194
0.67	0	11448	11631	4604	9207
0.67	0	11521	11694	4631	9263
0.67	0	11538	11729	4641	9281
0.67	0	11642	11836	4683	9365
0.67	0	11762	11943	4729	9458
0.67	0	11904	12084	4786	9571
0.67	0	12066	12266	4853	9706

TOTAL VOLUME	1 204 113	[M^3]
TOTAL MASS AT BULK DENSITY OF MATERIAL OF 1800 [kg/M^3]	2 167 403 520	[kg]

